



The University of  
**Nottingham**

School of Chemistry

# Immobilised Catalysts for Continuous Reactions in Supercritical Carbon Dioxide

**GEORGE GREEN LIBRARY OF  
SCIENCE AND ENGINEERING**

Bernadett Kondor, MSc

Thesis submitted to the University of Nottingham for the  
Degree of Doctor of Philosophy, April 2009

## Abstract

This Thesis investigates immobilised metal- and biocatalysts for continuous reactions in scCO<sub>2</sub>. Chemical transformations with high atom economy and low E-factor (amount of waste per kg of product) are highly desired in the green chemical viewpoint. One of the approaches to decrease the production of waste is the use of catalysis (possibly highly selective). Another approach is the use of a ‘green’ reaction medium as a substitute for traditional solvents that can reduce the production of harmful solvent waste. How this Thesis encompasses by these topics is discussed in Chapter 1.

The details of the apparatus, experimental and analytical equipments and procedures are reported in Chapter 2.

The field of asymmetric catalytic hydrogenation is a currently important and expanding field of research. In Chapters 3 and 4, the continuous asymmetric hydrogenation of dimethyl itaconate is covered. High enantioselectivity (*ees* up to 83 %) was obtained in the continuous asymmetric hydrogenation of dimethyl itaconate catalysed by supported homogeneous chiral Rh catalysts on alumina in scCO<sub>2</sub> (Chapter 3). This is one of the first examples of the use of chiral catalyst in a continuous flow system without the need for the addition of the chiral modifier. The continuous asymmetric hydrogenation of dimethyl itaconate was also examined with chiral Rh catalysts immobilised in ionic liquids in a biphasic system ionic liquid/scCO<sub>2</sub> (Chapter 4). High enantioselectivity was achieved in the continuous flow system: *ees* up to 76 %.

Chapter 5 describes the kinetic resolution of secondary alcohols catalysed by immobilised *Candida antarctica* lipase B (Cal B) in a continuous flow scCO<sub>2</sub> system. The continuous kinetic resolution of α-tetralol with Cal B immobilised in the form of Cross-Linked Enzyme Aggregate (CLEA) gave excellent enantioselectivity (*eeR* to 99 %). Different acyl donors (vinyl acetate, phenyl acetate and *p*-nitrophenyl acetate) were investigated, and were shown to influence the enantioselectivity of the reaction.

In Chapter 6, a two step catalytic cascade reaction is described in a continuous flow scCO<sub>2</sub> system: hydrogenation of acetophenone with a Pd catalyst (Pd Type 31) followed by the kinetic resolution of the product with Cal B CLEA. The series reaction gave good results even when un-optimised:

- Step 1 (hydrogenation of acetophenone): conversion up to 91 %
- Step 2 (kinetic resolution of (*R/S*)-1-phenylethanol): conversion of (*R*)-1-phenylethanol up to 22 %, enantioselectivity (*R*) > 99 %.

Chapter 7 details the preparation of cholesterol oxidase CLEA and combi-CLEA of cholesterol oxidase and catalase, and their application for the continuous oxidation of cholesterol in scCO<sub>2</sub> with ‘in-flow’ cholesterol extraction. CLEA were successfully prepared with high retained activity:

- Individual cholesterol oxidase CLEA: cholesterol oxidase activity up to 99 % (relative to native),
- Combi-CLEA: cholesterol oxidase activity up to 99 % (relative to native), catalase activity up to 53 % (relative to native).

Unfortunately, the activity of the CLEA in the continuous oxidation was low, however, the findings of this work will aid in improving the performance of the continuous catalytic oxidation of cholesterol in the future.

The possible future directions of this research are presented in Chapter 8.

## Acknowledgements

I would like to thank Martyn Poliakoff and Neil Thomas for firstly giving me the opportunity to undertake such an interesting project and also for their constant supervision and support. I would also like to thank Paul Hamley for his help in the arrangements related to the SubClean Probiomat Programme.

I would like to thank the members of the Clean Technology Group for making my time in Nottingham very enjoyable and also for their scientific support. I would like to thank Geoff Akien, Gabriele Aksomaityte, Karima Benaissi, Rich Bourne, Adrian Chapman, Peter Clark, Natalie Cozier, Peter Gooden, Helen Hobbs, Amrit Johal, Sunil Joshi, Ingrida Lapenaite, Peter Licence, Silvia Lidon, Kevin Lovelock, Dianne Mann, Andrew Parrott, Katherine Scovell, Stepan Shipovskov, Phil Stephenson, Jamie Stevens, Hareg Tadesse, Sam Tang, Morgan Thomas, and Nacho Villar. I also thank Hetti Forintos and Joan for welcoming me on my first days in Nottingham and for their constant support and friendship onwards. I also thank Adrien Davis, Jon MacMaster, and David Clift for their scientific help. I am grateful to Mark Guyler, Peter Fields, and Richard Wilson for all their technical help.

During my PhD, I had opportunity to work at other European universities which taught me more about academic research in Europe. I have been introduced to new areas of research and also to new cultures. I would like to thank Zoran Novak, Prof. Roger Sheldon, Dr. Michiel Janssen, Prof. Maria José Cocero, and Dr. Juan Garcia-Serna for their support and help.

I am grateful to Johnson Matthey (UK), Solvias AC (Switzerland) and CLEA Technologies BV (Netherlands) for catalyst samples, and for the financial support provided by the EU Marie Curie EST Network, SubClean Probiomat Programme.

I would also like to thank my 'new' Nottingham friends for all the great time we had together, which made my time even more enjoyable in Nottingham. I would like to thank Cedric and Yasmine Biguenet, Antonello Decortes, Hiromi Mori, Kiril Tankov, Arturo Martinez, Maria Gonzalez, Anna Lovrics, Rudolf Balla, Nicolas Rodriguez, Athith Shrivatagh, Chloe Focche, Barbara Hennequin, Dominika Sari, Elena Waltz,

I would also like to thank my family and my friends for all their support and love during my time at university - Szeretném köszönni családomnak és barátaimnak a folytonos támogatásukat és szeretetüket, ami a tanulmányaim során sok erőt adott.

# List of Abbreviations

## Methods and materials:

$\alpha$ -tetralol - 1,2,3,4-tetrahydro naphtol

AGG - Aggregate

Amms - Ammonium sulfate solution (aqueous, saturated)

Anl - *Aspergillus niger* lipase

BINAP - 2,2'-*bis*(diphenylphosphino)-1,1'-binaphthyl

[BMIM] - 1-butyl-3-methylimidazolium

[BMIM][BF<sub>4</sub>] - 1-butyl-3-methylimidazolium tetrafluoroborate

[BMIM][BTA] - 1-butyl-3-methylimidazolium bis(trifluoromethylsulfonyl) amide

[BMIM][N(CN)<sub>2</sub>] - 1-butyl-3-methylimidazolium dicyanamide

[BMIM][NTf<sub>2</sub>] - 1-butyl-3-methylimidazolium bis(trifluoromethylsulfonyl) imide

BPR - Back Pressure Regulator

Cal A - *Candida antarctica* lipase A

Cal B - *Candida antarctica* lipase B

CATAXA/Alumina - Rh[(COD)<sub>2</sub>]<sup>+</sup>[BF<sub>4</sub>]<sup>-</sup>/PTA/Alumina

CATAXA/Carbon - Rh[(COD)<sub>2</sub>]<sup>+</sup>[BF<sub>4</sub>]<sup>-</sup>/PTA/Carbon

CD - Cyclodextrin

CLE - Cross-Linked Enzyme

CLEA - Cross-Linked Enzyme Aggregate

CLEC - Cross-Linked Enzyme Crystal

COD - 1,5-cyclo-octadiene

CRY - Crystal

CSDE - Cross-Linked Spray Dried Enzyme

dH<sub>2</sub>O - Distilled water

DKR - Dynamic Kinetic resolution

DLS - Dynamic Light Scattering

DME - Dimethoxyethane (ethyleneglycol dimethyl ether)

DMIT - Dimethyl itaconate

DPA - Dextran polyaldehyde (solution in water)

DPA 200 - Dextran polyaldehyde (200 µL DPA solution/mL enzyme solution)

DPA 400 - Dextran polyaldehyde (400 µL DPA solution/mL enzyme solution)

[EMIM] - 1-ethyl-3-methylimidazolium

FAD - Flavin Adenine Dinucleotide

FID - Flame Ionisation Detector

GA - Glutaraldehyde

GA 10 - Glutaraldehyde (10 mM solution in water)

GA 50 - Glutaraldehyde (50 mM solution in water)

GLC - Gas-Liquid Chromatography

HPLC - High Performance Liquid Chromatography

HRP - Horseradish peroxidise

ICP-MS - Inductively Coupled Plasma Mass Spectrometry

IL - Ionic Liquid

IPA - Iso-propanol or 2-propanol

KR - Kinetic resolution

NADPH - Nicotinamide Adenosine Diphosphate

nbd - 2,5-norbornadiene

PTA - Phosphotungstic acid H<sub>3</sub>O<sub>40</sub>PW<sub>12</sub>

Rml - *Rhizomucor miehei* lipase

R<sub>2</sub>P\*-P\*R<sub>2</sub> - Bisphosphine ligand

RTIL - Room Temperature Ionic Liquid

sc - Supercritical

SCF - Supercritical fluid

SDE - Spray dried enzyme

SDS-PAGE - Sodium Dodecyl Sulfate Polyacrylamide Gel Electrophoresis

SEM - Scanning Electron Microscopy

SILP - Silica supported Ionic Liquid Phase

SPB-20 - Poly(20% phenyl/80% dimethylsiloxane)

SPB-35 - Poly(35% diphenyl/ 65% dimethylsiloxane)

TBDMS - *Tert*-butyldimethylsilyl

TfO - Trifluoromethanesulfonate

TMOS - Si(OMe)<sub>4</sub>

UV-Vis - Ultraviolet-Visible Spectroscopy

VOC - Volatile organic compound

VVVC - Variable volume view cell

**Physical-chemical parameters:**

$d_{inner}$  - Inner diameter of a tube

$ee$ - Enantiomeric excess, enantioselectivity

$$ee(\%) = \frac{[enantiomerA - enantiomerB]}{[enantiomerA + enantiomerB]} \times 100$$

E-value - A measure of enantioselectivity (value > 100 indicate highly enantioselective reaction). It is calculated using the equation below.

$$E = \frac{\ln[1 - c(1 + ee_{R-acetate})]}{\ln[1 - c(1 - ee_{R-acetate})]}$$

E-factor - defined as amount of waste per kg of product. A parameter to report waste emission rate of chemical processes.

EQ - Environmental quotient

ppm - Part per million

Q - Unfriendliness quotient

TON - Turnover Number

U - Enzyme Unit: that amount of the enzyme that catalyses the conversion of 1 micro mol of substrate per minute

**General:**

JM - Johnson Matthey Plc. (UK)

NIST - National Institute of Standards and Technology

SOP - Standard Operating Procedure

## Important notes

**CO<sub>2</sub> flow rate:** The flow rate is given as volumetric flow rate (mL/min). The corresponding temperature and pressure were -10 °C and 40-50 bar.

**Experimental error:** The experimental error (as standard deviation of enantioselectivity and conversion values) was not determined in each case throughout this study (Chapters 3 and 4), however, it is shown in most cases (Chapters 5, 6, and 7). Where no error bars are found in Chapters 5, 6, and 7 the experimental error was very low.

# Contents

<b>Chapter 1.....</b>	<b>1</b>
1.1. Green Chemistry.....	1
1.2. Catalyst Immobilisation.....	4
1.3. Alternative Solvents .....	8
1.3.1. Water	9
1.3.2. Fluorinated Solvents	10
1.4. Supercritical Fluids (SCFs) .....	11
1.4.1. Supercritical Carbon Dioxide (scCO <sub>2</sub> )	13
1.4.2. Reactions in Supercritical Carbon Dioxide	13
1.5. Aims and Objectives.....	14
References .....	14
<b>Chapter 2.....</b>	<b>19</b>
2.1. Catalyst Immobilisation.....	19
2.1.1. The Preparation of Alumina or Carbon Supported Chiral Rh Catalysts	20
2.1.1.1. Preparation of [Rh(COD)(ligand)] <sup>+</sup> [BF <sub>4</sub> ] <sup>-</sup> /PTA/Alumina .....	21
2.1.1.2. Preparation of [Rh(COD)(ligand)] <sup>+</sup> [BF <sub>4</sub> ] <sup>-</sup> /PTA/Carbon.....	22
2.1.2. Preparation of Aerogel Supported Chiral Rh Catalysts	23
2.1.3. Preparation of Ionic Liquid Supported Chiral Rh Catalysts	25
2.1.4. Preparation of Cross-Linked Enzyme Aggregate (CLEA)	25
2.2. Preparation of dextran polyaldehyde .....	28
2.3. Enzyme Assays.....	29
2.3.1. Cholesterol Oxidase Assay	29
2.3.2. Catalase Assay	30
2.4. Equipment Description .....	32
2.4.1. The Small Scale Hydrogenation Apparatus	33
2.4.2. The Small Scale Enzyme Reactor	36
2.4.3. The Small Scale Two-Stage Reactor	38
2.4.4. The Small Scale Oxidation Reactor	41
2.4.5. Gas Dosage	44
2.4.6. The Small Scale Screw Top Autoclave	45
2.4.7. The Small Scale Clamp Autoclave	46
2.4.8. The Variable Volume View Cell (VVVC)	49
2.5. Analytical Techniques .....	49
2.5.1. Gas-Liquid Chromatography (GLC)	50
2.5.2. High Performance Liquid Chromatography (HPLC)	51
2.5.3. Ultraviolet-Visible Spectroscopy (UV-Vis)	51
2.5.4. Inductively Coupled Plasma – Mass Spectrometry (ICP-MS)	52
2.5.5. Dynamic Light Scattering (DLS)	52
2.5.6. Scanning Electron Microscopy (SEM)	53
2.5.7. Sodium Dodecyl Sulfate Polyacrylamide Gel Electrophoresis (SDS-PAGE)	54
2.5.8. Karl-Fischer Titration	55
References .....	56

<b>Chapter 3.....</b>	<b>58</b>
3.1. Catalytic Asymmetric Hydrogenation .....	58
3.2. Continuous Catalytic Asymmetric Hydrogenation in SCFs.....	59
3.3. Supported Homogeneous Chiral Rh Catalysts .....	61
3.4. Continuous Asymmetric Hydrogenation of Dimethyl Itaconate in scCO <sub>2</sub> .....	64
3.5. The Development of the Josiphos Type Ligands .....	67
3.6. Results and Discussion .....	68
3.6.1. The Effect of the Bisphosphine Ligand on the Enantioselectivity	71
3.6.2. The Effect of the Cosolvent on the Enantioselectivity	83
3.6.3. The Effect of the Support Material on the Enantioselectivity	85
3.7. Conclusions .....	87
References .....	88
<b>Chapter 4.....</b>	<b>91</b>
4.1. Ionic Liquids.....	91
4.2. Reactions in Biphasic Systems Ionic Liquid/scCO <sub>2</sub> .....	92
4.3. Experimental.....	95
4.4. Results and Discussion .....	97
4.5. Conclusions .....	101
References .....	102
<b>Chapter 5.....</b>	<b>105</b>
5.1. Using Enzymes as Biocatalysts .....	105
5.2. Enzyme catalysed kinetic resolution in scCO <sub>2</sub> .....	107
5.3. Results and Discussion .....	111
5.4. Conclusions .....	122
References .....	123
<b>Chapter 6.....</b>	<b>126</b>
6.1. Multistep Catalytic Cascade Reactions .....	126
6.2. Reactor Design for Multistep Catalytic Cascade Reactions .....	128
6.3. Results and Discussion .....	130
6.4. Conclusions .....	137
References .....	138
<b>Chapter 7.....</b>	<b>140</b>
7.1. Cholesterol Oxidases .....	140
7.2. Enzyme Catalysed Coupled-/Cascade Reactions .....	144
7.3. Results and Discussion .....	147
7.3.1. Results of the Precipitation Screen of the Enzymes	148
7.3.2. CLEA Activity	151
7.3.3. Oxidation of Cholesterol in a Continuous Flow scCO <sub>2</sub> system	166
7.3.3.1. ‘In-flow’ Cholesterol Extraction in a Continuous Flow scCO <sub>2</sub> system .....	167
7.3.3.2. Oxidation of Cholesterol in a Continuous Flow scCO <sub>2</sub> system	174
7.3.3.3. Oxidation of Cholesterol in a Batch scCO <sub>2</sub> system.....	176
7.4. Conclusions .....	178
References .....	180

<b>Chapter 8.....</b>	<b>183</b>
8.1. Continuous Asymmetric Hydrogenation with Supported Homogeneous Chiral Rh Catalysts on Alumina in scCO <sub>2</sub> .....	183
8.2. Continuous Kinetic Resolution of $\alpha$ -tetralol Catalysed by Cal B CLEA in scCO <sub>2</sub> .....	184
8.3. Catalytic Cascade Reaction in a Continuous Flow scCO <sub>2</sub> system: Hydrogenation followed by the Kinetic Resolution of the Product .....	185
8.4. Combi-CLEA of Cholesterol Oxidase and Catalase for the Continuous Oxidation of Cholesterol in scCO <sub>2</sub> .....	185
8.5. Thesis Summary .....	188
References .....	188
<b>Appendix .....</b>	<b>190</b>

## Declaration

Except where specific reference is made to other sources or collaborators, the work presented in this Thesis is the original work of the author. It has not been submitted, in whole or in part, for any other Degree.

Signed: 

Bernadett Kondor

Date: 18/03/2010

# Chapter 1

## Introduction

This Thesis describes the use of supercritical flow reactors with heterogeneous catalysts (metal catalysts and enzymes). Supported homogeneous chiral Rh catalysts were used to investigate the enantioselective hydrogenation of dimethyl itaconate in a continuous flow scCO<sub>2</sub> system (Chapter 3 and Chapter 4). Immobilised lipase in the form of Cross-Linked Enzyme Aggregate (CLEA) was examined for the continuous kinetic resolution of α-tetralol in scCO<sub>2</sub> (Chapter 5), and for the continuous kinetic resolution of 1-phenylethanol in scCO<sub>2</sub> as a step of a catalytic cascade reaction (Chapter 6). Furthermore, CLEA of cholesterol oxidase and combi-CLEAs of cholesterol oxidase and catalase were investigated for the continuous oxidation of cholesterol in scCO<sub>2</sub> with ‘in-flow’ extraction of cholesterol (Chapter 7). The possible future directions are detailed in Chapter 8. The aim of this Chapter is to introduce the importance of Green Chemistry and Catalysis, followed by an outline of catalyst immobilisation techniques and the potentials of supercritical CO<sub>2</sub> (scCO<sub>2</sub>) and other alternative ‘green’ solvents.

### 1.1. Green Chemistry

Chemistry has greatly improved the quality of our life in the 20<sup>th</sup> century. Some of the first symptoms of the damage caused by the global development to be recognised are the climate change and depletion of the ozone layer.<sup>1-8</sup> New environmentally friendly, sustainable and also cost-effective products and processes are therefore required. Sustainable development will improve the quality of life, not just the rate of development.

Green chemistry is a comprehensive approach to the application of chemicals and their reactions, which aims to eliminate hazardous wastes and reduce pollution.<sup>9</sup> In 1998, the 12 principles of Green Chemistry were created which can serve as a rough guide for green chemical process design.<sup>9</sup> The 12 principles of Green Chemistry are the following.

- 1. Prevention:** It is better to prevent waste than to treat or clean up waste after it has been created.
- 2. Atom Efficiency:** Synthetic methods should be designed to maximise the incorporation of all materials used in the chemical process.
- 3. Less Hazardous Chemical Syntheses:** Wherever practicable, synthetic methodologies should be developed to use and generate substances that possess little or no toxicity to human health and the environment.
- 4. Designing Safer Chemicals:** Chemical products should be designed to preserve their efficacy of function while reducing toxicity.
- 5. Safer Solvents and Auxiliaries:** The use of auxiliary substances (e.g. solvents, separation agents, etc) should be made unnecessary wherever possible and, innocuous when used.
- 6. Design for Energy Efficiency:** Energy requirements should be recognised for their environmental and economic impacts and should be minimised. If possible, synthetic methods should be conducted at ambient temperature and pressure.
- 7. Use of Renewable Feedstocks:** A raw material or feedstock should be renewable rather than depleting wherever technically and economically practicable.
- 8. Minimise Derivatisation:** Unnecessary derivatisation (blocking group, protection/ deprotection, temporary modification of physical/ chemical processes) should be avoided whenever possible.
- 9. Catalysis:** Catalytic reagents (as selective as possible) are superior to stoichiometric reagents.
- 10. Design for Degradation:** Chemical products should be designed so that at the end of their function they do not persist in the environment and break down into innocuous degradation products.
- 11. Real-time Analysis:** Analytical methods should be developed to allow real-time *in situ* monitoring and control prior to the formation of hazardous substances.
- 12. Safer Chemical Processes for Accident Prevention:** Substances and the form of a substance used in a chemical process should be chosen so as to minimise the potential for chemical accidents, including releases, explosions and fires.

In this study, alternative solvents (Principle 5) and catalysis (Principle 9) were applied to design sustainable chemical processes. The environmental impact of chemical processes can be significantly reduced by the replacement of harmful solvents with more environmentally friendly/‘alternative’ solvents.<sup>10, 14</sup> A discussion of alternative solvents can be found below in this Chapter. The other approach was the application of catalysis in the production of chemicals, which can decrease the production of waste because catalytic reactions have high atom economy and catalysts can also be recycled.<sup>9, 10</sup>

It is important to quantify the sustainability and efficiency of chemical processes. As Lord Kelvin said “when you can measure what you are speaking about, and express it in numbers, you know something about it” (1883). One of the qualifying measures is the E-factor (amount of waste per kg of product) created by Roger Sheldon where waste is defined as everything produced in the process except the desired product.<sup>9-12</sup> The E-factors of various sectors of the chemical industry are available and shown in Table 1-1.

**Table 1-1. The E-factor for few segments of the chemical industry.<sup>11</sup>**

Industry sector	Product tonnage	kg waste/kg product
Oil refining	$10^6\text{--}10^8$	< 0.1
Bulk chemicals	$10^4\text{--}10^6$	< 1–5
Fine chemicals	$10^2\text{--}10^4$	5 → > 50
Pharmaceuticals	$10\text{--}10^3$	25 → > 100

The E-factor is a widely used parameter to report the waste emission rate of chemical processes. The E-factor is significantly larger for fine chemicals and pharmaceuticals probably due to the application of multi-step processes where many of these steps may use stoichiometric reagents rather than catalytic methods, and complex purification procedures, which can further increase the E-factor. Another measure, the environmental quotient (EQ) of individual chemical routes gives refined information about the environmental impact. The EQ is E-factor multiplied by an unfriendliness quotient (Q).<sup>13</sup> For example, NaCl could be assigned by a Q value of 1 and heavy metal salts by 100-1000, depending on their toxicity, ease of recycling, etc.

Waste production depends on the selectivity of each step of a synthetic process. By studying the overall stoichiometry of the reaction, the atom selectivity or atom utilisation can be measured. Using the atom utilisation of a reaction, the amount of waste generated can be quickly evaluated.<sup>14</sup>

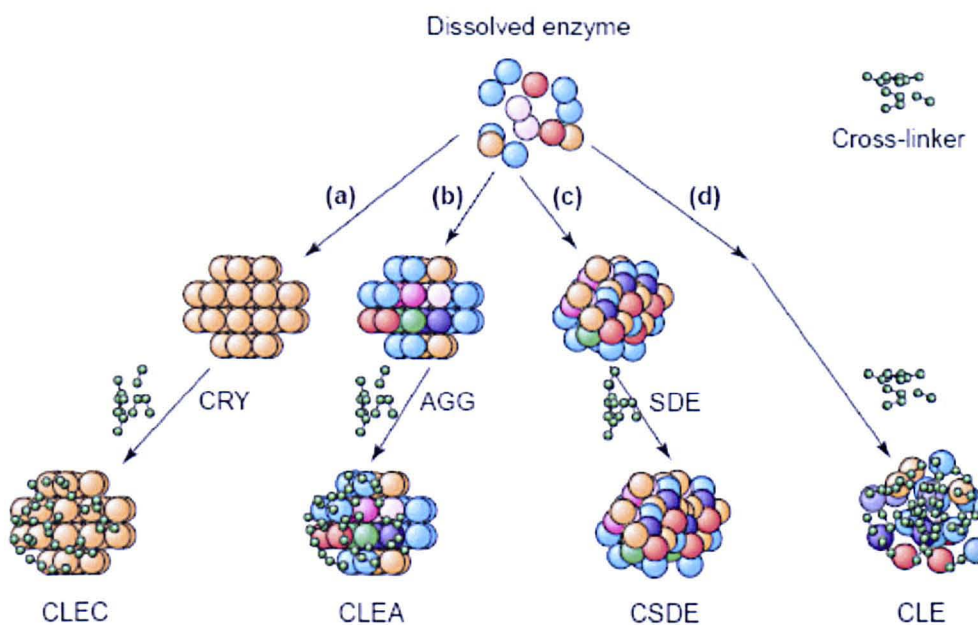
## 1.2. Catalyst Immobilisation

Catalysis is widely used in organic synthesis<sup>15, 16</sup> and can be performed under homogeneous or heterogeneous conditions. The heterogeneous system has several benefits over the homogeneous method. Heterogeneous catalysis facilitates the catalyst recovery and product separation which is complicated in a homogeneous system. The immobilisation of homogeneous catalysts may also improve the catalyst stability and performance.<sup>17-21</sup>

Immobilised catalysts can be discussed as carrier-bond and carrier-free.<sup>18</sup> Although the support material carries bulk matter into the system of carrier-bound enzymes, it can enhance the catalytic performance and stability.<sup>17-21</sup> Carrier-free immobilised catalysts can overcome the problem of the bulk matter by linking the catalyst particles to each other which is eliminating the need for support material.<sup>18</sup> In this case, the only inactive mass is that of the cross-linker that usually is negligible compared to the catalyst. Cross-Linked Enzymes (CLE), Cross-Linked Enzyme Crystals (CLEC), Cross-Linked Spray Dried Enzymes (CSDE) and Cross-Linked Enzyme Aggregates (CLEA) belong to the family of carrier-free immobilised enzymes.<sup>18</sup> They are discriminated from each other by the precursor that is cross-linked (Scheme 1-1). The advantages and disadvantages of carrier-free immobilised enzymes are summarised in Table 1-2.

**Table 1-2. The advantages and disadvantages of carrier-free immobilised enzymes.**

	Precursor	Advantages	Disadvantages
<b>CLE – Cross-Linked Enzyme</b>	Dissolved enzyme	Enhanced thermostability (that requires a delicate balance between the amount of cross linker, temperature, pH, ionic strength)	Low activity retain (usually below 50 % of the native enzyme) Poor reproducibility Low mechanical stability Difficulties in handling of gelatinous CLE and controlling geometric parameters
<b>CLEC – Cross-Linked Enzyme Crystal</b>	Crystalline enzyme	Relatively high retained activity (30 – 70 % of the native enzyme) <sup>23</sup> Enhanced thermostability and mechanical stability relative to CLE <sup>24</sup> Broad pH and temperature stability <sup>25, 26</sup> High stability against organic solvents <sup>26, 27</sup>	Need for high purity enzyme Need to crystallise the enzyme Crystal size is crucial for high activity <sup>26</sup> , therefore need for the optimisation of the crystal form
<b>CSDE – Cross-Linked Spray Dried Enzyme</b>	Spray dried enzyme	Powder – easy to handle CDSE is till to be exploited	Spray drying reversibly deactivates the enzyme Relatively low activity compared to CLE, CLEC, and CLEA <sup>28</sup>
<b>CLEA – Cross-Linked Enzyme Aggregates</b>	Physically aggregated enzyme	Simple preparation procedure Precursor is prepared by physical aggregation of the enzyme Precipitation also purifies the enzyme High thermostability, mechanical stability, and against organic solvents	The catalytic behaviour depends on the precipitant <sup>29</sup>

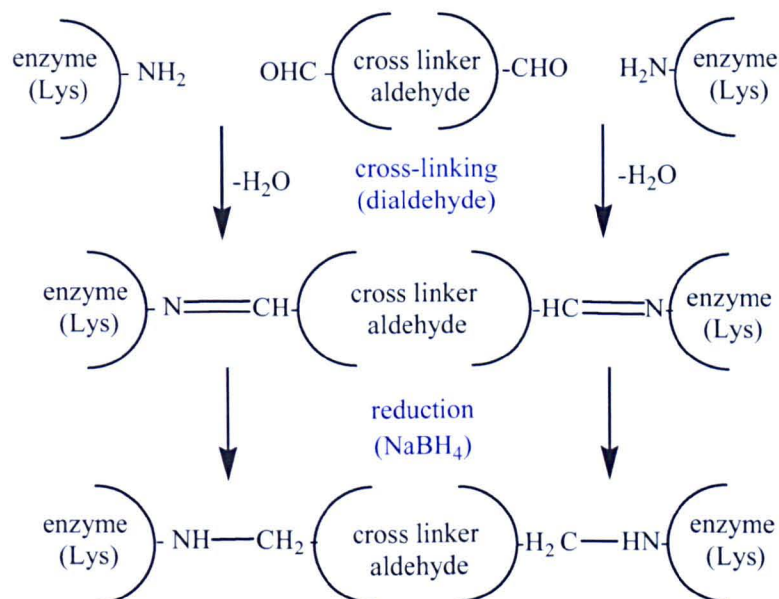


**Scheme 1-1. Carrier-free immobilised enzymes.<sup>18</sup>**

The Cross-Linked Enzyme Aggregate (CLEA) method is the most recently developed carrier-free immobilisation technique.<sup>29, 30</sup> A number of enzymes have already been immobilised successfully as CLEA<sup>10, 29, 31-41</sup> and there are few examples for combi-CLEA.<sup>10, 42-44</sup> The carrier-free nature, the high volumetric activity (U/g), the simple preparation, the high stability of the enzyme in the CLEA form, and the ease of recyclability make it widely attractive.<sup>21, 45</sup> A ‘spin-out’ company, CLEA Technologies<sup>46</sup> has been established by the developer, Professor Roger Sheldon where specific research on CLEA of various enzymes is being performed.

The CLEA is prepared by changing the proximity of the soluble enzyme particles to form aggregates: the addition of an appropriate aggregation agent changes the electrostatic properties of the solution and the enzyme particles associate and become insoluble. The aggregates of the native enzyme can be cross-linked using a bifunctional cross-linker (generally glutaraldehyde). The CLEAtion process consists of two steps, physical aggregation and cross-linking.<sup>30</sup> The most commonly used precipitants are iso-propanol, acetone, ethanol, tert-butanol, dimethoxyethane (ethyleneglycol dimethyl ether), acetonitrile (90 % v/v) and ammonium sulfate.<sup>30</sup> The second step of the process is the cross-linking of the solid particles which is performed with bifunctional linker molecules, usually dialdehydes. The most commonly used

linker is glutaraldehyde, however, other materials have also been used for example dextran polyaldehyde and polymeric dialdehydes.<sup>29, 47, 48</sup> The cross-linking requires amine groups of the lysine on the protein to be available to be linked to the aldehyde group of the cross-linker (Scheme 1-2). The success of the cross-linking depends on the number (and position) of available amine groups. The most reactive amine groups can be found on the lysine amino acid residue. If the cross-linker enters the active site of the enzyme and links to an amine group of a key amino acid, this particular enzyme unit will become inactive.



**Scheme 1-2. The cross-linking: reaction between an amino group of the lysine residue of the enzyme and an aldehyde group of the cross-linker.**

The work in this Thesis investigated the preparation of cholesterol oxidase CLEA and combi-CLEA of cholesterol oxidase and catalase. Cholesterol oxidase from *Nocardia sp.* and catalase from bovine liver were used for the studies. Both cholesterol oxidase from *Nocardia sp.* and catalase from bovine liver are cofactor dependent, FAD and NADPH, respectively, which are essential for their catalytic activity. The sequence and crystal structure of cholesterol oxidase from *Nocardia sp.* has not yet been published in the literature but cholesterol oxidase from *Streptomyces sp.* has been studied more extensively than cholesterol oxidase from *Nocardia sp.*, and more than 20 lysine residues were found in its structure.<sup>49</sup> (Detailed description of

cholesterol oxidases can be found in Chapter 7.) Cholesterol oxidase from *Nocardia sp.* is therefore assumed to contain a sufficient number of amine groups of lysine residue required for cross-linking. The second enzyme of the combi-CLEA was catalase from bovine liver that contains 108 lysines in its structure.<sup>50</sup> Due to the large number of lysine residues in the structure of both cholesterol oxidase from *Nocardia sp.* and catalase from bovine liver, they are both potentially good candidates for being immobilised by cross-linking.

Besides heterogenising homogeneous catalysts, the use of multiphase systems for catalytic reactions such as aqueous biphasic systems, fluorous biphasic systems, and a biphasic system ionic liquid/scCO<sub>2</sub> (where the homogeneous catalyst is immobilised in one of the phases) also offers promising opportunities. In principle, the catalyst is soluble only in one of the phases and the substrate/product in the other phase, which offers an easy separation of the catalyst and the product.<sup>10, 51-53</sup> A number of research groups has investigated this field as summarised in the reviews of Keim<sup>54</sup> and Tundo.<sup>55</sup>

### 1.3. Alternative Solvents

One of the main concerns in Green Chemistry is the replacement of 'traditional' solvents, chlorinated solvents and VOCs with environmentally benign (alternative) solvents.<sup>9, 10</sup> The application of alternative solvents in the manufacture of chemicals can reduce the environmental impact and can also provide benefits by their unique physical and chemical properties.<sup>56</sup> The ease of product and catalyst separation, and reduced waste disposal cost also create motivating aspects for their application.<sup>20, 51, 57-60</sup> Alternative solvents can be grouped as follows.

- i. Fluorinated solvents
- ii. Ionic liquids (detailed description in Chapter 4)
- iii. Supercritical fluids

Conducting reactions in a solventless environment<sup>52</sup> would be ideal in order to meet the conditions discussed previously but is not widely applicable because

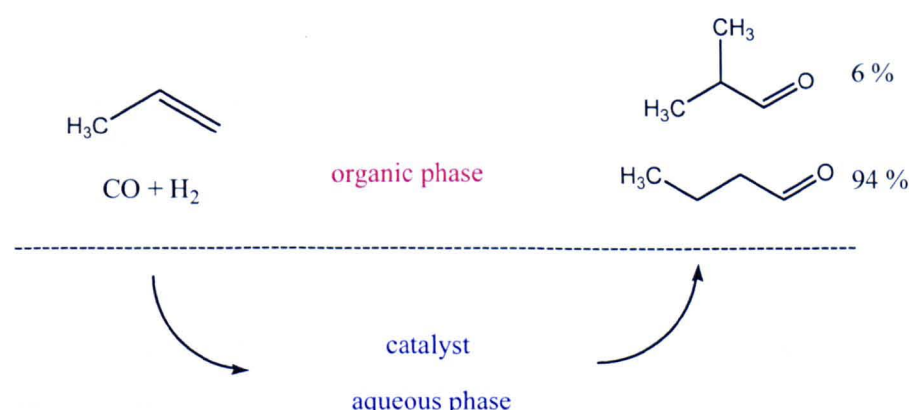
of the need to remove heat from the reaction, mix reagents, and transport reagents and products.

### 1.3.1. Water

Although water is not classed as an alternative solvent, it is discussed here because of its high environmentally benign nature. It is widely accepted that “the best solvent is no solvent” but when a solvent is required the second best is often water. Some of the advantages of water are the environmentally benign nature, non-toxicity and non-flammability. The disadvantages are the following

- Difficulty of recovering materials (product, catalyst) from water
- Purifying water before releasing it back to the ecosystem.

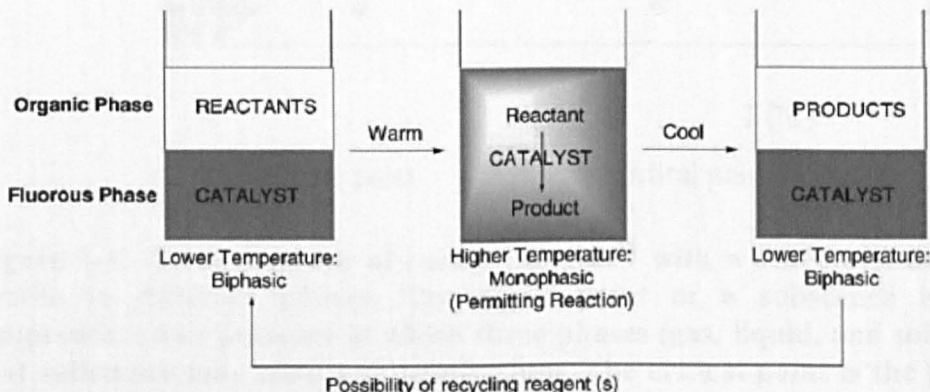
Reactions can be conducted in water or in aqueous biphasic system. There are several methods to make materials soluble/dispersible in water<sup>61</sup> for example use of surfactants, cosolvents, hydrophilic agents. In a liquid-liquid biphasic system where one of the immiscible phases is water, one of the phases dissolves the catalyst and the other one contains the substrate(s) and product(s), which therefore allows simple product separation and catalyst recovery. An example of large scale application of an aqueous biphasic system is the Ruhrchemie/Rhone-Poulenc process for the hydroformylation of propylene to n-butanal (Scheme 1-3).<sup>62, 63</sup>



**Scheme 1-3. The hydroformylation of propylene to n-butanal performed in aqueous biphasic system, the Ruhrchemie/Rhone-Poulenc process.<sup>62, 63</sup>**

### 1.3.2. Fluorinated Solvents

Fluorinated solvents are materials where the majority of C-H bonds have been replaced by C-F bonds. Fluorinated solvents can be used as reaction medium when an undesired reaction occurs in water and are usually used in a biphasic system. A fluorous biphasic system consist of a fluorous phase with the fluorous soluble reactants and catalyst, and a second organic or inorganic phase that has limited solubility with the fluorous phase.<sup>64</sup> The catalyst can be dissolved in a fluorinated solvent by linking fluorocarbon substituents to it.<sup>64</sup> Certain solvents can turn to a single phase by heating in a fluorous biphasic system<sup>65</sup>, for example *n*-hexane, toluene, or c-C<sub>6</sub>F<sub>11</sub>CF<sub>3</sub> at 36.5 °C, which can therefore combine the advantage of conducting the reaction in single phase at higher temperature and retaining the ease of separation by phase separation at lower temperature. The schematic of a fluorous biphasic catalytic system is shown in Scheme 1-4.



**Scheme 1-4. Fluorous biphasic catalysis.**<sup>66</sup> The reaction can be performed in single phase at higher temperature and the separation in a biphasic system at lower temperature in a system that becomes a single phase by increased temperature.

A disadvantage of fluorous biphasic catalysis is the high price of the fluorinated ligands and solvents and the environmental impact of these materials is also of concern.<sup>67</sup> A review from 2007 summarises the result obtained in the field to that date.<sup>52</sup>

## 1.4. Supercritical Fluids (SCFs)

Supercritical fluids (SCFs) are materials in a particular state above their critical pressure ( $p_c$ ) and critical temperature ( $T_c$ ) but below the pressure required to form a solid.<sup>68</sup> The pressure required to solidify for example carbon dioxide is, however, very high, 5700 bar at the critical temperature (31.1 °C).<sup>69</sup> A phase diagram with schematic density profile of the different phases can be seen in Figure 1-1.

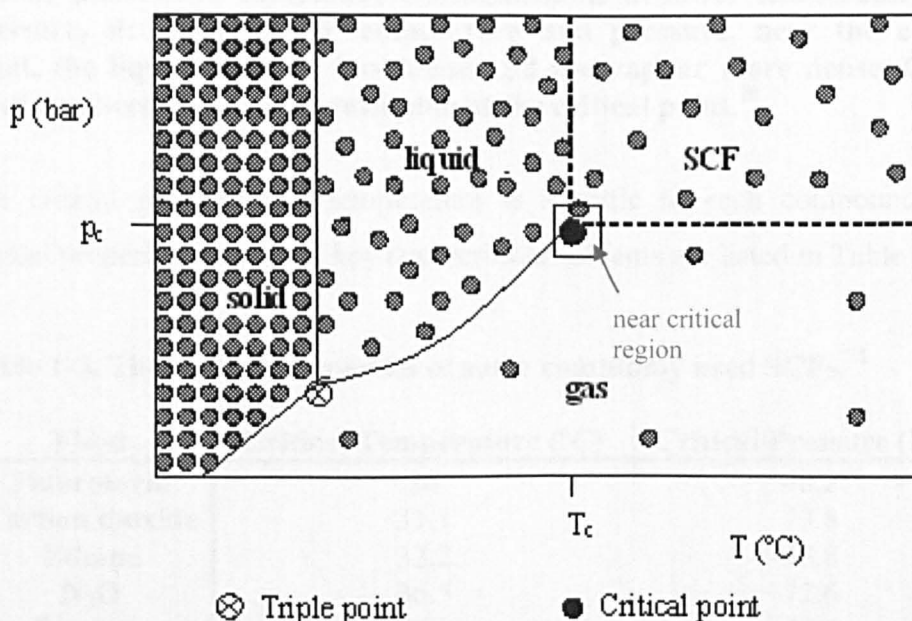


**Figure 1-1.** Phase diagram of carbon dioxide<sup>68</sup> with a schematic density profile in different phases. The triple point of a substance is the temperature and pressure at which three phases (gas, liquid, and solid) of that substance may coexist in equilibrium. The critical point is the phase termination point where the phases become indistinguishable.

Near to the critical point the gas becomes more dense and the liquid becomes less dense, and at the critical point the meniscus turns to indistinguishable between the two phases. The phase change to supercritical is demonstrated in Figure 1-2.

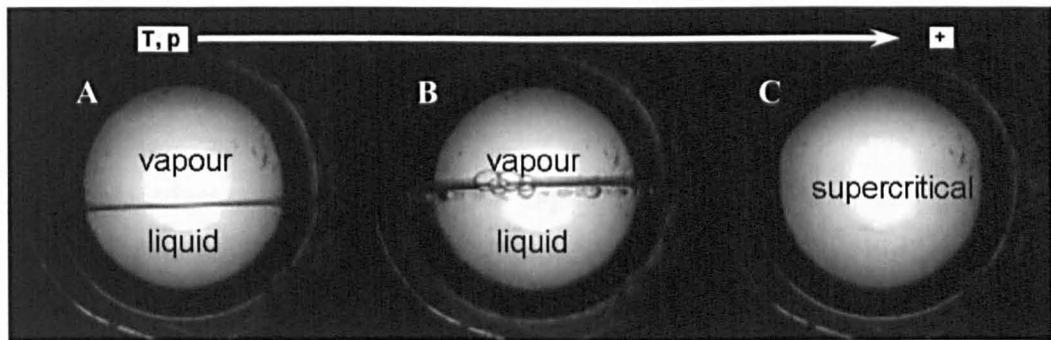


**Figure 1-2.** Phase change of a substance. A: Two phases, the liquid and the vapour phases are completely distinguishable at lower temperature and pressure, B: at increased temperature and pressure, near the critical point, the liquid becomes less dense and the vapour more dense, C: the meniscus becomes indistinguishable at the critical point.<sup>70</sup>

The critical pressure and temperature is specific to each compound. The critical properties of several key supercritical solvents are listed in Table 1-3.

**Table 1-3. The critical properties of some commonly used SCFs.<sup>71</sup>**

Fluid	Critical Temperature (°C)	Critical Pressure (bar)
Fluoroform	26	48.2
Carbon dioxide	31.1	73.8
Ethane	32.2	48.8
N <sub>2</sub> O	36.5	72.6
Propane	96.8	42.6
NH <sub>3</sub>	132.5	112.8
EtOH	243	63.8
Water	374	221

Many of the properties of SCFs are intermediate between liquid and gas, for instance the density, diffusivity, and viscosity, but not all properties of SCFs are intermediate, for instance compressibility and heat capacity. These are much higher in the near critical region and even in the supercritical phase than those in either liquid or in gas phase.<sup>68</sup> The density of supercritical fluids changes with applied pressure, particularly sharply in the compressible region (near critical point).<sup>68</sup> The dielectric constants ( $\epsilon$ ) of polar SCFs also change sharply with pressure in the near critical region, an effect connected with changes in density.<sup>68</sup> The effect is large in water<sup>72, 73</sup> and fluoroform<sup>74</sup> but the dielectric constant of CO<sub>2</sub> does not change much with pressure<sup>75</sup>. The

dielectric constant is a tuneable property of polar SCFs which can be utilised when working with SCFs but there are still gaps in the knowledge of this field.

The main advantage of SCFs is their liquid like solvent power and gas like diffusivity. Other important advantageous properties of SCFs are that many of them have no harmful environmental effect, they are non-toxic and non-flammable, they have high diffusivity, low viscosity, adjustable solvent power and density, and they are miscible with gases.<sup>68</sup>

#### **1.4.1. Supercritical Carbon Dioxide (scCO<sub>2</sub>)**

Carbon dioxide (CO<sub>2</sub>) is the most commonly used SCF because of its availability, low cost and properties. CO<sub>2</sub> is a greenhouse gas but if the by-product CO<sub>2</sub> from different industries is utilised for the production of chemicals, there will be no net increase in CO<sub>2</sub>. It can be recovered from ammonia and hydrogen production, and also from flue gases.<sup>76-78</sup>

The easily attainable critical parameters of CO<sub>2</sub>; temperature of 31.1 °C and pressure of 73.8 bar are mild in comparison with other SCFs (Table 1-3). Using supercritical CO<sub>2</sub> for conducting chemical transformations eliminates the production of solvent waste from the reaction medium. Many of the fluid properties of CO<sub>2</sub>, such as diffusion rate, viscosity, solvent power, and density are adjustable by changing the pressure and temperature which also makes scCO<sub>2</sub> widely attractive. The properties such as high diffusivity, complete miscibility with gases, high compressibility, no solvent residue production can also be highly beneficial. CO<sub>2</sub> is widely used in extraction processes. It is also used to conduct chemical transformations, including continuous flow processes when combined with a heterogeneous catalyst, and in multiphase catalysis.

#### **1.4.2. Reactions in Supercritical Carbon Dioxide**

Reactions with gaseous reactants in scCO<sub>2</sub> can occur at higher rates due to the complete miscibility of scCO<sub>2</sub> with gases such as H<sub>2</sub> and O<sub>2</sub>. This miscibility reduces the mass transport limitations that can occur at the catalyst surface with traditional solvent systems.<sup>79, 80</sup> Supercritical flow reactors are suitable for performing high pressure reactions. Effective gas mixing occurs with the lab scale dosing equipment used within the group at Nottingham.

## 1.5. Aims and Objectives

The areas of catalysis and use of alternative solvents are important topics within the field of Green Chemistry. The objective of this Thesis was to investigate continuous flow reactions with heterogeneous catalysts in scCO<sub>2</sub> in the following areas:

- Continuous asymmetric hydrogenation with supported homogeneous Rh catalysts modified with bisphosphine ligands in scCO<sub>2</sub>.
- Continuous kinetic resolution of secondary alcohols with immobilised Cal B in scCO<sub>2</sub>.
- Chemo-enzymatic catalytic cascade reaction in a continuous flow scCO<sub>2</sub> system.
- Continuous oxidation of cholesterol with combi-CLEA of cholesterol oxidase and catalase in scCO<sub>2</sub>.

The final aim was to draw conclusions on the compatibility of immobilised catalysts for continuous reactions in scCO<sub>2</sub>.

## References

1. Crowley, T. J., Causes of climate change over the past 1000 years. *Nature* **2000**, 289, 270-277.
2. Shindell, D. T., Rind, D., Lonergan, P., Increased polar stratospheric ozone losses and delayed eventual recovery owing to increasing greenhouse-gas concentrations. *Nature* **1998**, 392, 589-592.
3. Wigley, T. M. J., Raper, S.C.B., Implications for climate and sea level of revised IPCC emissions scenarios. *Nature* **1992**, 357, 293-300.
4. Solomon, S., Progress towards a quantitative understanding of Antarctic ozone depletion. *Nature* **1990**, 347, 347-354.
5. Walther, G. R., Ecological responses to recent climate change. *Nature* **2002**, 416, 389-395.
6. Fenger, J., Air pollution in the last 50 years – From local to global. *Atmospheric Environment* **2009**, 43, 13-22.
7. Gaffney, J. S., Marley, N.A., The impacts of combustion emissions on air quality and climate - From coal to biofuels and beyond. *Atmospheric Environment* **2009**, 43, 23-26.
8. Jacob, D. J., Winner, D.A., Effect of climate change on air quality. *Atmospheric Environment* **2009**, 43, 51-63.
9. Anastas, P. T., Warner, J.C., in *Green Chemistry: Theory and practice*. Oxford University Press, Oxford 1998.
10. Sheldon, R. A., Arends, I., Hanefeld, U., in *Green Chemistry and Catalysis*. Wiley-VCH, Weinheim 2007.

11. Sheldon, R. A., Atom efficiency and catalysis in organic synthesis. *Pure Applied chemistry* **2000**, 72, 1233-1246.
12. Sheldon, R. A., E factors, green chemistry and catalysis: an odyssey. *Chemical Communications* **2008**, 3352-3365.
13. Sheldon, R. A., Consider the environmental quotient. *Chemtech* **1994**, 38-47.
14. Clark, J., Macquarrie, D., in *Handbook of Green Chemistry and Technology*. Blackwell Publishing, Oxford **2002**.
15. Oakes, R. S., Clifford, A. A., Rayner, C. M., The use of supercritical fluids in synthetic organic chemistry. *Journal of the Chemical Society-Perkin Transactions* **2001**, 1, 917-941.
16. Blaser, H. U., Malan, C., Pugin, B., Spiendler, F., Steiner, H., Struder, M., Selective hydrogenation for fine chemicals: Recent trends and new developments. *Advanced Synthesis & Catalysis* **2003**, 345, 103-151.
17. Sevella, B., Biomérnöki műveletek és folyamatok (Biotechnology). *Műegyetemi Kiadó, Budapest (Hungary)* **1992**.
18. Cao, L., van Langen, L.M., Sheldon, R.A., Immobilised enzymes: carrier-bound or carrier-free? *Current Opinion in Biotechnology* **2003**, 14, 387-394.
19. Clark, D. S., Can immobilisation be exploited to modify enzyme activity. *Trends in Biotechnology* **1994**, 12, 439-444.
20. De Vos, D. E., Vankelecom, I.F.J., Jacobs, P.A., in Chiral catalyst immobilisation and recycling. Wiley-VCH **1998**.
21. Sheldon, R. A., Enzyme Immobilization: The Quest for Optimum Performance. *Advanced Synthesis & Catalysis* **2007**, 349, 1289-1307.
22. Messing, R. A., Immobilized Enzymes for Industrial Reactors. London: Academic Press **1975**.
23. Quiocho, F. A., Richards, F.M., Intermolecular cross-linking of a protein in the crystalline state: carboxypeptidase A. *Proceedings of the National Academy of Sciences USA* **1964**, 52, 833-839.
24. Quiocho, F. A., Richards, F.M., The enzyme behaviors of carboxypeptidase-A in the solid state. *Biochemistry* **1966**, 5, 4062-4076.
25. Tuchsen, E., Ottesen, M., Kinetic properties of subtilisin type Carlsberg in the crystalline state. *Carlsberg Research Communications* **1977**, 42, 407-420.
26. St Clair, N. L., Navia, M.A., Cross-linked enzyme crystals as robust biocatalysts. *Journal of the American Chemical Society* **1992**, 114, 7314-7316.
27. Lee, K. M., Blaghen, M., Samama, J.P., Biellmann, J.F., Cross-linked crystalline horse liver alcohol dehydrogenase as a redox catalyst: activity and stability towards organic solvent. *Bioorganic Chemistry* **1986**, 14, 202-210.
28. Cao, L., van Langen, L.M., Janssen, M.H.A., Sheldon, R.A., Preparation and properties of cross-linked aggregates of penicillin acylase and other enzymes. *European Patent Applications, EP1088887A1* **1999**.
29. Cao, L., van Rantwijk, F., Sheldon, R.A., Cross-linked enzyme aggregates: A simple and effective method for the immobilization of penicillin acylase. *Organic Letters* **2000**, 1, 1361-1364.
30. Schoevaart, R., Wolbers, M.W., Golubovic, M., Ottens, M., Kieboom, A.P.G., van Rantwijk, F., van der Wielen, L.A.M., Sheldon, R.A.,

- Preparation, optimization, and structures of cross-linked enzyme aggregates (CLEAs). *Biotechnology and Bioengineering* 2004, 87, (6), 754-762.
31. Lopez-Serrano, P., Cao, L., van Rantwijk, F., Sheldon, R.A., Cross-linked enzyme aggregates with enhanced activity: application to lipases. *Biotechnology Letters* 2002, 24, 1379-1383.
  32. Wilson, L., Betancor, L., Fernandez-Lorente, G., Fuentes, M., Hidalgo, A., Guisan, J.M., Pessela, B.C.C., Fernandez-Lafuente, R., Cross-linked aggregates of multimeric enzymes: A simple and efficient methodology to stabilize their quaternary structure. *Biomacromolecules* 2004, 5, 814-817.
  33. Bode, M. L., van Rantwijk, F., Sheldon, R.A., Crude Aminoacylase From Aspergillus sp. is a Mixture of Hydrolases. *Biotechnology and Bioengineering* 2003, 84, 710-713.
  34. Aytar, B. S., Bakir, U., Preparation of cross-linked tyrosinase aggregates. *Process Biochemistry* 2008, 43, 125-131.
  35. Kaul, P., Stoltz, A., Banerjeea, U.C., Cross-Linked Amorphous Nitrilase Aggregates for Enantioselective Nitrile Hydrolysis. *Advanced Synthesis & Catalysis* 2007, 349, 2167-2176.
  36. van Pelt, S., Quignard, S., Kubac, D., Sorokin, D.Y., van Rantwijk, F., Sheldon, R.A., Nitrile hydratase CLEAs: The immobilization and stabilization of an industrially important enzyme. *Green Chemistry* 2008, 10, 395-400.
  37. Cabana, H., Jones, J.P., Agathos, S.N., Preparation and characterization of cross-linked laccase aggregates and their application to the elimination of endocrine disrupting chemicals. *Journal of Biotechnology* 2007, 132, 23-31.
  38. van Langen, L. M., Selassa, R.P., van Rantwijk, F., Sheldon, R.A., Cross-Linked Aggregates of (R)-Oxynitrilase: A Stable, Recyclable Biocatalyst for Enantioselective Hydrocyanation. *Organic Letters* 2005, 7, 327-329.
  39. Chmura, A., van der Kraan, G.M., Kielar, F., van Langen, L.M., van Rantwijk, F., Sheldon, R.A., Cross-Linked Aggregates of the Hydroxynitrile Lyase from Manihot esculenta: Highly Active and Robust Biocatalysts. *Advanced Synthesis & Catalysis* 2006, 348, 1655-1661.
  40. Gaur, R., Pant, H., Jain, R., Khare, S.K., Galacto-oligosaccharide synthesis by immobilized Aspergillus oryzae b-galactosidase. *Food Chemistry* 2006, 97, 426-430.
  41. Sheldon, R. A., Schoevaart, R., van Langen, L.M., Cross-linked enzyme aggregates (CLEAs): A novel and versatile method for enzyme immobilization (a review). *Biocatalysis and Biotransformation* 2005, 23, 141-147.
  42. Dalal, S., Kapoor, M., Gupta, M.N., Preparation and characterization of combi-CLEAs catalyzing multiple non-cascade reactions. *Journal of Molecular Catalysis B: Enzymatic* 2007, 44, 128-132.
  43. Mateo, C., Chmura, A., Rustler, S., van Rantwijk, F., Stoltz, A., Sheldon, R.A., Synthesis of enantiomerically pure (S)-mandelic acid using an oxynitrilase-nitrilase bienzymatic cascade: a nitrilase surprisingly shows nitrile hydratase activity. *Tetrahedron: Asymmetry* 2006, 17, 320-323.
  44. Vafiadi, C., Topakas, E., Christakopoulos, P., Preparation of multipurpose cross-linked enzyme aggregates and their application to production of alkyl ferulates. *Journal of Molecular Catalysis B: Enzymatic* 2008, 54, 35-41.

45. Cao, L., van Langen, L.M., van Rantwijk, F., Sheldon, R.A., Cross-linked aggregates of penicillin acylase: robust catalysts for the synthesis of b-lactam antibiotics. *Journal of Molecular Catalysis A: Enzymatic* **2001**, 11, 665-670.
46. [www.cleatechnologies.com](http://www.cleatechnologies.com), accessed April/2009.
47. Schoevaart, R., Siebum, A., Sheldon, R.A., Kieboom, T., Glutaraldehyde cross-link analogues from carbohydrates. *Starch* **2005**, 57, 161-165.
48. Sorgedrager, M., PhD Thesis. *Delft University of Technology, Delft (Netherlands)* **2005**.
49. Yue, Q. K., Kass, I.J., Sampson, N.S., Vrielink, A., Crystal Structure Determination of Cholesterol Oxidase from Streptomyces and Structural Characterization of Key Active Site Mutants. *Biochemistry* **1999**, 38, 4277-4286.
50. Fita, I., Rossmann, M.G., The NADPH binding site on beef liver catalase. *Proceedings of the National Academy of Sciences USA* **1985**, 82, 1604-1608.
51. Mikami, K., in Green reaction media in organic synthesis. *Blackwell Publishing, Oxford* **2005**.
52. Hobbs, H. R., Thomas, N.R., Biocatalysis in supercritical fluids, in fluorous solvents, and under solvent-free conditions. *Chemical Reviews* **2007**, 107, 2786-2820.
53. van Rantwijk, F., Sheldon, R.A., Biocatalysis in Ionic Liquids. *Chemical Reviews* **2007**, 107, 2757-2785.
54. Keim, W., Multiphase catalysis and its potential in catalytic processes: the story of biphasic homogenous catalysis. *Green Chemistry* **2003**, 5, 105-111.
55. Tundo, P., Perosa, A., Multiphasic heterogeneous catalysis mediated by catalyst-philic liquid phases. *Chemical Society Reviews* **2007**, 36, 532-550.
56. Liu, Q. B., Janssen, M.H.A., van Rantwijk, F., Sheldon, R.A., Room-temperature ionic liquids that dissolve carbohydrates in high concentrations. *Green Chemistry* **2005**, 7, 39-42.
57. Brown, R. A., Pollet, P., McKoon, E., Eckhert, C.A., Liotta, C.L., Jessop, P.G., Asymmetric hydrogenation and catalyst recycling using ionic liquid and supercritical carbon dioxide. *Journal of the American Chemical Society* **2001**, 123, 1254-1255.
58. Liu, F., Abrams, M.B., Baker, R.T., Tumas, W., Phase-separable catalysis using room temperature ionic liquids and supercritical carbon dioxide. *Chemical Communications* **2001**, 433-434.
59. Sellin, M. F., Webb, P.B., Cole-Hamilton, D.J., Continuous flow homogeneous catalysis: hydroformylation of alkenes in supercritical fluid-ionic liquid biphasic mixtures. *Chemical Communications* **2001**, 781-782.
60. Bösmann, A., Francio, G., Janssen, E., Solinas, N., Leitner, W., Wasserscheid, P., Activation, Tuning, and Immobilization of Homogeneous Catalysts in an Ionic Liquid/Compressed CO<sub>2</sub> Continuous-Flow System. *Angewandte Chemie International Edition* **2001**, 40, 2697-2699.
61. Lindstrom, U. M., Stereoselective Organic Reactions in Water. *Chemical Reviews* **2002**, 102, 2751-2772.
62. Cornils, B., Wiebus, E., Virtually no environmental impact: The biphasic oxo process. *Recl. Trav. Chim. Pays-Bas* **1996**, 115, 211-215.

63. Kohlpaintner, C. W., Fischer, R. W., Cornils, B., Aqueous biphasic catalysis: Ruhrchemie/Rhone-Poulenc oxo process. *Applied Catalysis A: General* **2001**, 219-225.
64. Leitner, W., ed. Cornils, B., Herrmann, W.A., Horvath, I.T., Leitner, W., Mecking, S., Olivier-Bourbigou H., Vogt, D., in Multiphase Homogeneous Catalysis. *Wiley-VCH, Weinheim* **2005**, 605-750.
65. Munson, M. S. B., Solution of fluorocarbons + hydrocarbons. *Journal of Physical Chemistry* **1964**, 68, 796-&.
66. Dobbsa, A. P., Kimberley, M.R., Fluorous phase chemistry: a new industrial technology. *Journal of Fluorine Chemistry* **2002**, 118, 3-17.
67. Hua, Y., Birdsall D.J., Stuart A.M., Hope E.J., Xiao, J., Ruthenium-catalysed asymmetric hydrogenation with fluoroalkylated BINAP ligands in supercritical CO<sub>2</sub>. *Journal of Molecular Catalysis A: Chemical* **2004**, 219, 57-60.
68. Jessop, P., Leitner, W., in Chemical synthesis using supercritical fluids. *Wiley-VCH, Weinheim* **1999**.
69. Bridgeman, P. W., Change of Phase under Pressure. I. The Phase Diagram of Eleven Substances with Especial Reference to The Melting Curve. *Physical Reviews* **1914**, 3, 126-141, 153-203.
70. Hobbs, H. R., PhD Thesis. *University of Nottingham, Nottingham (UK) 2006*.
71. Weast, R. C., in Handbook of Chemistry and Physics, 53rd Edition. *The Chemical Rubber Co., Cleveland (USA) 1972-1973*.
72. Fernandez, D. P., Mulev, Y., Goodwin, A.R.H., Levelt Sengers, J.M.H., A database for the static dielectric-constant of water and steam. *Journal of Physical Chemistry* **1995**, 24, 33-69.
73. Uematsu, M., Franck, E.U., Static dielectric constant of water and steam. *Journal of Physical Chemistry* **1980**, 9, 1291-1306.
74. Downing, R. C., in Fluorocarbon refrigerants handbook. *Prentice-Hall, Englewood Cliffs, New York 1988*.
75. Kita, T., Uosaki, Y., Moriyoshi, T., in High pressure liquids and solutions. *Elsevier 1994*, 181-198.
76. Kroschwitz, J. I., Howe-Grant, M., in Encyclopedia of Chemical Technology, 4th Edition. *Wiley Interscience, New York 2005*, 5, 35-53.
77. Chapel, D. G., Mariz, C.L., Ernest, J., Recovery of CO<sub>2</sub> from Flue Gases: Commercial Trends. **1999**.
78. Granite, E. J., O'Brien, T., Review of novel methods for carbon dioxide separation from flue and fuel gases. *Fuel Processing Technology* **2005**, 86, 1423-1434.
79. Jessop, P. G., Subramaniam, B., Gas-expanded liquids. *Chemical Reviews* **2007**, 2666-2694.
80. van den Hark, S. H., M., Hydrogenation of oleochemicals at supercritical single-phase conditions: influence of hydrogen and substrate concentrations on the process. *Applied Catalysis A: General* **2001**, 210, 207-215.

## Chapter 2

### Experimental

This Chapter describes:

- i) The immobilisation techniques used for preparing supported homogeneous metal- and biocatalysts.
- ii) The enzyme assays used for determining the activity of immobilised biocatalysts.
- iii) The high pressure equipments used for examining the activity of supported catalysts in scCO<sub>2</sub>.
- iv) The analytical techniques used throughout this study.

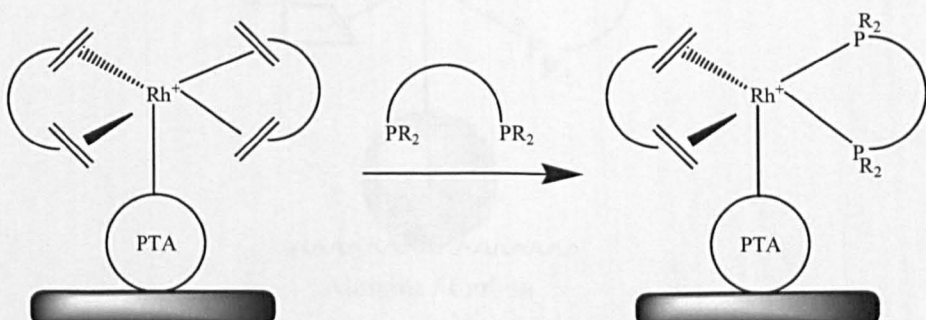
The immobilisation techniques used in this work include carrier-bound and carrier-free techniques. The metal catalysts, Rh and Pd were supported on different carrier materials while the enzymes, lipase B from *Candida antarctica*, cholesterol oxidase from *Nocardia sp.* and catalase from bovine liver were supported in a carrier-free form (Cross-Linked Enzyme Aggregate, CLEA). The Rh catalysts were further modified by the addition of a bisphosphine ligand. The aim of the study was the investigation of the activity of heterogeneous catalysts in a continuous flow scCO<sub>2</sub> system. The catalyst activity was also examined in a batch scCO<sub>2</sub> system in some cases. All scCO<sub>2</sub> systems used in this study were small scale due to the high cost of the catalysts. The scale-up of the system is possible but optimisation has to be performed.

#### 2.1. Catalyst Immobilisation

This section describes the immobilisation techniques used throughout this research project. Rh catalysts and enzymes were immobilised in different ways on a carrier material or *via* cross-linking in a carrier-free form. The Rh catalysts were also modified by the addition of a bisphosphine ligand either before or after the immobilisation of the catalyst.

### 2.1.1. The Preparation of Alumina or Carbon Supported Chiral Rh Catalysts

Chiral Rh catalysts supported on a solid support (alumina or carbon),  $[\text{Rh}(\text{COD})(\text{R}_2\text{P}^*\text{-PR}_2^*)]^+[\text{BF}_4]^-/\text{PTA}/\text{Alumina}$  or  $\text{Carbon}$  ( $\text{COD} = 1,5\text{-cyclo-octadiene}$ ,  $\text{R}_2\text{P}^*\text{-P}^*\text{R}_2 = \text{bisphosphine ligand}$ ,  $\text{PTA} = \text{phosphotungstic acid H}_3\text{O}_{40}\text{PW}_{12}$ ), a gift from Johnson Matthey (UK), were used to perform asymmetric hydrogenation in a continuous flow scCO<sub>2</sub> system. The chiral modification of the commercial alumina or carbon supported Rh catalyst was performed by us. The bisphosphine ligand ( $\text{R}_2\text{P}^*\text{-PR}_2^*$ ) (Josiphos type ligands, Solvias AG, Basel, Switzerland) was added after the immobilisation of the achiral catalyst. The ligand exchange reaction occurred between one of the COD ligands of  $\text{Rh}(\text{COD})_2$  ( $\text{COD} = 1,5\text{-cyclo-octadiene}$ ) and the bisphosphine ligand (Scheme 2-1). Calculations to determine the appropriate amount of  $[\text{Rh}(\text{COD})_2]^+[\text{BF}_4]^-/\text{PTA}/\text{Alumina}$  (CATAXA/Alumina) or  $[\text{Rh}(\text{COD})_2]^+[\text{BF}_4]^-/\text{PTA}/\text{Carbon}$  (CATAXA/Carbon) and ligand were based upon the Rh content (determined by Johnson Matthey), 35  $\mu\text{mol}$  of Rh in each gram of CATAXA/Alumina and less than 0.5 % of Rh in each gram of CATAXA/Carbon. A 1:1.5 molar ratio of Rh to ligand was used in each case, which is expected to provide a sufficient excess for the ligand exchange to be completed. Due to the air and moisture sensitivity of the Rh catalysts and the ligands, all preparation procedures were performed under an argon or nitrogen atmosphere in dry solvents.



Scheme 2-1. The ligand exchange reaction. The chiral catalyst is  $[\text{Rh}(\text{COD})(\text{R}_2\text{P}^*\text{-PR}_2^*)]^+[\text{BF}_4]^-/\text{PTA}/\text{Alumina}$  ( $\text{COD} = 1,5\text{-cyclo-octadiene}$ ,  $\text{R}_2\text{P}^*\text{-P}^*\text{R}_2 = \text{bisphosphine ligand}$ ,  $\text{PTA} = \text{phosphotungstic acid H}_3\text{O}_{40}\text{PW}_{12}$ ).

### 2.1.1.1. Preparation of $[\text{Rh}(\text{COD})(\text{ligand})]^+[\text{BF}_4]^-/\text{PTA}/\text{Alumina}$

The experiments were performed in a two-neck glass flask (oven dried, volume: 100 mL). The  $[\text{Rh}(\text{COD})_2]^+[\text{BF}_4]^-/\text{PTA}/\text{Alumina}$  catalyst ( $9.19 \times 10^{-6}$  mol Rh) and ligand ( $1.38 \times 10^{-5}$  mol) were mixed in anhydrous ethanol (99.8 %, Aldrich, 50 mL) using a suspended stirrer (Lab egg, IKA, Germany) overnight (16 hours) at ambient pressure and room temperature under an argon atmosphere. The following quantities of the Rh catalyst and ligand were used for preparing the supported homogeneous chiral catalysts.

- Josiphos 001 (0.0088g) :  $\text{Rh}[(\text{COD})_2]^+[\text{BF}_4]^-/\text{PTA}/\text{Alumina}$  (0.26 g)
- Josiphos 005 (0.009 g) :  $\text{Rh}[(\text{COD})_2]^+[\text{BF}_4]^-/\text{PTA}/\text{Alumina}$  (0.26 g)
- Walphos 002 (0.009 g) :  $\text{Rh}[(\text{COD})_2]^+[\text{BF}_4]^-/\text{PTA}/\text{Alumina}$  (0.26 g)
- Mandyphos 001 (0.0113 g) :  $\text{Rh}[(\text{COD})_2]^+[\text{BF}_4]^-/\text{PTA}/\text{Alumina}$  (0.26 g)
- Taniaphos 001 (0.0095 g) :  $\text{Rh}[(\text{COD})_2]^+[\text{BF}_4]^-/\text{PTA}/\text{Alumina}$  (0.26 g)
- Taniaphos 002(0.0098 g) :  $\text{Rh}[(\text{COD})_2]^+[\text{BF}_4]^-/\text{PTA}/\text{Alumina}$  (0.26 g)

The next morning, the solvent was removed and the catalyst was dried under vacuum (for approximately 15 minutes). The catalyst was then stored under an argon atmosphere until use. The structure of the Rh catalyst and the ligands are shown in Figure 2-1 and Figure 2-2, respectively.

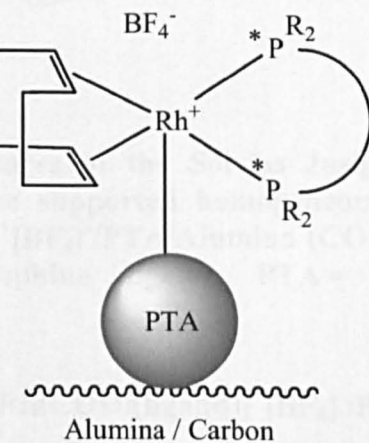


**Figure 2-1. General structure of the supported homogeneous Rh catalyst  $[\text{Rh}(\text{COD})(\text{R}_2\text{P}^*-\text{PR}_2^*)]^+[\text{BF}_4]^-/\text{PTA}/\text{Alumina}$  or Carbon where COD = 1,5-cyclo-octadiene,  $\text{R}_2\text{P}^*-\text{PR}_2^*$  = bisphosphine ligand, PTA = phosphotungstic acid  $\text{H}_3\text{O}_{40}\text{PW}_{12}$ .**

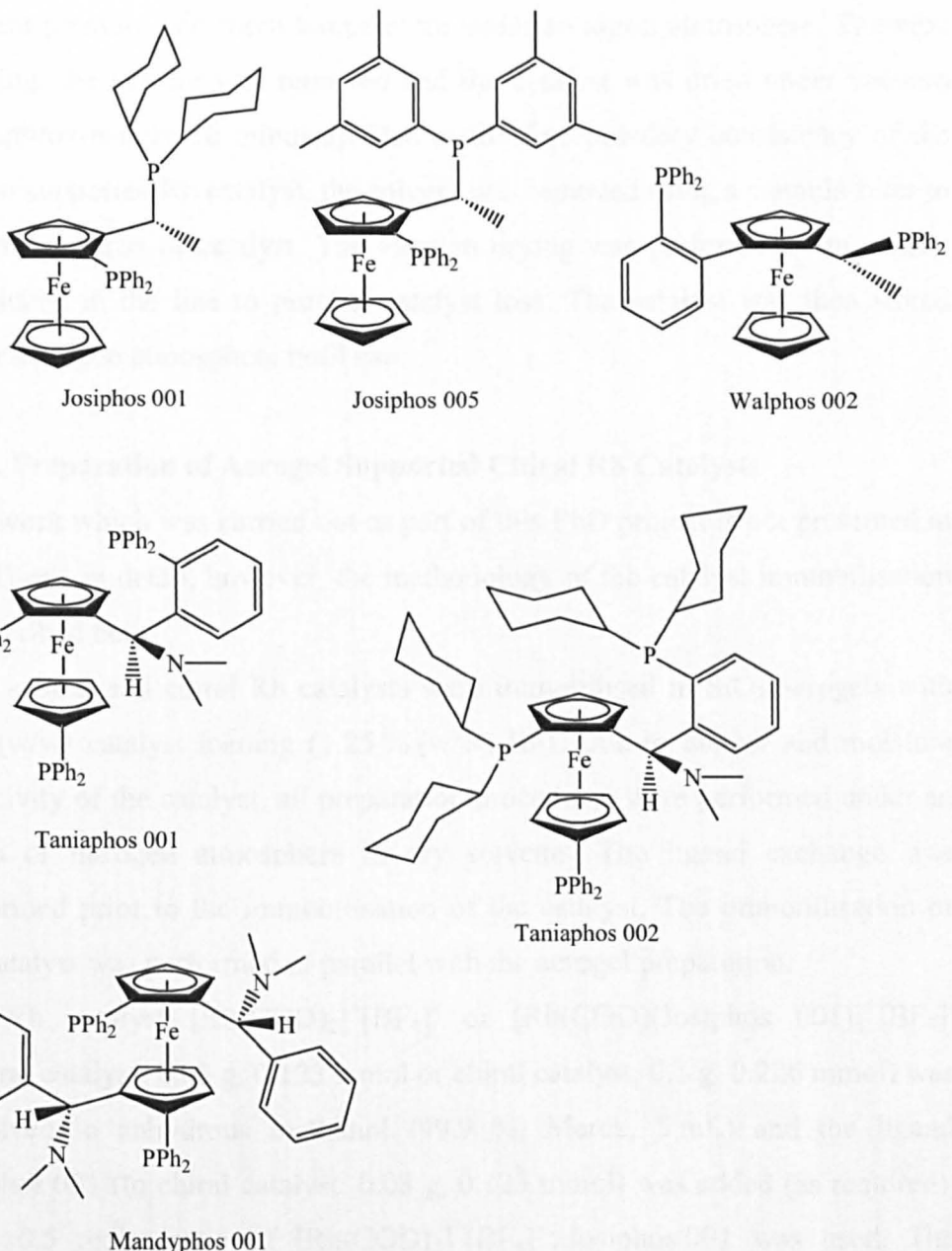


Figure 2-2. The structures of the Solvias Josiphos type ligands. The general structure of the supported homogeneous chiral Rh catalyst is  $[\text{Rh}(\text{COD})(\text{R}_2\text{P}^*-\text{PR}_2^*)]^+[\text{BF}_4^-]/\text{PTA}/\text{Alumina}$  ( $\text{COD} = 1,5\text{-cyclo-octadiene}$ ,  $\text{R}_2\text{P}^*-\text{PR}_2^* = \text{bisphosphine ligand}$ , PTA = phosphotungstic acid  $\text{H}_3\text{O}_{40}\text{PW}_{12}$ ).

#### 2.1.1.2. Preparation of $[\text{Rh}(\text{COD})(\text{ligand})]^+[\text{BF}_4]^-/\text{PTA}/\text{Carbon}$

The carbon supported Rh catalyst was modified with only one bisphosphine ligand, Josiphos 001.  $[Rh[(COD)_2]^+[BF_4]^-/PTA/Carbon$  (0.25 g, 12.1  $\mu\text{mol}$  Rh) and Josiphos 001 ligand (0.012 g, 18.2  $\mu\text{mol}$ ) were mixed in anhydrous ethanol (50 mL) using a two-neck glass flask (oven dried, volume: 100 mL). The solution was stirred with a suspended stirrer overnight (for 16 hours) at

ambient pressure and room temperature under an argon atmosphere. The next morning, the solvent was removed and the catalyst was dried under vacuum (for approximately 10 minutes). Due to the fine powdery consistency of the carbon supported Rh catalyst, the solvent was removed using a cannula filter to prevent any loss of catalyst. The vacuum drying was performed with a filter introduced in the line to prevent catalyst loss. The catalyst was then stored under an argon atmosphere until use.

### **2.1.2. Preparation of Aerogel Supported Chiral Rh Catalysts**

This work which was carried out as part of this PhD project is not presented in this Thesis in detail, however, the methodology of the catalyst immobilisation is described here.

Both achiral and chiral Rh catalysts were immobilised in SiO<sub>2</sub> aerogels with 5 % (w/w) catalyst loading (1.25 % (w/w) Rh). Due to the air and moisture sensitivity of the catalyst, all preparation procedures were performed under an argon or nitrogen atmosphere in dry solvents. The ligand exchange was performed prior to the immobilisation of the catalyst. The immobilisation of the catalyst was performed in parallel with the aerogel preparation.

The Rh catalyst [Rh(COD)<sub>2</sub>]<sup>+</sup>[BF<sub>4</sub>]<sup>-</sup> or [Rh(COD)(Josiphos 001)]<sup>+</sup>[BF<sub>4</sub>]<sup>-</sup> (achiral catalyst: 0.05 g, 0.123 mmol or chiral catalyst: 0.1 g, 0.226 mmol) was dissolved in anhydrous methanol (99.9 %, Merck, 5 mL) and the ligand Josiphos 001 (to chiral catalyst: 0.08 g, 0.123 mmol) was added (as required). A 1 : 0.5 molar ratio of [Rh(COD)<sub>2</sub>]<sup>+</sup>[BF<sub>4</sub>]<sup>-</sup>: Josiphos 001 was used. The ligand exchange reaction was performed in anhydrous methanol overnight (16 hours) at ambient pressure and room temperature under an argon atmosphere.

The aerogel was synthesised using the following procedure: SiO<sub>2</sub> aerogel was obtained using Si(OMe)<sub>4</sub> (TMOS) (Sigma, 1 mol), MeOH (99.8 %, Aldrich, 6 mol), deionised H<sub>2</sub>O (4 mol) and NH<sub>4</sub>OH (Fisher, 0.005 mol). The calculations were based upon the Rh loading: the quantity of SiO<sub>2</sub> was first determined and the quantities of the MeOH, H<sub>2</sub>O and NH<sub>4</sub>OH were then calculated considering the molar ratios described above. The quantities of the materials used are listed in Table 2-1.

**Table 2-1. The quantity of reagents used in the preparation of aerogel supported Rh catalysts. The catalyst : ligand molar ratio was 1 : 0.5.**

Entry	Catalyst loading (w/w %)	SiO <sub>2</sub> (g)	TMOS (g)	MeOH (g)	H <sub>2</sub> O (g)	NH <sub>4</sub> OH (g)
1	5 % [Rh(COD) <sub>2</sub> ] <sup>+</sup> [BF <sub>4</sub> ] <sup>-</sup> *	0.95	2.41	3.04	1.14	0.003
2	5 % [Rh(COD)(Josiphos 001)] <sup>+</sup> [BF <sub>4</sub> ] <sup>-</sup> **	3.38	8.57	10.82	4.05	0.01

\* Achiral catalyst: 0.05 g, 0.123 mmol

\*\* Chiral catalyst: [Rh(COD)<sub>2</sub>]<sup>+</sup>[BF<sub>4</sub>]<sup>-</sup> (0.1 g, 0.226 mmol) and Josiphos 001 (0.079 g, 0.123 mmol)

The precursor, TMOS was dissolved in water and was added to the Rh catalyst [Rh(COD)<sub>2</sub>]<sup>+</sup>[BF<sub>4</sub>]<sup>-</sup> (Fluka, cat.no. 14694) dissolved in anhydrous methanol (quantity: see Table 2-1). The solution was then stirred using a magnetic stirrer bar. Once a homogeneous solution was obtained, the NH<sub>4</sub>OH was added. Intense stirring was provided during the gel formation step to ensure a homogeneous solution and therefore presumably a homogeneous distribution of the Rh catalyst. Once the gelation was completed, the material was poured into a tube (open at both ends) and left until it solidified. The gel was removed from the tube and placed in methanol (250 mL), and aged for 2 days.

Supercritical drying using scCO<sub>2</sub> was performed to replace the liquid in the pores by gas.<sup>1</sup> The drying was performed using a 1 L volume high pressure vessel. The gel was placed in the vessel and the vessel was filled with methanol. The system was closed and the methanol was slowly flushed away by charging the system with CO<sub>2</sub> up to 100 bar and it was heated to 40 °C. The CO<sub>2</sub> was circulated in the system to completely remove the methanol. Wash samples (of methanol) were taken before and after drying to determine the catalyst loss during the preparation. The aerogel supported Rh catalyst was stored under an argon atmosphere until use.

In conclusions, the immobilisation technique was successful as low leaching of Rh was determined during the preparation (determined with ICP-MS). Although H<sub>2</sub>O was used for making the aerogel supported catalyst, the achiral catalyst [Rh(COD)<sub>2</sub>]<sup>+</sup>[BF<sub>4</sub>]<sup>-</sup>/SiO<sub>2</sub> aerogel showed high activity in the continuous asymmetric hydrogenation of dimethyl itaconate in scCO<sub>2</sub> (conversion to 100 %). The chiral catalyst [Rh(COD)(Josiphos 001)]<sup>+</sup>[BF<sub>4</sub>]<sup>-</sup>

/SiO<sub>2</sub> aerogel showed low enantioselectivity for the continuous asymmetric hydrogenation in scCO<sub>2</sub> (*ee<sub>R</sub>* < 10 %). The catalyst stability, however, was high in a continuous flow scCO<sub>2</sub> system as the Rh leaching of both achiral and chiral catalysts remained under 1 ppm in the continuous reactions at all conditions (determined with ICP-MS).

### **2.1.3. Preparation of Ionic Liquid Supported Chiral Rh Catalysts**

Chiral Rh catalysts immobilised in ionic liquids (ILs) were examined for the hydrogenation of dimethyl itaconate in a continuous flow scCO<sub>2</sub> system. The ILs [BMIM][BF<sub>4</sub>], [BMIM][Tf<sub>2</sub>N] and [BMIM][N(CN<sub>2</sub>)] were used as support material for [Rh(COD)<sub>2</sub>]<sup>+</sup>[BF<sub>4</sub>]<sup>-</sup> and [Rh(COD)(Josiphos 001)]<sup>+</sup>[BF<sub>4</sub>]<sup>-</sup>. The chiral catalyst was prepared prior to the immobilisation of the catalyst using a 1 : 0.5 molar ratio of [Rh(COD)<sub>2</sub>]<sup>+</sup>[BF<sub>4</sub>]<sup>-</sup> : Josiphos 001. The ionic liquids were prepared at Nottingham.<sup>2</sup> Due to the air and moisture sensitivity of the catalyst, all preparation procedures were carried out under an argon atmosphere in dry solvents.

The achiral Rh catalyst [Rh(COD)<sub>2</sub>]<sup>+</sup>[BF<sub>4</sub>]<sup>-</sup> (0.02 g, 50 µmol) was dissolved in anhydrous ethanol (10 mL) and an appropriate amount of Josiphos 001 ligand (to chiral catalyst: 0.016 g, 25 µmol) was added to the solution (as required). The ligand exchange reaction was performed in ethanol at room temperature and ambient pressure overnight (for 18 hours) with stirring. Once the ligand exchange reaction was completed, the IL (3 mL) was added to the solution and this was stirred for a further 30 minutes. The ethanol was then evaporated using vacuum. In order to remove the majority of contaminants including water, the vacuum drying was continued for a further 30 minutes. A sample of ethanol collected in the trap of the Schlenk line was kept to determine the catalyst loss during the preparation. The catalyst was stored under an argon atmosphere until use.

### **2.1.4. Preparation of Cross-Linked Enzyme Aggregate (CLEA)**

Individual CLEA of cholesterol oxidase (cholesterol oxidase from *Nocardia sp.* (batch 1: 19.5 U/mg protein - protein content 77.4 % or batch 2: 20.1 U/mg protein - protein content 84.2 %, E.C. 1.1.3.6., Merck 228230) and

catalase from bovine liver (batch 1: 2140 U/mg protein - protein content 63 % or batch 2: 4540 U/mg protein - protein content 65 %, E.C. 1.11.1.6, Sigma C-9322), and combi-CLEA of the two enzymes were prepared. Lipase from *Candida antarctica* (lipase B, E.C. 3.1.1.3) CLEA (28000 U/g solid, batch no 5790) was received as a gift from CLEA Technologies (Delft, Netherlands). All procedures were performed at 4 °C using chilled solvents.

The “CLEAtion” consists of two steps, physical aggregation and cross-linking.<sup>3</sup> The first step, the precipitation of the enzyme is commonly performed using organic solvents. The precipitants (ethanol, iso-propanol, acetone, dimethoxyethane (ethyleneglycol dimethyl ether), acetonitrile and ammonium sulfate) were screened for both cholesterol oxidase and catalase using a 1 to 5 volume ratio of enzyme aliquot to precipitant. The precipitation screen was performed using cholesterol oxidase from *Nocardia sp.* (33.3 U/mL, 0.3 mL, 10 U - batch 1) and catalase from bovine liver (11167 U/mL, 0.3 mL, 3348 U - batch 1) dissolved in phosphate buffer (5 mM, pH 7.0). Cholesterol oxidase was used in low concentration due to its high price. The precipitant (1.8 mL) was measured in a microfuge tube and the enzyme solution (0.3 mL, cholesterol oxidase: 10 U, catalase: 3348 U) was added dropwise while an intense stirring (using magnetic stirrer bar, 600 rpm). The solution was stirred for 30 minutes and centrifuged at 600 x g for 10 min (Denver Instrument, Force 13). The supernatant was decanted and the pellet was redissolved in phosphate buffer (5 mM, pH 7.0, 1.8 mL). The enzyme activity was assayed in both the supernatant and the enzyme aliquot of the redissolved pellet. The details of the enzyme assays are discussed below in this Chapter.

The enzymes were used in larger quantities for making CLEA. Individual cholesterol oxidase CLEA was prepared using cholesterol oxidase (100 U dissolved in 5 mM phosphate buffer, 0.5 mL, pH 7.0) with ammonium sulfate as precipitant (saturated, 2.5 mL) (total volume: 3 mL). The catalase CLEA was prepared using catalase (batch 1: 335000 U, batch 2: 737500 U, dissolved in 5 mM phosphate buffer, 5 mL, pH 7.0) with ammonium sulfate (saturated, 25 mL) or dimethoxyethane (25 mL) as precipitant (total volume: 30 mL). The combi-CLEA was prepared using cholesterol oxidase (100 U dissolved in 5 mM phosphate buffer, 0.5 mL, pH 7.0) and catalase (batch 1: 335000 U,

batch 2: 737500 U, dissolved in 5 mM phosphate buffer, 5 mL, pH 7.0) with ammonium sulfate (saturated, 24.5 mL) as precipitant (total volume: 30 mL). The precipitant (ammonium sulfate or dimethoxyethane) was measured in a centrifuge tube (volume: 10 or 50 mL) and the enzyme solution was added dropwise with intense stirring. The solution was stirred for 30 minutes.

The second step of the CLEAtion is the cross-linking of the solid enzyme particles. In this study, glutaraldehyde (25 % w/w, Fluka) and dextran polyaldehyde (prepared by us) were investigated as cross-linkers. Dextran (from *Leuconostoc mesenteroides*, average mol wt 5M-40M kDa, Sigma) was oxidised using sodium iodide (Montplet and Esteban SL. Barcelona).<sup>4</sup> The procedure for the preparation of dextran polyaldehyde is discussed below in this Chapter. Glutaraldehyde was used in 10 mM and 50 mM concentrations. Dextran polyaldehyde (DPA) was used in the following quantities 200 µL DPA solution /mL enzyme solution (DPA 200) and 400 µL DPA solution/mL enzyme solution (DPA 400). The cross-linking was performed in the same solution as the precipitation: the cross-linker was added to the suspension of the precipitated enzyme and was stirred overnight (18 hours) at 4 °C. The next morning, the CLEA was centrifuged at 1250 x g for 10 min (Fisher Accu spin 400) and washed twice with phosphate buffer (5 mM, pH 7.0) to remove the unreacted cross-linker (the volume of the phosphate buffer used for washing was half of the total volume). The supernatant was decanted and kept for further analysis. The CLEA was resuspended in phosphate buffer (5 mM, pH 7.0, total volume: 3 mL or 30 mL) and stored at 4 °C.

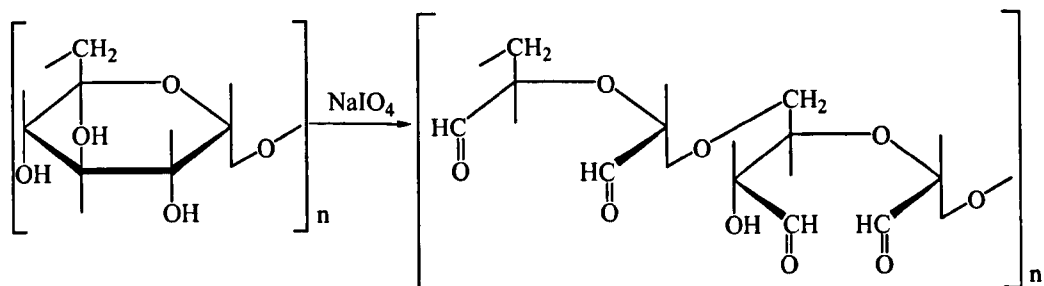
In some cases, a reduction step was also included in the preparation procedure following the cross-linking, using NaBH<sub>4</sub> (95+ %, Merck) as reducing agent. Before the reduction step, the CLEA was centrifuged at 1250 x g for 10 min and the supernatant was removed. The chilled borohydride solution (0.5 mg/mL, 2 mL for cholesterol oxidase CLEA, and 20 mL for catalase CLEA and combi-CLEA) was added to the suspension of the CLEA which was stirred for 30 minutes. The CLEA was centrifuged at 1250 x g for 10 min and washed twice with phosphate buffer (5 mM, pH 7.0) (the volume of the phosphate buffer used for washing was half of the total volume). The supernatant was decanted and kept for further analysis. The CLEA was

resuspended in phosphate buffer (5 mM, pH 7.0, total volume: 3 mL or 30 mL) and stored at 4 °C.

Combi-CLEA can be prepared by co- or separate precipitation of the enzymes of interest. Here, we examined both methods. When the enzymes were co-precipitated, ammonium sulfate was used as precipitant. When the enzymes were precipitated separately, ammonium sulfate (cholesterol oxidase and catalase) and dimethoxyethane (catalase) were used as precipitants and the aggregates were mixed before cross-linking. Glutaraldehyde and dextran polyaldehyde were examined as cross-linkers and a reduction step was included in some cases. The amount of the enzymes used for the particular batches is described in detail in Chapter 7. The procedure for preparation of the combi-CLEA was identical to the preparation procedure of individual CLEA as described above.

## 2.2. Preparation of dextran polyaldehyde

Dextran polyaldehyde (DPA) was prepared by the oxidation of dextran (Scheme 2-2). Dextran from *Leuconostoc mesenteroides* (1.65 g, average mol wt 5-40 kDa, Sigma) was dissolved in dH<sub>2</sub>O (100 mL) and sodium iodine (3.85 g, Montplet and Esteban SL. Barcelona) was added. The resulting solution was stirred at room temperature for 90 minutes. Subsequently, the solution was dialysed five times, using MW cutoff of 12 kDa dialysis sacks (Sigma, Cat. no D6191) against 5 L dH<sub>2</sub>O each time at room temperature during >2 hours and under stirring.<sup>4, 5</sup> DPA was used as cross-linker in the following quantities: 200 µL DPA solution/mL enzyme solution (DPA 200) or 400 µL DPA solution/mL enzyme solution (DPA 400).



Scheme 2-2. Preparation of dextran polyaldehyde from dextran.

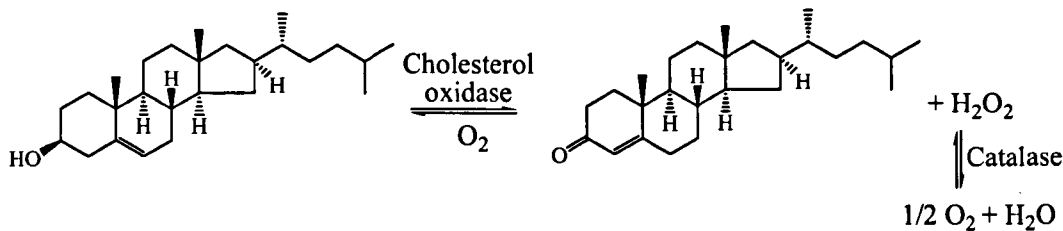
## 2.3. Enzyme Assays

The activity of the immobilised enzymes was determined to evaluate the relative activity of the CLEA compared to the activity of the non-immobilised enzyme. The oxidation of cholesterol (96%, Alfa Aesar) to 4-cholest-en-3-one (98%, Acros) (Scheme 2-3) with O<sub>2</sub> as oxidant was used to assay cholesterol oxidase activity. For catalase, two different assays were developed. One of them determined the amount of H<sub>2</sub>O<sub>2</sub> (30 % w/w, Sigma-Aldrich) reduced directly by measuring the H<sub>2</sub>O<sub>2</sub> concentration using a UV-Vis spectrophotometer (Agilent) at 240 nm. The other method consisted of two steps. First, catalase was incubated in a H<sub>2</sub>O<sub>2</sub> solution for exactly 1 min and the remaining H<sub>2</sub>O<sub>2</sub> was then determined in a coupling reaction catalysed by another enzyme horseradish peroxidise (HRP, Type II: 150-250 U/mg, Sigma).

### 2.3.1. Cholesterol Oxidase Assay

The oxidation of cholesterol (Scheme 2-3) was performed in sodium phosphate buffer (20 mM, pH 7.0) containing Triton X-100 surfactant (Sigma, 0.5 mL/L). Cholesterol was dissolved in iso-propanol (12 mM, IPA, 99.6 %, Fluka). An aqueous solution of cholesterol oxidase from *Nocardia sp.* (33.3 U/mL) was prepared in phosphate buffer (5 mM, pH 7.0, 3 mL).

The reaction was performed in a round bottom flask (volume: 100 mL) at room temperature using O<sub>2</sub> (99+ %, BOC) as oxidant. The reaction mixture consisted of phosphate buffer (20 mM, pH 7.0, 27.3 mL), alcoholic solution of cholesterol (in IPA, 12 mM, 2.5 mL) and aliquot of cholesterol oxidase solution or suspension of cholesterol oxidase CLEA (0.2 mL, 6.67 U). The flask was sealed with a septum (Suba-Seal) that allowed charging the flask with O<sub>2</sub> using a syringe. The reaction mixture was stirred with a magnetic stirrer bar. The reaction was run up to 5 hours. The samples for HPLC analysis (described below in this Chapter) were prepared by mixing a sample from the oxidation reaction (750 µl) and NaOH (0.2 M, 250 µl). The NaOH solution effectively stopped the enzymatic reaction and therefore allowed real time analysis and different time points to be taken from the same reaction.



**Scheme 2-3. The oxidation of cholesterol in a coupled-enzymatic reaction of cholesterol oxidase and catalase.**

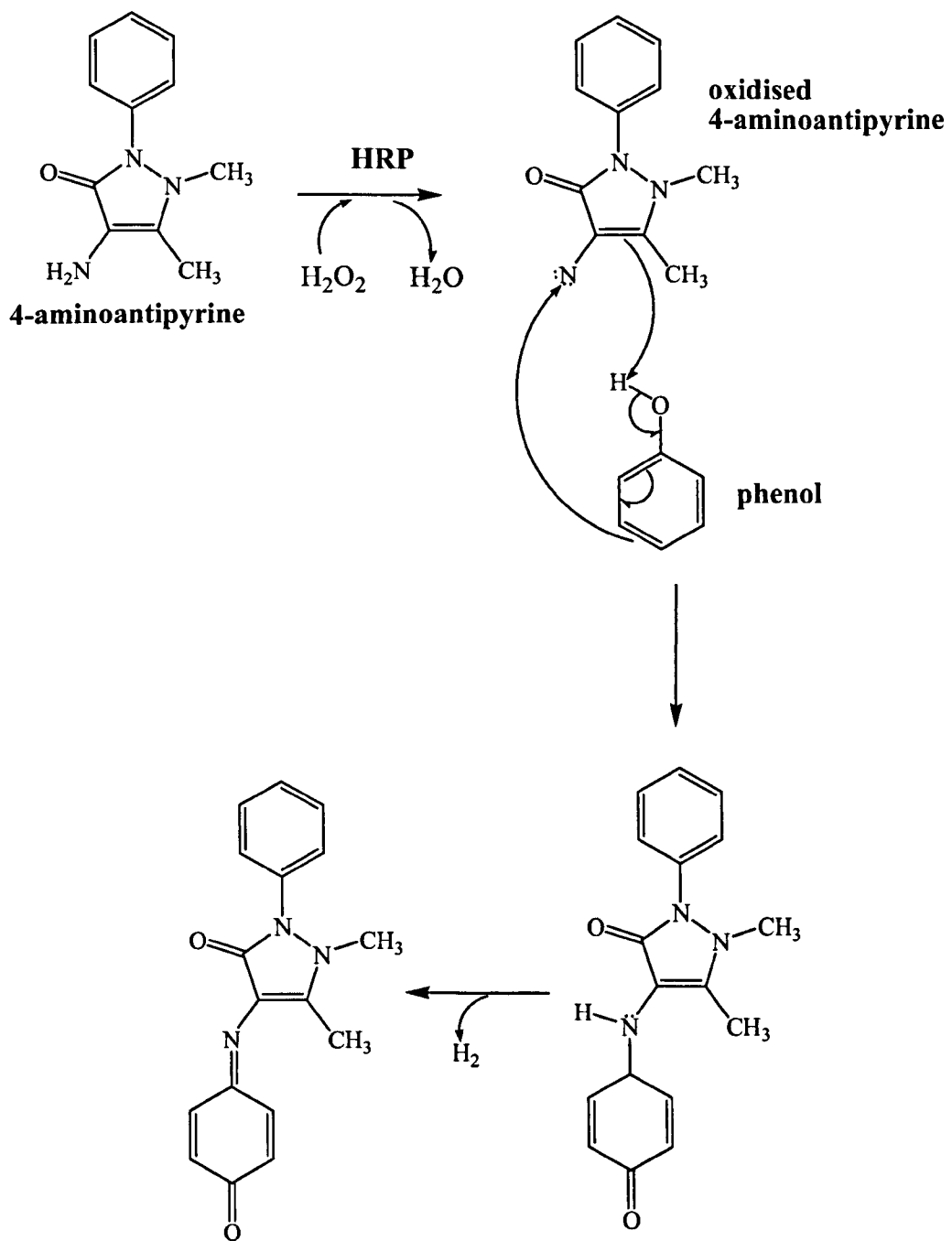
### 2.3.2. Catalase Assay

Two different catalase assays were used throughout this study. Both activity tests were performed in sodium phosphate buffer (20 mM, pH 7.0) containing Triton X-100 surfactant (0.5 mL/L). H<sub>2</sub>O<sub>2</sub> (30 % w/w in water) was used as received. An aqueous solution of catalase from bovine liver (batch 1: 11167 U/mL, batch 2: 24583 U/mL) was prepared in phosphate buffer (5 mM, pH 7.0).

In assay 1, the H<sub>2</sub>O<sub>2</sub> concentration was monitored directly using a UV-Vis spectrophotometer. The reaction was performed in a round bottom flask (volume: 50 mL) at room temperature. The reaction mixture consisted of sodium phosphate buffer (20 mM, pH 7.0, 6.8 mL), H<sub>2</sub>O<sub>2</sub> (30 % w/w in water, 3 ml) and aliquot of catalase solution or suspension of catalase CLEA (0.2 mL, batch 1: 2233 U). The reaction was run for up to 1 hour with stirring. The decrease in absorbance was measured at 240 nm.

The other catalase assay consisted of two steps. The first reaction was carried out in a round bottom flask (volume: 100 mL) at room temperature. The reaction mixture consisted of sodium phosphate buffer (20 mM, pH 7.0, 8.6 mL), H<sub>2</sub>O<sub>2</sub> (30 % w/w in water, 0.4 mL) and enzyme aliquot of catalase solution or suspension of catalase CLEA (0.2 mL, batch 2: 4917 U). The enzyme was added to a H<sub>2</sub>O<sub>2</sub> solution and incubated for exactly 1 min at room temperature with stirring. The reaction was stopped by the addition of an inhibitor sodium azide (1 mL, Fluka, 2 mg/mL). The remaining H<sub>2</sub>O<sub>2</sub> was determined with a coupling reaction. A coloured product (dye) was formed by the reaction occurring between 4-aminoantipyrine (97 %, Alfa Aesar) and phenol (99 + %, Alfa Aesar) catalysed by horseradish peroxidise (HRP) (Scheme 2-4). The reaction was performed at 37 °C in a 5 mL vial for

20 minutes with stirring. The reaction mixture consisted of sodium phosphate buffer (20 mM, pH 7.0, 0.9 mL), HRP reagent (1 mL), HRP enzyme solution (500 U/mL, 0.1 mL, 50 U) and sample (3 mL). The HRP reagent consisted of 4-aminoantipyrine (6.25 mM in 5 mM phosphate buffer pH 7.0) and phenol solutions (100 mM in 5 mM phosphate buffer pH 7.0) in 1 : 1 volume ratio. The amount of dye formed in the reaction was measured by UV-Vis at 500 nm. The activity of the enzyme was calculated from the absorbance data obtained for the second reaction of the assay (dye formation). This assay was also used to determine the remaining H<sub>2</sub>O<sub>2</sub> in the coupled-enzymatic reaction.



**Scheme 2-4. Dye formation.** The dye is formed by a reaction between 4-aminoantipyrine and phenol catalysed by horseradish peroxidase (HRP).<sup>6,7</sup>

## 2.4. Equipment Description

This section gives a detailed schematic diagram and description, and a standard operating procedure (SOP) for each reactor. Attention! Experiments performed

at high pressures and high temperatures require careful execution. The safety of the equipment is always the responsibility of the researcher.

#### 2.4.1. The Small Scale Hydrogenation Apparatus

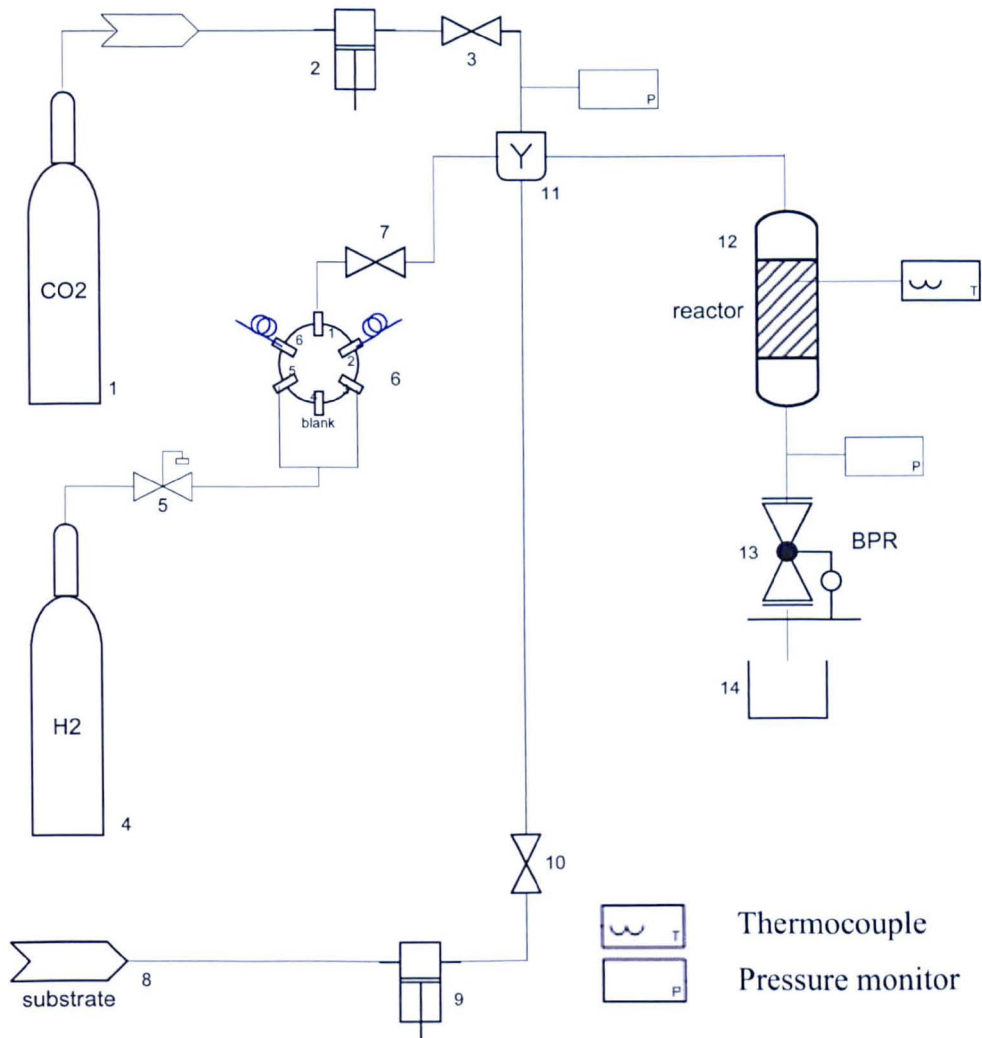


**Figure 2-3. The small scale continuous flow hydrogenation apparatus.** Parts are labelled as follows. 1: CO<sub>2</sub> cylinder, 2: Jasco CO<sub>2</sub> pump (CO<sub>2</sub> cooling unit and HPLC pump in one) (PU-1580-CO<sub>2</sub>), 3: SSI tap, 4: H<sub>2</sub> cylinder, 5: Maximator (H<sub>2</sub>), 6: Rheodyne gas dosage, 7: SSI tap, 8: Substrate reservoir, 9: Gilson pump (306-HPLC), 10: SSI tap, 11: Static mixer, 12: Reactor, 13: Jasco Back pressure regulator (BPR) (Jasco BP-1580-81), 14: Collection vial. All components were connected by 1/16" 316 stainless steel tubing. The feed streams were mixed in a heated, static mixer before being passed through the reactor (1.5 cm<sup>3</sup> in volume). Products were collected by continuous depressurisation of the reaction mixture using an electronic BPR, and analysed by chiral GLC.

Figure 2-3 shows the reactor setup used to perform asymmetric hydrogenation in a continuous flow scCO<sub>2</sub> system. The system consisted of several cylinders,

pumps and taps and all components were connected by 1/16" 316 stainless steel tubing (Swagelok). The CO<sub>2</sub> (98 + %, BOC) was supplied *via* a cylinder (1) to a supercritical fluid Jasco CO<sub>2</sub> cooler and pump (PU-1580-CO<sub>2</sub>) (2). The pump cooled down the CO<sub>2</sub> to -10 °C and fed it to a heated static mixer (11). The H<sub>2</sub> (99.99 %, BOC) was supplied *via* a cylinder (4) to a gas booster pump (5) that could generate an overpressure of the H<sub>2</sub> using compressed air. The H<sub>2</sub> was fed in a Rheodyne gas dosage unit (6) that forwarded the gas to a heated static mixer (11). The description of the Rheodyne system can be found below in this Chapter. The organic substrate was supplied using a Gilson pump (306-HPLC) (9) and fed to a heated static mixer (11). All reagents and CO<sub>2</sub> were mixed and heated in a static mixer (11) filled with glass beads before entering the reactor (12) filled with catalyst. A metal filter 'frit' (Supelco, pore size: 0.5 µm, diameter: 1/4") was placed in the bottom of the reactor to ensure that the catalyst remained in the reactor. The system pressure was controlled using an automatic Jasco back pressure regulator (BPR) (BP-1580-81) (13) that also allowed the continuous depressurisation of the system and product collection. The Jasco CO<sub>2</sub> pump (2) and the BPR (13) both had a build-in pressure monitor. For further safety, the pressure of the system was monitored by external pressure monitors attached to membrane pressure transducers (RDP-A105). The temperature of the static heater (11) and the reactor (12) were heated using a band heater (230 V) and aluminium heating blocks (230 V) equipped with thermocouples, respectively, and monitored by a temperature monitor. (The pressure monitors, temperature monitors and heaters were manufactured at the School of Chemistry, the University of Nottingham.) The pumps and heaters were connected to a trip system controlled by a set overpressure and overtemperature (on the pressure and temperature monitors). The trip switched off all pumps and heaters if overpressure or overtemperature was recorded.

The standard operating procedure (SOP) of the small scale hydrogenation reactor was the following (see Figure 2-3 for numbering of taps, pumps, etc.).

Start up:

1. Fill up the reactor with a weighed amount of catalyst
2. Attach the reactor to the apparatus and tighten the fittings

3. Set BPR to the desired pressure
4. Open the CO<sub>2</sub> cylinder and let the Jasco pump cool down the CO<sub>2</sub>
5. Open tap 3, start pumping the CO<sub>2</sub> with 3 mL/min flow rate and leave the system to reach the set pressure
6. Set the desired CO<sub>2</sub> flow rate
7. Leak test all pressurized fittings at operating pressure
8. Open the H<sub>2</sub> cylinder and set overpressure on valve 5 (usually 50 bar over the system pressure)
9. Set the pre-calculated H<sub>2</sub> dosage rate on the Rheodyne (6) (data from The National Institute of Standards and Technology (NIST) database<sup>8</sup> were used to calculate H<sub>2</sub> correct dosage rate)
10. Attach heating blocks and secure thermocouples
11. Turn heaters and temperature monitors on and set to the desired temperatures
12. Leave CO<sub>2</sub> and H<sub>2</sub> flowing to reduce the catalyst and allow the system to reach a steady state for approximately 20 minutes

Reaction:

13. Prime the Gilson pump (9) with the substrate and set to the desired flow rate
14. Open tap 10 to allow the substrate flowing and start pumping
15. Allow the substrate to flow for approximately 20 minutes to establish a steady state
16. Take a sample
17. Leave the substrate flowing and once a sufficient amount of sample has been obtained submit for analysis
18. Stop the substrate flow
19. If the reaction conditions are to be altered set the new parameters and repeat steps 13-18

Shutdown:

20. Close tap 10
21. Stop H<sub>2</sub> dosing by switching off Rheodyne
22. Decompress and shut off the maximator (5) and close the H<sub>2</sub> cylinder
23. Turn the heaters off and let the system cool down
24. Leave CO<sub>2</sub> flowing to flush the system through for 15-20 minutes

25. Stop pumping CO<sub>2</sub>, close tap 3 and close the CO<sub>2</sub> cylinder
26. Depressurise the system by decreasing the pressure on the BPR (13) stepwise.

#### 2.4.2. The Small Scale Enzyme Reactor

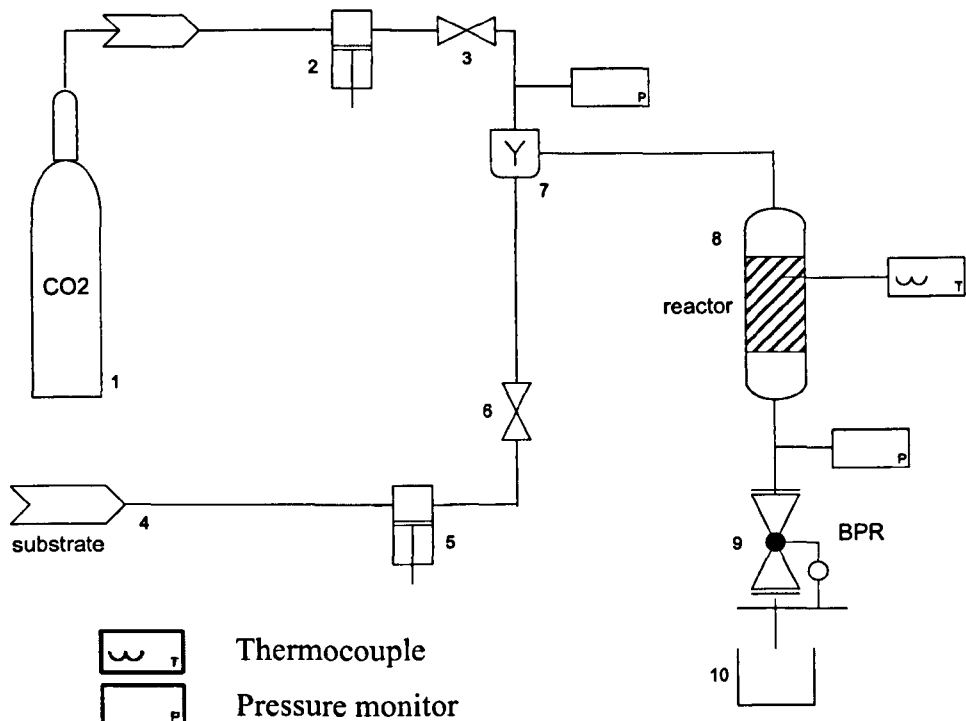


**Figure 2-4. The small scale enzyme reactor. Parts are labelled as follows.** 1: CO<sub>2</sub> cylinder, 2: Jasco CO<sub>2</sub> pump (CO<sub>2</sub> cooling unit and HPLC pump in one) (PU-1580-CO<sub>2</sub>), 3: SSI tap, 4: Substrate reservoir, 5: Gilson pump (306-HPLC), 6: SSI tap, 7: Static mixer, 8: Reactor, 9: Jasco Back pressure regulator (BPR) (Jasco BP-1580-81), 10: Collection vial. All components were connected by 1/16" 316 stainless steel tubing. The feed streams were mixed in a heated, static mixer before being passed through the reactor (1.5 cm<sup>3</sup> in volume). Products were collected by continuous depressurisation of the reaction mixture using an electronic BPR, and analysed by chiral GLC.

The equipment used for conducting enzymatic reactions in flow scCO<sub>2</sub> was similar to the small scale hydrogenation apparatus that is described above in this Chapter in detail. The only difference compared to the hydrogenation rig was the lack of the H<sub>2</sub> line, otherwise all parts of the enzyme reactor were identical with the parts used for the small scale hydrogenation reactor.

The SOP of the continuous flow enzyme reactor was as follows (see Figure 2-4 for numbering of taps, pumps, etc.).

**Start up:**

1. Fill up the reactor with a weighed amount of catalyst
2. Attach the reactor to the apparatus and tighten the fittings
3. Set BPR to the desired pressure
4. Open the CO<sub>2</sub> cylinder and let the Jasco pump cool down the CO<sub>2</sub>
5. Open tap 3, start pumping the CO<sub>2</sub> with 3 mL/min flow rate and leave the system to reach the set pressure
6. Set the desired CO<sub>2</sub> flow rate
7. Leak test of all pressurized fittings at operating pressure
8. Attach heating blocks and secure thermocouples
9. Turn heaters and temperature monitors on and set to the desired temperatures
10. Leave CO<sub>2</sub> flowing to allow the system to reach a steady state

**Reaction:**

11. Prime Gilson pump (5) with the substrate and set to the desired flow rate
12. Open tap 6 to allow the substrate flowing and start pumping
13. Allow the substrate to flow for approx 20 minutes to establish a steady state
14. Take a sample
15. Leave the substrate flowing and once a sufficient amount of sample obtained submit for analysis
16. Stop the substrate flow
17. If the reaction conditions are to be altered set the new parameters and repeat steps 11-16

**Shutdown:**

18. Close tap 6
19. Turn the heaters off and let the system cool down
20. Leave CO<sub>2</sub> flowing to flush the system through for 15-20 minutes
21. Stop pumping CO<sub>2</sub> and close tap 3 and close the CO<sub>2</sub> cylinder
22. Depressurise the system by decreasing the pressure on the BPR (9) stepwise.

### 2.4.3. The Small Scale Two-Stage Reactor

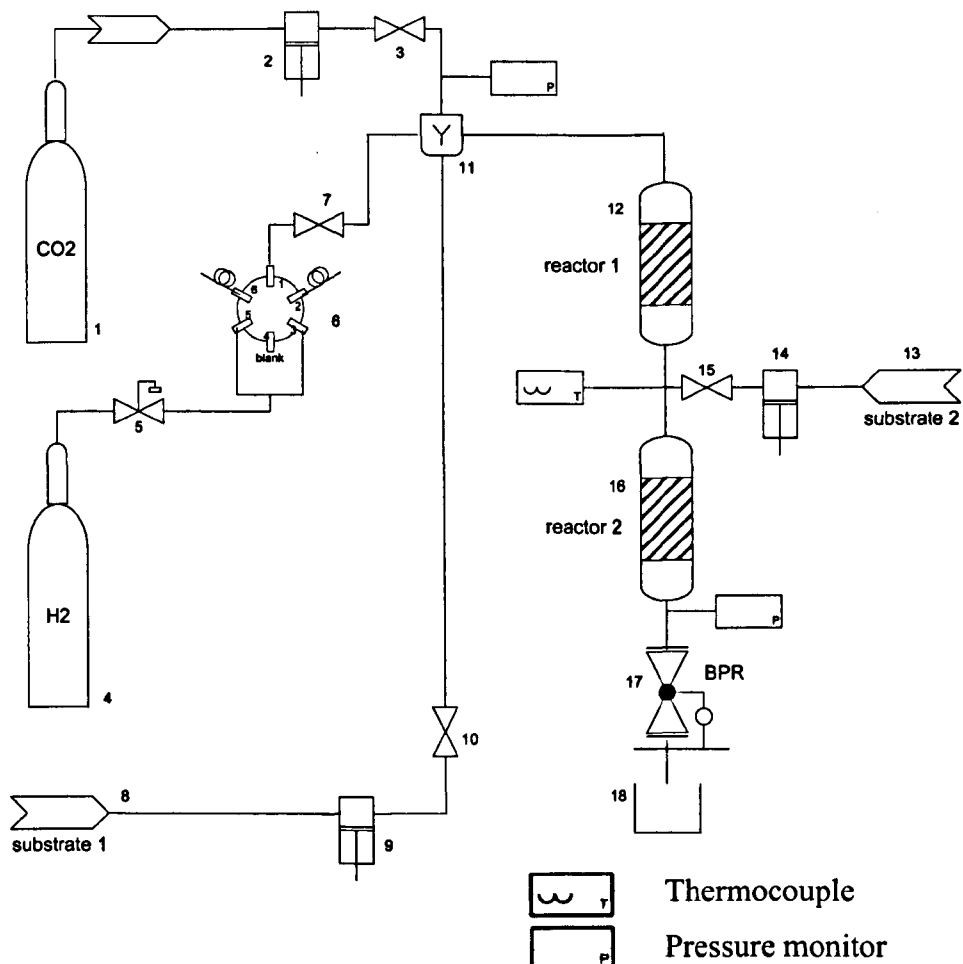


**Figure 2-5. The small scale two-stage reactor.** Parts are labelled as follows. 1:  $\text{CO}_2$  cylinder, 2: Jasco  $\text{CO}_2$  pump (CO<sub>2</sub> cooling unit and HPLC pump in one) (PU-1580-CO<sub>2</sub>), 3: SSI tap, 4:  $\text{H}_2$  cylinder, 5: Maximator ( $\text{H}_2$ ), 6: Rheodyne gas dosage, 7: SSI tap, 8: Substrate (1) reservoir, 9: Gilson pump (1) (306-HPLC), 10: SSI tap, 11: Static mixer, 12: Reactor (1), 13: Substrate (2) reservoir, 14: Gilson pump (2) (306-HPLC), 15: SSI tap, 16: Reactor (2), 17: Jasco Back pressure regulator (BPR) (Jasco BP-1580-81), 18: Collection vial. All components were connected by 1/16" 316 stainless steel tubing. The feed streams were mixed in a heated, static mixer before being passed through the reactor (1.5 cm<sup>3</sup> in volume). Products were collected by continuous depressurisation of the reaction mixture using an electronic BPR, and analysed by chiral GLC.

The reactor shown in Figure 2-5 was used to perform series reactions in a continuous flow scCO<sub>2</sub> system. The system was slightly different from the hydrogenation apparatus. The changes were in the number of reactors and number of substrate streams. The system description is the following. The CO<sub>2</sub> was supplied *via* a cylinder (1) to a supercritical fluid Jasco CO<sub>2</sub> cooler and pump (2). The pump cooled down the CO<sub>2</sub> to -10 °C and fed it to a heated

static mixer (11). The H<sub>2</sub> was supplied *via* a cylinder (4) to a gas booster pump (5) that could generate an overpressure of H<sub>2</sub> using compressed air. The H<sub>2</sub> was fed in a Rheodyne gas dosage unit (6) that forwarded the gas to a heated static mixer (11). The organic substrate 1 (8) was supplied using a Gilson pump (306-HPLC) (9) and fed to a heated static mixer (11). CO<sub>2</sub>, H<sub>2</sub> and substrate 1 were mixed and heated in a static mixer (11) filled with glass beads before entering the first reactor (12) filled with catalyst. Another organic stream (13) was introduced in the system after the first reactor which was supplied using a Gilson pump (306-HPLC) (14). The entry position of the second substrate was carefully chosen in order to avoid any reaction that could be catalysed by the catalyst loaded in the first reactor. The stream of substrate 2 and all other streams met in a cross-piece mixer before passing through the second reactor (16) filled with catalyst. A metal filter ‘frit’ (Supelco, pore size: 0.5 µm, diameter: ¼”) was placed in the bottom of each reactor to ensure that the catalyst remained in the reactor. The system pressure was controlled using an automatic Jasco back pressure regulator (BPR) (BP-1580-81) (17) that also allowed the continuous depressurisation of the system and the product collection. The pressure monitors, temperature monitors and heater were identical to the ones used for the small scale hydrogenation apparatus.

The SOP of the two-stage reactor was the following (see Figure 2-5 for numbering of taps, pumps, etc.).

Start up:

1. Fill up the reactors with weighed amount of catalysts
2. Attach the reactors to the apparatus and tighten the fittings
3. Set BPR to the desired pressure
4. Open the CO<sub>2</sub> cylinder and let the Jasco pump cool down the CO<sub>2</sub>
5. Open tap 3 and start pumping the CO<sub>2</sub> with 3 mL/min flow rate and leave the system to reach the set pressure
6. Set the desired CO<sub>2</sub> flow rate
7. Leak test of all pressurized fittings at operating pressure
8. Open H<sub>2</sub> cylinder and set overpressure on valve 5 (usually 50 bar over system pressure)

9. Set the pre-calculated H<sub>2</sub> dosage rate on the Rheodyne (6) (data from The National Institute of Standards and Technology (NIST) database<sup>8</sup> were used to calculate H<sub>2</sub> correct dosage rate)
10. Attach heating blocks and secure thermocouples
11. Turn heaters and temperature monitors on and set to the desired temperatures
12. Leave CO<sub>2</sub> and H<sub>2</sub> flowing to reduce the catalyst and allow the system to reach a steady state for approximately 40 minutes

Reaction:

13. Prime Gilson pumps (9 and 14) and set to the desired flow rates
14. Open taps 10 and 15 to allow the substrates flowing and start pumping
15. Allow the substrate flowing for approximately 40 minutes to establish a steady state
16. Take a sample
17. Leave the substrate to flow and once a sufficient amount of sample obtained submit for analysis
18. Stop the substrate flows
19. If the reaction conditions are to be altered set the new parameters and repeat steps 13-18

Shutdown:

20. Close taps 10 and 15
21. Stop H<sub>2</sub> dosing by switching off Rheodyne (6)
22. Decompress and shut off the maximator (5) and close the H<sub>2</sub> cylinder
23. Turn off the heaters and let the system cool down
24. Leave CO<sub>2</sub> flowing to flush the system through for 20-25 minutes
25. Stop pumping CO<sub>2</sub> and close tap 3 and close the CO<sub>2</sub> cylinder
26. Depressurise the system by decreasing the pressure on the BPR (17) stepwise.

#### 2.4.4. The Small Scale Oxidation Reactor

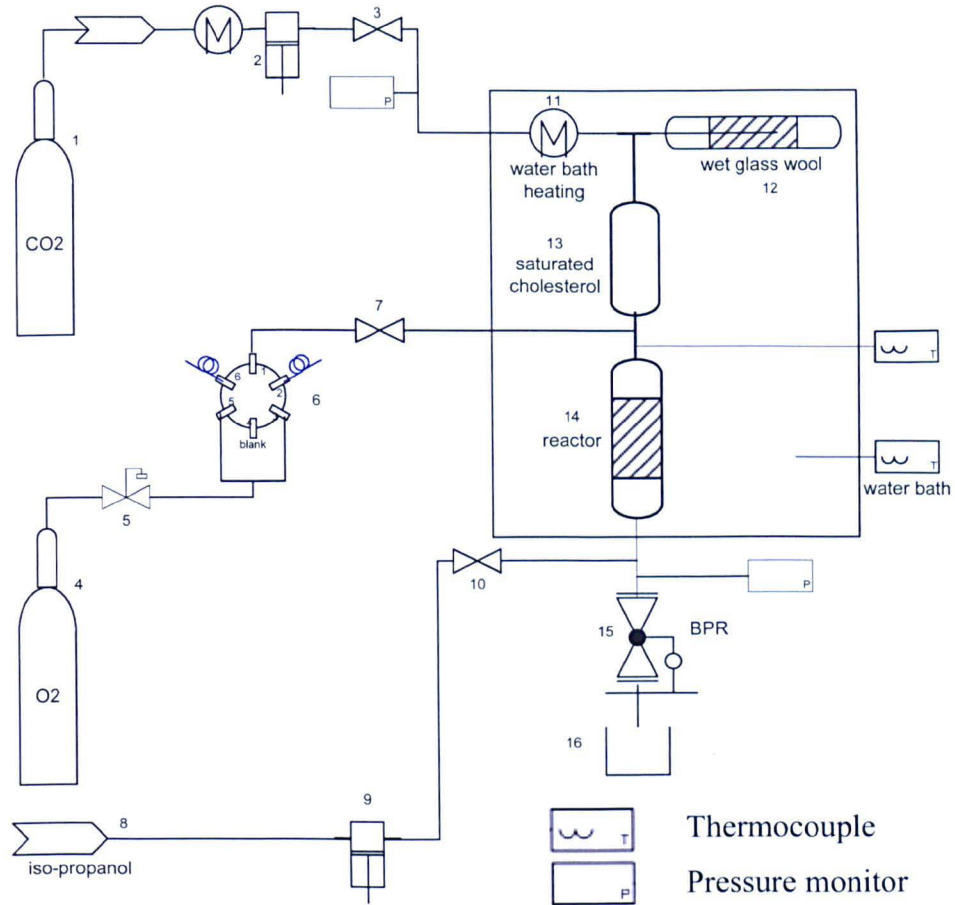


**Figure 2-6. The small scale continuous flow reactor.** Parts are labelled as follows. 1: CO<sub>2</sub> cylinder, 2: CO<sub>2</sub> cooling unit and HPLC pump, 3: Parker ball valve, 4: O<sub>2</sub> cylinder, 5: Manual pressure regulator, 6: Waters switching valve for O<sub>2</sub> dosage (two-position six-port switching valve), 7: Parker ball valve, 8: substrate/solvent reservoir, 9: HPLC pump, 10: Parker ball valve, 11: Water bath heater, 12: Vessel for CO<sub>2</sub> saturation with H<sub>2</sub>O, 13: Cholesterol vessel ( $d_{inner}=1$  cm, length 19 cm), 14: Reactor ( $\frac{1}{4}$ "  $d_{inner}=3$  mm, length 10 cm), 15: GO valve - manual back pressure regulator (BPR), 16: Collection vial. All components were connected by 1/16" 316 stainless steel tubing. The feed streams were mixed in a heated T-piece mixer before being passed through the cholesterol vessel (14.92 cm<sup>3</sup> in volume) and the reactor (0.7 cm<sup>3</sup> in volume). The cholesterol extraction was performed up flow. Products were collected by continuous depressurisation of the system using a manual backpressure regulator, and analysed by reverse phase HPLC.

The small scale oxidation reactor was slightly different from the equipments described above. The substrate was extracted 'in-flow' instead of introducing it into the system with a liquid pump. This part of the research was performed at a partner University (University of Valladolid, Spain) and therefore the components used were different from those at Nottingham. The continuous

flow oxidation equipment consisted of several cylinders, pumps and taps and all components were connected by 1/16" 316 stainless steel tubing (Gyrolok). The CO<sub>2</sub> (99.9 %, Carburos Metalicos) was supplied *via* a cylinder (1) to a cold bath that fed the cold CO<sub>2</sub> to an HPLC pump (2). The cooling system cooled down the CO<sub>2</sub> to -20 °C but the temperature was rising during the continuous flow experiment up to -12 °C. The CO<sub>2</sub> passed thorough a vessel filled with wet glass wool (12) in order to obtained water-saturated CO<sub>2</sub>. The water-saturated CO<sub>2</sub> entered the cholesterol vessel (13) filled with alternate layers of cholesterol and glass beads, and 'extracted' cholesterol. The O<sub>2</sub> (99.9 %, Carburos Metalicos) was supplied *via* a cylinder (4) to a manual regulator (5) where the desired O<sub>2</sub> pressure could be set (normally 20 bar overpressure to the system pressure). The O<sub>2</sub> was fed in a Waters switching valve (6) that forwarded the gas to a heated T-piece mixer (7). The mechanism of the Waters switching valve (Waters Two-Position Six-Port Switch Valve) was identical to the one of the Rheodyne system and described below in this Chapter. The stream of CO<sub>2</sub> saturated with cholesterol and mixed with O<sub>2</sub> passed thorough the reactor (14) filled with catalyst. A metal filter 'frit' (Supelco, pore size: 0.5 µm, diameter: 1/4") was placed in the bottom of the reactor to ensure that the catalyst remained in the reactor. An organic stream (8) was introduced after the reactor using a HPLC pump (9) in order to solubilise the oxidation product and the unreacted cholesterol. The system pressure was controlled using a manual BPR ('GO' valves) (15) that also allowed the continuous depressurisation of the system and product collection. The CO<sub>2</sub> pump (2) and the liquid pump (9) had build-in pressure monitors. For further safety, the pressure of the system was monitored by manometers attached to the beginning and the end of the continuous flow system. The heating of the system was performed using a water bath that provided a homogeneous temperature.

The SOP of the oxidation reactor was the following (see Figure 2-6 for numbering of taps, pumps, etc.).

Start up:

1. Fill up the vessel (12) with wet glass wool
2. Fill up the vessel (13) with weighed amount of cholesterol glass beads
3. Fill up the reactor with weighed amount of catalyst

4. Attach the vessels (12) and (13), and the reactor to the system and tighten the fittings
5. Close the GO valve (BPR) (15) approximately half way
6. Open the CO<sub>2</sub> cylinder and tap 3, let the cooling bath chill the CO<sub>2</sub>
7. Start pumping the CO<sub>2</sub> with 10 mL/min flow rate and leave the system to reach the working pressure
8. Set the desired CO<sub>2</sub> flow rate and the operating pressure by adjusting the GO valve
9. Leak test all pressurised fittings at the operating pressure
10. Open the O<sub>2</sub> cylinder and set overpressure on valve 5 (usually 20 bar overpressure compared to the system pressure)
11. Set the pre-calculated O<sub>2</sub> dosage rate on the switching valve (data from The National Institute of Standards and Technology (NIST) database<sup>8</sup> used to calculate O<sub>2</sub> correct dosage rate)
12. Fill up the bath with water, turn the heater and temperature monitors on, and set to the desired temperatures
13. Start the flow of the organic solvent if needed (entry after the reactor in order to obtain the product in solution after depressurisation)
14. Leave CO<sub>2</sub>, O<sub>2</sub> and the organic solvent flowing to reach a steady state

Reaction:

15. Take a sample after the system has reached steady state
16. Leave all streams running and once a sufficient amount of sample obtained submit for analysis
17. If the reaction conditions are to be altered, set the new parameters and repeat steps 13-15

Shutdown:

18. Stop O<sub>2</sub> dosing by switching off 6
19. Close the O<sub>2</sub> cylinder and tap 7
20. Stop the organic flow and close tap 10
21. Turn the heater off and let the system cool down
22. Leave CO<sub>2</sub> flowing to flush the remaining organic solvent in the system
23. Stop pumping CO<sub>2</sub>, close tap 3 and the CO<sub>2</sub> cylinder
24. Depressurise the system stepwise.

#### 2.4.5. Gas Dosage

Flow controller with low flow rates is not available commercially and therefore the gases ( $H_2$  and  $O_2$ ) were supplied using a dosage unit (Rheodyne or Waters switching valve). The pressure of the gases was always set higher than the system pressure (50 bar overpressure for  $H_2$  and 20 bar overpressure for  $O_2$ ) in order to ensure that the gas enters the system. Both dosage units were two-position six-port switching valves that could dose the gas into the system nearly in a continuous manner. The continuity depended on the volume of the loops and switch rate: the smaller volume loops and the faster switch rate, the ‘more continuous’ the flow. The mechanism of the valves is shown in Figure 2-7.

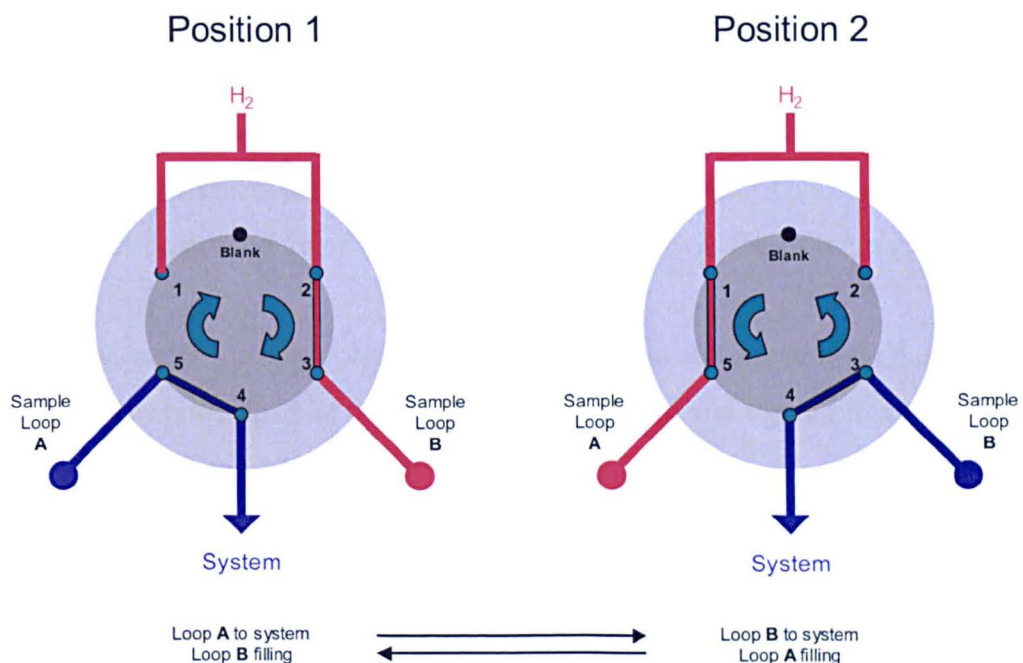


Figure 2-7. The switch mechanism of the valves.<sup>9</sup>

Two loops of the same volume were attached to two ports of the six-port valve. There were two inlets of the gas ( $H_2$  or  $O_2$ ). One port was the entry to the system and the remaining sixth port was blanked. When the valve was in position 1, loop A was emptied into the system and loop B was filled up with gas. In position 2, loop A was filled with gas from the cylinder and loop B was emptied into the system. The switch rate was calculated using the database

provided by the National Institute of Standards and Technology<sup>8</sup> to obtain the desired gas to substrate ratio.

#### **2.4.6. The Small Scale Screw Top Autoclave**

A small volume 60 mL screw top autoclave was used to perform batch hydrogenation reactions at Nottingham. The autoclave consists of a body and a head that can be screwed together with a force of 220 Nm. The autoclave had two inlets/outlets. A 1/8" pipe was attached to one of the inlets that allowed charging the vessel and monitoring the pressure during an experiment. A thermocouple was introduced through the other inlet to monitor the temperature inside the reactor. A 230 V band heater was attached to the body of the cell and heated to the desired temperature. Pressure and temperature monitors were attached to a trip that switched off the heating when an overpressure or overtemperature was recorded. The stirring of the reaction mixture could be provided by placing a magnetic stirrer bar in the cell that was controlled by a stirrer plate placed underneath the reactor.

The operation procedure of the screw top autoclave was the following.

Start up:

1. Measure the appropriate amount of catalysts and substrate in the reactor
2. Attach the head of the autoclave to the body and tighten it with a force of 220 Nm using a torque wrench
3. Attach the outlet of the autoclave to the H<sub>2</sub> cylinder equipped with a low pressure manual regulator (up to 10 bars)
4. Open the H<sub>2</sub> cylinder and set 1 bar pressure on the regulator
5. Open the tap attached to the outlet pipe of the autoclave and charge the vessel
6. Close the tap after approximately 30 seconds and disconnect the autoclave from the cylinder, close the regulator and the cylinder
7. Open the tap and release the gas
8. Repeat steps 3-7 to flush any residual air trapped in the autoclave
9. Repeat steps 3-6 and charge the vessel with H<sub>2</sub> up to the desired pressure (the amount of the gas needed was pre-calculated)
10. Weigh the autoclave

11. Attach the outlet of the autoclave to outlet of the booster pump connected to a CO<sub>2</sub> cylinder
12. Open the CO<sub>2</sub> cylinder, open the inlet of the reactor and then the outlet of the booster pump
13. Open the taps attached to the pump and the autoclave
14. Charge the autoclave with a small amount of CO<sub>2</sub>
15. Weigh the autoclave and if more CO<sub>2</sub> is needed repeat steps 10-14 (the amount of CO<sub>2</sub> was pre-calculated to obtain the desired pressure at a particular reaction temperature)
16. Attach the band heater to the autoclave
17. Place the autoclave on a stirrer plate and attach the outlet to a pressure monitor
18. Open the tap attached to the autoclave
19. Turn heaters and temperature monitors on and set to the desired temperatures
20. Turn the stirring plate on and set the desired speed

Reaction:

21. Continue heating and stirring for a desired time

Shutdown:

22. Turn the heater and the stirring off and let the system cool down
23. Disconnect the band heater
24. Place the autoclave in dry ice and spill acetone on the ice for further cooling while monitoring the pressure of the cell continuously
25. Once the system pressure reaches 1 bar the autoclave is safe to open
26. Open tap of the autoclave and open the autoclave using a torque wrench
27. Collect the product and the catalyst.

#### **2.4.7. The Small Scale Clamp Autoclave**

A small volume 8 mL clamp autoclave (Figure 2-8) was used to perform oxidation in batch at Nottingham. The body and the head of the autoclave were sealed together with a clamp with an O-ring as seal (BSL: EPDM 70, size: 42 x 2 mm) between the two parts. The autoclave had one inlet and one outlet of a 1/8" pipe. The temperature of the cell could be monitored by a thermocouple

inserted in the cell *via* another 1/8" pipe. A 230 V band heater was attached to the body of the cell and heated to the desired temperature. Pressure and temperature monitors were attached to a trip that switched off the heating when an overpressure or overtemperature was recorded. Stirring of the reaction mixture could be provided by placing a magnetic stirrer bar in the cell that was controlled by a stirrer plate placed underneath the reactor.

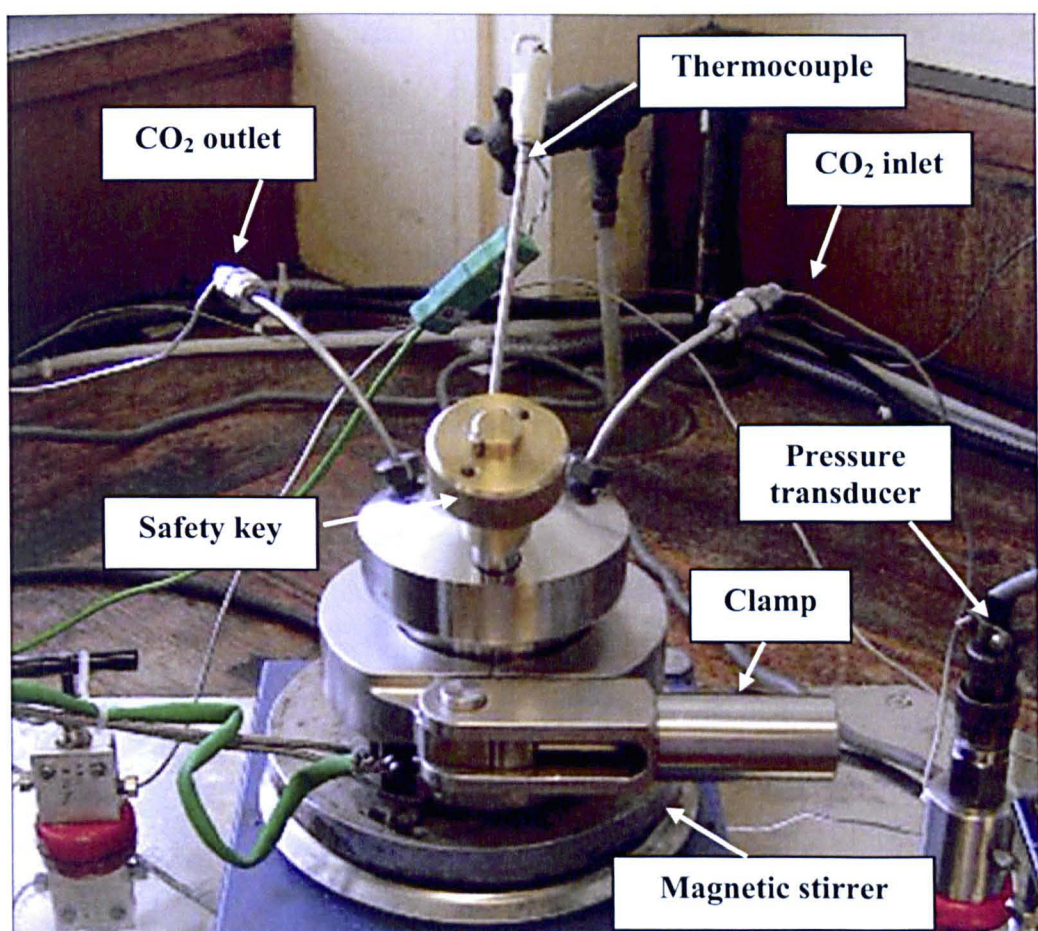


**Figure 2-8. The clamp autoclave.**

The standard operation procedure of the clamp autoclave was the following.

Start up:

1. Measure the appropriate amount of catalysts and substrate in the reactor
2. Attach the head of the autoclave to the body, place in the O-ring seal and close it with the clamp
3. Place the safety key in the cell
4. Attach the inlet pipe of the autoclave to the O<sub>2</sub> cylinder equipped with a low pressure manual regulator (up to 8 bars)

5. Open the O<sub>2</sub> cylinder and set 0.5 bar pressure on the regulator
6. Open the tap attached to the inlet pipe of the autoclave and charge the vessel
7. Open the tap attached to the outlet pipe of the autoclave and flush the system to remove any residual air trapped in the cell
8. Close the outlet tap of the autoclave and charge the cell with O<sub>2</sub> up to the desire pressure and close the tap. Attention! It is important to consider the explosion limits! (Lower Explosive Limit for IPA is 2.02 %, Upper Explosive Limit for IPA is 11.8 %, as percentage-by-volume in air.<sup>10</sup>)
9. Attach the inlet and outlet pipes of the autoclave back to the system
10. Attach the band heater to the autoclave and place the autoclave on a stirrer plate and start stirring
11. Heat the autoclave to the desired temperature
12. Once reaches the desired temperature, open the tap attached to the inlet pipe of the autoclave and charge the cell with CO<sub>2</sub> using a booster pump up to the desired pressure
13. Close the tap attached to the inlet pipe of the autoclave and keep supervising the reaction

Reaction:

14. Continue heating and stirring for a desired time

Shutdown:

15. Turn the heater and the stirring off and let the system cool down
16. Disconnect the band heater
17. Place the autoclave in dry ice and spill acetone on the ice for further cooling while monitoring the pressure continuously
18. Once the system pressure reaches 1 bar the autoclave is safe to open
19. Open the outlet tap of the autoclave and open the autoclave by removing the safety key and opening the clamp
20. Leave the body of the cell under a fume hood to let the CO<sub>2</sub> evaporate
21. Collect the product and the catalyst.

#### 2.4.8. The Variable Volume View Cell (VVVC)

Experiments using a variable volume view cell (VVVC) were performed to investigate the solubility of  $\alpha$ -tetralol in scCO<sub>2</sub>. Details of the VVVC have been described elsewhere<sup>11</sup> and therefore only a brief description is given here. The VVVC is a stainless steel vessel with two sapphire windows that allows the user to have a clear view of the cell contents. A white backlight is used to illuminate the cell. The rear sapphire window can be moved using a piston, and therefore can be used to alter the volume and thus the pressure of the cell (Figure 2-9). The body of the cell can also be heated. Different conditions can be investigated by changing the pressure and temperature.

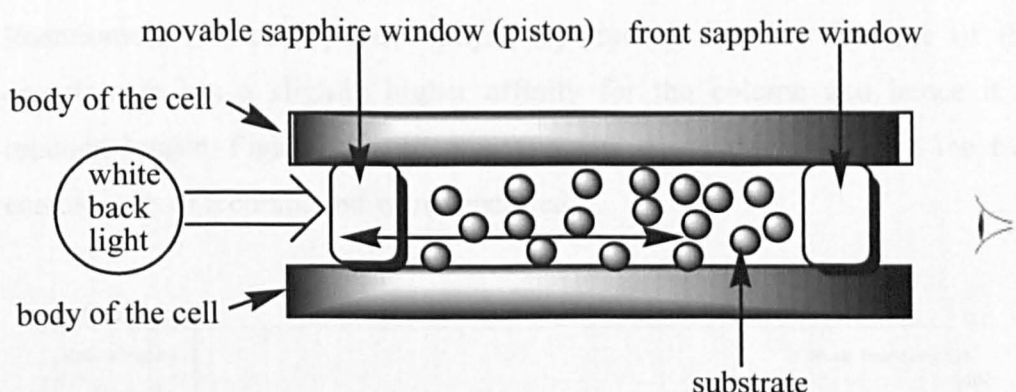


**Figure 2-9. Schematic diagram of the variable volume view cell (VVVC).** The VVC is a stainless steel vessel with two sapphire windows. White light is used to obtain a clear view of the cell content for the user. As the rear piston can be moved, the volume of the cell and therefore the pressure inside can be altered. The body of the cell can be heated. The heaters are located in the body of the cell. Different conditions can be investigated by changing the pressure and temperature.

#### 2.5. Analytical Techniques

In this section, the analytical techniques used throughout this study are detailed. Different chromatography (GLC, HPLC) and spectroscopy techniques (UV-Vis, NMR, ICP-MS), dynamic light scattering (DLS), scanning electron microscopy (SEM), gel electrophoresis (SDS-PAGE) and Karl Fischer titration were used to analyse the reaction products and to characterise the immobilised catalysts. The more commonly used analytical techniques are described in less detail than the ones less commonly used.

### 2.5.1. Gas-Liquid Chromatography (GLC)

The products of the hydrogenation reactions examined throughout this study were analysed by chiral gas-liquid chromatography (chiral GLC). Shimadzu GC17A and GC2010 chromatographs equipped with a Shimadzu 2011 autosampler were used. Chiral columns beta-dex 225 and beta-dex 110 type (Supelco) were used for the analysis of the samples from the hydrogenation and the kinetic resolution reactions, respectively.

The beta-dex 225 column contains 25% modified  $\beta$ -cyclodextrin (CD) (2,3-di-O-acetyl-6-O-TBDMS- $\beta$ -CD) embedded in SPB-20 poly(20% phenyl/80% dimethylsiloxane). The beta-dex 110 column 10% consists of permethylated  $\beta$ -cyclodextrin in SPB-35 (poly (35% diphenyl/65% dimethylsiloxane)). Enantiomers can be separated physically due to the fact that one of the enantiomers has a slightly higher affinity for the column and hence it is retained longer. Figure 2-10 represents a GC chromatogram where the two enantiomers of a compound were separated.

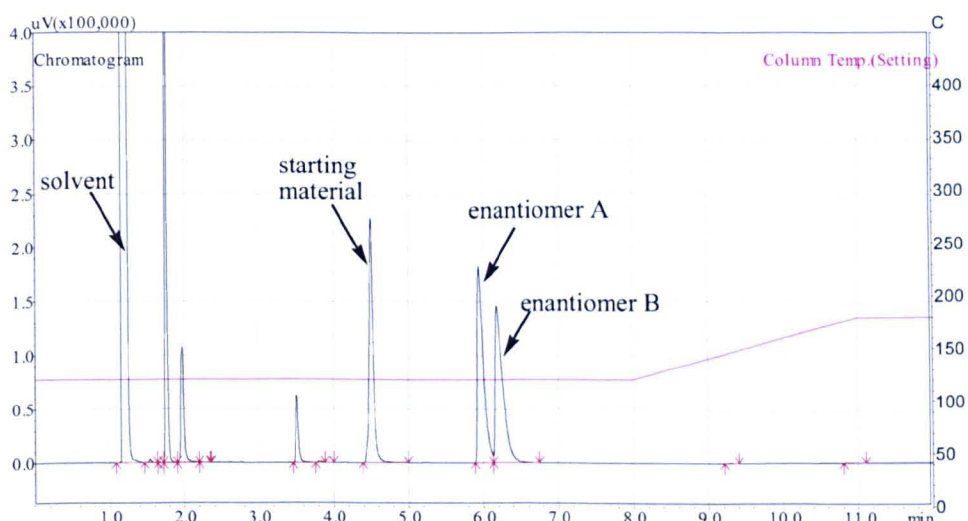


**Figure 2-10. Enantiomer separation by GC. The chromatogram shows the separation of two enantiomers of a compound.**

A flame ionization detector (FID) heated to 300 °C was used for the analysis. Helium was used as the carrier gas. The samples were prepared in 2 mL septum-capped glass vials in appropriate concentrations using acetone as the solvent.

The response factor of the FID is linear in a certain range and can be determined by plotting standards. Therefore calibration had to be performed for all compounds analysed to give accurate analysis. As all compounds are ionised to different extents, standard samples in known concentration have to be prepared.<sup>12</sup> The retention time obtained from the analysis of standards enables to identify the target compound in the reaction mixture. The relationship between the concentration and area % can be established by analysing standards in known concentration.

The enantiomeric excess (*ee*) was calculated by using peak area values measured for each of the enantiomers (Equation 2-1).

$$ee \text{ (%)} = \frac{[\text{enantiomer (a)} - \text{enantiomer (b)}]}{[\text{enantiomer (a)} + \text{enantiomer (b)}]} \times 100$$

**Equation 2-1. The calculation of the enantiomeric excess (*ee*).**

### **2.5.2. High Performance Liquid Chromatography (HPLC)**

The samples from the oxidation of cholesterol were analysed using HPLC. The difference in polarity of cholesterol and its oxidation product 4-cholest-3-one allowed the separation.

A HPLC instrument (Merck Hitachi gradient D-7000 or Waters isocratic 1515) equipped with an autosampler (Merck Hitachi L-7200 or Waters 717) was used. The column was a reverse phase C18 column (XTerra by Waters, 150mm length, 3.0 mm I.D. or Waters 150 mm length, 0.5 mm I.D.). The mobile phase was 100 % acetonitrile at flow rates 0.4 mL/min or 0.6 mL/min. The column was heated to 40 °C or 60 °C. A UV detector was used at 210 nm. The samples were prepared in 1.5 mL septum-capped glass vials in appropriate concentrations.

### **2.5.3. Ultraviolet-Visible Spectroscopy (UV-Vis)**

UV-Vis (200-700 nm) spectroscopy was used to monitor the activity of catalase by measuring the absorbance of H<sub>2</sub>O<sub>2</sub> at 240 nm and also to analyse the dye formation reactions at 500 nm (UV spectrometer: Agilent 8453). The reaction medium of both activity assays was sodium phosphate buffer (20 mM,

pH 7.0) containing Triton X-100 surfactant (0.5 mL/L) which was used as UV blank.

#### **2.5.4. Inductively Coupled Plasma – Mass Spectrometry (ICP-MS)**

ICP-MS was used to determine the Rh leaching during the catalyst immobilisation and the continuous flow hydrogenation reactions. The ligand leaching could also be determined by analysing the Fe content of the samples. ICP-MS is the combination of inductively coupled plasma and mass spectrometer that can be used to detect traces of metals. An aqueous sample is introduced into the plasma that evaporates any solid and breaks the sample into its component atoms. The plasma temperature is very high, of the order of 10000 K which ionises most atoms of many chemical elements. The mass spectrometer receives the ions from the plasma and separates them according to their mass-to-charge ratio. The ion signal received by the mass spectrometer detector is proportional to the concentration.<sup>13</sup>

An ICP-MS instrument (Thermo-Fisher Scientific X-Series<sup>II</sup>) with a ‘hexapole collision cell’ (7 % H<sub>2</sub> in helium) upstream of the analytical quadrupole was used for the analysis. Samples were introduced from an autosampler (Cetac ASX-520) through a concentric glass venturi nebuliser (Thermo-Fisher Scientific; 1 mL/min). Samples of 10 mL were prepared (standards and unknown samples) using a 2 % nitric acid solution. The calibration standards of Rh and Fe were run covering the range 0 to 100 ppb. The samples collected during the continuous flow experiments and catalyst immobilisation were diluted to the concentration range 0 to 100 ppb. Three replicates were measured for each sample. The data processing was undertaken using Plasmalab software (version 2.5.4; Thermo-Fisher Scientific) set to employ separate calibration blocks and, where necessary, instrument cross calibration was used to calculate results for those samples that had tripped from pulse counting detection mode to analogue mode.

#### **2.5.5. Dynamic Light Scattering (DLS)**

It was attempted to measure the particle size of the CLEA using dynamic light scattering technique. The description of the technique can be found in detail in another Thesis<sup>14</sup> and therefore only a brief description is given here. Dynamic

light scattering is used to determine particle size distribution by measuring the fluctuation of the scattered light. The intensity of the scattered light depends on the size of the particles. The instrument used here was a Malvern Zetasizer Nano S equipped with a back scattering detector and a He-Ne laser as light source.

Unfortunately, the particle size determination of the CLEA using DLS was unsuccessful. The suspension of the CLEA was very unstable and settled too quickly. The suspension was then diluted, but its stability was still very poor and the results of the DLS analysis were not reproducible. Flow DLS equipment may be suitable for analysing the particle size of CLEA but it was not available to us. Scanning electron microscopy (SEM) has been shown previously to be appropriate for analysing the morphology and particle size of CLEA<sup>3</sup> and was also used in this work.

#### **2.5.6. Scanning Electron Microscopy (SEM)**

Scanning electron microscopy (SEM) was used to determine the size and morphology of the CLEA. In SEM, a high energy electron beam is focused on the sample. The electrons interact with the atoms of the sample and the electrons scattered or emitted by the sample are detected.<sup>15</sup>

The samples were prepared using a single drop of liquid from the top portion of each sample (suspension of CLEA) that was pipetted onto a glass cover slip and dried at room temperature. The samples were then gold coated under vacuum. High vacuum mode using secondary electron detection was used for viewing the samples. The images were taken using a FEI Quanta 600 or Quanta 200 scanning electron microscope. The image shown in Figure 2-11 represents an SEM image of *Candida antarctica* lipase CLEA.

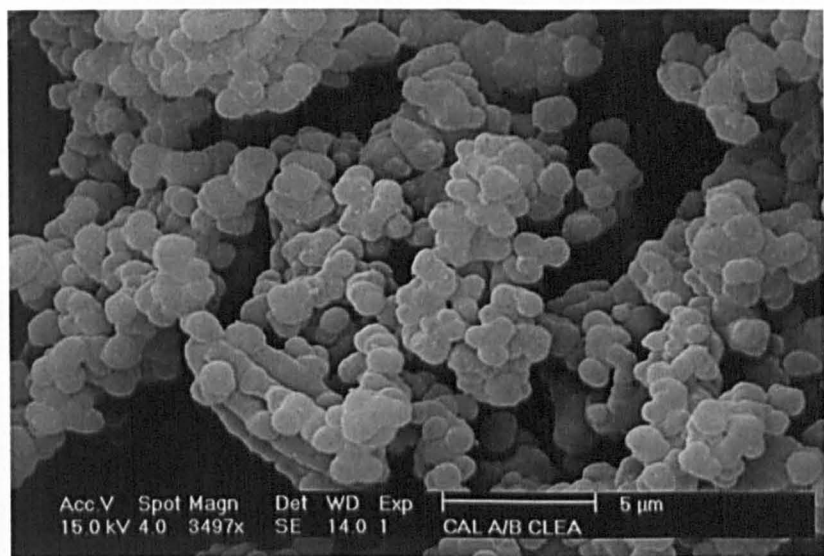


**Figure 2-11. SEM image of *Candida antarctica* lipase A/B CLEA.<sup>3</sup>**

### 2.5.7. Sodium Dodecyl Sulfate Polyacrylamide Gel Electrophoresis (SDS-PAGE)

SDS-PAGE analysis was used to quantify the released protein from catalase under different conditions, which was used to evaluate the efficiency of the cross-linking. In SDS-PAGE, the protein fractions can be separated according to their size (electrophoretic mobility).

By boiling the samples, the catalase tetramer breaks to subunits of which size can be determined by electrophoresis. The samples of the supernatant collected during the preparation of the CLEA were analysed.

Precast gels (Criterion XT) and synthesized gels were used for the analysis. The ‘home made’ gels were prepared using an 8 % resolving gel and a 6 % stacking gel. The samples were prepared using 30 μL sample mixed with 30 μL loading dye (2x concentrated) or with 10 μL loading dye (4x concentrated) on the ‘home made’ or the precast gels, respectively. The mixture of the sample and loading dye was boiled for 5 minutes before loading on the gel. 30 μL sample was loaded on the gel in both cases. A marker (30 μL, BioRad Precision Plus Protein Standards, Blue Prestained) was also loaded on each gel. The gel was run at 100 V for 180 minutes in order to obtain a good quality separation. To visualize the bands on the gel, a Comassie Blue staining solution was used. The gel was placed in the staining solution and left there for 1 hour with agitation. (The precast gel was washed before the

staining step using a dilute MeOH solution in order to remove the membrane of the gel.) The following step was destaining. The gel was agitated in the destaining solution (containing 20% MeOH) for 30 minutes and it was repeated 3 times using a fresh solution or until the bands became clearly visible. The gel was then photographed and analysed considering the standard. A sample gel is presented below for further explanation (Figure 2-12).

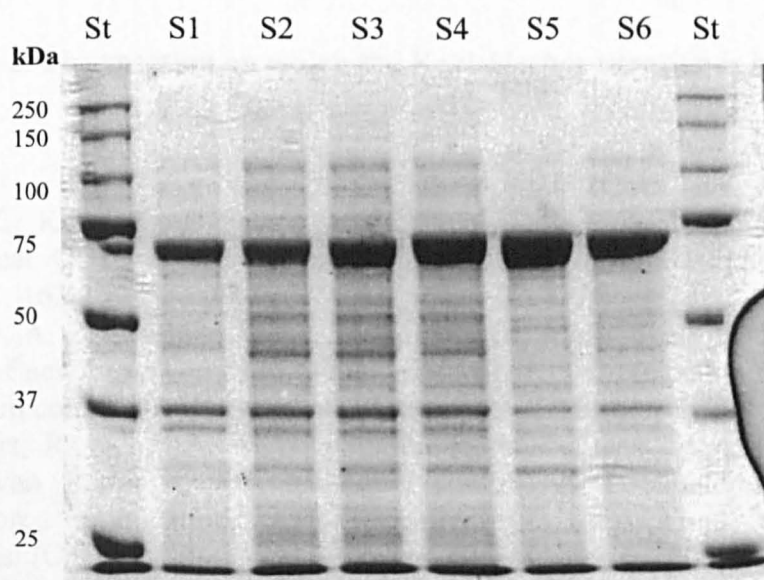


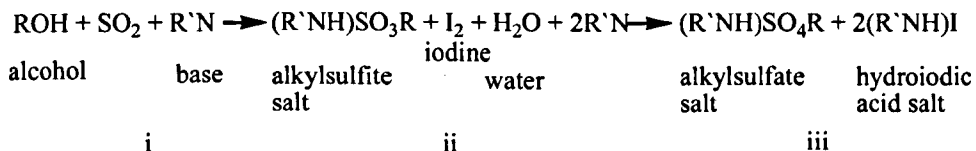
**Figure 2-12. SDS-PAGE analysis of protein samples.<sup>16</sup>** In this Figure ‘St’ stands for standard (protein standard) and ‘S1’-‘S6’ are unknown samples. The size of the protein fractions contained in the standards is marked in the Figure on the left hand side that was considered for the size determination of the proteins in the unknown samples.

#### 2.5.8. Karl-Fischer Titration

Karl-Fischer titration was used to quantify the water content in the solvents used for conducting kinetic resolution. The aim of the research was to investigate enzymatic reactions in a non-aqueous medium and therefore the amount of water present was important.

The titration is based on a reaction between an alcohol (ROH) and sulfur dioxide (SO<sub>2</sub>), and a base (R'N) to form an intermediate (alkylsulfite salt). The intermediate alkylsulfite salt is oxidised to an alkylsulfate by iodine. Sulphur dioxide (i), pyridine (i) and iodine (ii) are contained in the Karl Fischer reagent. Methanol was used as alcohol (ROH) (i) and water (ii) was present as water content of the solvent to be analysed. The oxidation reaction consumes

water and once all the water is used, the iodine excess is detected voltammetrically by the titrator indicator electrode. To obtain an accurate analysis, triplicates of the same samples were analysed. The Karl-Fischer titration is based on the reaction shown in Equation 2-2.



**Equation 2-2. The reaction on which the Karl-Fischer titration is based.**

## References

- Novak, Z., Knez, Z., Diffusion of methanol-liquid CO<sub>2</sub> and methanol-supercritical CO<sub>2</sub> in silica aerogels. *Journal of Non-Crystalline Solids* **1997**, 221, 163-169.
- Suarez, P. A. Z., Dullius, J.E.L., Einloft, S., de Souza, R.F., Dupont, J., The use of new ionic liquids in two-phase catalytic hydrogenation reaction by rhodium complexes. *Polyhedron* **1996**, 15, 1217-1219.
- Schoevaart, R., Wolbers, M.W., Golubovic, M., Ottens, M., Kieboom, A.P.G., van Rantwijk, F., van der Wielen, L.A.M., Sheldon, R.A., Preparation, optimization, and structures of cross-linked enzyme aggregates (CLEAs). *Biotechnology and Bioengineering* **2004**, 87, (6), 754-762.
- Drobchenko, S. N., Isaeva-Ivanova, L.S., Kleiner, A.R., Lomakin, A.V., Kolker, A.R., Noskin, V.A., An investigation of the structure of periodate-oxidised dextran. *Carbohydrate Research* **1993**, 241, 189-199.
- Sorgedrager, M., PhD Thesis. *Delft University of Technology, Delft (Netherlands)* **2005**.
- Holt, A., Palcic, M.M., A peroxidase-coupled continuous absorbance plate-reader assay for flavin monoamine oxidases, copper-containing amine oxidases and related enzymes. *Nature Protocols* **2006**, 1, 2498-2505.
- Aparicio, J. F., Martin, J.F., Microbial cholesterol oxidases: bioconversion enzymes or signal proteins? *Molecular biosystems* **2008**, 4, (8), 804-809.
- Linstrom, P. J., Mallard, W.G., NIST Chemistry WebBook, NIST Standard Reference Database Number 69. *National Institute of Standards and Technology, Gaithersburg MD, 20899*, <http://webbook.nist.gov>.
- Stephenson, P., PhD Thesis. *University of Nottingham, Nottingham (UK)* **2005**.
- Weast, R. C., in Handbook of Chemistry and Physics, 53rd Edition. *The Chemical Rubber Co., Cleveland (USA)* **1972-1973**.
- Woods, H. M., PhD Thesis. *University of Nottingham, Nottingham (UK)* **2005**.
- Douglas, A., Skoog, F., Holler, J., Nieman, T.A., in Principles of instrumental analysis. *Saunders, Philadelphia* **1997**.
- Browner, R. F., et.al., edited by Montaser, A., in Inductively coupled plasma mass spectrometry. *Wiley-VCH, London* **1996**.

14. Hobbs, H. R., PhD Thesis. *University of Nottingham, Nottingham (UK) 2006.*
15. Keyse, R. J., Introduction to scanning transmission electron microscopy. *Oxford: BIOS Scientific 1998.*
16. Kondor, B., Master Thesis. *Budapest University of Technology and Economics, Budapest (Hungary) and Lund University, Lund (Sweden) 2005.*

## Chapter 3

# Continuous Asymmetric Hydrogenation using Alumina Supported Homogeneous Chiral Rh Catalysts in scCO<sub>2</sub>

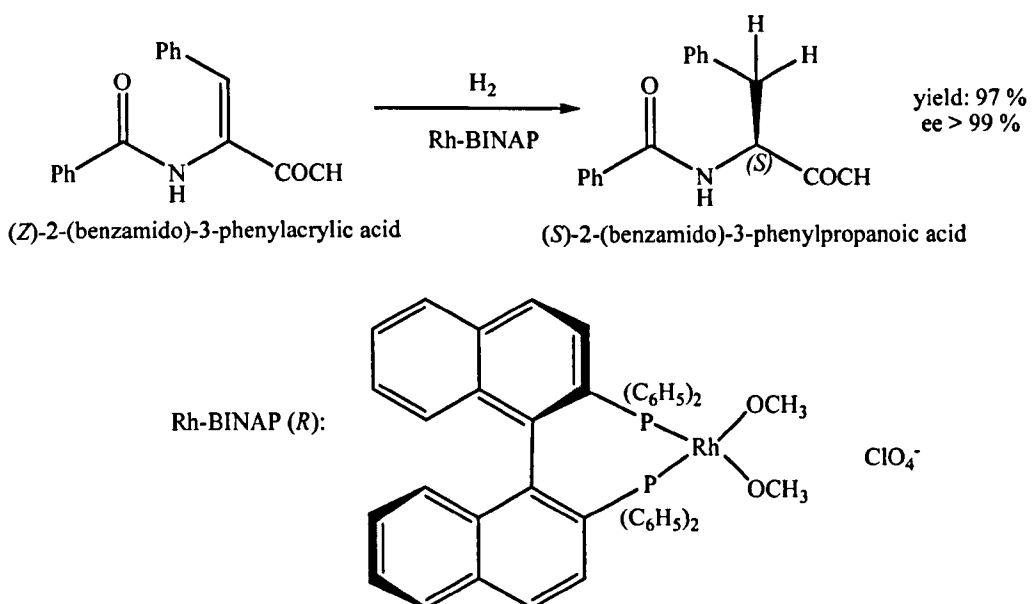
This Chapter begins with an overview of catalytic asymmetric hydrogenation in scCO<sub>2</sub> reported to date. It then describes the progress achieved in continuous flow asymmetric hydrogenation during this research project.

### 3.1. Catalytic Asymmetric Hydrogenation

The production of enantiomerically pure compounds has become increasingly important because the two enantiomers of the same compound can have completely different biological activities, which is of great concern in the pharmaceutical industry. One of the most widely known examples of the different effect of two enantiomers is thalidomide which was used in the 1960s to reduce nausea and vomiting during pregnancy. One enantiomer in the drug is causing birth defects (monster making) such as missing or stunted limbs.<sup>1</sup>

Until the 1970's, the primary method for obtaining pure enantiomeric compounds was the resolution of racemic mixtures.<sup>2</sup> Through the development of asymmetric catalysis, a small amount of chirally modified catalyst can produce large amounts of enantiopure product.<sup>3,4</sup>

Hydrogenation is one of the most common reactions in the chemical industry.<sup>5</sup> Catalytic asymmetric hydrogenation enables the production of enantiomerically pure compounds in a single step from a prochiral substrate<sup>3,4</sup>. One of the first examples of asymmetric catalytic hydrogenation to produce enantiomerically pure compounds was performed by Noyori and co-workers applying a bisphosphine ligand in 1980. The pioneering research of Sharpless, Knowles and Noyori was recognised by Nobel Prize for Chemistry in 2001: “the development of catalytic asymmetric synthesis”. The enantioselective hydrogenation of  $\alpha$ -(acylamino)acrylic acids using a Rh catalyst modified with 2,2'-*bis*(diphenylphosphino)-1,1'-binaphthyl (BINAP) ligand was performed in EtOH and high enantioselectivity was observed (Scheme 3-1).<sup>6</sup>



**Scheme 3-1.** An example for the asymmetric hydrogenation of  $\alpha$ -(acylamino)acrylic acids using an Rh(I)-BINAP catalyst.<sup>6</sup>

Reaction conditions: H<sub>2</sub> pressure: 3-4 bar, 0.5-1.0 mmol of substrate in 20-30 mL EtOH.

There are two classes of enantioselective catalysts: homogeneous metal complexes containing chiral ligands and heterogeneous metal catalysts in the presence of chiral modifiers. The metal component is the activating function while the ligand is responsible for the enantiocontrol. The most commonly used metals are Cu, Ir, Mn, Os, Pd, Pt, Rh, Ru, and Ti. The majority of the ligands used presently in asymmetric catalysis are phosphorous based.<sup>2, 7, 8</sup> The review by Tang list a large number of phosphorous ligands that can be used for the asymmetric hydrogenation of various substrates.<sup>9</sup>

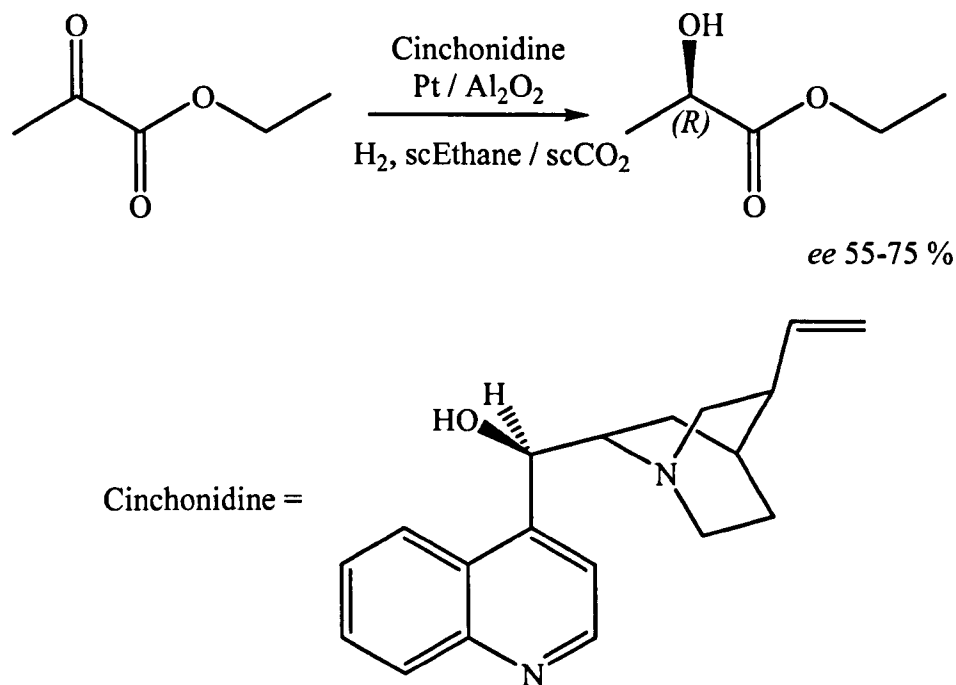
### 3.2. Continuous Catalytic Asymmetric Hydrogenation in SCFs

Hydrogenation has been shown to be possible under classical conditions (in organic solvents: gas-phase hydrogenation, liquid-gas system) and also in supercritical fluids (SCFs).<sup>10-13</sup> Despite the need for high pressure reactors when using SCFs as solvent for conducting chemical transformations, SCFs (especially supercritical CO<sub>2</sub>) have become increasingly important as alternative reaction medium. The advantages of supercritical CO<sub>2</sub> (scCO<sub>2</sub>) for hydrogenation reactions are the following.<sup>10</sup>

- i) Complete miscibility of scCO<sub>2</sub> with H<sub>2</sub> that reduces the mass transport difficulties compared to a liquid-gas system.
- ii) Adjustable solvent density (viscosity, and solute solubility) by altering the pressure and temperature.
- iii) Easy separation of the solvent from the product by simple decompression of the high pressure system.
- iv) Reduction in the use of volatile organic solvents.

The production of fine chemicals in a flow system gives the advantage of continuous manufacture and also a reduced risk due to smaller reactor size and reduced amount of reactants present at any one time as compared to a batch system.

A number of papers have been published on homogeneously catalysed asymmetric hydrogenation in SCFs<sup>14-17</sup> but only a few have reported continuous enantioselective hydrogenation in SCFs<sup>18-20</sup> including two papers<sup>19, 20</sup> published by our group. The latter<sup>20</sup> describes the results presented here. The continuous asymmetric hydrogenation of ethyl pyruvate in continuous flow SCF system was performed by Baiker and co-workers with continuous feed of the chiral modifier (Scheme 3-2).<sup>18</sup> The hydrogenation of ethyl pyruvate (and other substrates) has also been performed in a non-supercritical continuous flow toluene or toluene + acetic acid system using a H-Cube reactor<sup>21</sup> with the chiral modifier continuously fed, as shown previously in SCFs by Baiker.



**Scheme 3-2. Continuous asymmetric hydrogenation of ethyl pyruvate in SCFs over cinchonidine modified Pt catalyst performed by Baiker and co-workers.<sup>18</sup>**

### 3.3. Supported Homogeneous Chiral Rh Catalysts

The reason why there are very few publications on continuous asymmetric hydrogenation in a flow system may be the poor availability of heterogeneous chiral catalysts. Recently, Augustine *et al.* developed a technique to anchor homogeneous catalysts<sup>22</sup> that has been shown to work successfully for enantioselective hydrogenation.<sup>23</sup> The Augustine anchored catalyst, with general formula of  $[\text{Rh}(\text{nbd})_2/\text{PTA}/\text{Alumina}]^+[\text{BF}_4]^-/\text{PTA}/\text{Alumina}$  ( $\text{nbd} = 2,5\text{-norbornadiene}$ , PTA = phosphotungstic acid  $\text{H}_3\text{O}_{40}\text{PW}_{12}$ ) and brand name of CATAXA, is a Rh based catalyst immobilised on alumina.<sup>22</sup> The Rh is bound to alumina *via* phosphotungstic acid binder. The schematic structure of the chiral catalyst is shown in Figure 3-1.

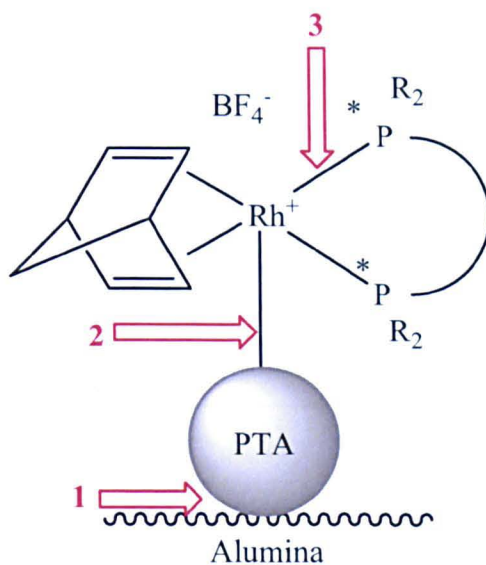
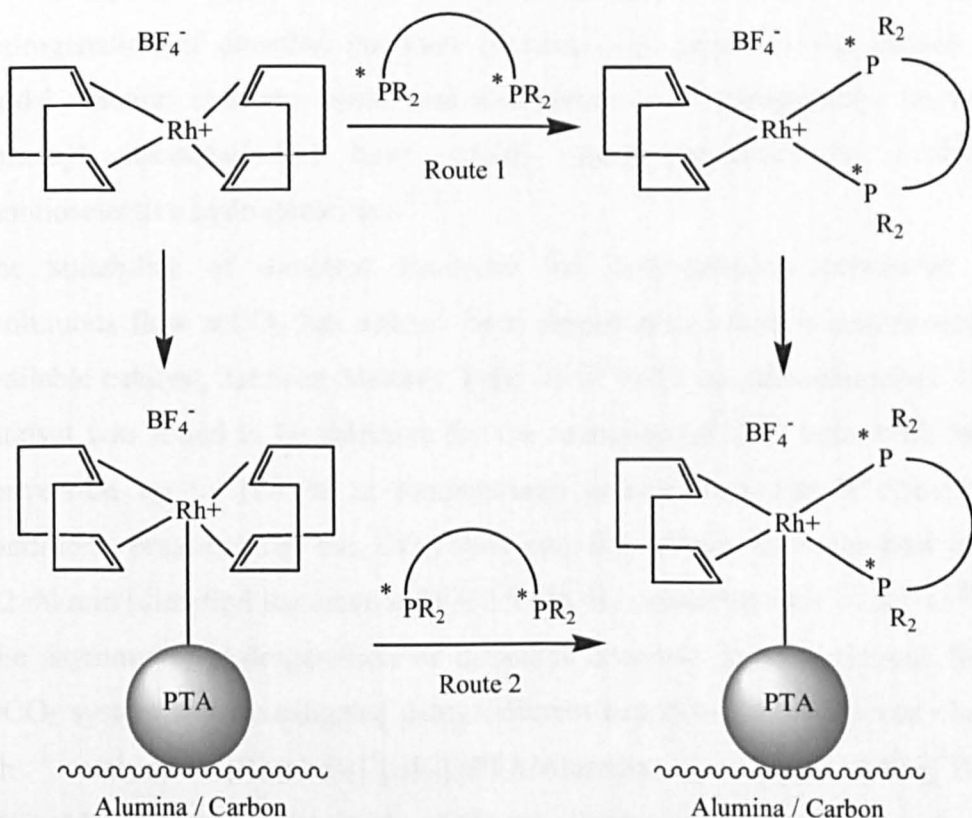


**Figure 3-1. General structure of the Augustine anchored catalyst.  $[\text{Rh}(\text{nbd})(\text{PR}_2^*\text{-}\text{PR}_2^*)]^+[\text{BF}_4^-]/\text{PTA}/\text{Alumina}$  where nbd: 2,5-norbornadiene,  $\text{PR}_2^*\text{-}\text{PR}_2^*$ : bisphosphine ligand, PTA: phosphotungstic acid  $\text{H}_3\text{O}_{40}\text{PW}_{12}$ .**

The numbers (in red) in Figure 3-1 indicate the positions of possible cleavage to loss of chiral or total activity. The stability of the chiral catalyst  $[\text{Rh}(\text{nbd})(\text{Skewphos})]^+[\text{BF}_4^-]/\text{PTA}/\text{Alumina}$  has been investigated previously in a continuous flow hydrogenation reaction in scCO<sub>2</sub> by Stephenson at Nottingham.<sup>24</sup> The Rh and W content of the product collected by continuous depressurisation of the flow system was determined using ICP-MS analysis. The tungsten leaching was found to be very low (below 1 ppm) at all reaction conditions (reaction conditions: pressure: 100 bar, temperature up to 100 °C, CO<sub>2</sub> flow rate: 0.5 ml/min, substrate flow rate: 0.2 ml/min (dimethyl itaconate in IPA 2.5 M), H<sub>2</sub> : substrate ratio = 2.5 : 1). As there was no tungsten leaching observed, the tungsten-alumina link (1 in Figure 3-1) should be stable and the rupture of Rh(nbd)<sub>2</sub>/PTA or Rh(nbd)(ligand)/PTA from the alumina should not be expected. The Rh leaching was above 8 ppm at higher temperatures (above 100 °C) which suggests that the PTA-Rh link (2 in Figure 3-1) should be less stable at high temperatures. The ligand leaching, the stability of the Rh-ligand link (3 in Figure 3-1) was not studied at this time. The achiral CATAXA ( $[\text{Rh}(\text{nbd})_2]^+[\text{BF}_4^-]/\text{PTA}/\text{Alumina}$ ) can be modified with bisphosphine ligands, which produces supported homogenous chiral catalysts. The chiral ‘motif’ of the catalyst is obtained *via* a ligand exchange between the original nbd (or COD) ligand and the bisphosphine ligand. The Augustine

supported homogeneous chiral catalyst can be prepared in two ways: 1) synthesis of the chiral species before immobilisation and 2) immobilisation of the achiral species before the addition of the ligand (Scheme 3-3). A variety of bisphosphine ligand can be added to the Augustine catalyst<sup>25</sup>, and therefore various substrate specific chiral catalysts can be prepared.



**Scheme 3-3. The preparation of the supported homogeneous Rh catalyst. Route 1: the synthesis of the chiral species before immobilisation, Route 2: the immobilisation of the achiral species before the addition of the ligand.**

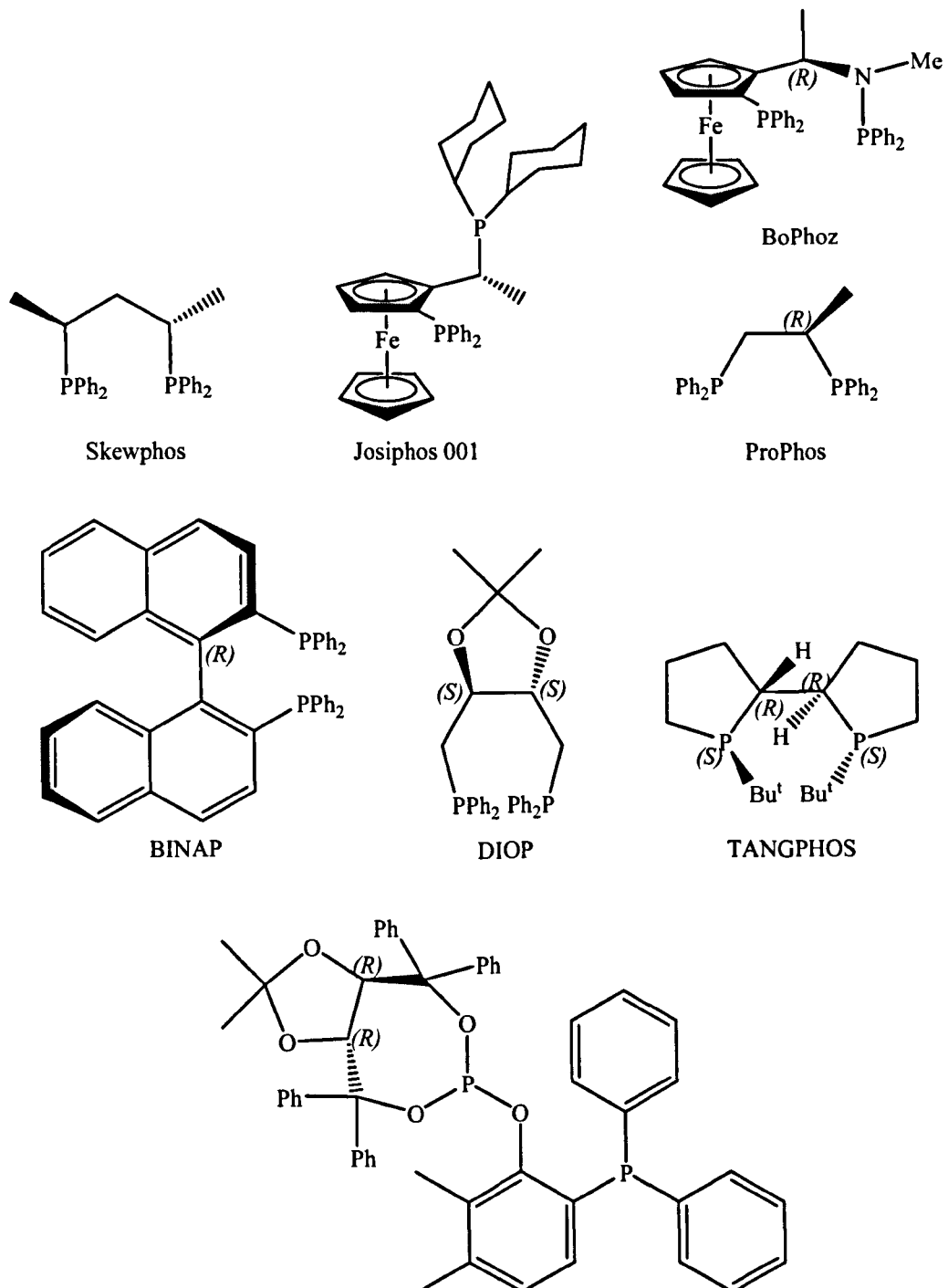
Route 1 was investigated by Johnson Matthey (JM) and various supported homogeneous chiral catalysts were prepared. Route 2 was investigated at Nottingham. Comparing the results of the asymmetric hydrogenation of dimethyl itaconate in a continuous flow scCO<sub>2</sub> system with [Rh(nbd)(Skewphos)]<sup>+</sup>[BF<sub>4</sub>]<sup>-</sup>/PTA/Alumina prepared *via* route 1 (by JM) and route 2 (at Nottingham), the viability of the catalyst preparation in route 2 could be evaluated. The conversion and enantioselectivity of the reaction were similar with both chiral catalysts. Having confirmed that route 2 is viable for preparing supported homogeneous chiral catalyst<sup>24</sup>, this method was used throughout this research project. A detailed procedure for the chiral catalyst preparation is described in Chapter 2.

### 3.4. Continuous Asymmetric Hydrogenation of Dimethyl Itaconate in scCO<sub>2</sub>

The activity of supported homogeneous chiral Rh catalysts was examined for the asymmetric hydrogenation of alkenes in a continuous flow scCO<sub>2</sub> system at Nottingham prior to this research project.<sup>19, 24</sup> The asymmetric hydrogenation of dimethyl itaconate (Scheme 3-5, page 66) was chosen as model reaction to study continuous enantioselective hydrogenation because dimethyl itaconate has been widely used previously to evaluate enantioselective hydrogenations.<sup>26, 27</sup>

The suitability of dimethyl itaconate for hydrogenation conducted in continuous flow scCO<sub>2</sub> has already been demonstrated with a commercially available catalyst, Johnson Matthey Type 31 (2 % Pd on silica/alumina). The catalyst was found to be selective for the reduction of C=C bond with high conversion up to 100 % at temperatures greater than 100 °C (reaction conditions: pressure: 100 bar, CO<sub>2</sub>: flow rate: 0.5 ml/min, substrate flow rate: 0.2 ml/min (dimethyl itaconate in IPA 2.5 M), H<sub>2</sub> : substrate ratio = 2.5:1).<sup>24</sup>

The asymmetric hydrogenation of dimethyl itaconate in a continuous flow scCO<sub>2</sub> system was investigated using different supported homogeneous chiral Rh catalysts [Rh(nbd)<sub>2</sub>]<sup>+</sup>[BF<sub>4</sub>]<sup>-</sup>/PTA/Alumina or [Rh(COD)<sub>2</sub>]<sup>+</sup>BF<sub>4</sub><sup>-</sup>/PTA/Alumina modified with different bisphosphine ligands such as Skewphos, Josiphos 001, BoPhoz, Prophos, BINAP, DIOP, TANGPHOS and a Phosphine-Phospite ligand.<sup>24</sup> The structures of the ligands are depicted in Figure 3-2.



Chiral phosphine-phosphite ligand (LigBank)

**Figure 3-2. The structure of the ligands used for preparing supported homogeneous chiral catalyst  $[\text{Rh}(\text{nbd})(\text{Skewphos})]^+[\text{BF}_4]^-/\text{PTA}/\text{Alumina}$  or  $[\text{Rh}(\text{COD})(\text{R}_2\text{P}^*\text{-PR}_2^*)]^+[\text{BF}_4]^-/\text{PTA}/\text{Alumina}$  where nbd: 2,5-norbornadiene, COD: 1,5-cyclo-octadiene,  $\text{R}_2\text{P}^*\text{-PR}_2^*$ : bisphosphine ligand, PTA: phosphotungstic acid  $\text{H}_3\text{O}_{40}\text{PW}_{12}$ . The activity of the chiral catalysts was investigated in the asymmetric hydrogenation of dimethyl itaconate in continuous flow scCO<sub>2</sub>.**

The results of the asymmetric hydrogenation using supported homogeneous chiral Rh catalysts  $[\text{Rh}(\text{nbd})(\text{Skewphos})]^+[\text{BF}_4]^-/\text{PTA}/\text{Alumina}$  or  $[\text{Rh}(\text{COD})(\text{PR}_2^*-\text{PR}_2^*)]^+[\text{BF}_4]^-/\text{PTA}/\text{Alumina}$  are listed in Table 3-1.

**Table 3-1. The results of the asymmetric hydrogenation of dimethyl itaconate in continuous flow scCO<sub>2</sub>.<sup>19, 24</sup>**

Entry	Ligand	T (°C)	P (bar)	Conv (%)	ee (%)
1 <sup>a</sup>	Skewphos	25-70	100	22-41	6-31
2 <sup>a</sup>	Josiphos 001(batch 1)	30-75	100	8-22	3-53
3 <sup>a</sup>	Josiphos 001(batch 1)	30-50	160	25-35	48-77
4 <sup>b</sup>	BoPhoz	30-150	100	0-15	0-3
5 <sup>b</sup>	Prophos	30-70	100	27-34	0-1
6 <sup>b</sup>	Prophos	30, 40	200	14-37	0-1
7 <sup>c</sup>	BINAP	30-60	100	5-19	0-11
8 <sup>c</sup>	BINAP	30-50	200	20-26	9
9 <sup>c</sup>	DIOP	35-55	100	42-61	10-18
10 <sup>c</sup>	DIOP	35-55	160	45-67	10-12
11 <sup>c</sup>	TANGPHOS	35-55	100	0-17	0-1
12 <sup>c</sup>	TANGPHOS	35-55	160	0-24	0
13 <sup>c</sup>	Phosphine-phosphite	50-100	100	0-93	0-4
14 <sup>c</sup>	Phosphine-phosphite	30-70	200	0-80	0-4

\* The catalyst was  $[\text{Rh}(\text{nbd})(\text{Skewphos})]^+[\text{BF}_4]^-/\text{PTA}/\text{Alumina}$  where nbd: 2,5-norbornadiene, PTA: phosphotungstic acid  $\text{H}_3\text{O}_{40}\text{PW}_{12}$ . In all other cases the catalyst was  $[\text{Rh}(\text{COD})(\text{R}_2\text{P}^*-\text{PR}_2^*)]^+[\text{BF}_4]^-/\text{PTA}/\text{Alumina}$  where COD: 1,5-cyclo-octadiene,  $\text{PR}_2^*-\text{PR}_2^*$ : bisphosphine ligand.

<sup>a</sup>) Reaction conditions: CO<sub>2</sub> flow rate: 0.5 mL/min, substrate flow rate: 0.2 mL/min (DMIT in IPA 2.5 M), H<sub>2</sub> : substrate ratio = 2.5 : 1.

<sup>b</sup>) Reaction conditions: CO<sub>2</sub> flow rate: 0.25 mL/min, substrate flow rate: 0.1 mL/min (DMIT in IPA 2.5 M), H<sub>2</sub> : substrate ratio = 2.5 : 1.

<sup>c</sup>) Reaction conditions: CO<sub>2</sub> flow rate: 0.5 mL/min, substrate flow rate: 0.15 mL/min (DMIT in IPA 2.5 M), H<sub>2</sub> : substrate ratio = 4 : 1.

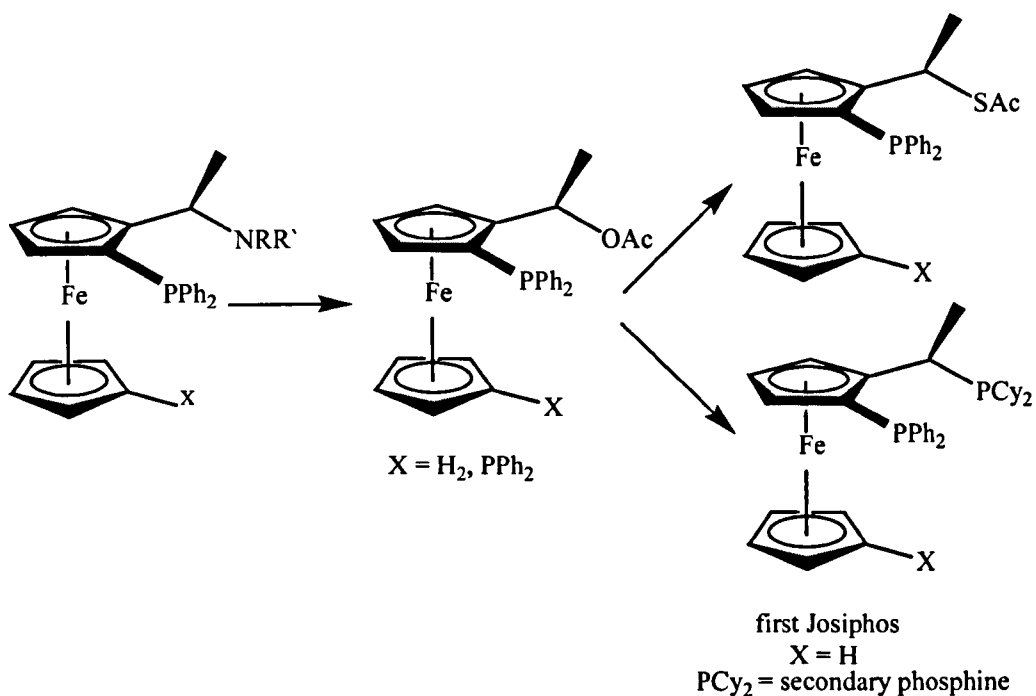
The supported homogeneous chiral Rh catalyst modified with Josiphos 001 ligand,  $[\text{Rh}(\text{COD})(\text{Josiphos 001})]^+[\text{BF}_4]^-/\text{PTA}/\text{Alumina}$ , was found to be the most successful for the continuous asymmetric hydrogenation of dimethyl itaconate in scCO<sub>2</sub>. This catalyst was the most active at temperatures between 35 °C and 55 °C at 100 bar (reaction conditions: CO<sub>2</sub> flow rate: 0.5 ml/min, substrate flow rate: 0.2 ml/min (dimethyl itaconate in IPA 2.5 M), H<sub>2</sub> : substrate ratio = 2.5 : 1). Above 55 °C, the enantioselectivity and the conversion both reached a plateau. The effect of the pressure was also

examined between 60 bar and 180 bar at 60 °C. A peak was observed in the enantioselectivity and conversion at 120 bar but lower activity was found with a further increase in pressure. The reaction gave the best results at 60 °C at 120 bar: enantioselectivity (*S*) 73 % and conversion 39 %.

As the best results were obtained with Josiphos 001 among the other bisphosphine ligands examined by Stephenson, it was thought that similar ligands to Josiphos 001 may be highly active. Several bisphosphine ligands similar to Josiphos 001 have been developed at Solvias AG (Basel, Switzerland), which were investigated for continuous asymmetric hydrogenation of dimethyl itaconate in scCO<sub>2</sub> in this work.

### 3.5. The Development of the Josiphos Type Ligands

The discovery of the Josiphos type ligands began at the Central Research Laboratories of the former Ciba-Geigy. The starting point was the preparation of ferrocenyl ligands carrying different side chains.<sup>25</sup> It was found later that the acetate group at the stereogenic centre could be replaced (upper right part in Scheme 3-4, X = PPh<sub>2</sub>).<sup>28, 29</sup> This finding led to the idea of introducing different PR<sub>2</sub> groups (lower right part in Scheme 3-4). The first example of a Josiphos ligand was X = H. The synthetic route of the first Josiphos type ligand is shown in Scheme 3-4.<sup>30, 31</sup> The first catalytic test was the Rh-catalysed enamide hydrogenation, which showed high success with enantioselectivity > 99 % and a Turn-Over Number (TON, moles of product per mole of catalyst) of around 1000 h<sup>-1</sup>.<sup>30</sup> The whole ligand family was named after a technician Josi Puelo who prepared the first example for the novel chelating ligands bearing two different PR<sub>2</sub> groups.

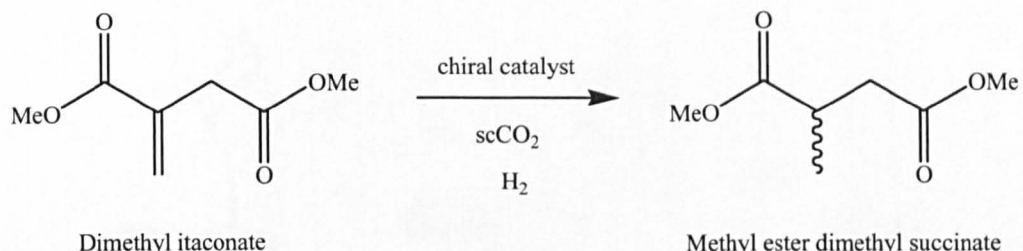


**Scheme 3-4. Synthetic route of the first Josiphos ligand. Substitution reactions at the stereogenic centre of ethyl ferrocene derivatives.<sup>30</sup>**

The synthesis of Josiphos type bisphosphine ligands has continued because the substituents of the ligands are modular and tuneable. This property allows further development of the ligands to obtain high enantioselectivity for a particular reaction.<sup>31</sup>

### 3.6. Results and Discussion

Solvias AG, the trader of the Josiphos type ligands, kindly offered to donate several Josiphos type ligands to determine their activity for continuous asymmetric hydrogenation in scCO<sub>2</sub>. Their performance is evaluated here for the hydrogenation of dimethyl itaconate (Scheme 3-5) using supported homogeneous chiral catalysts [Rh(COD)(R<sub>2</sub>P\*-PR<sub>2</sub>\*)]<sup>+</sup>[BF<sub>4</sub>]<sup>-</sup>/PTA/Alumina or Carbon (Figure 3-3) where PR<sub>2</sub>\*-PR<sub>2</sub>\* was a Josiphos type ligand (Figure 3-4). The results of the research performed prior to this study determined a range of temperature and pressure where the asymmetric hydrogenation of dimethyl itaconate was the most successful in scCO<sub>2</sub>.<sup>24</sup> The Josiphos type ligands were examined in this ‘optimal’ temperature and pressure range.



**Scheme 3-5.** The enantioselective hydrogenation of dimethyl itaconate using supported homogeneous chiral Rh catalyst.

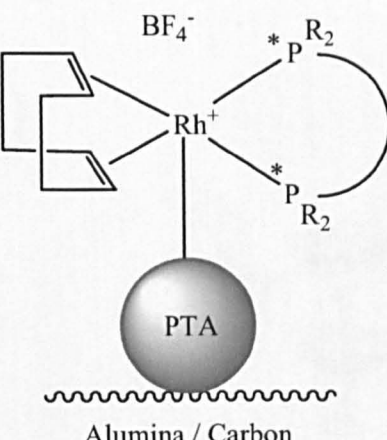


**Figure 3-3.** General structure of the supported homogeneous Rh catalyst  $[Rh(COD)(R_2P^*-PR_2^*)]^+[BF_4]^-$ /PTA/Alumina or Carbon where COD = 1,5-cyclo-octadiene,  $R_2P^*-PR_2^*$  = bisphosphine ligand, PTA = phosphotungstic acid  $H_3O_{40}PW_{12}$ .

The continuous asymmetric hydrogenation of dimethyl itaconate was investigated using  $[\text{Rh}(\text{COD})(\text{PR}_2^*-\text{PR}_2^*)]^+[\text{BF}_4^-]/\text{PTA}/\text{Alumina}$  modified with six different Josiphos type ligands: Josiphos 001, Josiphos 005, Walphos 002, Mandyphos 001, Taniaphos 001, Taniaphos 002. The structures of the ligands are shown in Figure 3-4. The preparation of the chiral catalyst was performed *via* immobilisation of the achiral species before the addition of the bisphosphine ligand (Route 2, Scheme 3-3). The procedure for preparation of the chiral catalysts is described in detail in Chapter 2. Dimethyl itaconate is solid at room temperature and therefore a cosolvent was needed to bring the material into solution. Iso-propanol (IPA) and methanol were used in this work.

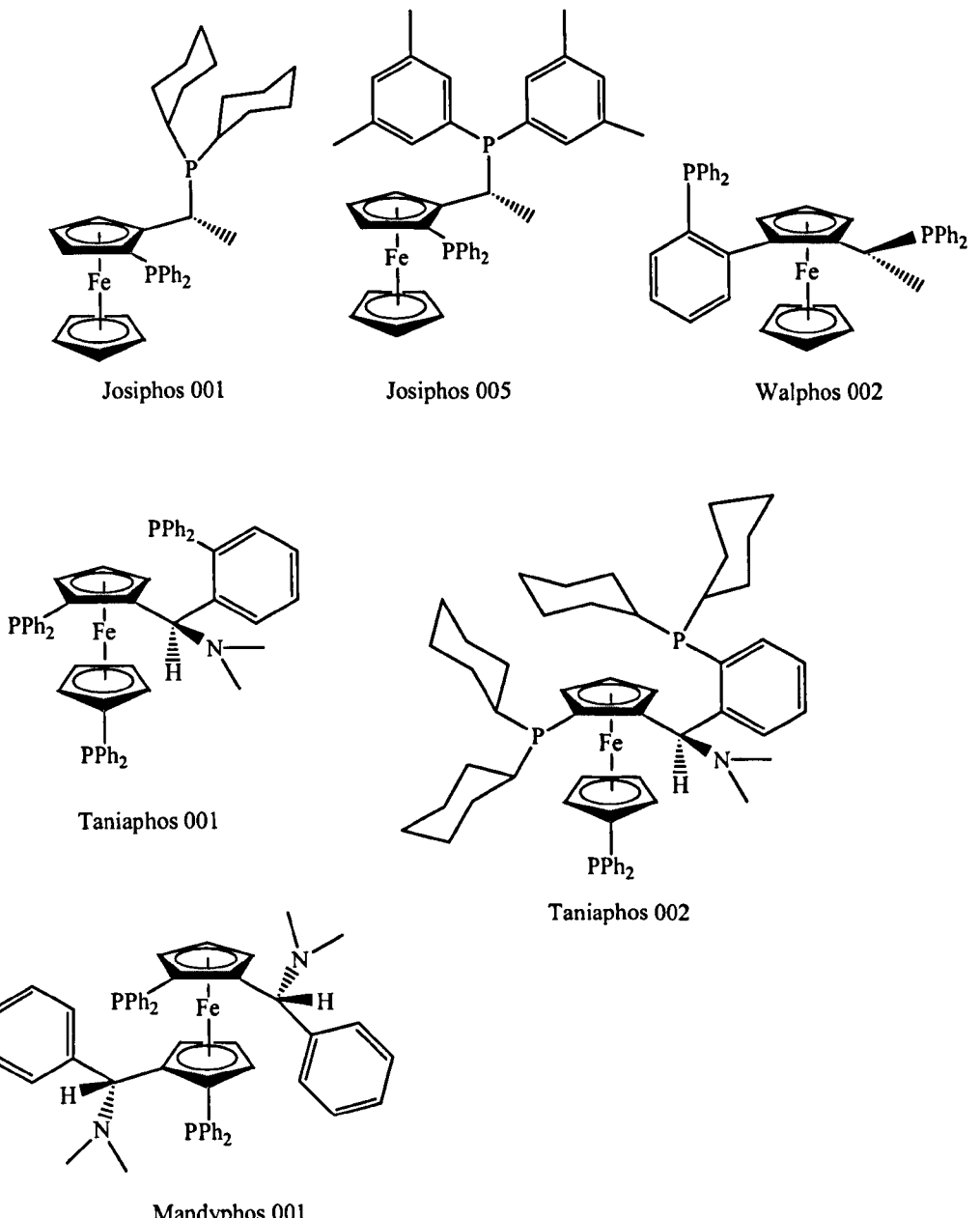


**Figure 3-4.** The structures of the Solvias Josiphos type ligands. The general structure of the supported homogeneous chiral Rh catalyst is  $[\text{Rh}(\text{COD})(\text{R}_2\text{P}^*\text{-PR}_2^*)]^+[\text{BF}_4]^-/\text{PTA}/\text{Alumina}$  ( $\text{COD} = 1,5\text{-cyclo-octadiene}$ ,  $\text{R}_2\text{P}^*\text{-PR}_2^* = \text{bisphosphine ligand}$ , PTA = phosphotungstic acid  $\text{H}_3\text{O}_{40}\text{PW}_{12}$ ).

This research focused on achieving highly enantioselective hydrogenation *via* two key routes i) altering the temperature and pressure of the continuous flow scCO<sub>2</sub> system and ii) changing the bisphosphine ligand attached to the Rh catalyst (CATAXA). The bisphosphine ligands examined here belong to the Solvias Josiphos family. The ligands differentiate in electronic properties and size, which can influence the activity of the whole catalyst system. In addition,

different cosolvents (used to bring the solid dimethyl itaconate into solution) were also examined. The polarity and dielectric constant of the solvent may influence the hydrogenation. Furthermore, different support materials, alumina and carbon, were also investigated. The enantioselectivity will be discussed here in more detail as the main aim of this work was achieving high enantioselectivity for the continuous asymmetric hydrogenation of dimethyl itaconate in scCO<sub>2</sub>.

### **3.6.1. The Effect of the Bisphosphine Ligand on the Enantioselectivity**

The chiral Rh catalysts modified with Josiphos type ligands (Figures 3-3 and 3-4) were examined for the continuous asymmetric hydrogenation of dimethyl itaconate in flow scCO<sub>2</sub> (Scheme 3-5) at temperatures 35-55 °C at 100 bar and 170 bar. Small amount of each chiral catalyst was used because a limited amount of CATAXA was available in the lab. The quantity of the catalyst used in the particular experiment could affect the conversion of the substrate but it could be increased by using a larger amount of catalyst and/or increasing the residence time (by decreasing the flow rate). It has been shown previously that an increase in CO<sub>2</sub> flow rate did not affect greatly the enantioselectivity of the reaction, while it significantly decreased the conversion of the substrate to product.<sup>24</sup> Figure 3-5 shows the experimental results of the continuous asymmetric hydrogenation of dimethyl itaconate in flow scCO<sub>2</sub> with [Rh(nbd)(Skewphos)]<sup>+</sup>[BF<sub>4</sub>]<sup>-</sup>/PTA/Alumina.<sup>24</sup>

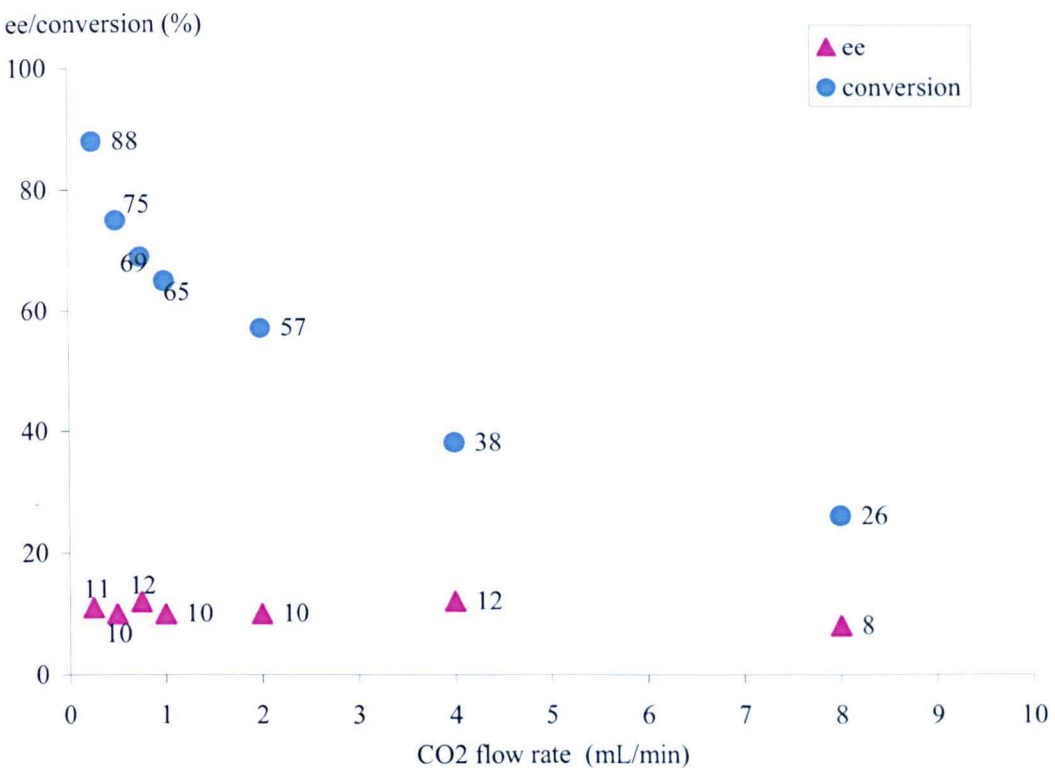


**Figure 3-5.** The effect of the flow rate on the enantioselective hydrogenation of dimethyl itaconate in continuous flow scCO<sub>2</sub> with [Rh(nbd)(Skewphos)]<sup>+</sup>[BF<sub>4</sub>]<sup>-</sup>/PTA/Alumina.<sup>24</sup>

**Reaction conditions:** temperature: 60 °C, substrate flow rate: 0.2 ml/min (DMIT in IPA 2.5 M), H<sub>2</sub> : substrate ratio = 2.5 : 1.

Before the screening of the Josiphos type ligands for the continuous asymmetric hydrogenation of dimethyl itaconate in scCO<sub>2</sub>, the reproducibility of the results of Stephenson<sup>24</sup> was examined using freshly prepared [Rh(COD)(Josiphos 001)]<sup>+</sup>[BF<sub>4</sub>]<sup>-</sup>/PTA/Alumina. The experiments were performed using a small scale hydrogenation equipment described in Chapter 2. The samples were analysed by chiral GC and the enantioselectivity was calculated as described in Chapter 2. The results are shown in Table-3-2.

**Table 3-2.** The results of the asymmetric hydrogenation of dimethyl itaconate using  $[\text{Rh}(\text{COD})(\text{Josiphos } 001)]^+[\text{BF}_4^-]$ /PTA/Alumina. The results of the research performed prior to the current study are marked as Josiphos - batch 1.<sup>24</sup> The results of this work are shown as Josiphos - batch 2.

Entry	Ligand	T (°C)	P (bar)	Conv (%)	<i>ee</i> <sub>S</sub> (%)
1	Josiphos - batch 1	30	100	12	3
2	Josiphos - batch 1	35	100	10	8
3	Josiphos - batch 1	40	100	8	18
4	Josiphos - batch 1	45	100	10	39
5	Josiphos - batch 1	50	100	19	52
6	Josiphos - batch 1	55	100	19	51
7	Josiphos - batch 1	60	100	22	52
8	Josiphos - batch 1	65	100	21	52
9	Josiphos - batch 1	70	100	21	52
10	Josiphos - batch 1	75	100	22	53
11	Josiphos - batch 1	60	120	39	73
12	Josiphos - batch 1	60	160	40	63
13	Josiphos - batch 1	60	180	38	59
14*	Josiphos - batch 2	35	100	29	26
15*	Josiphos - batch 2	45	100	29	47
16*	Josiphos - batch 2	55	100	65	83
17*	Josiphos - batch 2	35	170	17	16
18*	Josiphos - batch 2	45	170	29	74
19*	Josiphos - batch 2	55	170	80	77

Reaction conditions: CO<sub>2</sub> flow rate: 0.5 ml/min, substrate flow rate: 0.2 ml/min (DMIT in IPA 2.5 M), H<sub>2</sub> : substrate ratio = 2.5 : 1.

\* Reaction conditions: CO<sub>2</sub> flow rate: 0.5 ml/min, substrate flow rate: 0.2 ml/min (DMIT in IPA 2.5 M), H<sub>2</sub> : substrate ratio = 3 : 1.

For better visualization of the results, the enantioselectivity is shown in a graph as well (Figure 3-6).

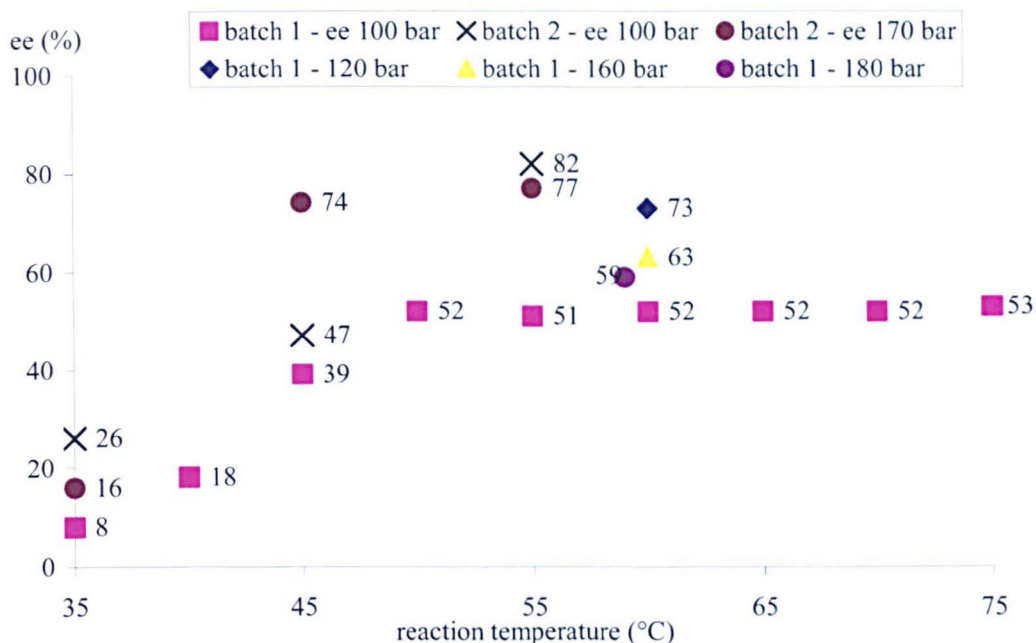


**Figure 3-6.** The enantioselectivity of the asymmetric hydrogenation of dimethyl itaconate using  $[\text{Rh}(\text{COD})(\text{Josiphos 001})]^+[\text{BF}_4]^-/\text{PTA}/\text{Alumina}$ . The results of the research preformed prior to this work are marked as batch 1.<sup>24</sup> The results of this work are shown as batch 2.

Reaction conditions:  $\text{CO}_2$  flow rate: 0.5 ml/min, substrate flow rate: 0.2 ml/min (DMIT in IPA 2.5 M),  $\text{H}_2$  : substrate ratio = 2.5 : 1 for batch 1, and 3 : 1 for batch 2.

The enantioselectivities displayed by the chiral catalyst  $[\text{Rh}(\text{COD})(\text{Josiphos 001})]^+[\text{BF}_4]^-/\text{PTA}/\text{Alumina}$  with Josiphos 001 from different batches were different, but showed a similar trend: the enantioselectivity increased with an increase in the reaction temperature. (It is not unusual that the catalyst activity varies when it originates from different batches.) Normally, higher enantioselectivity is expected at low temperature, the energetic difference between the paths leading to the two enantiomers is so small that it is reasonable to assume that low energy would lead to a higher enantioselectivity. The reason for higher enantioselectivity at higher temperature might be due to changes in the phase behaviour of the system because the solubility of substrates normally increases with an increase in temperature. The phase behaviour of dimethyl itaconate/IPA/sc $\text{CO}_2$  mixture was determined at Nottingham<sup>24</sup> and is shown in Figure 3-7. The addition of  $\text{H}_2$  to the system slightly shifted the phase boundary line upwards but only a slight difference (up to 5 bar at  $\text{H}_2$  : substrate ratio = 8 : 1) was observed (conditions used in this work: maximum  $\text{H}_2$  : substrate ratio = 3 : 1).<sup>24</sup>

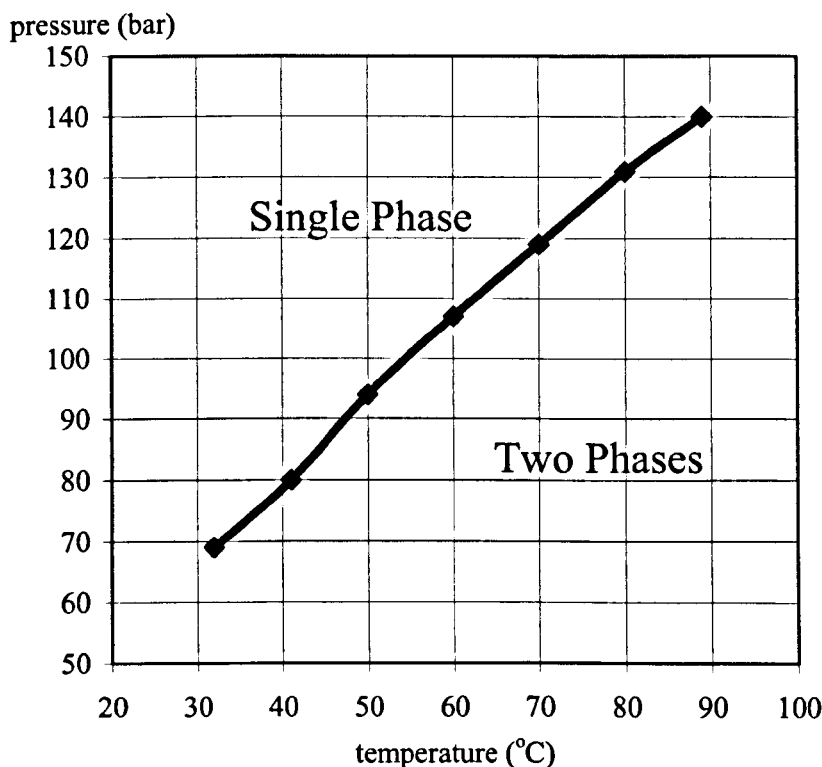


**Figure 3-7. Phase behaviour of dimethyl itaconate/IPA/scCO<sub>2</sub> mixture.<sup>24</sup>**

Most conditions examined here lay in the single phase region. The asymmetric hydrogenation using Josiphos 001 from the first batch reached a plateau above 50 °C at 100 bar. The highest enantioselectivity (73 %) was obtained at 60 °C at 120 bar where the reactants and scCO<sub>2</sub> were present in a single phase. From all the work with [Rh(COD)(Josiphos 001)]<sup>+</sup>[BF<sub>4</sub>]<sup>-</sup>/PTA/Alumina, the best result was obtained using the chiral catalyst modified with Josiphos 001 ligand from the second batch at 55 °C at 100 bar: ee<sub>S</sub> = 83 %. The phase boundary line goes through the point of 55 °C at 100 bar which might influence the reaction. However, high enantioselectivity was observed with the chiral catalyst modified with Josiphos 001 ligand from the first batch at 60 °C and 120 bar ee<sub>S</sub> = 73 %, and from the second batch at 55 °C and 170 bar ee<sub>S</sub> = 77 %, which were both in the one phase region. Therefore, the phase behaviour of the system should not have a significant effect on the reaction. The enantioselectivity of the asymmetric hydrogenation increased with an increase in temperature at both pressures examined here (100 bar and 170 bar) using [Rh(COD)(Josiphos 001)]<sup>+</sup>[BF<sub>4</sub>]<sup>-</sup>/PTA/Alumina (this study). The reason for higher enantioselectivity at higher temperature may be due to changes in

the density of CO<sub>2</sub>: it decreases with an increase in temperature, which therefore results in a slight flow rate change as ‘weaker’ reaction medium flows through the system. The removal of the product from the catalyst surface may also be faster at higher flow rates and higher temperatures, which can improve the performance of the chiral catalyst. The effect of an increased pressure was not clearly shown here.

The hydrogenation with [Rh(COD)(Josiphos 001)]<sup>+</sup>[BF<sub>4</sub>]<sup>-</sup>/PTA/Alumina with Josiphos 001 from the second batch was performed 3 times using a freshly made chiral catalyst in each case. The description of the process for preparation can be found in detail in Chapter 2. The ligand exchange was performed over 16 hours (overnight) with stirring under an argon atmosphere. One of the batches was prepared with a 4-hour ligand exchange reaction rather than 16 hours. In another case, technical problems occurred during the preparation (the stirrer stopped after circa 8 hours). In both cases a very low enantioselectivity was obtained for the asymmetric hydrogenation. The results presented here are from the experiments using the chiral catalyst [Rh(COD)(Josiphos 001)]<sup>+</sup>[BF<sub>4</sub>]<sup>-</sup>/PTA/Alumina prepared in the route described in Chapter 2 without any malfunction. It therefore suggests that the catalyst preparation may have a significant effect on the catalyst performance, and therefore the chiral catalyst must be prepared with a great care.

The chiral catalysts [Rh(COD)(ligand)]<sup>+</sup>[BF<sub>4</sub>]<sup>-</sup>/PTA/Alumina using Josiphos type ligands were examined at temperatures 35 °C, 45 °C and 55 °C and at pressures 100 bar and 170 bar. The enantioselectivity values are plotted in two graphs. The enantioselectivity obtained at 100 bar is shown in Figure 3-8.

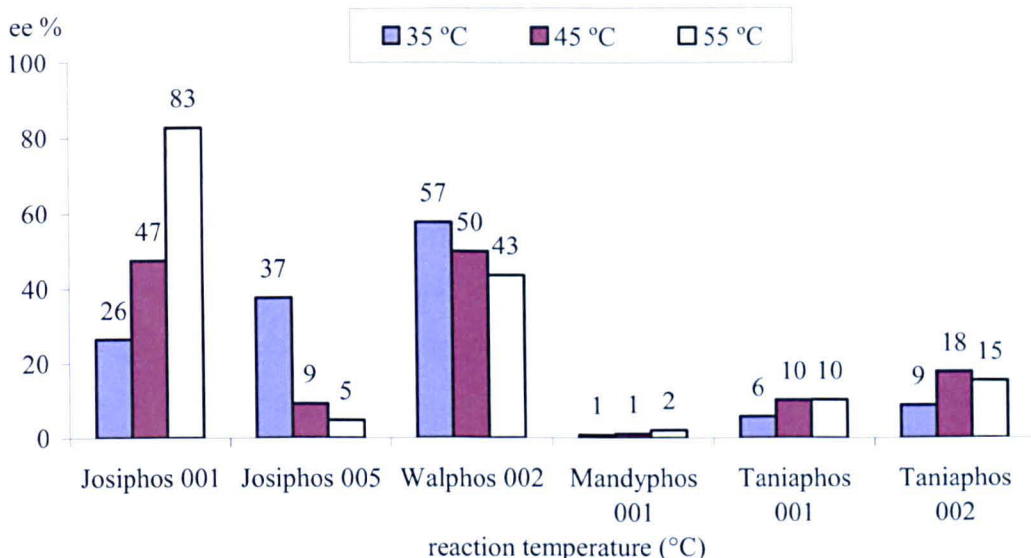


**Figure 3-8. The enantioselectivity of the asymmetric hydrogenation of dimethyl itaconate using CATAXA modified with bisphosphine ligands  $[\text{Rh}(\text{COD})(\text{ligand})]^+[\text{BF}_4]^-/\text{PTA}/\text{Alumina}$  at 100 bar.**

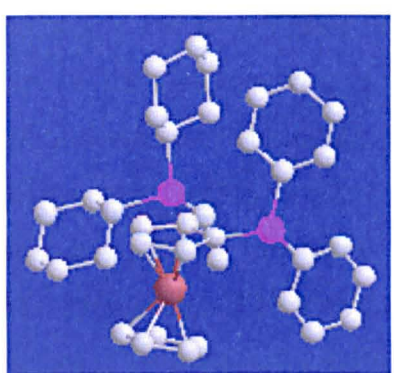
**Reaction conditions:** pressure: 100 bar,  $\text{CO}_2$  flow rate: 0.5 ml/min, substrate flow rate: 0.2 ml/min (DMIT in IPA 2.5 M),  $\text{H}_2$  : substrate ratio = 3:1.

It can be seen from Figure 3-8 that the enantioselectivity of the hydrogenation was highly dependent on the ligand attached to the Rh complex. (The conversion is shown in Figure 3-11, page 83) The enantioselectivity increased with an increase in temperature using Josiphos 001, Taniaphos 001, Taniaphos 002 and Mandyphos 001. The enantioselectivity using Mandyphos 001 was very low which is within the experimental error. The enantioselectivity produced using Josiphos 001, Taniaphos 001 and Taniaphos 002 ligands increased with increasing temperature. This increase is counter-intuitive, the energetic difference between the paths producing the two enantiomers is very small and therefore it can be assumed increasing energy would lead to lower enantioselectivity. The results of the reaction using  $[\text{Rh}(\text{COD})(\text{Josiphos 001})]^+[\text{BF}_4]^-/\text{PTA}/\text{Alumina}$  are also described in detail above. The expected trend, decreasing enantioselectivity with increasing temperature, was observed with Josiphos 005 and Walphos 002 ligands.

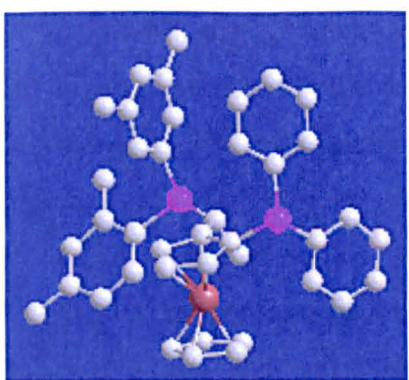
The variation in enantioselectivity using different ligands can be rationalised on the basis of the electron withdrawing/donating properties and size of the ligands. All of the ligands used in this work have electron donating groups attached to the phosphine. The most strongly electron donating ligand was

assumed to be Walphos 002 which gave an enantioselectivity up to 58 %. The highest enantioselectivity was obtained using Josiphos 001 ligand, which was thought to have the weakest electron donating properties of the six ligands. Therefore the size and steric effects also need to be considered. The sterics of the two might have a more significant effect than size on the chiral catalyst performance. Josiphos 001 is the smallest ligand in size among these six Josiphos type ligands and it showed the highest enantioselectivity. Walphos 002 is slightly larger than Josiphos 001 and it showed the second highest chiral activity. The remaining four ligands (Josiphos 005, Mandyphos 001, Taniaphos 001 and Taniaphos 002) are all larger in size than either Josiphos 001 or Walphos 002 and gave lower enantioselectivities. Small differences in size may change the effect of the ligand on the chiral performance of the catalyst *via* steric inhibition. Furthermore, steric problems could also cause incompatibility of some ligands with the CATAXA system, which could be the origin of the low activity in some cases. The incompatibility of a ligand could have been determined by analysing the iron (from the ligand) present in the samples collected during the chiral catalyst preparation but unfortunately, there was no access to an ICP-MS instrument at the time these experiments were conducted. Even if the ligand could be attached to the Rh, steric inhibition could still be the source of the low enantioselectivity: the substrate might not reach the active centre of the catalyst because it was blocked by the ligand.

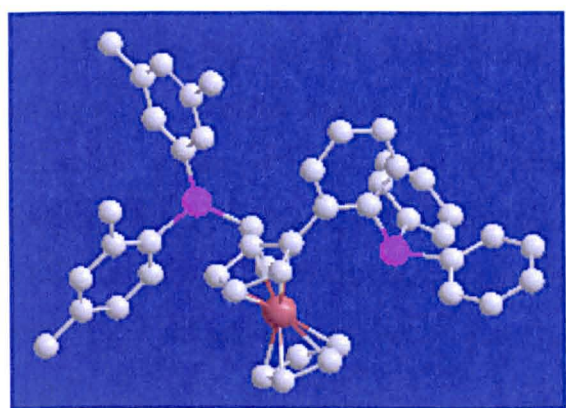
Molecular modelling (Spartan, Semi Empirical using PM3) of the Josiphos type ligands (the structures of the ligands is shown in Figure 3-4) was performed to demonstrate the differences in size (Figure 3-9).



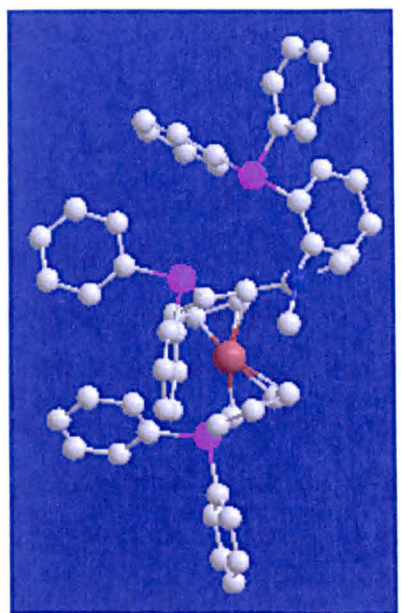
Josiphos 001 ( $\text{ee}_S = 83\%$ )



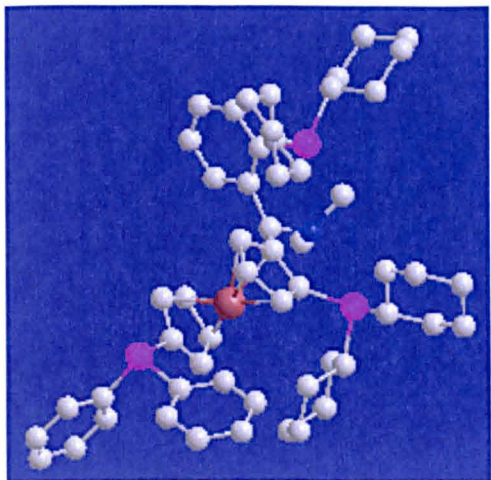
Josiphos 005 ( $\text{ee}_S = 37\%$ )



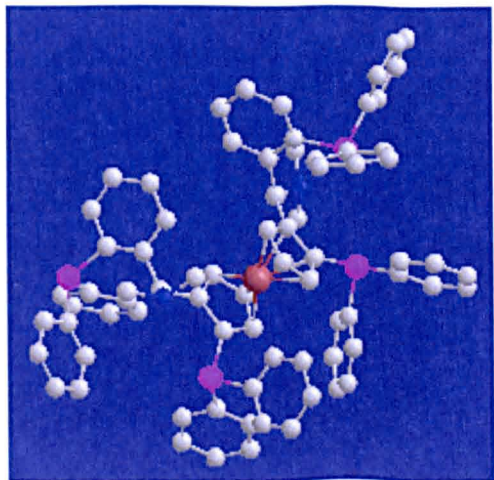
Walphos 002 ( $\text{ee}_R = 57\%$ )



Taniaphos 001 ( $\text{ee}_R = 10\%$ )



Taniaphos 002 ( $\text{ee}_R = 18\%$ )

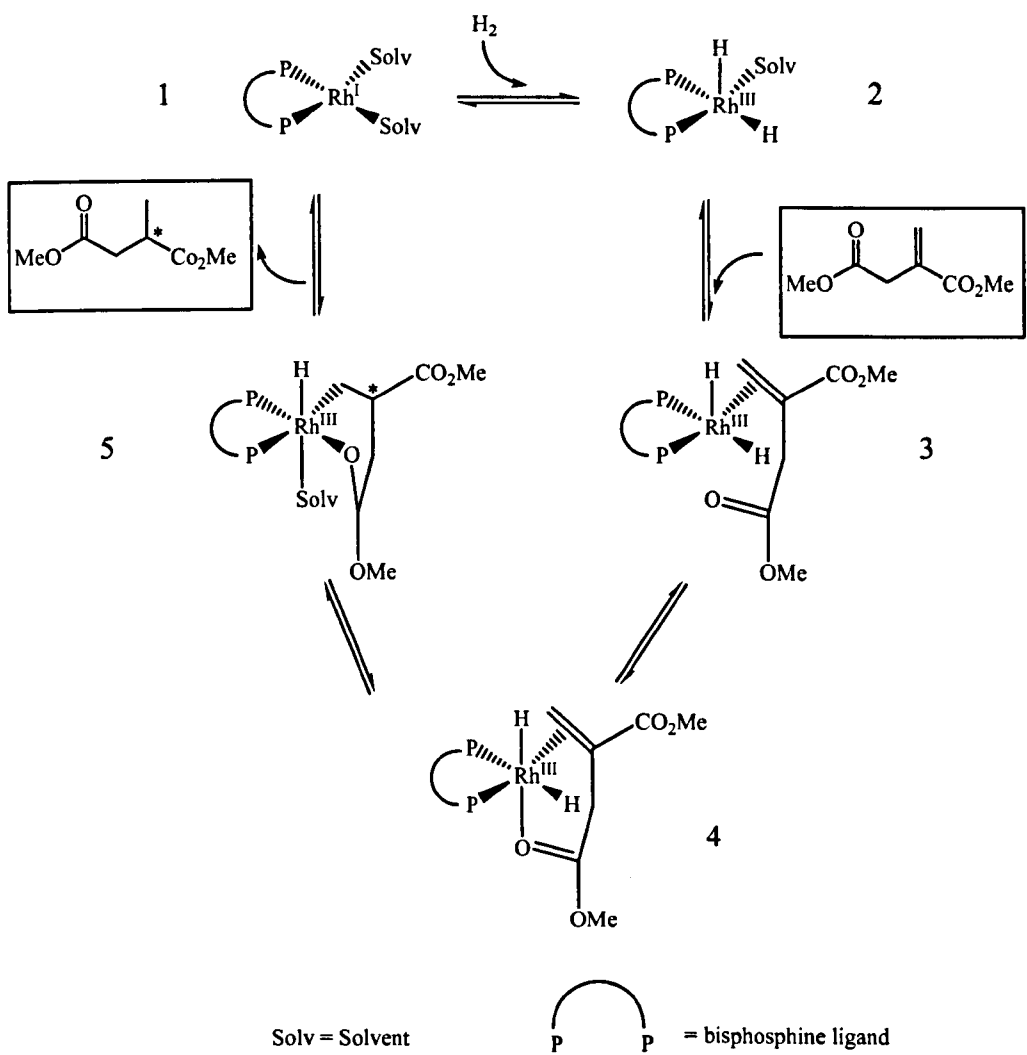


Mandyphos 001 ( $\text{ee}_R = 3\%$ )

**Figure 3-9.** The structures of the Solvias Josiphos type ligands. The calculations were performed on Spartan, Semi Empirical using PM3. (The highest enantioselectivity obtained with the particular ligand is shown in brackets.)

Although, the 3D dimensions of the ligands are not available, the difference in size of the ligands can be seen clearly and is in a good agreement with the enantioselectivity observed in the asymmetric hydrogenation of dimethyl itaconate in scCO<sub>2</sub>: (order of size and enantioselectivity): Josiphos 001 > Walphos 002 > Josiphos 005 > Taniahos 002 > Taniaphos 001 > Mandyphos 001. Although Josiphos 005 ligand is the second smallest ligand, it has conjugated substituents that will decrease the electron withdrawing/donating properties, which can explain why it produced lower enantioselectivity than Walphos 002 (no conjugated system) which is larger in size.

A mechanism for the homogenously catalysed hydrogenation of dimethyl itaconate has been proposed previously.<sup>2, 32</sup> The orientation and therefore the selectivity of the reaction is dependent on how the substrate binds to the catalyst.<sup>2</sup> In Scheme 3-6, the binding of H<sub>2</sub> is prior to the binding of the substrate which is presumably occurring in the continuous asymmetric hydrogenation of dimethyl itaconate in scCO<sub>2</sub> because H<sub>2</sub> was used in excess to the substrate. If the bisphosphine ligand is too large the substrate might not go through the catalytic cycle.



**Scheme 3-6. The mechanism of the homogenous catalytic asymmetric hydrogenation in conventional solvents.**

The continuous asymmetric hydrogenation of dimethyl itaconate in scCO<sub>2</sub> was also examined at a higher pressure. The results of the experiments at 170 bar are shown in Figure 3-10.

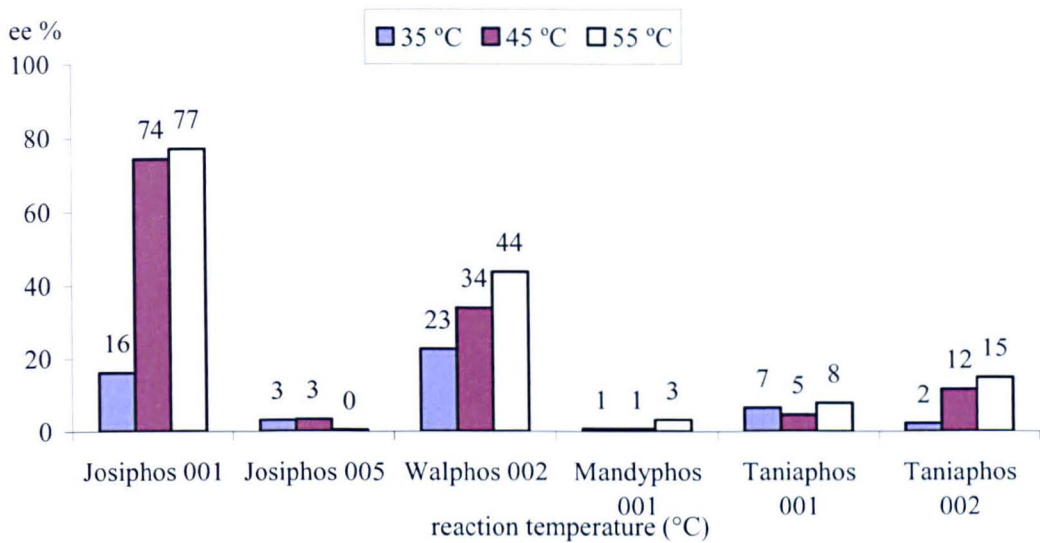


**Figure 3-10. The enantioselectivity of the asymmetric hydrogenation of dimethyl itaconate using CATAXA modified with bisphosphine ligands  $[\text{Rh}(\text{COD})(\text{ligand})]^+[\text{BF}_4]^-/\text{PTA}/\text{Alumina}$  at 170 bar.**

**Reaction conditions:** pressure: 170 bar,  $\text{CO}_2$  flow rate: 0.5 ml/min, substrate flow rate: 0.2 ml/min (DMIT in IPA 2.5 M),  $\text{H}_2$  : substrate ratio = 3 : 1.

Comparing the results shown in Figures 3-8 and 3-10, it can be observed that the enantioselectivity was lower with all chiral catalysts at higher pressure. (The conversion is shown in Figure 3-11, page 83) The enantioselectivity increased with an increase in temperature using either ligand, however, the enantioselectivity was very low in most cases. The experiments at 170 bar were performed after those at 100 bar in the same set. The catalyst might have become deactivated *via* the reverse water gas-shift reaction  $\text{CO}_2 + \text{H}_2 \rightarrow \text{H}_2\text{O} + \text{CO}$ .<sup>11</sup> The negative effect of the reverse water gas-shift reaction might possibly be more significant on the chiral catalyst if it had been kept under  $\text{CO}_2$  and  $\text{H}_2$  for a longer period of time. Furthermore, the ligand could be washed away during the experiment and therefore the enantioselectivity might drop with time.

The conversion of dimethyl itaconate using  $[\text{Rh}(\text{COD})(\text{ligand})]^+[\text{BF}_4]^-/\text{PTA}/\text{Alumina}$  with Josiphos 001 and Walphos 002 ligands are presented in Figure 3-11.

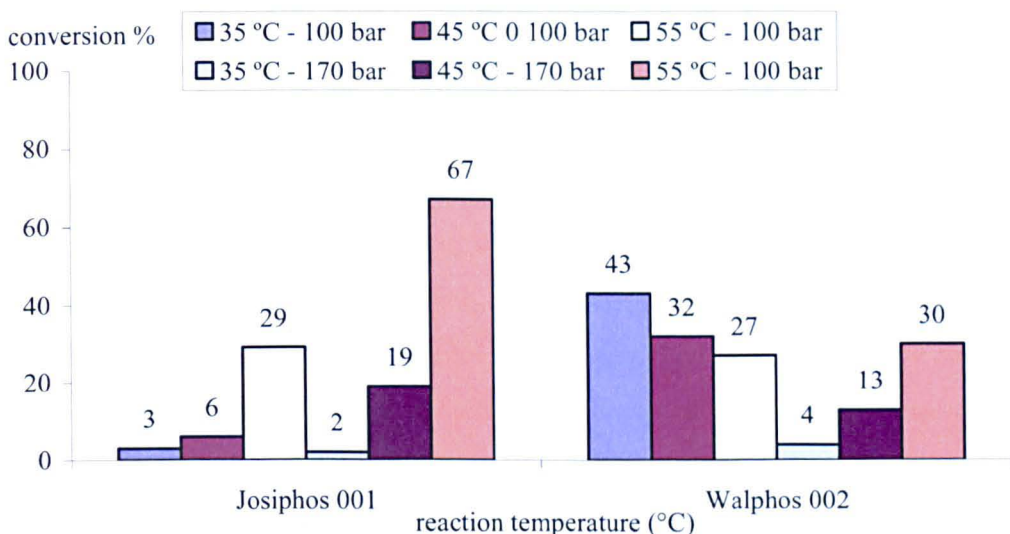


**Figure 3-11.** The level of conversion obtained in the asymmetric hydrogenation of dimethyl itaconate using  $[\text{Rh}(\text{COD})(\text{ligand})]^+[\text{BF}_4]^-$ /PTA/Alumina modified with Josiphos 001 and Walphos 002 ligands.  
Reaction conditions:  $\text{CO}_2$  flow rate: 0.5 ml/min, substrate flow rate: 0.2 ml/min (DMIT in IPA 2.5 M),  $\text{H}_2$  : substrate ratio = 3 : 1.

The results in Figure 3-11 show that the conversion of the substrate in the continuous asymmetric hydrogenation increased by an increase in temperature in most cases. An increased pressure increased the conversion of dimethyl itaconate using  $[\text{Rh}(\text{COD})(\text{Josiphos 001})]^+[\text{BF}_4]^-$ /PTA/Alumina, while decreased the conversion using  $[\text{Rh}(\text{COD})(\text{Walphos 002})]^+[\text{BF}_4]^-$ /PTA/Alumina. An increase in pressure increases the density of the  $\text{CO}_2$  and therefore the residence time of the reaction. An increased residence time can lead to higher conversion as it has also been shown previously (Figure 3-5). The conversion of dimethyl itaconate decreased using  $[\text{Rh}(\text{COD})(\text{Walphos 002})]^+[\text{BF}_4]^-$  at 100 bar with temperature, which might be due to catalyst leaching during the reaction. The highest conversion obtained at 170 bar did not exceed significantly the lowest conversion at 100 bar, which supports this hypothesis.

### 3.6.2. The Effect of the Cosolvent on the Enantioselectivity

The cosolvent used might affect the reaction as a change in solvent polarity influences the dielectric constant of the reaction medium. Iso-propanol was used as a cosolvent in the experiments described so far. To investigate the effect of the cosolvent on the reaction, the asymmetric hydrogenation of

dimethyl itaconate in continuous flow scCO<sub>2</sub> was also performed using methanol as cosolvent.

The polarity indexes of IPA and methanol are 3.9 and 5.1, respectively. The dielectric constants of CO<sub>2</sub> (liquid), IPA and methanol are 1.6, 18 and 33, respectively.<sup>33</sup> Although, scCO<sub>2</sub> is a favoured solvent due its low dielectric constant, a medium with higher dielectric constant may improve the enantioselectivity of asymmetric hydrogenations. The enantioselectivity of the asymmetric hydrogenation of dimethyl itaconate in continuous flow scCO<sub>2</sub> using [Rh(COD)(Walphos 002)]<sup>+</sup>[BF<sub>4</sub>]<sup>-</sup>/PTA/Alumina with different cosolvents is shown in Figure 3-12.

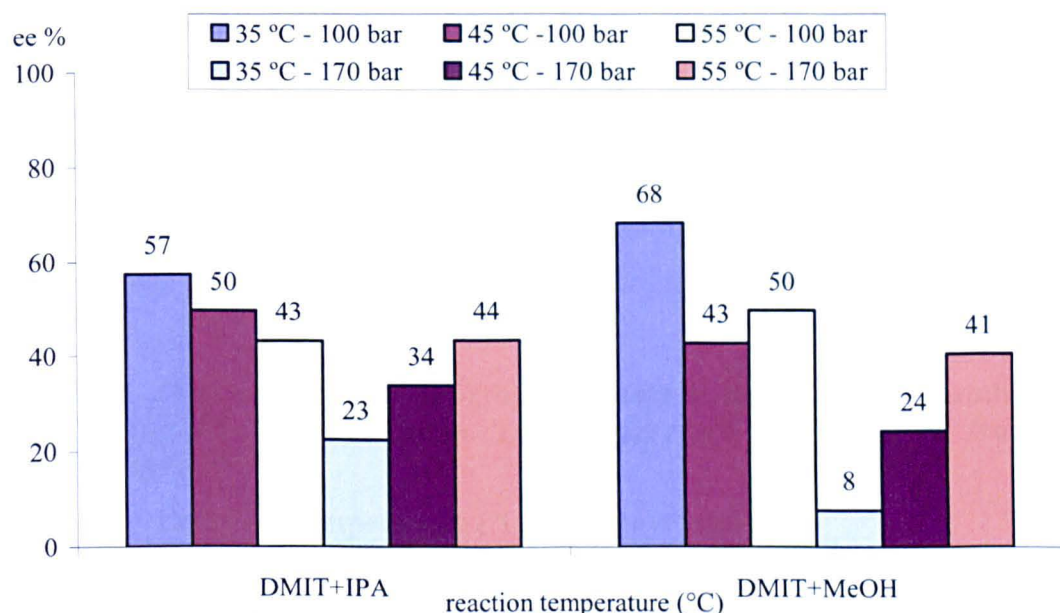


**Figure 3-12. The enantioselectivity of the asymmetric hydrogenation of dimethyl itaconate using CATAXA modified with Walphos 002 ligand [Rh(COD)(Walphos 002)]<sup>+</sup>[BF<sub>4</sub>]<sup>-</sup>/PTA/Alumina and different cosolvents. Reaction conditions: CO<sub>2</sub> flow rate: 0.5 ml/min, substrate flow rate: 0.2 ml/min (DMIT in IPA or MeOH 2.5 M), H<sub>2</sub> : substrate ratio = 3 : 1.**

The enantioselectivity of the reaction was slightly higher at 35 °C and 55 °C at 100 bar when using methanol as cosolvent than that using IPA as cosolvent. At all other conditions, the enantioselectivity was lower using methanol than that using IPA as cosolvent. The inconsistency could be due to experimental error. A reaction medium with higher dielectric constant can positively influence the chiral motif of a catalyst by providing a more ionic medium. In this case, the

dielectric constant was not clearly shown to be crucial for achieving high chiral performance.

Unfortunately, there was limited amount of CATAXA/Alumina available in the lab and further supplies of the same catalyst could not be obtained. A catalyst with similar structure to  $[\text{Rh}(\text{COD})_2]^+[\text{BF}_4]^-$ /PTA/Alumina was received from Johnson Matthey as a gift. The only difference was the support material.

### 3.6.3. The Effect of the Support Material on the Enantioselectivity

$[\text{Rh}(\text{COD})_2]^+[\text{BF}_4]^-$ /PTA/Carbon was used to establish whether the support material has any effect on catalyst performance. The results of the hydrogenation (achiral) of dimethyl itaconate with  $[\text{Rh}(\text{COD})_2]^+[\text{BF}_4]^-$ /PTA/Alumina are shown in Table 3-3, and those for  $[\text{Rh}(\text{COD})_2]^+[\text{BF}_4]^-$ /PTA/Carbon are listed in Tables 3-4 and 3-5. Table 3-5 lists the level of conversion for the asymmetric hydrogenation with  $[\text{Rh}(\text{COD})_2]^+[\text{BF}_4]^-$ /PTA/Carbon examined at decreasing temperature from 80 °C to 35 °C.

**Table 3-3. The conversion of dimethyl itaconate using CATAXA/Alumina  $[\text{Rh}(\text{COD})_2]^+[\text{BF}_4]^-$ /PTA/Alumina. The temperature was increased from 30 °C to 70 °C.<sup>24</sup>**

Entry	Temperature (°C)	Conversion (%)
1	30	68
2	40	68
3	50	51
4	60	36
5	70	22

Reaction conditions: pressure: 100 bar,  $\text{CO}_2$  flow rate: 0.25 ml/min, substrate flow rate: 0.1 ml/min (DMIT in IPA 2.5 M),  $\text{H}_2$  : substrate ratio = 2.5 : 1.

**Table 3-4.** The conversion of dimethyl itaconate using CATAXA/Carbon  $[\text{Rh}(\text{COD})_2]^+[\text{BF}_4]^-$ /PTA/Carbon. The temperature was increased from 35 °C to 80 °C.

Entry	Temperature (°C)	Conversion (%)
1	35	60
2	45	98
3	55	99
4	65	99
5	80	99

Reaction conditions: pressure: 100 bar,  $\text{CO}_2$  flow rate: 0.5 ml/min, substrate flow rate: 0.2 ml/min (DMIT in IPA 2.5 M),  $\text{H}_2$  : substrate ratio = 3 : 1.

**Table 3-5.** The conversion of dimethyl itaconate using CATAXA/Carbon  $[\text{Rh}(\text{COD})_2]^+[\text{BF}_4]^-$ /PTA/Carbon. The temperature was decreased from 80 °C to 35 °C.

Entry	Temperature (°C)	Conversion (%)
1	80	99
2	65	98
3	55	99
4	45	98
5	35	94

Reaction conditions: pressure: 100 bar,  $\text{CO}_2$  flow rate: 0.5 ml/min, substrate flow rate: 0.2 ml/min (DMIT in IPA 2.5 M),  $\text{H}_2$  : substrate ratio = 3 : 1.

While the conversion of dimethyl itaconate using  $[\text{Rh}(\text{COD})_2]^+[\text{BF}_4]^-$ /PTA/Alumina decreased with increasing temperature, the conversion increased using  $[\text{Rh}(\text{COD})_2]^+[\text{BF}_4]^-$ /PTA/Carbon. The reason for lower conversion using  $[\text{Rh}(\text{COD})_2]^+[\text{BF}_4]^-$ /PTA/Alumina could be due to catalyst loss, however, no Rh leaching was observed below 100 °C (determined by ICP-MS analysis).<sup>24</sup> The activity of the carbon supported Rh catalyst remained high even when the reaction temperature was decreased from 80 °C to 35 °C. The slight decrease with a decrease in temperature might be due to catalyst loss or reaction rate decrease.

Following that the catalyst  $[\text{Rh}(\text{COD})_2]^+[\text{BF}_4]^-$ /PTA/Carbon has been confirmed to be suitable for performing continuous hydrogenation in sc $\text{CO}_2$ , a chiral catalyst  $[\text{Rh}(\text{COD})(\text{Josiphos } 001)]^+[\text{BF}_4]^-$ /PTA/Carbon was examined

for the enantioselective hydrogenation of dimethyl itaconate. The enantioselectivities of the asymmetric hydrogenation of dimethyl itaconate at different conditions with  $[\text{Rh}(\text{COD})(\text{Josiphos 001})]^+[\text{BF}_4]^-/\text{PTA}/\text{Alumina}$  and Carbon are shown in Figure 3-13.

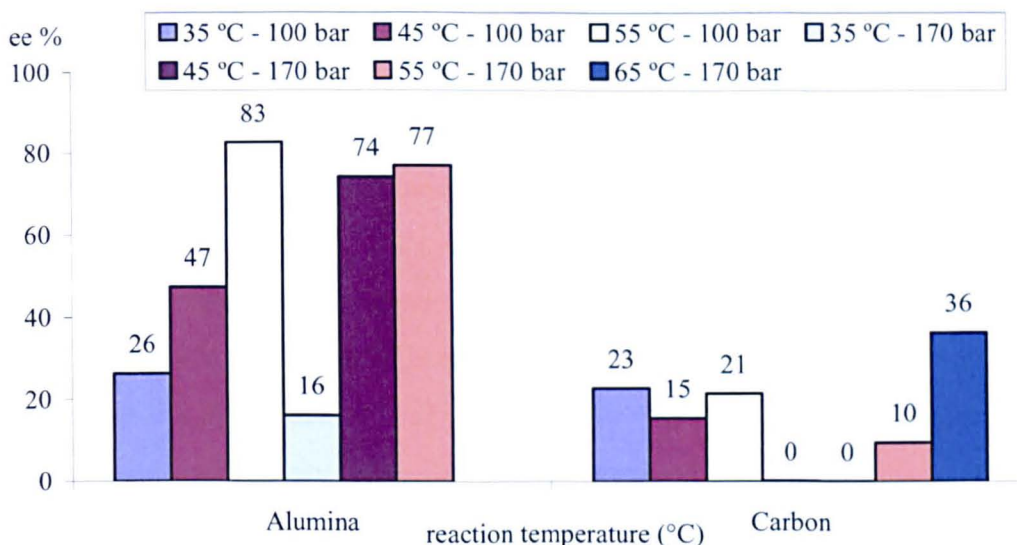


**Figure 3-13. The enantioselectivities of the asymmetric hydrogenation of dimethyl itaconate using  $[\text{Rh}(\text{COD})(\text{Josiphos 001})]^+[\text{BF}_4]^-/\text{PTA}/\text{Alumina}$  or Carbon at 100 bar and 170 bar.**

**Reaction conditions:**  $\text{CO}_2$  flow rate: 0.5 ml/min, substrate flow rate: 0.2 ml/min (DMIT in IPA 2.5 M),  $\text{H}_2$  : substrate ratio = 3:1.

The carbon supported chiral catalyst displayed much lower enantioselectivity than the alumina supported catalyst, at all conditions.  $[\text{Rh}(\text{COD})_2]^+[\text{BF}_4]^-/\text{PTA}/\text{Carbon}$  has a very fine powdery consistency and it might have become compacted under pressure. Therefore the catalyst could become a monolith and the reactants might flow around rather than through the catalyst bed. However, the achiral catalyst was highly active in the continuous flow sc $\text{CO}_2$  system. The chiral modification might be the source of the low activity rather than the compaction of the catalyst bed under pressure.

### 3.7. Conclusions

The work in this Chapter demonstrates one of the first examples of continuous asymmetric hydrogenation using heterogeneous chiral catalyst without the need for the addition of the chiral modifier.

The following parameters were examined here for the continuous asymmetric hydrogenation of dimethyl itaconate in scCO<sub>2</sub> i) the ligand attached to the Rh complex, ii) the cosolvent used for the reaction, and iii) the support material of the chiral catalyst. Among these parameters, the ligand was shown to be the most important factor. The electron withdrawing/donating properties, the size, and the sterics of the bisphosphine ligand could all highly influence the enantioselectivity, but the size and sterics of the ligand might have a more significant effect on the catalyst performance.

The temperature of the continuous flow scCO<sub>2</sub> system greatly influenced the asymmetric hydrogenation. The system pressure had less significant effect. An unexpected trend, an increase in enantioselectivity by an increase in temperature was observed in some cases which can be explained by the changes in the properties of CO<sub>2</sub> (density, viscosity, and solvent power). The highest enantioselectivity ( $ee_R = 83\%$ ) was obtained at 55 °C at 100 bar with [Rh(COD)(Josiphos 001)]<sup>+</sup>[BF<sub>4</sub>]<sup>-</sup>/PTA/Alumina.

## References

1. Anastas, P. T., Warner, J.C., in *Green Chemistry: Theory and practice*. *Oxford University Press, Oxford 1998*.
2. Noyori, R., in *Asymmetric catalysis in organic synthesis*. *Wiley, New York 1994*.
3. Knowles, W. S., Asymmetric hydrogenations (Nobel lecture). *Angewandte Chemie International Edition* **2002**, 42, 1999-2007.
4. Noyori, R., Asymmetric catalysis: Science and opportunities (Nobel lecture). *Angewandte Chemie International Edition* **2002**, 42, 2008-2022.
5. Blaser, H. U., Malan, C., Pugin, B., Spindler, F., Steiner, H., Struder, M., Selective hydrogenation for fine chemicals: Recent trends and new developments. *Advanced Synthesis & Catalysis* **2003**, 345, 103-151.
6. Miyashita, A., Yasuda, A., Takaza, H., Toriumi, K., Ito, T., Souchi, T., Noyori, R., Synthesis of 2,2'-bis(diphenylphosphino)-1,1'-binaphthyl (BINAP), an atropisomeric chiral bis(triaryl)phosphine, and its use in the rhodium(1)-catalyzed asymmetric hydrogenation of α-(acylamino)acrylic acids. *Journal of the American Chemical Society* **1980**, 102, 7932-7934.
7. Shaw, N. M., Robins, K.T., Kiener, A., Eds Blaser, H.U., Schmidt, E., in *Asymmetric Catalysis on Industrial Scale: Challenges, Approaches, and Solutions*. *Wiley-VHC, Weinheim 2004*.
8. Blaser, H. U., Pugin, B., Spindler, F., Progress in enantioselective catalysis assessed from an industrial point of view. *Journal of Molecular Catalysis A: Chemical* **2005**, 231, 1-20.
9. Tang, W. J., Zhang, X.M., New Chiral Phosphorous Ligands for Enantioselective Hydrogenation. *Chemical Reviews* **2003**, 103, 3029-3069.

10. Jessop, P., Leitner, W., in *Chemical synthesis using supercritical fluids*. Wiley-VCH, Weinheim 1999.
11. Seki, T., Grunwaldt, J.D., Baiker, A., Heterogeneous asymmetric hydrogenation in supercritical fluids: Potentials and limitations. *Industrial & Chemical Engineering Research* 2008, 47, 4561-4585.
12. Beckman, E. J., Supercritical and near-critical CO<sub>2</sub> in green chemical synthesis and processing. *Journal of Supercritical Fluids* 2003, 1-77.
13. Leitner, W., Supercritical carbon dioxide as a green reaction medium for catalysis. *Accounts of Chemical Research* 2002, 35, 746-756.
14. Kainz, S., Brinkmann, A., Leitner, W., Pfaltz, A., Iridium-catalyzed enantioselective hydrogenation of imines in supercritical carbon dioxide. *Journal of the American Chemical Society* 1999, 121, 6421-6429.
15. Jessop, P. G., Ikariya, T., Noyori, R., Homogeneous catalysis in supercritical fluids. *Chemical Reviews* 1999, 99, 475-493.
16. Xiao, J., Nefkens, S.C.A., Jessop, P.G., Ikayira, T., Noyori, R., Asymmetric hydrogenation of alpha, beta-unsaturated carboxylic acids in supercritical carbon dioxide. *Tetrahedron Letters* 1996, 37, (16), 2812-2816.
17. Jessop, P. G., Homogeneous catalysis using supercritical fluids: Recent trends and systems studied. *Journal of Supercritical Fluids* 2006, 38, 211-231.
18. Wandeler, W., Künzle, N., Schneider, M., Mallat, T., Baiker, A., Continuous platinum-catalyzed enantioselective hydrogenation in 'supercritical' solvents. *Chemical Communications* 2001, 673-674.
19. Stephenson, P., Licence, P., Ross, S.K., Poliakoff, M., Continuous catalytic asymmetric hydrogenation in supercritical CO<sub>2</sub>. *Green Chemistry* 2004, 6, 521-525.
20. Stephenson, P., Kondor, B., Peter Licence, P., Scovell, K., Ross, S.K., Poliakoff, M., Continuous asymmetric hydrogenation in supercritical carbon dioxide using an immobilised homogeneous catalyst. *Advanced Synthesis & Catalysis* 2006, 348, 1605-1610.
21. Szöllősi, G., Hermán, B., Fülöp, F., Bartók, M., Continuous enantioselective hydrogenation of activated ketones on a Pt-CD chiral catalyst: use of H-Cube reactor system. *Reaction Kinetics and Catalysis Letters* 2006, 88, (2), 391-398.
22. Augustine, R. T., Anderson, S.; Yang, H., A new technique for anchoring homogeneous catalysts. *Chemical Communications* 1999, 1257-1258.
23. Augustine, R. L., et al., Anchored homogeneous catalysts: high turnover number applications. *Journal of Molecular Catalysis A: Chemical* 2004, 215, (2), 189-197.
24. Stephenson, P., PhD Thesis. University of Nottingham, Nottingham (UK) 2005.
25. Togni, A., Developing new chiral ferrocenyl ligands for asymmetric catalysis: A personal account. *Chimia* 1996, 50, 86-93.
26. Hua, Y., Birdsall D.J., Stuart A.M., Hope E.J., Xiao, J., Ruthenium-catalysed asymmetric hydrogenation with fluoroalkylated BINAP ligands in supercritical CO<sub>2</sub>. *Journal of Molecular Catalysis A: Chemical* 2004, 219, 57-60.
27. Gergely, I., Hegedus, C., Szollosy, A., Monsees, A., Riermeier, T., Bakos, J., Electronic and steric effects of ligands as control elements for rhodium-

- catalyzed asymmetric hydrogenation. *Tetrahedron Letters* **2003**, 44, 9025-9028.
- 28. Togni, A., Häusel, R., A new entry into sulphur-containing ferrocenylphosphine ligands for asymmetric catalysis. *Synlett* **1990**, 633-635.
  - 29. Togni, A., G. Rihs, G., Blumer, R.E., Thiolato ligands derived from chiral ferrocenylphosphines: Synthesis and structure of the trimeric copper (I) complex  $\left[\{(R)-(S)-CpFe(\eta.5-C_5H_3(1-PPh_2)(2-CH(CH_3)S)\}Cu\right]_3$ . *Organometallics* **1992**, 11, 613-621.
  - 30. Blaser, H. U., Solvias Josiphos ligands: from discovery to technical application. *Topics in Catalysis* **2002**, 19, (1), 3-16.
  - 31. Yasuike, S., Kofink, C.C., Kloetzing, R.J., Gommermann, N., Tappe, K., Gavryushin, A., Knochel, P., Synthesis of JOSIPHOS-type ligands via a diastereoselective three-component reaction and their application in asymmetric rhodium-catalyzed hydroborations. *Tetrahedron: Asymmetry* **2005**, 16, 3385-3393.
  - 32. Sawamura, M., Kuwano, R., Ito, Y., Enantioselective hydrogenation of beta-distributed alpha-acetamidoacrylates catalyzed by rhodium complexes with TRAP trans-chelating chiral phosphine ligands. *Journal of the American Chemical Society* **1995**, 117, 9602-9603.
  - 33. Weast, R. C., in *Handbook of Chemistry and Physics*, 53rd Edition. *The Chemical Rubber Co., Cleveland (USA)* **1972-1973**.

## Chapter 4

### Continuous Asymmetric Hydrogenation with Ionic Liquid Supported Homogeneous Chiral Rh Catalysts in scCO<sub>2</sub>

This Chapter outlines the advantages of ionic liquids and their application for catalytic reactions in a biphasic system with scCO<sub>2</sub>. The performance of chiral Rh catalysts immobilised on alumina in a continuous flow scCO<sub>2</sub> system was discussed in Chapter 3. In this Chapter, [Rh(COD)(Josiphos 001)]<sup>+</sup> immobilised in ionic liquids was examined for the continuous asymmetric hydrogenation of dimethyl itaconate in a biphasic system ionic liquid/scCO<sub>2</sub>.

#### 4.1. Ionic Liquids

Ionic liquids (ILs) are liquids that contain only ionic species and are liquid below 100 °C. (They are termed as room temperature ionic liquids, RTILs, if they are liquid at room temperature or below).<sup>1, 2</sup> ILs are composed of anions and cations, which can be widely varied to allow the properties of the IL to be tuned. The large number of the known anions and cations make a huge number of potential combinations possible.<sup>1</sup> The most commonly used ionic partners are shown in Figure 4-1.

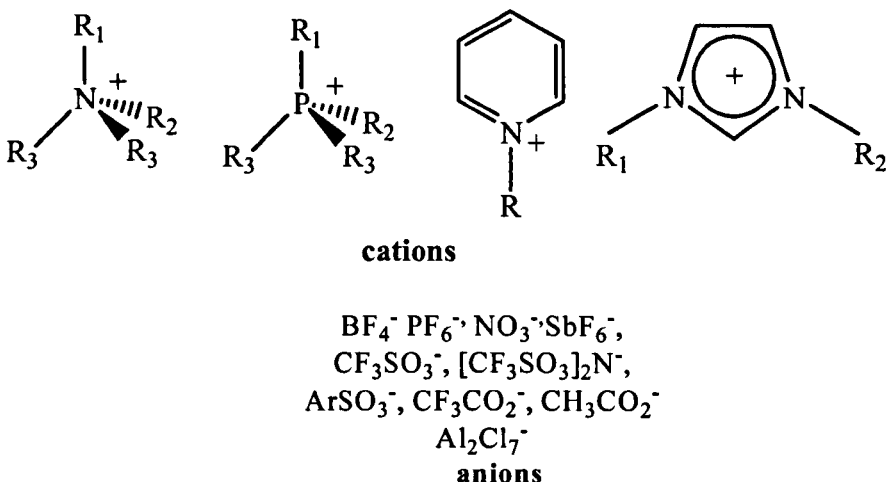


**Figure 4-1.** Typical ions found in common ionic liquids. Most common ILs are composed of an organic cation and a polyatomic anion. The properties of ILs vary depending on which ions are present, leading to them to be described as tuneable solvents.

It is possible to choose the desired solvation and the physical-chemical properties of an ILs by combining the appropriate anions and cations. At the same time, ILs are immiscible with several organic solvents and therefore can be used in a biphasic system. ILs possess several advantageous properties such as negligible vapour pressure, non-flammability, high thermal stability, and large liquid range. ILs are as essentially non-volatile and therefore the evaporative loss of solvent to the environment is avoided.<sup>3-6</sup> The disadvantage of ILs is that they may be toxic. The least toxic ILs have alkylsulfate anions and they are biodegradable. ILs have been used in many areas for example as solvents in catalytic synthesis, as supports for the immobilisation of catalysts, as electrolytes in electrochemistry, in fuel and solar cells, and as lubricants.<sup>1, 4, 7-9</sup>

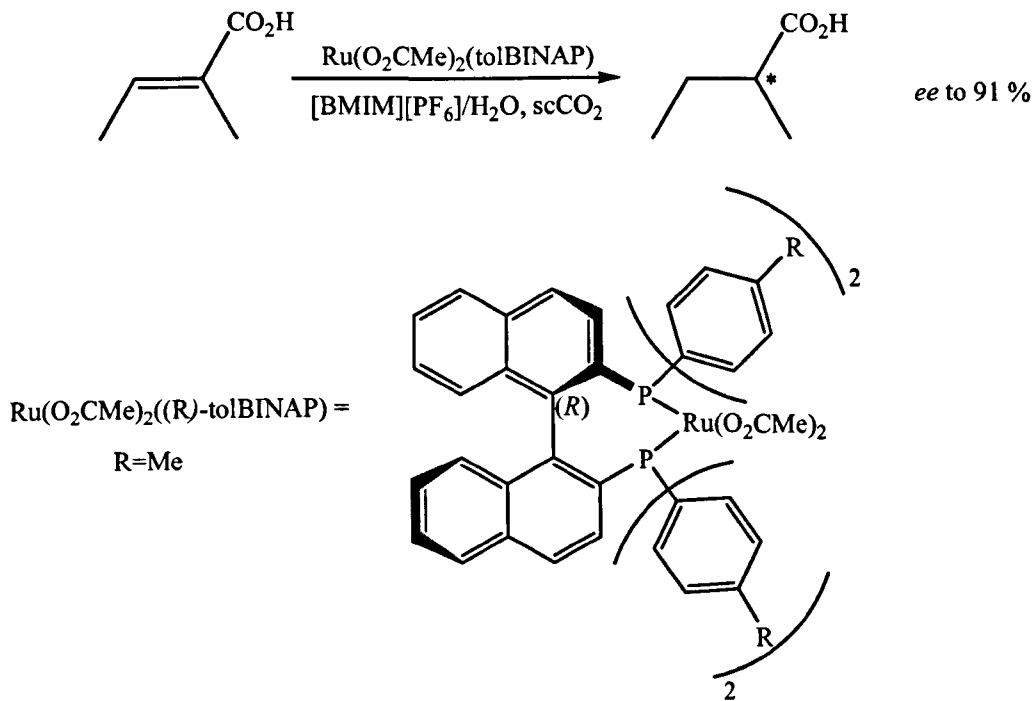
#### 4.2. Reactions in Biphasic Systems Ionic Liquid/scCO<sub>2</sub>

The recovery of the product and the recycling of the catalyst are problems associated with catalysis in ILs. The product may be recovered by distillation or extraction, or a biphasic system can be used. If an organic solvent is used for the extraction or in a biphasic system the overall benefit will decrease. If scCO<sub>2</sub> is

used instead of an organic solvent in a biphasic system, where the catalyst remains in the IL phase and product is extracted by scCO<sub>2</sub>, the problem of catalyst recycling and product recovery can be solved in a green way.<sup>10</sup>

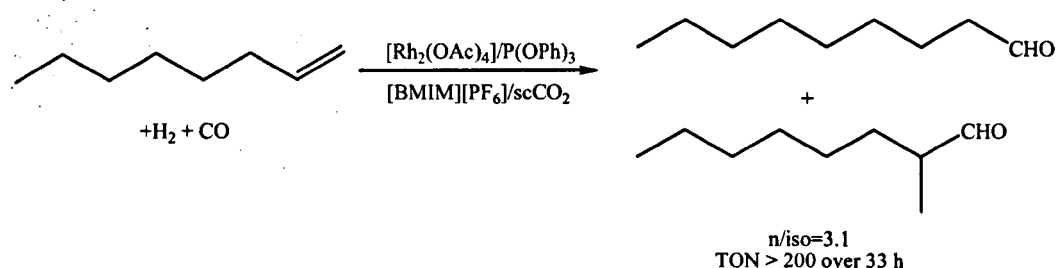
Another advantage of using CO<sub>2</sub> and ILs is that CO<sub>2</sub> is soluble in ILs but ILs are not appreciably soluble in CO<sub>2</sub>, therefore allowing extraction of the product with scCO<sub>2</sub> without contamination by IL.<sup>11</sup> Extraction of materials from the ionic liquid phase with scCO<sub>2</sub> has been successfully performed, including soil remediation<sup>12</sup>, product recovery of a chemical reaction<sup>13</sup>, and chemical-<sup>14-20</sup> and biocatalytic reactions.<sup>4, 21-23</sup>

The first report on asymmetric hydrogenation in [BMIM][PF<sub>6</sub>] with extraction of the product by scCO<sub>2</sub> was published by Jessop and co-workers.<sup>20</sup> High enantioselectivity (up to 99 %) was obtained and the product could be cleanly extracted from the IL with scCO<sub>2</sub> without contamination of the product by IL. The reaction and the catalyst are depicted in Scheme 4-1.



**Scheme 4-1.** The asymmetric hydrogenation of tiglic acid using Ru(O<sub>2</sub>CMe)<sub>2</sub>((R)-tolBINAP) in [BMIM][PF<sub>6</sub>]. The product was extracted with scCO<sub>2</sub>.<sup>20</sup>

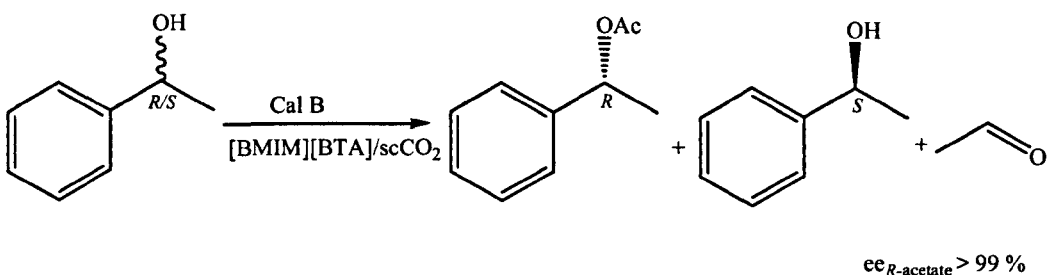
Reports of continuous catalytic reactions in a biphasic system IL/scCO<sub>2</sub> can also be found. The first example was demonstrated by Cole-Hamilton and co-workers.<sup>8,17,18,24</sup> They investigated the Rh-catalysed hydroformylation of 1-octene using [BMIM][PF<sub>6</sub>] (Scheme 4-2). The catalyst was found to be highly stable (Rh leaching into the scCO<sub>2</sub>/product stream was less than 1 ppm) over a long period of time (33 h).



**Scheme 4-2.** The continuous hydroformylation of 1-octene using a  $[\text{Rh}(\text{OAc})_4]/\text{P}(\text{OPh})_3$  in the biphasic system of  $[\text{BMIM}]\text{[PF}_6\text{]}/\text{scCO}_2$ .<sup>17, 24</sup>

During the continuous reaction, the alkene, CO, H<sub>2</sub> and CO<sub>2</sub> were separately fed into the reactor which contained the IL catalyst solution. The products, non-converted substrate and reactants were removed from the IL still dissolved in scCO<sub>2</sub>. After decompression, the liquid was collected and analysed. The description of the reactor for the continuous hydroformylation in a biphasic system IL/scCO<sub>2</sub> can be found in Reference<sup>17</sup>, which was indeed very similar to the reactor used in this study.

Enzymatic reactions have also been successfully demonstrated in a biphasic system IL/scCO<sub>2</sub>. Leitner and co-workers investigated continuous enzyme catalysed kinetic resolution of alcohols in 1-butyl-3-methylimidazolium bis(trifluoromethylsulfonyl)amide [BMIM][BTA] with subsequent extraction of the ester derivatives by scCO<sub>2</sub> (Scheme 4-3), and achieved high enantioselectivity.<sup>23, 25</sup> The reactor used by Leitner to investigate the continuous enzymatic reactions was very similar to the reactor used in this study.



**Scheme 4-3. Continuous enzymatic kinetic resolution of 1-phenylethanol using ionic liquid/scCO<sub>2</sub> media.<sup>23</sup>**

Another approach to perform continuous reactions with IL as catalytic phase is the use of solid, silica supported ionic liquid phase (SILP) catalysts. It has already been demonstrated to be successful. The first application of SILP catalysts was reported by Fehrmann: the continuous gas-phase carbonylation of methanol with [BMIM][Rh(CO)<sub>2</sub>I<sub>2</sub>]-[BMIM]I-SiO<sub>2</sub>.<sup>26</sup>

Continuous asymmetric reactions in a biphasic system IL/scCO<sub>2</sub> have been demonstrated successfully by various research groups, however, this research field is still to be extended. The aim of this study was to investigate the continuous asymmetric hydrogenation of dimethyl itaconate with a chiral Rh catalyst in a biphasic system ILs/scCO<sub>2</sub> and to determine the effect of the IL on the catalyst performance.

### 4.3. Experimental

The ILs [BMIM][BF<sub>4</sub>] (1-butyl-3-methylimidazolium tetrafluoroborate), [BMIM][NTf<sub>2</sub>] (1-butyl-3-methylimidazolium bis(trifluoromethylsulfonyl) imide), and [BMIM][N(CN)<sub>2</sub>] (1-butyl-3-methylimidazolium dicyanamide) were used to immobilise the chiral Rh catalyst [Rh(COD)(Josiphos 001)]<sup>+</sup>[BF<sub>4</sub>]<sup>-</sup>. The choice of these ILs was according to their properties discussed below in this Chapter. The structures of the ILs used here are shown in Figure 4-2.

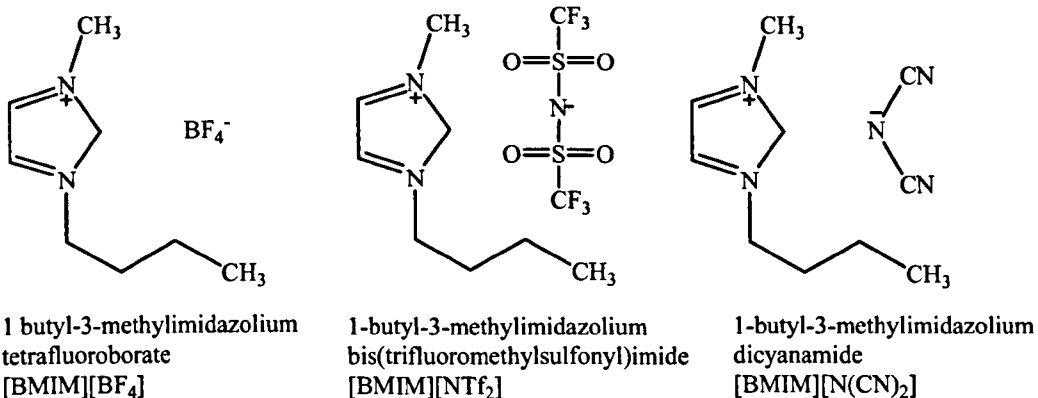


**Figure 4-2. The structure of the ionic liquids used in this work.**

The solubility of CO<sub>2</sub> and H<sub>2</sub> is different in these ILs and therefore allows to compare the performance of the catalyst under different conditions. In general, the solubility of CO<sub>2</sub> in ILs decreases with an increase in temperature, and increases with an increase in pressure. The solubility of CO<sub>2</sub> in ILs also depends on the properties of the IL.<sup>27</sup> It has been shown that CO<sub>2</sub> solubility is dependent on the anion in imidazolium based ILs and they can be classed in three main groups.<sup>27, 28</sup>

- i) The solubility of CO<sub>2</sub> in [BMIM] ILs is the highest when a fluoroalkyl group is the anion, for example [TfO], [NTf<sub>2</sub>], [methide].
- ii) The solubility of CO<sub>2</sub> in [BMIM] ILs is the lowest when a non-fluorinated group is the anion, for example [NO<sub>3</sub>], [N(CN)<sub>2</sub>].
- iii) Inorganic fluorinated anions belong to group possessing intermediate solubility of CO<sub>2</sub> in [BMIM] ILs ([BF<sub>4</sub>], [PF<sub>6</sub>]).

The solubility of H<sub>2</sub> in [BMIM][BF<sub>4</sub>] ( $0.86 \times 10^3$  [H<sub>2</sub>]/M) is higher than in [BMIM][NTf<sub>2</sub>] ( $0.77 \times 10^3$  [H<sub>2</sub>]/M).<sup>28, 29</sup> (No data were found for [BMIM][N(CN)<sub>2</sub>].) The solubility of H<sub>2</sub> in these ILs is approximately 4.5 fold lower than that in MeOH ( $3.75 \times 10^3$  [H<sub>2</sub>]/M).<sup>28, 29</sup>

In the continuous hydrogenation in a biphasic system IL/scCO<sub>2</sub>, the catalyst was dissolved in the IL phase ([BMIM][BF<sub>4</sub>], [BMIM][NTf<sub>2</sub>] or [BMIM][N(CN)<sub>2</sub>]). The CO<sub>2</sub> stream carried the substrate and H<sub>2</sub> to the catalyst dissolved in IL, and then extracted the product and unreacted reactants. The stream of CO<sub>2</sub> was

bubbled through the IL phase. The reactor used in this work to investigate continuous asymmetric hydrogenation in a biphasic system of IL/scCO<sub>2</sub> is shown in Figure 4-3.

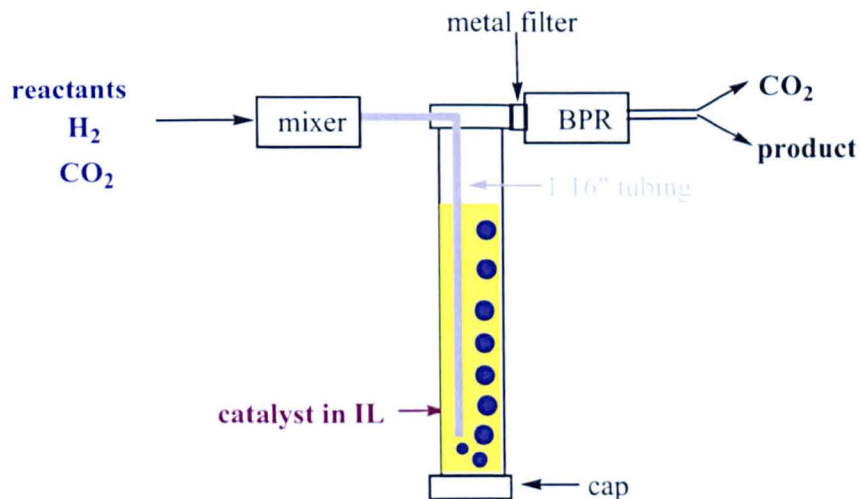
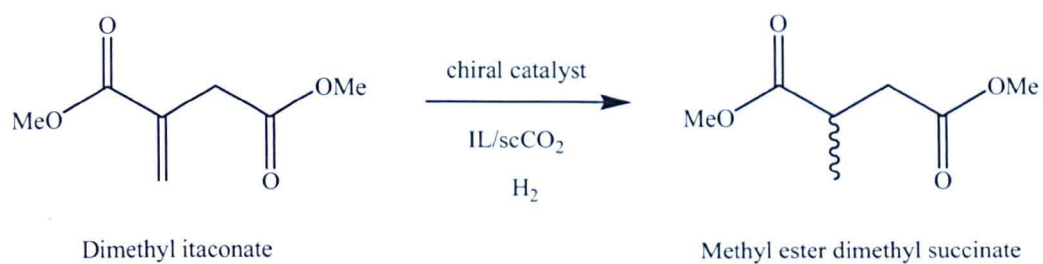


**Figure 4-3. The reactor for continuous asymmetric hydrogenation in a biphasic system IL/scCO<sub>2</sub>.**

#### 4.4. Results and Discussion

The reaction of interest was the asymmetric hydrogenation of dimethyl itaconate (Scheme 4-4). It has been investigated previously in a continuous flow scCO<sub>2</sub> system using an alumina supported chiral Rh catalyst which gave enantioselectivity to 83 % (*S*) (Chapter 3). Here, the continuous asymmetric hydrogenation was investigated with a chiral Rh catalyst in a biphasic system ILs/scCO<sub>2</sub> where the chiral Rh catalyst was immobilised in the IL phase. Different ILs were used to immobilise the catalyst to determine effect of the IL on the catalyst performance.



**Scheme 4-4.** The enantioselective hydrogenation of dimethyl itaconate using a chiral Rh catalyst.

First, the suitability of the reactor and the catalyst was evaluated. The continuous hydrogenation (achiral) of dimethyl itaconate was investigated with  $[\text{Rh}(\text{COD})_2]^+[\text{BF}_4]^-$  in a biphasic system  $[\text{BMIM}][\text{BF}_4]/\text{scCO}_2$  using the reactor shown in Figure 4-3. The results are shown in Figure 4-4.

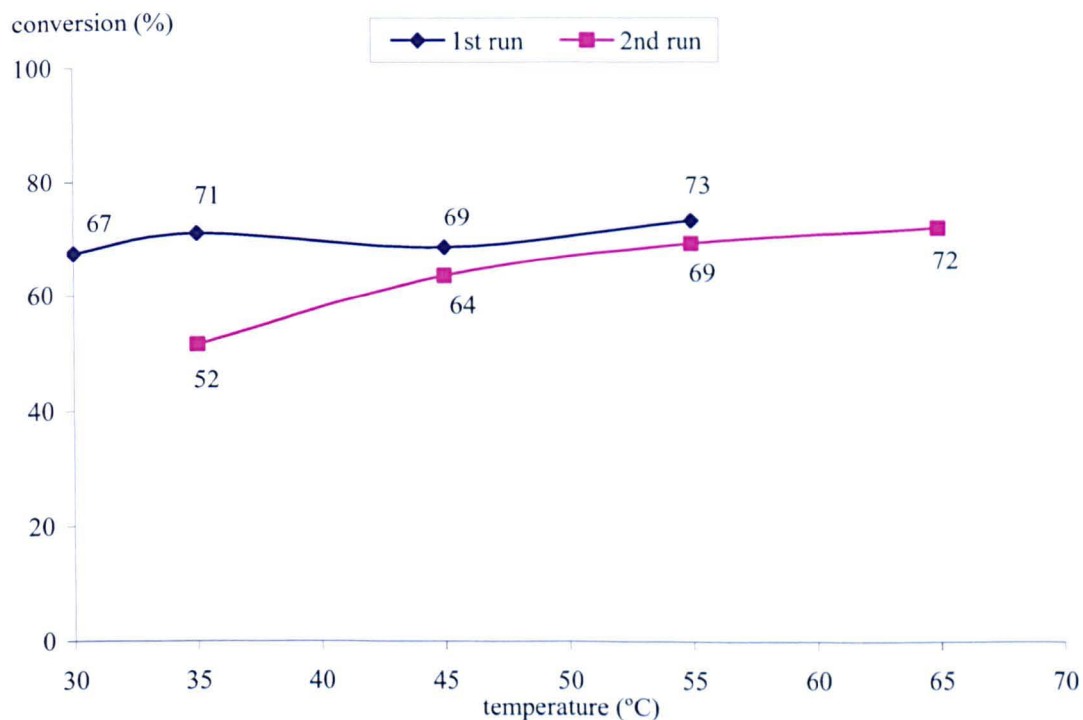


**Figure 4-4.** The conversion of the continuous hydrogenation of dimethyl itaconate with  $[\text{Rh}(\text{COD})_2]^+$  in the biphasic  $[\text{BMIM}][\text{BF}_4]/\text{scCO}_2$  system. Reaction conditions: system pressure: 100 bar,  $\text{CO}_2$  flow rate: 0.5 ml/min, substrate flow rate: 0.1 ml/min (2.5 M DMIT in IPA),  $\text{H}_2$ : substrate molar ratio = 3 : 1, catalyst: 16.7 mM (The molarity of the catalyst was calculated assuming the presence of 50  $\mu\text{mol}$  catalyst in 3 mL ionic liquid. The procedure for preparation is discussed in Chapter 2).

The conversion obtained with  $[\text{Rh}(\text{COD})_2]^+[\text{BF}_4]^-$  in the biphasic system  $[\text{BMIM}][\text{BF}_4]/\text{scCO}_2$  was comparable with the conversion obtained in the continuous hydrogenation with  $[\text{Rh}(\text{COD})_2]^+[\text{BF}_4]^-/\text{PTA}/\text{Alumina}$  in  $\text{scCO}_2$  (Chapter 3, Table 3-3). Having confirmed that the reactor and the catalyst were suitable, the asymmetric hydrogenation of dimethyl itaconate was then investigated. The ILs  $[\text{BMIM}][\text{BF}_4]$ ,  $[\text{BMIM}][\text{NTf}_2]$  and  $[\text{BMIM}][\text{N}(\text{CN})_2]$  were examined to immobilise the chiral catalyst  $[\text{Rh}(\text{COD})(\text{Josiphos } 001)]^+[\text{BF}_4]^-$ . The enantioselectivity of the continuous asymmetric hydrogenation in a biphasic system IL/ $\text{scCO}_2$  is shown in Figure 4-5.

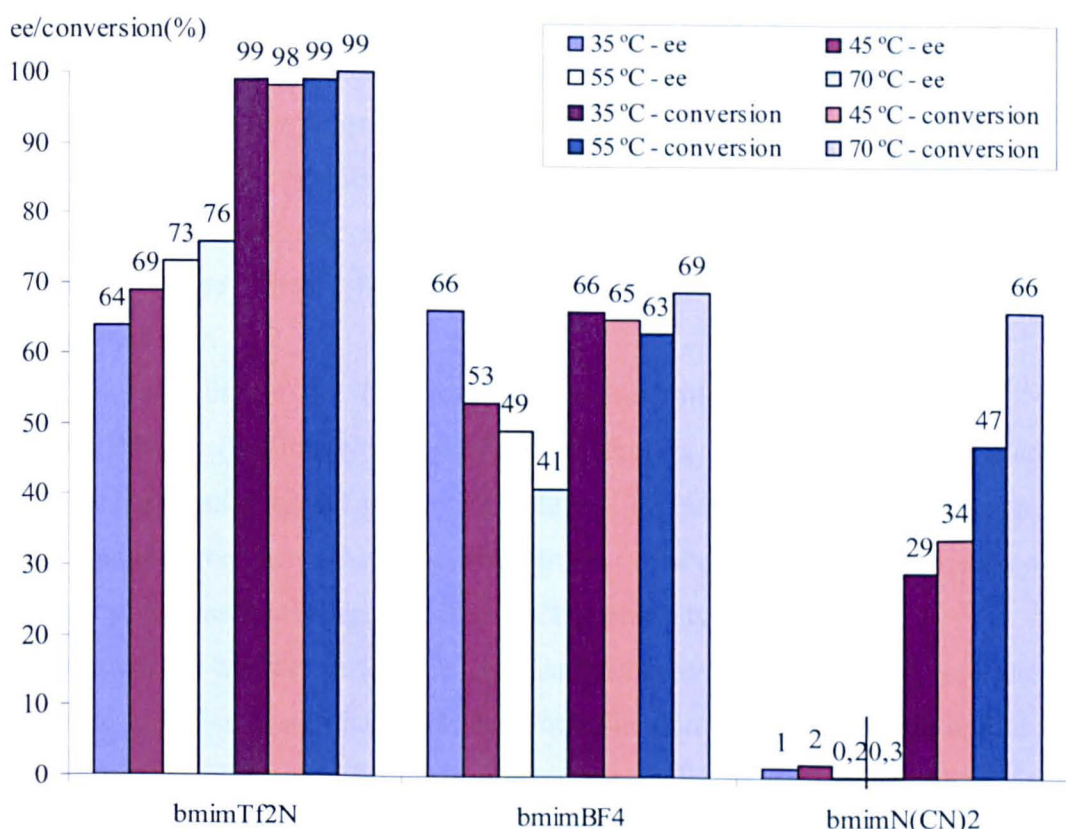


**Figure 4-5. The enantioselectivity and level of conversion of the continuous asymmetric hydrogenation of dimethyl itaconate with  $[\text{Rh}(\text{COD})(\text{Josiphos 001})]^+[\text{BF}_4]^-$  in a biphasic system IL/ $\text{scCO}_2$ .**

Reaction conditions: system pressure: 100 bar,  $\text{CO}_2$  flow rate: 0.5 ml/min, substrate flow rate: 0.1 ml/min (2.5 M DMIT in IPA),  $\text{H}_2$  : substrate molar ratio = 3 : 1, catalyst concentration: 16.7 mM.

\*  $[\text{Rh}(\text{COD})(\text{Josiphos 001})]^+[\text{BF}_4]^-$ /PTA/Alumina, Reaction conditions: pressure: 100 bar,  $\text{CO}_2$  flow rate: 0.5 ml/min, substrate flow rate: 0.2 ml/min (DMIT in IPA 2.5 M),  $\text{H}_2$  : substrate ratio = 3:1, chiral catalyst: 16.7 mM (The molarity of the chiral catalyst was calculated assuming the presence of 50  $\mu\text{mol}$  chiral catalyst in 3 mL ionic liquid. The procedure for preparation is discussed in Chapter 2).

The enantioselectivity of the reaction varied between the different ILs used to immobilise the chiral catalyst. The  $\text{H}_2$  solubility is higher in [BMIM][BF<sub>4</sub>] than that in [BMIM][NTf<sub>2</sub>]. (No literature data was found for the solubility of  $\text{H}_2$  in [BMIM][N(CN)<sub>2</sub>]). The enantioselectivity was higher using [BMIM][NTf<sub>2</sub>] than that using [BMIM][BF<sub>4</sub>], and much higher than that using [BMIM][N(CN)<sub>2</sub>]. The enantioselectivity observed for the continuous asymmetric hydrogenation in a

biphasic system IL/scCO<sub>2</sub> using the ILs [BMIM][BF<sub>4</sub>] and [BMIM][NTf<sub>2</sub>] was in a good agreement with the H<sub>2</sub> solubility in these ILs [BMIM][BF<sub>4</sub>] > [BMIM][NTf<sub>2</sub>]. The enantioselectivity in the biphasic system [BMIM][N(CN)<sub>2</sub>]/scCO<sub>2</sub> was lower than that using the other two ILs. This suggests the H<sub>2</sub> solubility in [BMIM][N(CN)<sub>2</sub>] may be lower than that in [BMIM][BF<sub>4</sub>] and [BMIM][NTf<sub>2</sub>], and therefore the catalyst displayed lower enantioselectivity.

The CO<sub>2</sub> solubility in the ILs used here is the following: [BMIM][NTf<sub>2</sub>] > [BMIM][BF<sub>4</sub>] > [BMIM][N(CN)<sub>2</sub>]. The introduction of CO<sub>2</sub> in the IL phase improves the mass transport which can influence the performance of the catalyst, which was observed here: the enantioselectivity of the asymmetric hydrogenation of dimethyl itaconate was higher at higher CO<sub>2</sub> solubility.

Another reason for the difference in enantioselectivity could be due to the difference in the estimated nucleophilicity/coordination strength of the IL anions. The enantioselectivity dropped with a decrease in nucleophilicity/coordination strength of the anion [NTf<sub>2</sub>] > [BF<sub>4</sub>] > [N(CN)<sub>2</sub>]. The anion choice was demonstrated to be crucial in achieving high enantioselectivity here and also by another research group<sup>19</sup> for the asymmetric hydrovinylation of styrene.

An interesting phenomenon was observed using [BMIM][NTf<sub>2</sub>] to immobilise [Rh(COD)(Josiphos 001)]<sup>+</sup>[BF<sub>4</sub>]<sup>-</sup>. The enantioselectivity increased with an increase in temperature, when, generally the opposite is expected (decrease in enantioselectivity with an increase in temperature). An increase in temperature can increase the rate of the slower reaction of an asymmetric hydrogenation and therefore the enantioselectivity decreases. In a biphasic system IL/scCO<sub>2</sub>, the solubility of the substrate in the IL may increase with an increase in temperature and, therefore higher enantioselectivity may result from lower mass transport limitations. The reason for this increase in enantioselectivity with temperature is not yet completely clear. However, the same trend was observed using Rh(COD)(Josiphos 001)]<sup>+</sup>[BF<sub>4</sub>]<sup>-</sup>/PTA/Alumina in the continuous asymmetric hydrogenation of dimethyl itaconate in scCO<sub>2</sub>.

The variation in conversion between different ILs was probably due to the differences in solubility of CO<sub>2</sub> in the particular IL. The conversion would be expected to increase when the mass transport limitations are lower which occurs with the introduction of CO<sub>2</sub> in the IL phase. The solubility of CO<sub>2</sub> in ILs was in a good agreement with the conversion observed [BMIM][NTf<sub>2</sub>] > [BMIM][BF<sub>4</sub>] > [BMIM][N(CN)<sub>2</sub>]. The nucleophilicity strength of the IL anion could also influence the performance of the catalyst: the higher the nucleophilicity strength the higher the conversion ([Tf<sub>2</sub>N] > [BF<sub>4</sub>] > [N(CN)<sub>2</sub>]), which was observed by us and previously by another research group.<sup>19</sup>

In the biphasic system [BMIM][N(CN)<sub>2</sub>]/scCO<sub>2</sub>, the enantioselectivity was low, while the conversion was high. This suggests that this IL might influence the chiral motif of the catalyst by interacting with Fe of the ligand.

#### 4.5. Conclusions

The ILs [BMIM][BF<sub>4</sub>], [BMIM][NTf<sub>2</sub>], and [BMIM][N(CN)<sub>2</sub>] were used to immobilise [Rh(COD)(Josiphos 001)]<sup>+</sup>[BF<sub>4</sub>]<sup>-</sup>. The immobilised catalyst was examined for the continuous asymmetric hydrogenation of dimethyl itaconate in a biphasic system IL/scCO<sub>2</sub>. The enantioselectivity and conversion of the reaction varied between using different ionic liquids in the biphasic system. The best results were observed in [BMIM][NTf<sub>2</sub>]/scCO<sub>2</sub> with enantioselectivity up to 76 % (*S*) and conversion up to 99 %. The solubility of H<sub>2</sub> in the IL, the solubility CO<sub>2</sub> in the IL, and the anion nucleophilicity/coordination strength were found to be the main factors that might influence the performance of the chiral catalyst.

#### References

1. Wasserscheid, P., Welton, T., in Ionic liquids in synthesis. *Wiley-VCH, Weinheim 2003*.
2. Anastas, P. T., Warner, J.C., in Green Chemistry: Theory and practice. *Oxford University Press, Oxford 1998*.
3. Rogers, R. D., Seddon, K.R., Chemistry. Ionic liquids-solvents of the future? *Science 2003, 302, 792-793*.
4. Sheldon, R. A., Arends, I., Hanefeld, U., in Green Chemistry and Catalysis. *Wiley-VCH, Weinheim 2007*.

5. Sheldon, R. A., Selective catalytic synthesis of fine chemicals: Opportunities and trends. *Journal of Molecular Catalysis A: Chemical* 1996, 107, 75-83.
6. Liu, Q. B., Janssen, M.H.A., van Rantwijk, F., Sheldon, R.A., Room-temperature ionic liquids that dissolve carbohydrates in high concentrations. *Green Chemistry* 2005, 7, 39-42.
7. Wagner, M., Ionic liquids: commercial success stories and further challenges. *Chimica Oggi - Chemistry Today* 2007, 25, 14-16.
8. Wasserscheid, P., Continuous Reaction Using Ionic Liquids as Catalytic Phase. *Journal of Industrial and Engineering Chemistry* 2007, 13, 325-338.
9. Dupont, J., de Souza, R.F., Suarez, P.A.Z. , Ionic liquid (molten salt) phase organometallic catalysis. *Chemical Reviews* 2002, 102, 3667-3691.
10. Scurto, A., Leitner, W., Expanding the useful range of ionic liquids: melting point depression of organic salts with carbon dioxide for biphasic catalytic reactions. *Chemical Communications* 2006, 3681-3683.
11. Blanchard, L. A., Hancu, D., Beckman, E.J., Brennecke, J.F. , Green processing using ionic liquids and CO<sub>2</sub>. *Nature* 1999, 399, 28-29.
12. Keskin, S., Akman, U., Hortacsu, O., Soil remediation via an ionic liquid and supercritical CO<sub>2</sub>. *Chemical Engineering and Processing* 2008, 47, 1693-1704.
13. Kroon, M. C., van Spronsen, J., Peters, C.J., Sheldon, R.A., Witkamp, G.J., Recovery of pure products from ionic liquids using supercritical carbon dioxide as a co-solvent in extractions or as an anti-solvent in precipitations. *Green Chemistry* 2006, 8, 246-249.
14. Ahosseini, A., Ren, W., Scurto, A.M., Homogeneous catalysis in biphasic ionic liquid/CO<sub>2</sub> systems. *Chimica Oggi - Chemistry Today* 2007, 25, 40-42
15. Kuhne, E., Perez, E., Witkamp, G.J., Peters C.J. , Solute influence on the high-pressure phase equilibrium of ternary systems with carbon dioxide and an ionic liquid. *Journal of Supercritical Fluids* 2008, 45, 27-31.
16. Liu, F., Abrams, M.B., Baker, R.T., Tumas, W., Phase-separable catalysis using room temperature ionic liquids and supercritical carbon dioxide. *Chemical Communications* 2001, 433-434.
17. Sellin, M. F., Webb, P.B., Cole-Hamilton, D.J., Continuous flow homogeneous catalysis: hydroformylation of alkenes in supercritical fluid-ionic liquid biphasic mixtures. *Chemical Communications* 2001, 781-782.
18. Webb, P. B., Sellin, M.F., Kunene, T.E., Williamson, S., Slawin, A.M.Z., Cole-Hamilton, D.J., Continuous Flow Hydroformylation of Alkenes in Supercritical Fluid-Ionic Liquid Biphasic Systems. *Journal of the American Chemical Society* 2003, 125, 15577-15588.
19. Bösmann, A., Francio, G., Janssen, E., Solinas, N., Leitner, W., Wasserscheid, P., Activation, Tuning, and Immobilization of Homogeneous Catalysts in an Ionic Liquid/Compressed CO<sub>2</sub> Continuous-Flow System. *Angewandte Chemie International Edition* 2001, 40, 2697-2699.
20. Brown, R. A., Pollet, P., McKoon, E., Eckhert, C.A., Liotta, C.L., Jessop, P.G., Asymmetric hydrogenation and catalyst recycling using ionic liquid and supercritical carbon dioxide. *Journal of the American Chemical Society* 2001, 123, 1254-1255.

21. van Rantwijk, F., Sheldon, R.A., Biocatalysis in Ionic Liquids. *Chemical Reviews* **2007**, 107, 2757-2785.
22. Lozano, P., de Diego, T., Carrié, d., Vaultier, M., Iborra, J.L., Continuous green biocatalytic processes using ionic liquids and supercritical carbon dioxide. *Chemical Communications* **2002**, 692-693.
23. Reetz, M. T., Wiesenhöfer, W., Franciò, G., Leitner, W., Biocatalysis in ionic liquids: batchwise and continuous flow processes using supercritical carbon dioxide as the mobile phase. *Chemical Communications* **2002**, 992-993.
24. Jessop, P. G., Homogeneous Catalysis and Catalyst Recovery Using Supercritical Carbon Dioxide and Ionic Liquids. *Journal of Synthetic Organic Chemistry, Japan* **2003**, 484-488.
25. Reetz, M. T., Wiesenhofer, W., Francio, G., Leitner, W., Continuous Flow Enzymatic Kinetic Resolution and Enantiomer Separation using Ionic Liquid/Supercritical Carbon Dioxide Media. *Advanced Synthesis & Catalysis* **2003**, 345, 1221-1228.
26. Rusager, A., Jorgensen, B., Wasserscheid, P., Fehrmann, R., First application of supported ionic liquid phase (SILP) catalysis for continuous methanol carbonylation. *Chemical Communications* **2006**, 994-996.
27. Aki, S. N. O. V. K., Mellein, B.R., Saurer, E.M., Brennecke, J.F., High-pressure phase behavior of carbon dioxide with imidazolium-based ionic liquids. *Journal of Physical Chemistry B* **2004**, 108, 20355-20365.
28. Anthony, J. L., Anderson, J.L., Maginn, E.J., Brennecke, J.F., Anion effects on gas solubility in ionic liquids. *Journal of Physical Chemistry B* **2005**, 13, 6366-6374.
29. Dyson, P. J., Laurenczy, G., Ohlin, C.A., Vallance, J., Welton, T., Determination of hydrogen concentration in ionic liquids and the effect (or lack of) on rates of hydrogenation. *Chemical Communications* **2003**, 2418-2419.
30. Jessop, P. G., Stanley, R.R., Brown, R.A., Eckert, C.A., Liotta, C.L., Ngo, T.T., Pollet, P., Neoteric solvents for asymmetric hydrogenation: supercritical fluids, ionic liquids, and expanded ionic liquids. *Green Chemistry* **2003**, 5, 123-128.
31. Anthony, J. L., Maginn, E.J., Brennecke, J.F., Solubilities and thermodynamic properties of gases in the ionic liquid 1-n-butyl-3-methylimidazolium hexafluorophosphate. *Journal of Physical Chemistry B* **2002**, 106, 7315-7320.
32. Seddon, K. R., Stark, A., Torres, M.J., Influence of chloride, water, and organic solvents on the physical properties of ionic liquids. *Pure Applied Chemistry* **2000**, 72, 2275-2287.

## Chapter 5

### Continuous Kinetic Resolution of $\alpha$ -tetralol Catalysed by Cal B CLEA in scCO<sub>2</sub>

The production of enantiomerically pure compounds was investigated using heterogeneous chiral Rh catalysts in scCO<sub>2</sub> in Chapters 3 and 4. In this Chapter, immobilised enzymes are examined for enantioselective reactions in scCO<sub>2</sub>. The continuous kinetic resolution of  $\alpha$ -tetralol was studied with *Candida antarctica* lipase B (Cal B) immobilised in the form of Cross-Linked Enzyme Aggregate (CLEA).

#### 5.1. Using Enzymes as Biocatalysts

Enzymes fall into one of the six classes depending on the type of reaction they catalyse.<sup>1</sup> The six classes are the following:

- i) Oxidoreductases
- ii) Transferases
- iii) Hydrolases
- iv) Lyases
- v) Isomerasases
- vi) Ligases

Enzymes as catalysts have two main advantages; they operate well at mild conditions, and they are highly chemo-, regio- and enantio-selective.<sup>2</sup> Despite these advantages, enzymes have not been widely applied in industry. This is because, like phosphine ligands, they have high substrate specificity and therefore limited to perform reactions with few structurally analogous substrates.<sup>3</sup> The ideal properties of an enzyme/biocatalyst would be high thermal stability, high stability against organic solvents, and high activity for many starting materials. Therefore the majority of applications of enzyme biocatalysts in synthetic chemistry have

been limited to few commercially available enzymes, namely lipases, proteases, and glycosidases.<sup>4</sup> These enzymes belong to the family of hydrolases and are widely used because they are usually less substrate specific than other enzymes and they normally function without a cofactor. Hydrolases catalyse the hydrolysis of chemical bonds; lipases, proteases, and glycosidases break ester, amide and glycoside bonds, respectively.

In this work, the activity of lipase from *Candida antarctica* (lipase B from *Candida antarctica*, Cal B) has been investigated for a transesterification reaction. Cal B is one of the most widely used lipases because it is active with a broad range of substrates.<sup>5,6</sup> Cal B hydrolyses triglycerides and is of particular interest because it displays strong stereospecificity on chiral substrates. The structure of Cal B<sup>7</sup> has been resolved and is shown in Figure 5-1. An Asp-His-Ser catalytic triad has been shown to be its active site.<sup>7</sup> The reaction mechanism of the transesterification of alcohols by Cal B has been investigated by many groups and was shown to follow a ping-pong bi-bi ordering.<sup>8, 9</sup> (The mechanism of the transesterification of  $\alpha$ -tetralol by Cal B is shown below in Scheme 5-3, page 115).

Although many enzymes have been shown to be active in organic solvents<sup>10-12</sup>, their application still has the drawback of homogeneously catalysed reactions, the difficulty of the recovery and recycling of the enzyme. Immobilisation of the enzyme facilitates the recovery and also opens up the possibility of using the enzyme in a highly efficient continuous process.<sup>13</sup> Besides the ease of recovery, immobilisation can also increase the stability.<sup>13</sup> A discussion on catalyst immobilisation can be found in Chapter 1. The Cross-Linked Enzyme Aggregate (CLEA) technique<sup>14</sup> is a novel method to immobilise enzymes in a carrier-free form. It has already been demonstrated to be suitable for various enzymes<sup>14-26</sup>, including lipases from different sources<sup>15</sup> (*Candida antarctica* lipase A and B - Cal A and Cal B, *Rhizomucor miehei* lipase - Rml, *Aspergillus niger* lipase - Anl) which have already been shown to be active in conventional media. If the immobilised enzymes that work well in traditional solvents can be shown to work in alternative solvents, the sustainability of the reactions can be improved.

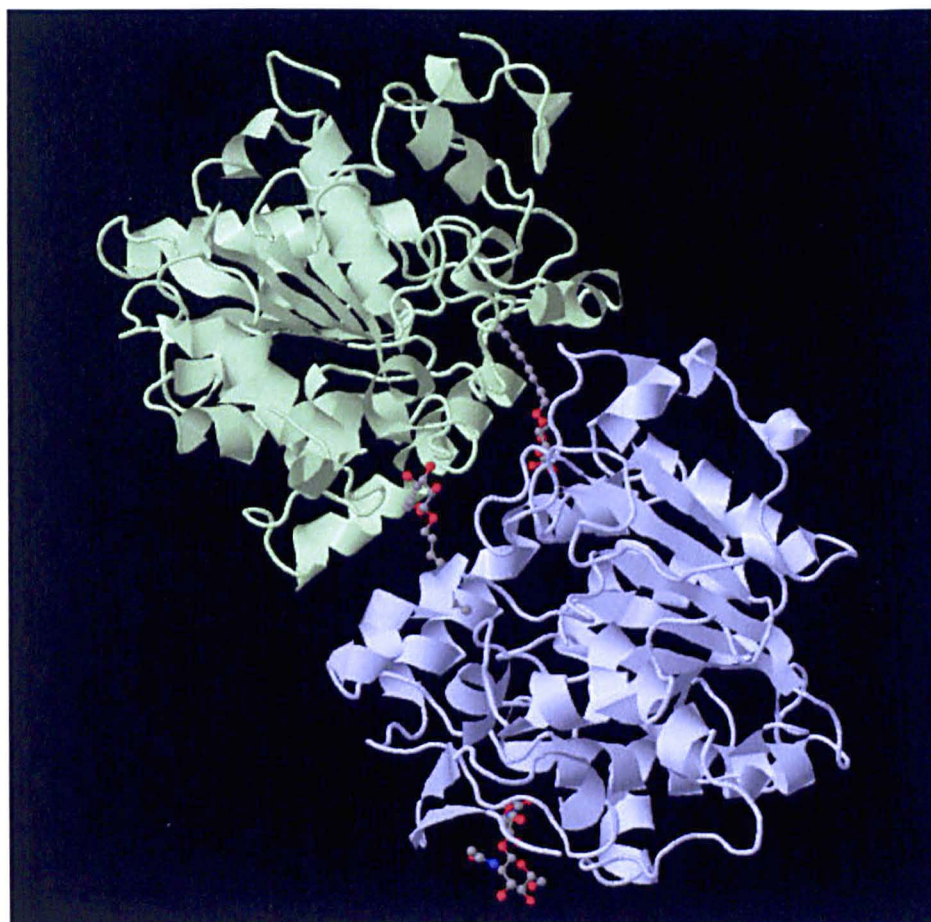


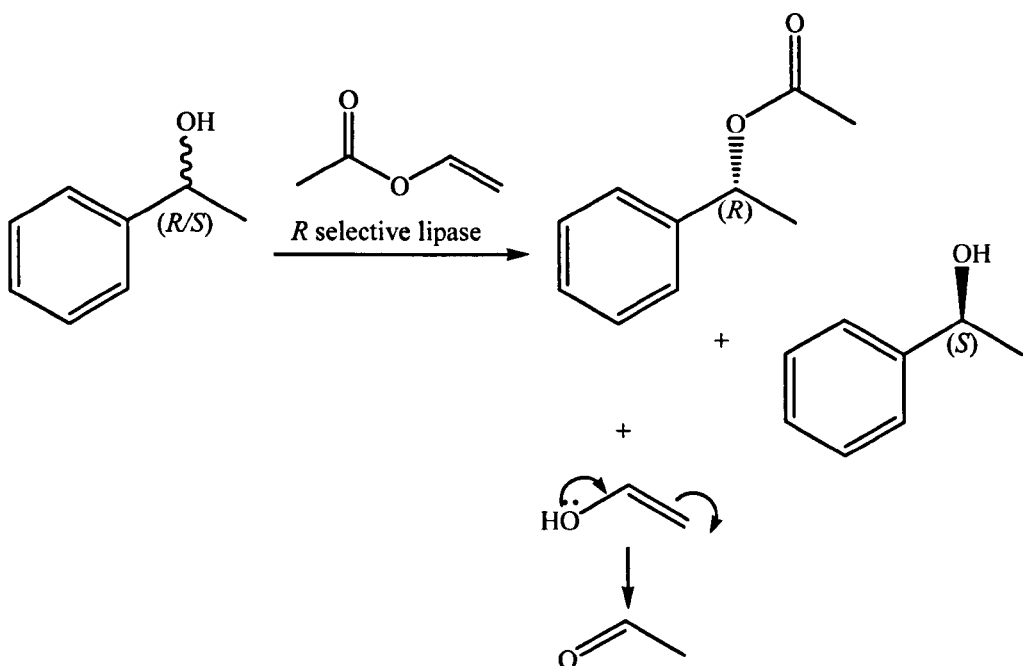
**Figure 5-1.** The structure of *Candida antarctica* lipase B (Cal B). Cal B has a molecular weight of 33.5 kDa and it is an  $\alpha/\beta$  type protein (build up of mostly parallel  $\beta$ -sheet surrounded by  $\alpha$ -helices). It has two asymmetric units. The crystal structure was obtained from Protein DataBank.<sup>7</sup> The picture was prepared using Jmol.

## 5.2. Enzyme catalysed kinetic resolution in scCO<sub>2</sub>

Kinetic resolution, an approach to produce enantiomerically pure compounds, can also be catalysed by enzymes. In a kinetic resolution, one of the enantiomers reacts more rapidly than the other. Due to the enhanced reaction rate of one of the enantiomers, a selective reaction can be performed. In kinetic resolutions catalysed by enzymes, only one enantiomer of the substrate is converted into the product and the other enantiomer is left unreacted or reacts considerably more slowly.<sup>26</sup> Lipase B from *Candida antarctica* is selective for the (*R*) enantiomer. The products of the kinetic resolution of alcohols are therefore (*R*)-ester, unreacted

(*S*)-alcohol, and a by-product from the acyl donor. Vinyl acetate is commonly used as acyl donor because the produced acetaldehyde cannot be re-acylated and therefore the reaction is driven towards the formation of the product. The kinetic resolution of 1-phenylethanol catalysed by lipase is one of the most widely studied reactions in organic solvents and also in alternative solvents.<sup>5, 6, 11, 12, 27-33</sup> The reaction is depicted in Scheme 5-1.

A disadvantage of kinetic resolution is that only one of the enantiomers is transformed with a highly selective catalyst, and therefore the maximum conversion of the reaction is 50 %. If the unreacted alcohol is racemised in situ, full conversion of the substrate to product can be achieved. This technique is known as dynamic kinetic resolution (DKR).



**Scheme 5-1. The kinetic resolution of 1-phenylethanol catalysed by an (*R*) selective lipase with vinyl acetate as acyl donor.**

The use of alternative solvents is of interest to in the fine chemical industry. Immobilised lipases have already been used for reactions in scCO<sub>2</sub>. The following advantages were found.<sup>27, 28, 30</sup>

- i) Highly enantioselective.
- ii) Work well at low temperatures and in a wide range of pressures.

- iii) Applicable to a range of substrates.
- iv) Highly active requiring a small amount of catalyst.
- v) Use of an alternative solvent.
- vi) Can be used in continuous processes.

Matsuda showed one of the first examples for the continuous kinetic resolution of 1-phenylethanol (Scheme 5-1) in scCO<sub>2</sub>. The catalyst was Novozym 435 (Cal B adsorbed on a macroporous resin) which displayed high enantioselectivity and E-value (a measure of enantioselectivity, value > 100 indicate highly enantioselective reaction<sup>34</sup>, Note! E-value is different than E-factor) in a continuous flow scCO<sub>2</sub> system.<sup>27</sup> The conversion of R-phenyl alcohol was calculated using the equation shown in Equation 5-1. The results of Matsuda's work are presented in Table 5-1.

$$c = ee_{S-alcohol} / (ee_{S-alcohol} + ee_{R-acetate})$$

**Equation 5-1. Calculation of the conversion of an enantioselective reaction.**

$$E = \frac{\ln[1 - c(1 + ee_{R-acetate})]}{\ln[1 - c(1 - ee_{R-acetate})]}$$

**Equation 5-2. Calculation of the E-value.**

**Table 5-1. Results of Matsuda's continuous kinetic resolution of 1-phenylethanol with vinyl acetate catalysed by Novozym 435 in scCO<sub>2</sub>.**<sup>27</sup>

Entry	Ratio <sup>a</sup>	P (bar)	ee alcohol (%)	ee acetate (%)	Conv <sup>b</sup> (%)	E-value <sup>c</sup>
1	1 : 0.5	130	89.6	99.7	47	>1000
2	1 : 0.6	130	98.8	99.2	50	>1000
3	1 : 1.3	129	>99.5	99	50	>1000
4	1 : 1.3	89	>99.5	99	50	>1000
5	1 : 1.3	200	>99.5	99	50	>1000

Reaction conditions: temperature: 42 - 43 °C, CO<sub>2</sub> flow rate: 1.0 mL/min, substrate flow rate: 0.2 mL/min.

a: Ratio of 1-phenyl ethanol : vinyl acetate

b: Conversion was calculated using Equation 5-1.

c: E-value was calculated using Equation 5-2.

The continuous kinetic resolution of 1-phenylethanol in scCO<sub>2</sub> was repeated at Nottingham and the results showed similarly high success (Table 5-2).<sup>35</sup>

**Table 5-2. Results of the continuous kinetic resolution of 1-phenylethanol with vinyl acetate using Novozym 435 as catalyst in scCO<sub>2</sub>.**<sup>35</sup>

Entry	T (°C)	ee alcohol (%)	ee acetate (%)	Conv (%)	E-value
1	35	94	95	50	140
2	40	95	96	50	180
3 *	40	85	99	46	520
4 **	45	99	99	50	1060
5	45	99	98	50	530
6	50	97	98	50	420

**Reaction conditions:** pressure: 110 bar, CO<sub>2</sub> flow rate: 1.0 mL/min, substrate flow rate: 0.2 mL/min (1 : 1 vol. ratio of 1-phenyl ethanol : vinyl acetate).

\* Reaction conditions: pressure: 110 bar, CO<sub>2</sub> flow rate: 1.0 mL/min, substrate flow rate: 0.2 mL/min (1 : 0.5 vol. ratio of 1-phenyl ethanol : vinyl acetate).

\*\* Reaction conditions: pressure: 200 bar, CO<sub>2</sub> flow rate: 1.0 mL/min, substrate flow rate: 0.2 mL/min (1 : 1 vol. ratio of 1-phenyl ethanol : vinyl acetate).

Nottingham has had a great interest in biocatalytic reactions in scCO<sub>2</sub> and as the results of Matsuda's work could be reproduced at Nottingham, the investigation of the kinetic resolution of secondary alcohols was continued. CLEA of Cal B has been successfully prepared but their activity has not yet been widely studied. Here, their activity for the kinetic resolution of 1-phenylethanol in a continuous flow scCO<sub>2</sub> system has been investigated. The results are shown in Table 5-3.

**Table 5-3. Results of the continuous kinetic resolution of 1-phenylethanol with vinyl acetate catalysed by Cal B CLEA in scCO<sub>2</sub>.**<sup>35</sup>

Entry	T (°C)	ee alcohol (%)	ee acetate (%)	E-value
1	30	60	99	> 1000
2	40	89	99	> 1000
3	45	92	99	> 1000
4	50	98	99	1000

**Reaction conditions:** pressure: 110 bar, CO<sub>2</sub> flow rate: 0.25 mL/min, substrate flow rate: 0.05 mL/min (1 : 1 vol. ratio of 1-phenyl ethanol : vinyl acetate).

The kinetic resolution of 1-phenylethanol was successfully performed in a continuous flow scCO<sub>2</sub> system using Cal B CLEA. The enantioselectivities obtained by Cal B CLEA were comparable with those obtained by Novozym 435. Following the success with Cal B CLEA in the continuous kinetic resolution of 1-phenylethanol in scCO<sub>2</sub>, the investigation of the activity of Cal B CLEA continued at Nottingham.

The kinetic resolution of 1-phenylethanol has been widely studied but the kinetic resolution of other secondary alcohols has been explored less. The activity of Cal B CLEA (donated by the first mentor of Cal B CLEA Professor Roger Sheldon, CLEA Technologies, Delft, Netherlands) was examined here for the kinetic resolution of another secondary alcohol,  $\alpha$ -tetralol, in a continuous flow scCO<sub>2</sub> system. To achieve high enantioselectivity, different reaction conditions and acyl donors were examined.

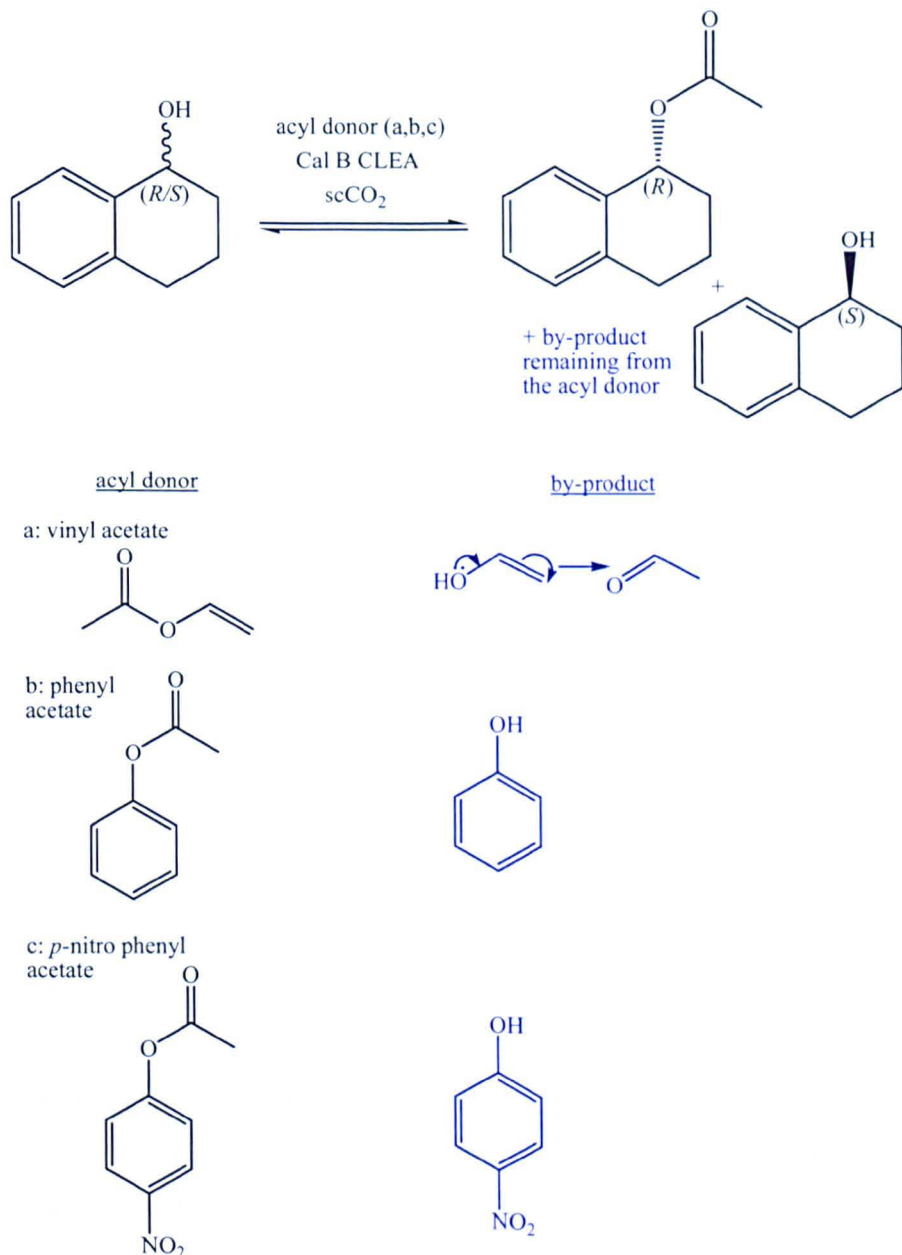
### 5.3. Results and Discussion

$\alpha$ -tetralol (1,2,3,4-tetrahydro naphthol) is a secondary alcohol and is slightly larger than 1-phenylethanol. The two compounds are different also in their solubility in scCO<sub>2</sub>: 1-phenylethanol<sup>36</sup> is highly soluble in scCO<sub>2</sub>, while  $\alpha$ -tetralol<sup>37</sup> is only slightly soluble in scCO<sub>2</sub> (52 mmol/L at 40 °C and 138 bar).

The kinetic resolution of  $\alpha$ -tetralol was examined with Cal B (E.C. 3.1.1.3) CLEA (28000 U/g solid, batch no 5790) in a continuous flow scCO<sub>2</sub> system. The continuous flow high pressure reactor is described in Chapter 2. The following parameters were investigated for the reaction.

- i) The effect of different acyl donors at different temperatures and pressures.
- ii) The effect of the immobilisation technique used to heterogenise Cal B at different temperatures.
- iii) The effect of the substrate to acyl donor ratio.
- iv) The effect of the use of a cosolvent.
- v) The effect of the phase behaviour.

In fact, enzymatic esterification is a reversible reaction and characterized by equilibrium constant. The reaction can become irreversible when the acyl donor forms a non-nucleophilic product (by-product in the reaction). To optimise the catalyst performance, different acyl donors were investigated for the kinetic resolution of  $\alpha$ -tetralol (Scheme 5-2) in a continuous flow scCO<sub>2</sub> system. The results are shown in Figure 5-2..



**Scheme 5-2.** The kinetic resolution of  $\alpha$ -tetralol using different acyl donors catalysed by Cal B CLEA in scCO<sub>2</sub>.

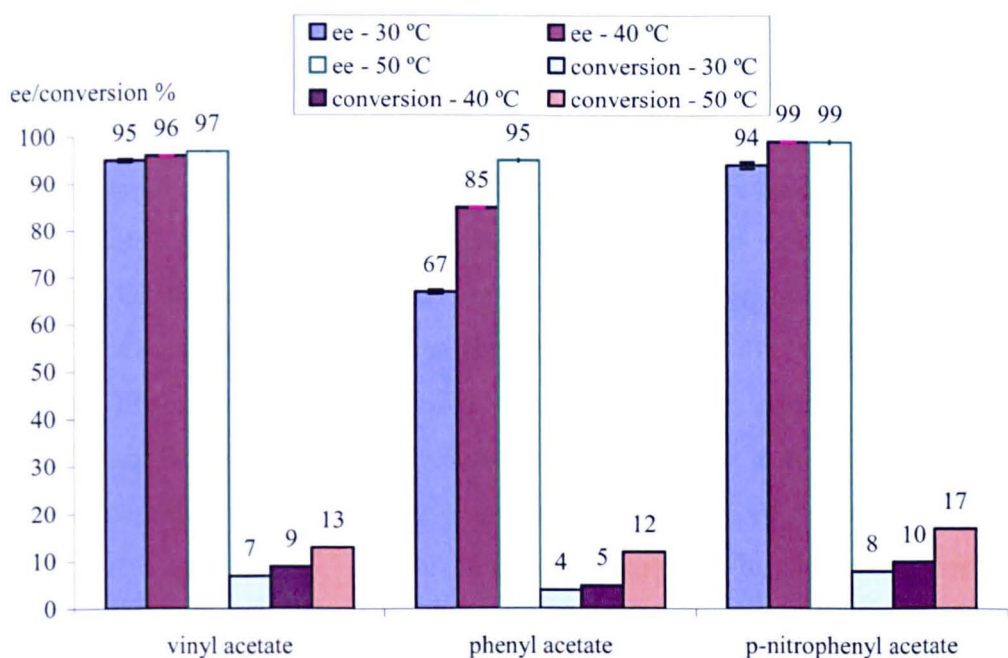


**Figure 5-2.** The enantioselectivity and the level of conversion of the continuous kinetic resolution of  $\alpha$ -tetralol using different acyl donors catalysed by Cal B CLEA (60 mg, 1680 U) in scCO<sub>2</sub>.

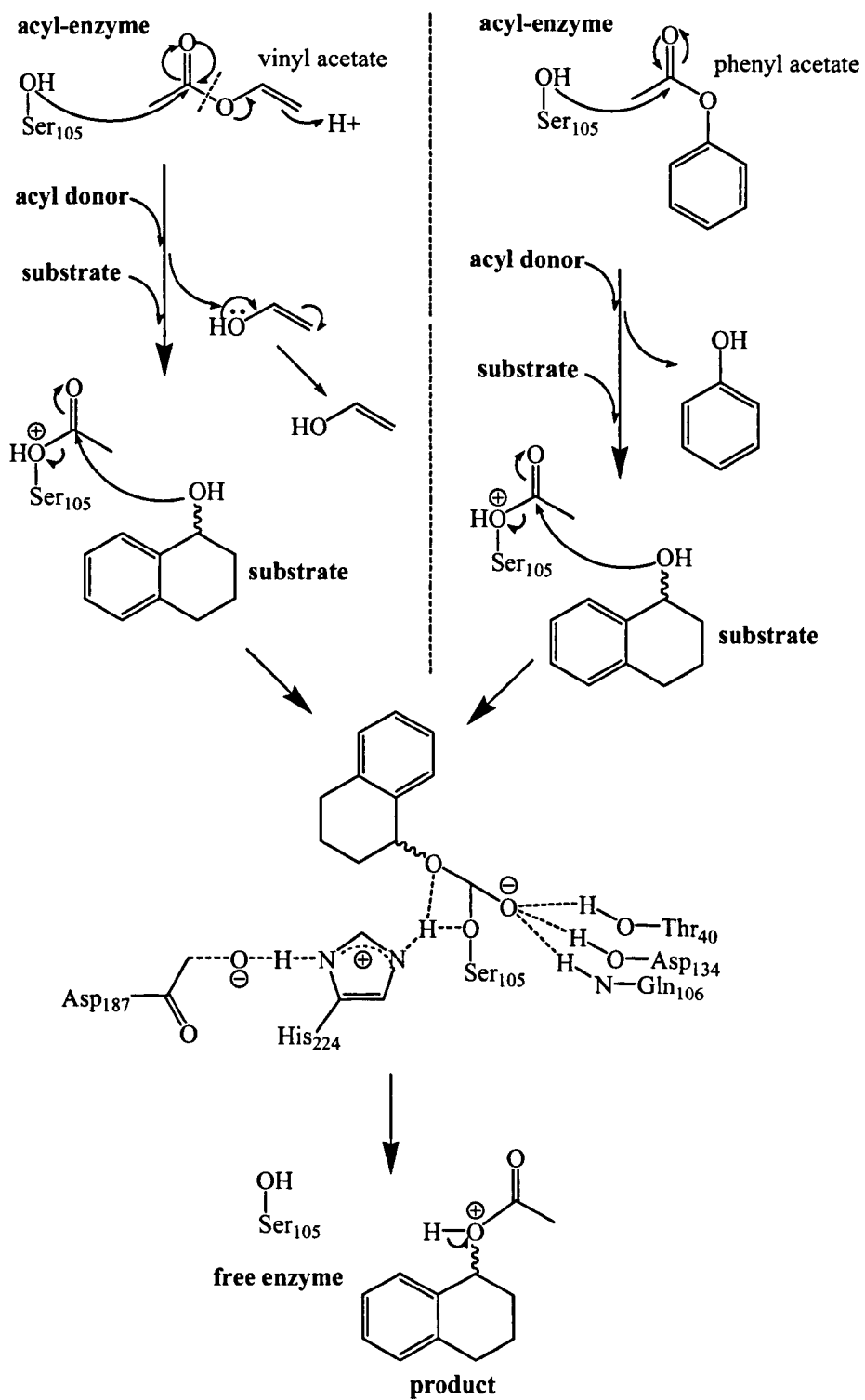
Reaction conditions: pressure: 100 bar, CO<sub>2</sub> flow rate: 1 mL/min, substrate flow rate: 0.2 mL/min ( $\alpha$ -tetralol : acyl donor = 1 : 1.5 molar ratio).

It can be seen in Figure 5-2 that the enantioselectivity of the reaction increased with an increase in temperature using all acyl donors. The solubility of  $\alpha$ -tetralol in scCO<sub>2</sub> is very poor but it increases with increased temperature<sup>37</sup>, which might influence the enantioselectivity. An increase in temperature can also increase the performance of the enzyme by providing more optimal conditions.

The different acyl donors influenced the enantioselectivity. If the acyl donor is vinyl acetate the product enol, tautomerises to acetaldehyde, therefore the reaction is irreversible and high enantioselectivity is expected. The other two acyl donors used here were phenyl acetate and *p*-nitrophenyl acetate. These acyl donors do not render the reaction irreversible but they can shift it towards the product where the driving force is the stability of the leaving group. The ability to deprotonate the consumed acyl donor is less for *p*-nitrophenyl acetate than that for phenyl acetate. Therefore the equilibrium of the reaction is more shifted towards the product formation using *p*-nitrophenyl acetate than phenyl acetate. Additionally, the

carbonyl group of *p*-nitrophenyl acetate is easier to attack and therefore the formation of the acyl-enzyme intermediate is faster in this case than that is with the other two acyl donors.

The enantioselectivity of the reaction was higher using *p*-nitrophenyl acetate than vinyl acetate. Although the kinetic resolution of  $\alpha$ -tetralol becomes irreversible using vinyl acetate as acyl donor, the driving force of the reaction towards product might be stronger when using *p*-nitrophenyl acetate due to the high stability of the product. The enantioselectivity was the lowest using phenyl acetate. The formation of acyl-enzyme intermediate might be slower using phenyl acetate because the carbonyl group is less electrophilic than that of the other two acyl donors. The mechanism of the reaction including the formation of the acyl-enzyme intermediate is shown in Scheme 5-3.



**Scheme 5-3.** The mechanism of the kinetic resolution of  $\alpha$ -tetralol using different acyl donors: vinyl acetate (left) and phenyl acetate (right). The mechanism of Cal B is proposed to be ping-pong bi-bi. Cal B has an Asp187-His224-Ser105 catalytic triad in its active site.

The level of conversion observed in the kinetic resolution of  $\alpha$ -tetralol (Figure 5-2, page 113) was low (maximum conversion in an enzymatic kinetic resolution is 50 %) but only a small amount of enzyme was used. In all cases, the level of conversion increased with an increase in temperature. An increase in temperature increases the solubility of reactants in  $\text{CO}_2$ , which may result in a higher reaction rate, and therefore higher conversion can be obtained. Besides, the activity of the enzyme can be influenced by the changes in temperature because enzymes have an optimal temperature where they display their highest performance.

The acyl donor had similar effect on the conversion of  $\alpha$ -tetralol as on the enantioselectivity. The changes in both enantioselectivity and conversion suggest that the rate of the acyl-enzyme intermediate formation might have a significant effect on the kinetic resolution of  $\alpha$ -tetralol.

A cosolvent (toluene) had to be used to bring *p*-nitrophenyl acetate into solution. The presence of the cosolvent in the reaction medium could influence the solvent power of  $\text{CO}_2$  which might increase the reaction rate when using *p*-nitrophenyl acetate as acyl donor. The water present in toluene (210±4 ppm determined by Karl-Fischer titration) might also enhance the enzyme activity. However, further evidence is required to confirm these hypotheses.

The phase behaviour might also influence the kinetic resolution of  $\alpha$ -tetralol because  $\alpha$ -tetralol is only slightly soluble in sc $\text{CO}_2$ .<sup>37</sup> As vinyl acetate is soluble in sc $\text{CO}_2$ ,<sup>38</sup>  $\alpha$ -tetralol and vinyl acetate may be present in two distinct phases in the  $\alpha$ -tetralol/vinyl acetate/sc $\text{CO}_2$  system. In a continuous flow sc $\text{CO}_2$  system, vinyl acetate might flow through the catalyst bed faster than  $\alpha$ -tetralol, which therefore provides shorter reaction time. The solubility of phenyl acetate and *p*-nitrophenyl acetate in sc $\text{CO}_2$  are unknown. In the case of 1-phenylethanol, all reactants and sc $\text{CO}_2$  are in a single phase. The kinetic resolution of 1-phenylethanol in a continuous flow sc $\text{CO}_2$  system with vinyl acetate as acyl donor reached maximum conversion 50 % and high enantioselectivity  $ee_R > 99\%$  (Tables 5-1, 5-2 and 5-3).

The kinetic resolution of  $\alpha$ -tetralol in a continuous flow scCO<sub>2</sub> system using vinyl acetate as acyl donor reached conversion up to 13 % and enantioselectivity (*R*) up to 97 %. The differences in conversion and enantioselectivity in the kinetic resolution of these substrates suggest that the phase behaviour may have a significant effect on the reaction, however, further evidence is required to confirm this.

The effect of the immobilisation method could be determined by comparing the results obtained by Cal B CLEA (cross-linking of solid enzyme molecules) and Novozym 435 (adsorption on a carrier material) in the continuous kinetic resolution of  $\alpha$ -tetralol in scCO<sub>2</sub>. The activity of Novozym 435 for the reaction was determined previously by Stephenson at Nottingham.<sup>35</sup> The enantioselectivities with Novozym 435 and Cal B CLEA are shown in Figure 5-3.

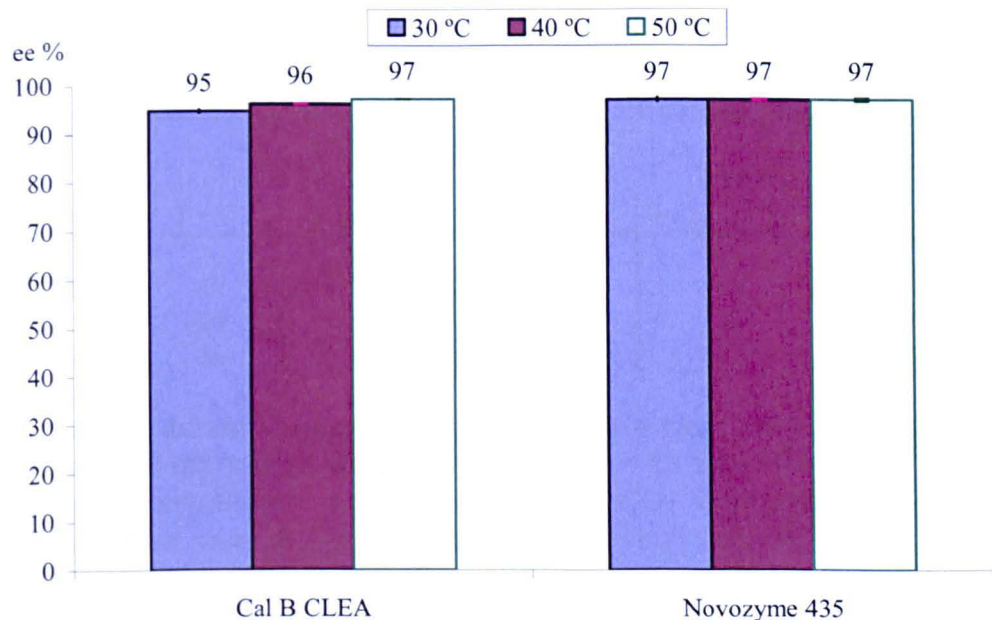


**Figure 5-3.** The enantioselectivity of the continuous kinetic resolution of  $\alpha$ -tetralol in scCO<sub>2</sub> using vinyl acetate as acyl donor catalysed by Cal B CLEA (25 mg, 700 U) and Novozym<sup>35</sup> 435 (25 mg, 87.5 U).

Reaction conditions: pressure: 100 bar, CO<sub>2</sub> flow rate: 1.0 mL/min, substrate flow rate: 0.2 mL/min ( $\alpha$ -tetralol : vinyl acetate = 1 : 1.5 molar ratio).

The enantioselectivity of the kinetic resolution of  $\alpha$ -tetralol was high using both catalysts in a continuous flow scCO<sub>2</sub> system. While the enantioselectivity of the reaction with Cal B CLEA was influenced by the changes in temperature, Novozym 435 displayed the same enantioselectivity at all temperatures examined. The immobilisation technique of Novozym 435 (Cal B adsorbed on a macroporous resin) might be more beneficial for continuous flow reactions in scCO<sub>2</sub> as it showed higher enantioselectivity even using less enzyme (lower number of enzyme unit) of Novozym 435 (87.5 U) than Cal B CLEA (700 U) under the same reaction conditions.

In a continuous flow system, the conversion can increase by using a larger amount of catalyst and/or increasing the residence time. To investigate this, the continuous kinetic resolution of  $\alpha$ -tetralol was also examined using different amounts of catalyst. The results are shown in Table 5-4.

**Table 5-4. The conversion of the continuous kinetic resolution of  $\alpha$ -tetralol in scCO<sub>2</sub> catalysed by Cal B CLEA (25 mg, 700 U or 60 mg, 1680 U).**

Entry	T (°C)	25 mg - 700 U		60 mg - 1680 U	
		ee acetate (%)	Conv (%)	ee acetate (%)	Conv (%)
1	30	88	4	95	7
2 *	30	91	4	94	6
3	40	93	6	96	9
4	50	95	8	97	13

**Reaction conditions:** pressure: 100 bar, CO<sub>2</sub> flow rate: 1.0 mL/min, substrate flow rate: 0.2 mL/min ( $\alpha$ -tetralol: vinyl acetate = 1 : 1.5 molar ratio).

\* Reaction conditions: pressure: 200 bar, CO<sub>2</sub> flow rate: 1.0 mL/min, substrate flow rate: 0.2 mL/min ( $\alpha$ -tetralol: vinyl acetate = 1 : 1.5 molar ratio).

Lower conversion was observed using less catalyst (25 mg, 700 U) than a larger amount of catalyst (60 mg, 1680 U) as expected. The enantioselectivity of the reaction was also lower using less catalyst. The enantioselectivity can increase by using a larger amount of catalyst because it may be a function of conversion.

An increase in pressure can increase the solubility of substrates in scCO<sub>2</sub> and can also change the properties of CO<sub>2</sub> (the density of CO<sub>2</sub> increases with an increase in pressure). The results of the kinetic resolution of  $\alpha$ -tetralol at different pressures are shown in Figure 5-4.

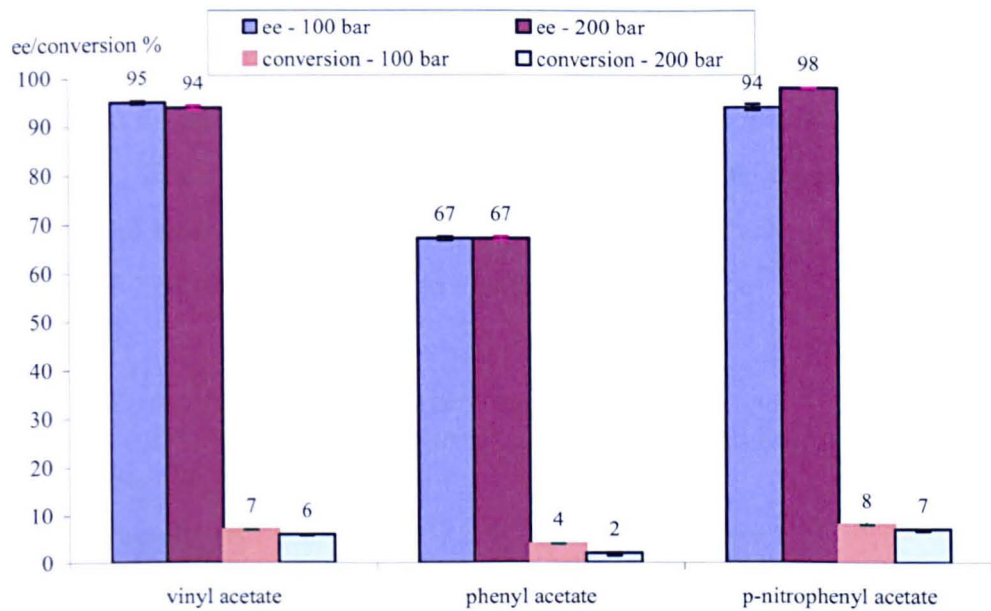


**Figure 5-4. The effect of the pressure on the enantioselectivity and conversion of the continuous kinetic resolution of  $\alpha$ -tetralol catalysed by Cal B CLEA (60 mg, 1680 U) in scCO<sub>2</sub>.**

Reaction conditions: temperature: 30 °C, CO<sub>2</sub> flow rate: 1 mL/min, substrate flow rate: 0.2 mL/min ( $\alpha$ -tetralol : vinyl acetate = 1 : 1.5 molar ratio).

An increase in pressure did not have a great influence on the enantioselectivity of the reaction using vinyl acetate and phenyl acetate as acyl donor. The enantioselectivity of the reaction improved with an increase in pressure using *p*-nitrophenyl acetate as acyl donor, however, the difference in enantioselectivity was small almost within the experimental error (includes the errors originating from the inaccuracy of the pumps, sample preparation, and analysis).

The conversion of the reaction decreased with an increase in pressure using all acyl donors. An increase in pressure could create a more significant difference in solubility between the substrate and the acyl donor in a continuous flow scCO<sub>2</sub> system: one of the reactants (acetate) might be flushed through the catalyst faster

with scCO<sub>2</sub> than the other (substrate) and thus the residence time could be reduced. Furthermore, the catalyst bed could become more compacted under higher pressure which might cause higher mass transport limitations.

The kinetic resolution of 1-phenylethanol (Scheme 5-1) was investigated with the acyl donor at various concentrations by Matsuda and co-workers.<sup>27</sup> It has been shown that the reaction improved using the acyl donor in excess of the substrate (Table 5-1). The effect of the substrate to acyl donor ratio on the kinetic resolution of α-tetralol was examined using a molar ratio of 1 : 1.5 and 1 : 1 of substrate : acyl donor. The results are shown in Figure 5-5.

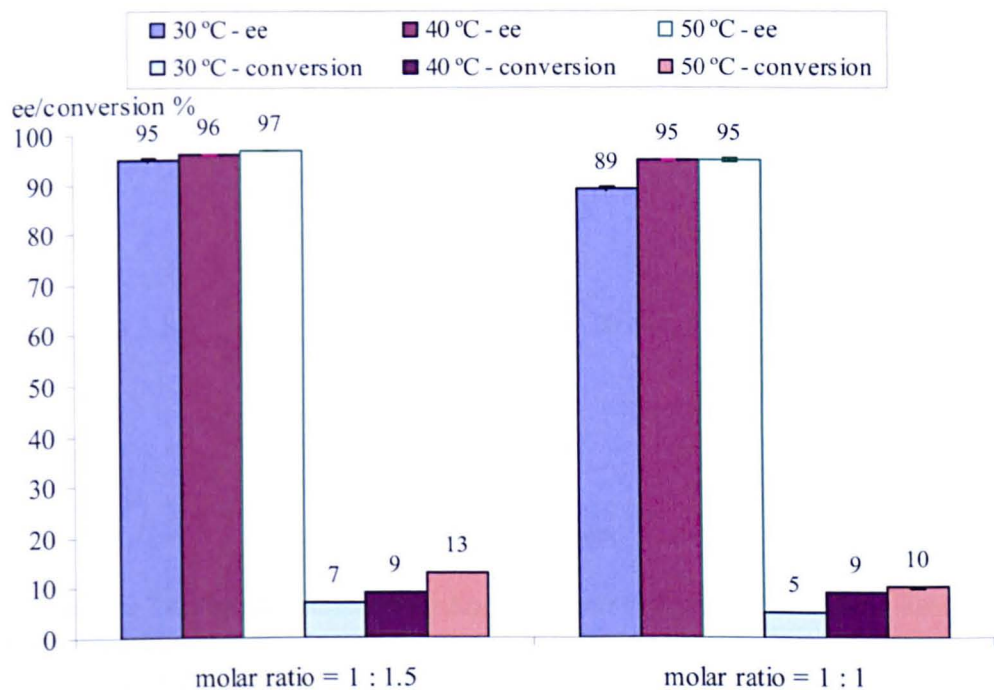


**Figure 5-5. The effect of the substrate : acyl donor ratio on the continuous kinetic resolution of α-tetralol catalysed by Cal B CLEA (60 mg, 1680 U) in scCO<sub>2</sub>.**

**Reaction conditions:** pressure 100 bar, CO<sub>2</sub> flow rate: 1 mL/min, substrate flow rate: 0.2 mL/min (α-tetralol + vinyl acetate).

Similarly to the kinetic resolution of 1-phenylethanol performed by Matsuda, the enantioselectivity and the conversion of kinetic resolution of α-tetralol increased

using the acyl donor in excess to the substrate. The concentration of acyl donor might influence the reaction rate and therefore higher enantioselectivity and conversion could be obtained using the acyl donor in excess to the substrate. The study should be extended to examine other conditions, which could provide further evidence to confirm this hypothesis.

The kinetic resolution of  $\alpha$ -tetralol was also examined in batch in n-hexane (without  $\text{CO}_2$ ). All reactants are soluble in hexane and therefore a single phase system is obtained. The results are shown in Figure 5-6.

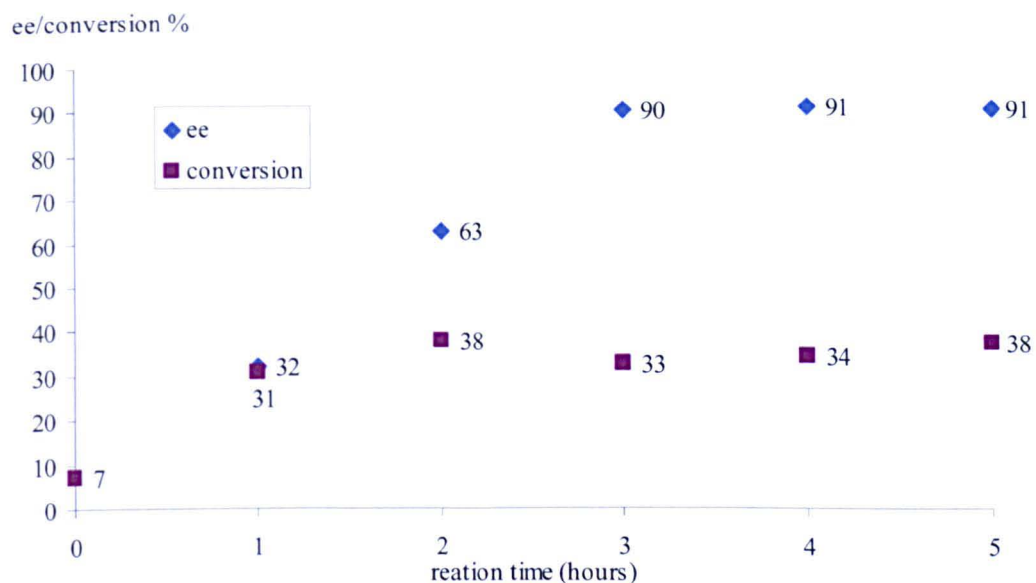


**Figure 5-6. The enantioselectivity and the conversion of the kinetic resolution of  $\alpha$ -tetralol in batch using n-hexane as solvent.**

Reaction conditions: temperature: 40 °C, hexane: 5 mL, substrate: 1 mL ( $\alpha$ -tetralol : vinyl acetate = 1 : 1.5 molar ratio), catalyst: Cal B CLEA (5.2 mg, 146 U).

The kinetic resolution of  $\alpha$ -tetralol reached a plateau in enantioselectivity and conversion after 3 hours. The enantioselectivity and conversion of the kinetic resolution of  $\alpha$ -tetralol in hexane were lower than those in a continuous flow  $\text{scCO}_2$  system despite a significantly longer reaction time and a single phase system. The reaction medium may influence the reaction and therefore the catalyst

performance can decrease. In order to determine whether the solvent has an effect on the reaction, the kinetic resolution of  $\alpha$ -tetralol should be examined in a batch scCO<sub>2</sub> system and also in other solvents. The reaction could also be inhibited by the presence of the product in batch. The product is continuously removed from the catalyst surface in a flow scCO<sub>2</sub> system and therefore no inhibition by the product is expected. An extensive investigation should be performed to determine the rate limiting step of the reaction but it could not be performed due to the limited amount of materials available.

#### 5.4. Conclusions

The continuous kinetic resolution of  $\alpha$ -tetralol has been performed successfully using different acyl donors (vinyl acetate, phenyl acetate, *p*-nitro phenyl acetate) catalysed by Cal B CLEA in scCO<sub>2</sub>. The enzyme displayed high enantioselectivity (*ee<sub>R</sub>* up to 99 %) for the reaction and was highly influenced by the acyl donor. The reaction might be driven towards the product more when the stability of the by-product remaining from the acyl donor was higher. The enantioselectivity was found to be a function of conversion in the continuous kinetic resolution of  $\alpha$ -tetralol in scCO<sub>2</sub>. The same phenomenon was observed in the lipase catalysed kinetic resolution of secondary alcohols in propylene carbonate by another research group.<sup>31</sup> The conversion of the reaction remained low using all acyl donors but it could be increased by using a larger amount of catalyst.

Both the enantioselectivity and the conversion increased with an increase in temperature using all acyl donors. It is possibly due to an increased solubility of the substrate in CO<sub>2</sub> at higher temperatures. The enzyme could also be more active if it was closer to its optimal temperature. An increase in pressure did not influence the catalyst performance significantly.

Cal B CLEA gave lower enantioselectivity and conversion for the continuous kinetic resolution of  $\alpha$ -tetralol than for the continuous kinetic resolution of 1-phenylethanol, in scCO<sub>2</sub>. Cal B CLEA may have higher specificity towards 1-phenylethanol than for  $\alpha$ -tetralol, which can be due to differences in their size: 1-phenylethanol is smaller and therefore it may fit the active site of Cal B better

than  $\alpha$ -tetralol.<sup>39</sup> The differences in phase behaviour may also affect the catalyst performance (1-phenylethanol<sup>36</sup> is completely miscible with CO<sub>2</sub>, while  $\alpha$ -tetralol<sup>37</sup> is only slightly soluble in CO<sub>2</sub>).

## References

1. Anthonsen, F., Ed Straathof, A.J.J., in Applied Biocatalysis. *Harwood Academic Publishers* 2000.
2. Sheldon, R. A., van Rantwijk, F., Biocatalysis for sustainable organic synthesis. *Australian Journal of Chemistry* 2004, 57, 281-289.
3. Demirjiam, D. C., Shah, P.C., Moris-Varas, F., Ed Fessner, W.D., in Biocatalysis - From Discovery to Application. *Springer, Berlin* 1999.
4. Shaw, N. M., Robins, K.T., Kiener, A., Eds Blaser, H.U., Schmidt, E., in Asymmetric Catalysis on Industrial Scale: Challenges, Approaches, and Solutions. *Wiley-VHC, Weinheim* 2004.
5. Anderson, E. M., Larsson, K.M., Kirk, O., One biocatalyst - many applications: the use of *Candida antarctica* B-lipase in organic synthesis. *Biocatalysis and Biotransformation* 1998, 16, 181-204.
6. Garcia-Urdiales, E., Alfonso, I., Gotor, V., Enantioselective Enzymatic Desymmetrizations in Organic Synthesis. *Chemical Reviews* 2005, 105, 313-354.
7. Uppenberg, J., Hansen, M.T., Patkar, S., Jones, T.A., The sequence, crystal structure determination and refinement of two crystal forms of lipase B from *Candida antarctica*. *Structure* 1994, 2, 293-308.
8. Bousquet-Dubouch, M. P., Gruber, M., Sousa, N., Lamare, S., Legoy, M.D., Alcoholysis catalyzed by *Candida antarctica* lipase B in a gas/solid system obeys a Ping Pong Bi Bi mechanism with competitive inhibition by the alcohol substrate and water. *Biochimica et Biophysica Acta* 2001, 1550, 90-99.
9. Martinelle, M., Hult, K., Kinetics of acyl transfer reaction in organic media catalysed by *Candida antarctica* lipase B. *Biochimica et Biophysica Acta* 1995, 1251, 191-197.
10. Vulfson, E. N., Halling, P.J., Holland, H.L., in Enzymes in Non-Aqueous Solvents. *Humana Press, New Jersey* 2001.
11. Hobbs, H. R., Thomas, N.R., Biocatalysis in supercritical fluids, in fluorous solvents, and under solvent-free conditions. *Chemical Reviews* 2007, 107, 2786-2820.
12. van Rantwijk, F., Sheldon, R.A., Biocatalysis in Ionic Liquids. *Chemical Reviews* 2007, 107, 2757-2785.
13. De Vos, D. E., Vankelecom, I.F.J., Jacobs, P.A., in Chiral catalyst immobilisation and recycling. *Wiley-VCH* 1998.
14. Cao, L., van Rantwijk, F., Sheldon, R.A., Cross-linked enzyme aggregates: A simple and effective method for the immobilization of penicillin acylase. *Organic Letters* 2000, 1, 1361-1364.

15. Lopez-Serrano, P., Cao, L., van Rantwijk, F., Sheldon, R.A., Cross-linked enzyme aggregates with enhanced activity: application to lipases. *Biotechnology Letters* **2002**, 24, 1379-1383.
16. Wilson, L., Betancor, L., Fernandez-Lorente, G., Fuentes, M., Hidalgo, A., Guisan, J.M., Pessela, B.C.C., Fernandez-Lafuente, R., Cross-linked aggregates of multimeric enzymes: A simple and efficient methodology to stabilize their quaternary structure. *Biomacromolecules* **2004**, 5, 814-817.
17. Bode, M. L., van Rantwijk, F., Sheldon, R.A., Crude Aminoacylase From Aspergillus sp. is a Mixture of Hydrolases. *Biotechnology and Bioengineering* **2003**, 84, 710-713.
18. Aytar, B. S., Bakir, U., Preparation of cross-linked tyrosinase aggregates. *Process Biochemistry* **2008**, 43, 125-131.
19. Kaul, P., Stoltz, A., Banerjeea, U.C., Cross-Linked Amorphous Nitrilase Aggregates for Enantioselective Nitrile Hydrolysis. *Advanced Synthesis & Catalysis* **2007**, 349, 2167-2176.
20. van Pelt, S., Quignard, S., Kubac, D., Sorokin, D.Y., van Rantwijk, F., Sheldon, R.A., Nitrile hydratase CLEAs: The immobilization and stabilization of an industrially important enzyme. *Green Chemistry* **2008**, 10, 395-400.
21. Cabana, H., Jones, J.P., Agathos, S.N., Preparation and characterization of cross-linked laccase aggregates and their application to the elimination of endocrine disrupting chemicals. *Journal of Biotechnology* **2007**, 132, 23-31.
22. van Langen, L. M., Selassa, R.P., van Rantwijk, F., Sheldon, R.A., Cross-Linked Aggregates of (R)-Oxynitrilase: A Stable, Recyclable Biocatalyst for Enantioselective Hydrocyanation. *Organic Letters* **2005**, 7, 327-329.
23. Chmura, A., van der Kraan, G.M., Kielar, F., van Langen, L.M., van Rantwijk, F., Sheldon, R.A., Cross-Linked Aggregates of the Hydroxynitrile Lyase from Manihot esculenta: Highly Active and Robust Biocatalysts. *Advanced Synthesis & Catalysis* **2006**, 348, 1655-1661.
24. Gaur, R., Pant, H., Jain, R., Khare, S.K., Galacto-oligosaccharide synthesis by immobilized Aspergillus oryzae b-galactosidase. *Food Chemistry* **2006**, 97, 426-430.
25. Sheldon, R. A., Schoevaart, R., van Langen, L.M., Cross-linked enzyme aggregates (CLEAs): A novel and versatile method for enzyme immobilization (a review). *Biocatalysis and Biotransformation* **2005**, 23, 141-147.
26. Sheldon, R. A., Arends, I., Hanefeld, U., in *Green Chemistry and Catalysis*. Wiley-VCH, Weinheim **2007**.
27. Matsuda, T., Watanabe, K., Harada, T., Nakamura, R., Arita, Y., Misumi, Y., Ichikawa, S., Ikariya, T., High-efficiency and minimum-waste continuous kinetic resolution of racemic alcohols by using lipase in supercritical carbon dioxide. *Chemical Communications* **2004**, 2286-2287.
28. Hobbs, H. R., Kondor, B., Stephenson, P., Sheldon, R.A., Thomas, N.R., Poliakoff, M., Continuous kinetic resolution catalysed by cross-linked enzyme aggregates, 'CLEAs', in supercritical CO<sub>2</sub>. *Green Chemistry* **2006**, 8, 816-821.
29. Lozano, P., Villora, G., Gómez, D., Gayo, A.B., Sánchez-Conesa J.A., Rubio, M., Iborra, J.L., Membrane reactor with immobilized Candida antarctica lipase

- B for ester synthesis in supercritical carbon dioxide. *Journal of Supercritical Fluids* **2004**, *121-128*.
- 30. Dijkstra, Z. J., Merchant, R., Keurentjes, J.T.F., Stability and activity of enzyme aggregates of Calb in supercritical CO<sub>2</sub>. *Journal of Supercritical Fluids* **2007**, *41*, 102-108.
  - 31. Wu, X. M., Sun, W., Xin, J.Y., Xia, C.G., Lipase-catalysed kinetic resolution of secondary alcohols with improved selectivity in propylene carbonate. *World Journal of Microbiology and Biotechnology* **2008**, *24*, 2421-2424.
  - 32. Shah, S., Gupta, M.N., Kinetic resolution of ( $\pm$ )-1-phenylethanol in [Bmim][PF6] using high activity preparations of lipases. *Bioorganic and Medicinal Chemistry Letters* **2007**, *17*, 921-924.
  - 33. Overmeyer, A., Schrader-Lippelt, S., Kasche, V., Brunner, G., Lipase-catalysed kinetic resolution of racemates at temperatures from 40 C to 160 C in supercritical CO<sub>2</sub>. *Biotechnology Letters* **1999**, *21*, 65-69.
  - 34. Chen, C. S., Fujimoto, Y., Girdaukas, G., Sih, C.J., Quantitative Analyses of Biochemical Kinetic Resolutions of Enantiomers. *Journal of the American Chemical Society* **1982**, *104*, 7294-7299.
  - 35. Stephenson, P., PhD Thesis. *University of Nottingham, Nottingham (UK) 2005*.
  - 36. Hobbs, H. R., PhD Thesis. *University of Nottingham, Nottingham (UK) 2006*.
  - 37. Borg, P., Jaubert, J.N., Denet, F., Solubility of alpha-tetralol in pure carbon dioxide and in a mixed solvent formed by ethanol and carbon dioxide. *Fluid Phase Equilibria* **2001**, *191*, (1-2), 59-69.
  - 38. Hobbs, H. R., The phase behaviour of 1-phenyl ethanol, vinyl acetate and scCO<sub>2</sub> was examined in a variable volume view cell and no phase separation was observed. Therefore it was assumed that vinyl acetate was soluble in scCO<sub>2</sub>. **2006**.
  - 39. Ottosson, J., Fransson, L., King., J.W., Hult, K., Size as a parameter for solvent effects on Candida antarctica lipase B enantio selectivity. *Biochimica et Biophysica Acta - Protein Structure and Molecular Enzymology* **2002**, *1594*, 325-334.

## Chapter 6

### Two-Step Catalytic Cascade Reaction in a Continuous Flow scCO<sub>2</sub> system: Hydrogenation followed by the Kinetic Resolution of the Product

One potential method to obtain a more environmentally viable process compared to the existing ones is to use a cheap raw material. The price of acetophenone is much lower than that of (*R/S*)-1-phenylethanol. If acetophenone is hydrogenated to (*R*)-1-phenylethanol and the formed intermediate is acylated to (*R*)-1-phenylethyl acetate, the cost of the process for the production of (*R*)-1-phenylethyl acetate will decrease, especially if the catalysts can be recycled. The work in this Chapter investigated this process in a two-step catalytic cascade reaction with heterogeneous catalysts in a continuous flow scCO<sub>2</sub> system. The Chapter also discusses the advantages of multistep catalytic cascade reactions and the importance of reactor design for these reactions.

#### 6.1. Multistep Catalytic Cascade Reactions

A well known example for multistep reactions is the Rhodia process for vanillin manufacture starting from phenol that involves four steps each with heterogeneous catalyst.<sup>1</sup> This process involves a series of catalytic steps where the product of each step is isolated (and in many cases purified) before the next step. The ultimate aim is the combination of several steps, preferably in one pot. Multistep catalytic cascade reactions can possess the following advantages.<sup>2</sup>

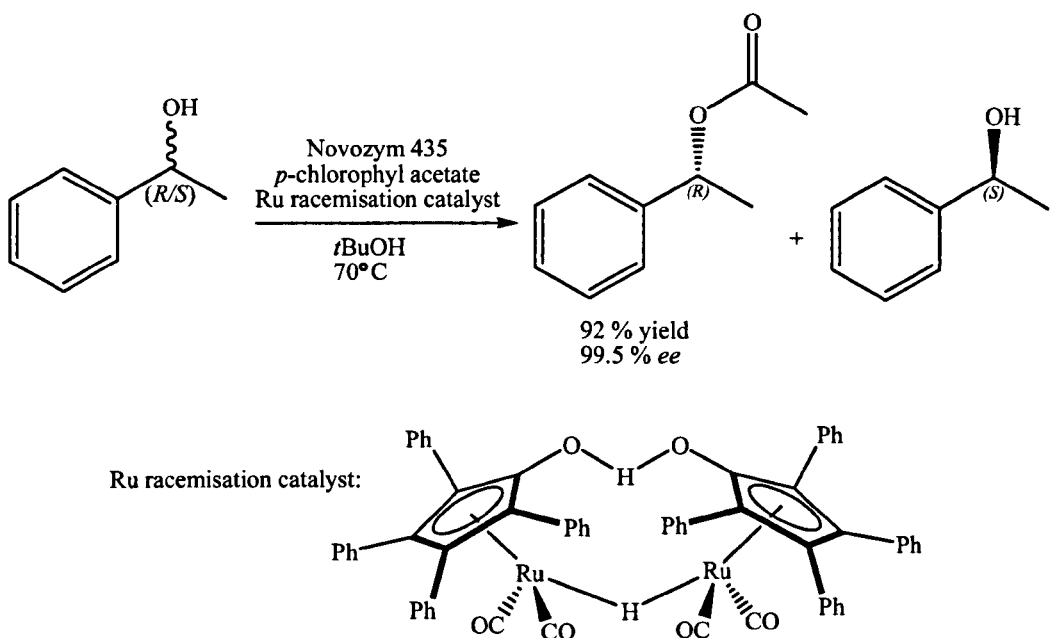
- i) No need for the separation of intermediates.
- ii) Fewer unit operation.
- iii) Less total reactor volume.
- iv) Higher volumetric and space time yield.
- v) Less waste (lower E-factor) (the E-factor is different than the enzymic E-value, E-factor: amount of waste per kg of product).

- vi) The reaction equilibrium may be driven towards the favoured direction.
- vii) Lower energy consumption.
- viii) Lower cost.

On the other hand, multistep catalytic cascade reactions have some limitations.<sup>2</sup>

- i) Incompatibility of the catalysts.
- ii) Different reaction rates.
- iii) Difficulty to optimise the reaction temperature, pressure, pH, and solvent.
- iv) Complicated catalyst recovery and recycling.

An example for catalytic cascade reactions is dynamic kinetic resolution (DKR) that is the combination of kinetic resolution and racemisation and is commonly performed with a catalyst system of a metal catalyst and a biocatalyst. The incompatibility of the catalysts is often a problem associated with DKR. Another limiting factor in DKR is the racemisation step. The DKR of alcohols is widely investigated where the kinetic resolution is commonly performed with lipase that is combined with a racemisation Rh or Ru catalyst. Among the large number of publications on DKR<sup>3-8</sup>, one of the early results was reported by Bäckvall who performed the DKR of (*R/S*)-1-phenylethanol catalysed by lipase and a racemisation Ru catalyst (Scheme 6-1).<sup>3</sup> By optimising the reaction conditions, high enantioselectivity and product yield was obtained.



**Scheme 6-1. DKR of (R/S)-1-phenylethanol using lipase and Ru catalyst.<sup>3,9</sup>**

The catalyst recovery and recycling are essential for an efficient catalytic cascade reaction. Catalyst immobilisation, the use of thermoregulated catalysts or tunable solvents (e.g. fluorous solvents) can be successful approaches for achieving high efficiency.<sup>10</sup> The work in this Thesis investigated a chemoenzymatic cascade reaction with heterogeneous catalysts. The cascade reaction was examined in series in a continuous flow scCO<sub>2</sub> system where a specially designed flow reactor was used to overcome the problem of the incompatibility of the catalysts.

## 6.2. Reactor Design for Multistep Catalytic Cascade Reactions

Multistep catalytic cascade reactions are normally performed in one pot where the incompatibility of the catalysts can cause limitations. Besides, the optimisation of the reaction conditions and the catalyst recycling can also be difficult. The incompatibility of the catalysts can be overcome by separating the catalysts. The physical separation of the catalysts can be solved for example by the use of a continuous flow system where the catalysts are separated in different reactors,

which also allows separate control of the temperature of each step and the ease of catalyst recovery and recycling.

In this work, a multistep catalytic cascade reaction was examined in a continuous flow scCO<sub>2</sub> system: hydrogenation followed by the kinetic resolution of the product. A heterogeneous metal catalyst Pd 2 % Type 31 (Johnson Matthey - UK) was used as catalyst of the hydrogenation step of the cascade. The catalyst of the second step (kinetic resolution) was a heterogeneous biocatalyst, Cal B CLEA. The Pd catalyst (Pd 2 % Type 31 by Johnson Matthey - UK) has been shown previously to be effective at higher temperatures (> 100 °C).<sup>11</sup> The activity of Cal B drops significantly at temperatures above 100 °C.<sup>12</sup> Two reactors were therefore used to control the temperature of each step separately. The reactor setup is shown in Figure 6-1. The acyl donor required by the kinetic resolution of (*R/S*)-1-phenylethanol was introduced after the hydrogenation reactor in order to avoid any reaction of the acyl donor over the Pd catalyst. It also helped to cool the main stream (150 °C - 200 °C). The temperature of the enzyme reactor was monitored in the reactor and the desired temperature was observed (40 °C, 50 °C or 60 °C).

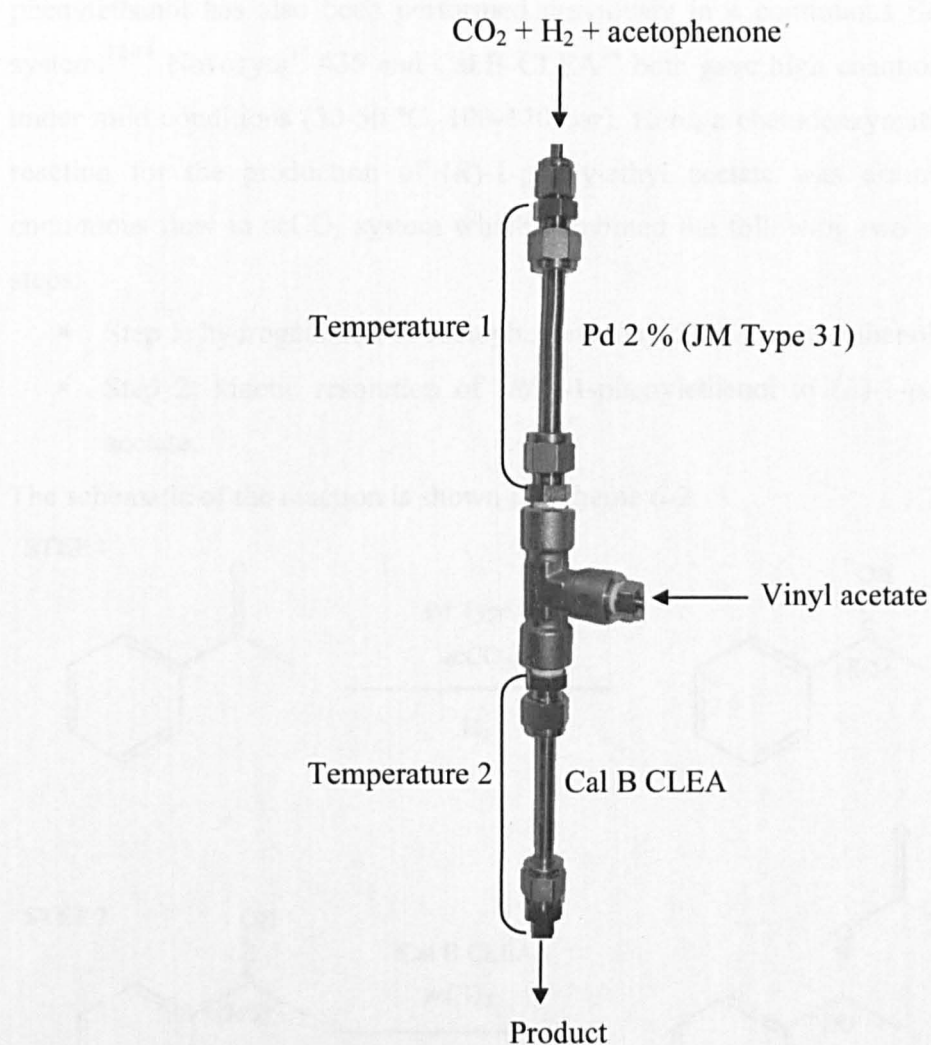


**Figure 6-1.** The reactor configuration for the continuous cascade reaction.  $\text{CO}_2$ ,  $\text{H}_2$  and acetophenone were mixed and heated in a static mixer before entering the hydrogenation reactor. Vinyl acetate, the acyl donor required to the kinetic resolution was introduced after the hydrogenation reactor. A detailed description of reactor can be found in Chapter 2.

All experiments were carried out using the reactor setup shown in Figure 6-1 where the reaction temperature, system pressure and  $\text{CO}_2$  flow rate were changed.

### 6.3. Results and Discussion

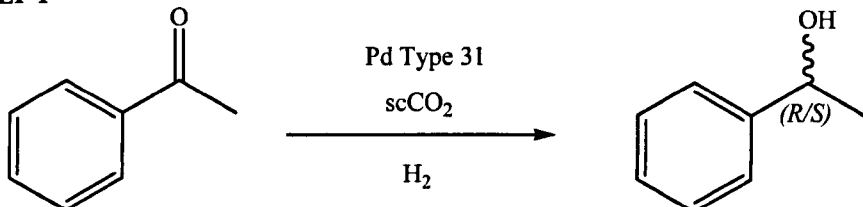
The continuous hydrogenation of acetophenone to (*R/S*)-1-phenylethanol has been shown previously to be successful with Pd Type 31 catalyst (Pd 2 % Type 31 by Johnson Matthey - UK) in sc $\text{CO}_2$ .<sup>11</sup> The kinetic resolution of (*R/S*)-1-

phenylethanol has also been performed previously in a continuous flow scCO<sub>2</sub> system.<sup>12-14</sup> Novozym<sup>13</sup> 435 and Cal B CLEA<sup>14</sup> both gave high enantioselectivity under mild conditions (30-50 °C, 100-170 bar). Here, a chemoenzymatic cascade reaction for the production of (*R*)-1-phenylethyl acetate was examined in a continuous flow in scCO<sub>2</sub> system which combined the following two subsequent steps:

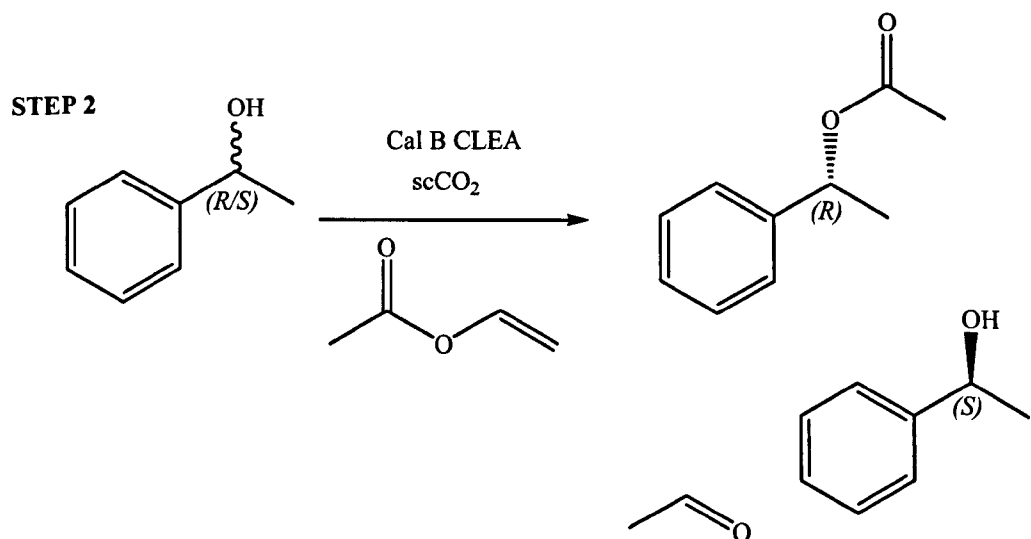
- Step 1: hydrogenation of acetophenone to (*R/S*)-1-phenylethanol
- Step 2: kinetic resolution of (*R/S*)-1-phenylethanol to (*R*)-1-phenylethyl acetate.

The schematic of the reaction is shown in Scheme 6-2.

**STEP 1**



**STEP 2**



**Scheme 6-2.** Two step catalytic cascade reaction: hydrogenation of acetophenone over an achiral Pd catalyst to produce racemic 1-phenylethanol that was kinetically resolved by Cal B CLEA (*R* selective).

The performance of the hydrogenation of acetophenone was examined at different temperatures and pressures. The results are shown in Figure 6-2.

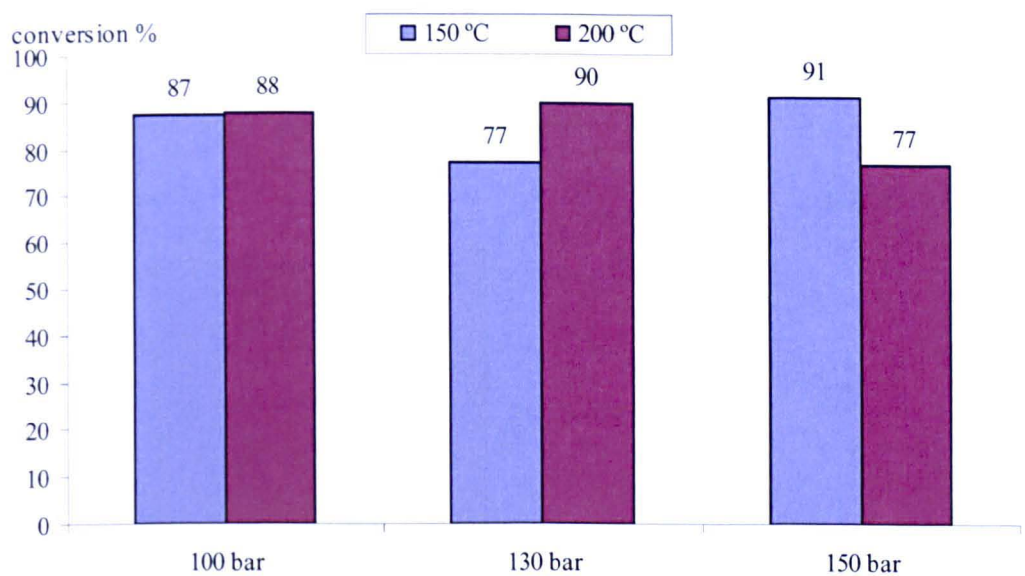


**Figure 6-2. Conversion of acetophenone catalysed by Pd (JM Type 31: 2 % on silica/alumina) (270 mg) (first step of the cascade reaction).**  
**Reaction conditions:** CO<sub>2</sub> flow rate: 1 mL/min, substrate flow rate: 0.1 mL/min (acetophenone), H<sub>2</sub> : substrate ratio = 4 : 1.

An increase in pressure had different effect at different temperatures. Acetophenone/H<sub>2</sub>/CO<sub>2</sub> forms one phase at all conditions examined here.<sup>11</sup> The phase behaviour of the system should therefore not affect the reaction significantly. The viscosity and density of CO<sub>2</sub> decreases with an increase in temperature and it might produce higher conversion at higher temperatures because the mass transport of the substrate to the catalyst could improve.

At 150 bar, the conversion of acetophenone was lower at 200 °C than at 150 °C. The continuous cascade reactions were examined at different conditions that were changed in a particular order. The experiment at 150 bar and 200 °C was the last in the row and therefore the catalyst had been under CO<sub>2</sub> and H<sub>2</sub> for a longer time than in other cases (1. 100 bar, 150 °C, 2. 130 bar, 150 °C, 3. 150 bar, 150 °C, 4. 100 bar, 200 °C, 130 bar, 200 °C, 6. 150 bar, 200 °C). The catalyst might have been poisoned by the reverse water gas-shift reaction (H<sub>2</sub>+CO<sub>2</sub>→H<sub>2</sub>O+CO)<sup>15</sup>, which could cause a drop in conversion.

The temperature of the kinetic resolution catalysed by Cal B CLEA was varied between 40 - 60 °C. The results are shown in Figure 6-3.

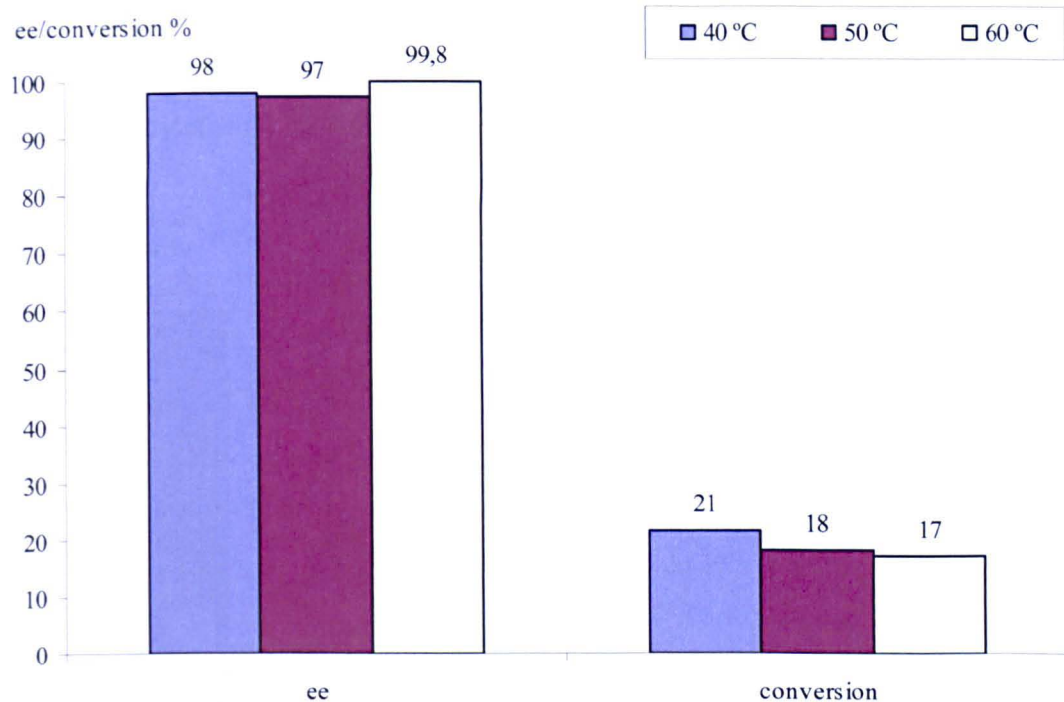


**Figure 6-3:** The enantioselectivity (*R*-acetate) and the level of conversion (conversion of (*R*)-1-phenylethanol) at different temperatures catalysed by Cal B CLEA (60-70 mg, 1680-1960 U) (second step of the cascade reaction). Reaction conditions: pressure: 100 bar, CO<sub>2</sub> flow rate: 1 mL/min, substrate flow rate: 0.1 mL/min (acetophenone, 1-phenyl ethanol, vinyl acetate).

High enantioselectivity was observed in the kinetic resolution of (*R/S*)-1-phenylethanol at all conditions examined. The highest enantioselectivity ( $ee_R$  acetate > 99 %) was observed at 60 °C which could be closer to the optimal temperature of the enzyme.

The conversion of (*R*)-1-phenylethanol decreased with an increase in temperature. Generally, the conversion of a reaction in scCO<sub>2</sub> increases with an increase in temperature due to an increase in solubility of the reactants in scCO<sub>2</sub> at higher temperatures which can improve the mass transport. Here, a decrease in conversion with an increase in temperature was observed. Cal B may be affected by H<sub>2</sub> if kept for a longer period of time (the order of the reaction conditions: 1. 40

$^{\circ}\text{C}$ , 2.  $50\text{ }^{\circ}\text{C}$ , 3.  $60\text{ }^{\circ}\text{C}$ ). Conformational changes of enzyme might be caused by the rupture of disulfide bonds of cysteine residues (discussed in detail below), and therefore the enzyme activity could decrease.

The effect of an increased pressure on the kinetic resolution of (*R/S*)-1-phenylethanol was also examined. The results are shown in Figure 6-4.

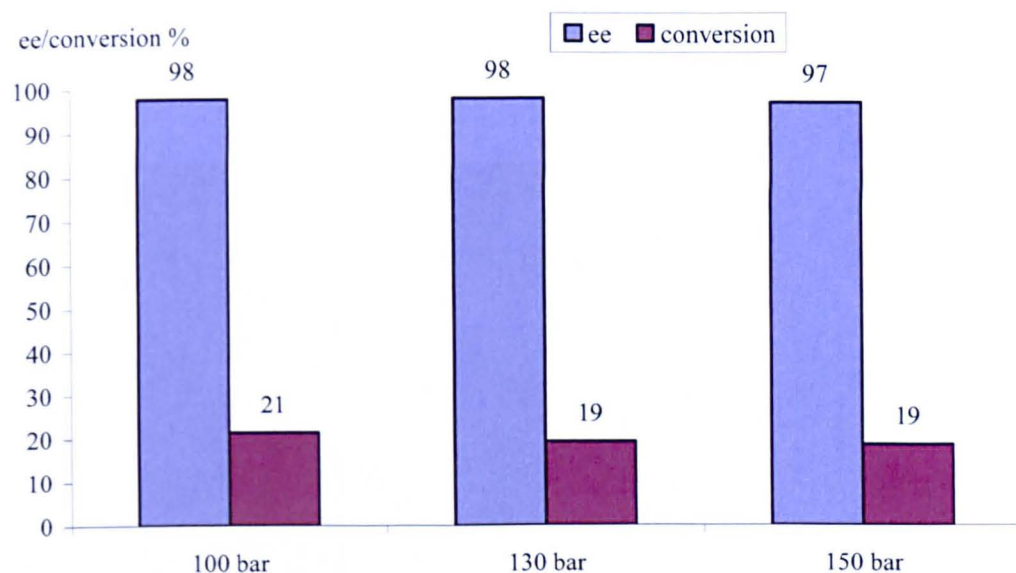


**Figure 6-4. The enantioselectivity (*R*-acetate) and the level of conversion (conversion of (*R*)-1-phenylethanol) at different pressures catalysed by Cal B CLEA (60-70 mg, 1680-1960 U) (second step of the cascade reaction).**  
**Reaction conditions:** temperature:  $40\text{ }^{\circ}\text{C}$ ,  $\text{CO}_2$  flow rate: 1 mL/min, substrate flow rate: 0.1 mL/min (acetophenone, 1-phenylethanol, vinyl acetate).

The enantioselectivity of the kinetic resolution did not change with pressure at  $40\text{ }^{\circ}\text{C}$ , while the conversion of (*R*)-1-phenylethanol slightly decreased with pressure. The level of conversion in  $\text{scCO}_2$  is expected to increase with an increase in pressure due to an increase in the density of  $\text{CO}_2$  that increases the residence time. On the other hand, high pressure could compress the catalyst and could thus create a less favoured flow profile (the stream of the reactants flows around the catalyst bed rather than through), however, further evidence is needed to confirm this.

The conversion of (*R*)-1-phenylethanol in the kinetic resolution step of the cascade reaction reached 22 %, while the kinetic resolution of (*R/S*)-1-phenylethanol as individual reaction<sup>13</sup> displayed 50 % conversion. The unused H<sub>2</sub> from the first step (H<sub>2</sub>:acetophenone = 4:1) could decrease the efficiency of the enzymatic reaction by causing conformational changes in the enzyme. Cal B contains six cysteines (Cys) in its structure. Cysteine contains a thiol group that can form disulfide bonds (Figure 6-5). Disulfide bonds help to stabilise the catalytically active structure of the enzyme and therefore if a disulfide bond breaks for example by H<sub>2</sub> treatment, the enzyme may become inactive because of conformation changes.

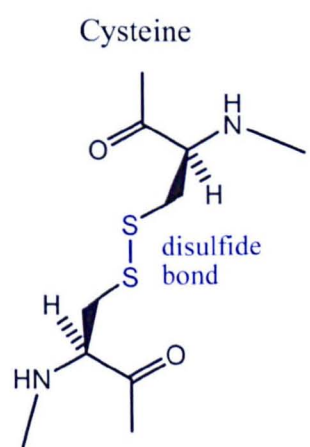
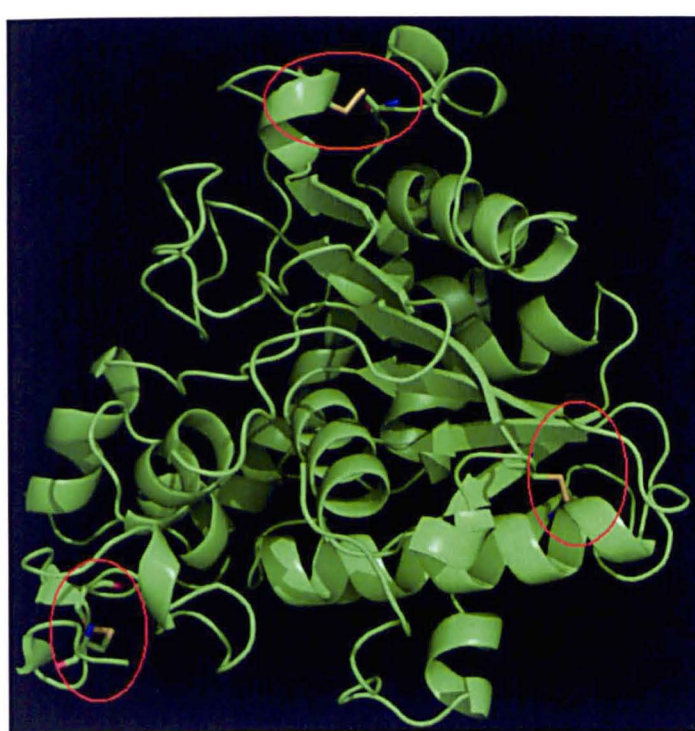


**Figure 6-5. A 3D structure of *Candida antarctica* lipase B (Cal B).** Cal B contains six cysteines in its structure Cys22 - Cys64, Cys216 - Cys258, Cys293 - Cys311 (marked with red). Disulfide bonds are formed by connecting two sulfurs contained in cysteine. If a disulfide bond is broken the 3D structure of the protein might change and thus the enzyme could become inactivated. The structure of Cal B (1TCA) was obtained from Protein DataBank. The figure was generated with Pymol (<http://pymol.sourceforge.net>).

The effect of different CO<sub>2</sub> flow rates was also examined. The results are listed in Table 6-1.

**Table 6-1. Two step catalytic cascade reaction: hydrogenation of acetophenone with Pd Type 31 (270 mg) followed by the kinetic resolution of the product, (*R/S*)-1-phenylethanol, with Cal B CLEA (60-70 mg, 1680-1960 U).**

Entry	CO <sub>2</sub> flow rate (mL/min)	Conv (%) acetophenone	ee <sub>S</sub> (%)	ee <sub>P</sub> (%)	Conv (%) ( <i>R</i> )-1-phenylethanol
1	1 <sup>a</sup>	87	19	98	21
2	0.5 <sup>b</sup>	91	28	98	22

Reaction conditions: pressure: 100 bar, substrate flow rate: 0.1<sup>a</sup> / 0.05<sup>b</sup> mL/min (acetophenone/vinyl acetate), H<sub>2</sub>:substrate ratio = 4:1, T (Pd): 150 °C, T (enzyme reactor): 40 °C.

The conversion of both steps of the catalytic cascade reaction increased with a decrease in CO<sub>2</sub> flow rate, while the enantioselectivity of the kinetic resolution of (*R*)-1-phenylethanol did not change. By decreasing the CO<sub>2</sub> flow rate, longer residence time is provided in the continuous flow reactor which expectedly resulted in higher conversion.

The cascade reaction has been studied previously using Pd Type 31 and Novozym 435 by Stephenson at Nottingham.<sup>14</sup> The results are listed in Table 6-2. The results obtained in this work for first step of the cascade, the hydrogenation of acetophenone, were better than those obtained by Stephenson. The conversion of acetophenone could be improved by optimising reaction conditions (temperature, pressure, CO<sub>2</sub> flow rate). The performance of the kinetic resolution of (*R/S*)-1-phenylethanol was higher with Novozym 435<sup>14</sup> than that with Cal B CLEA, which could be due to differences in the immobilisation of Cal B. The same phenomenon was observed in the kinetic resolution of α-tetralol using Novozym 435 and Cal B CLEA (Chapter 5).

**Table 6-2. Results of the series reaction using Pd Type 31 and Novozym 435 (250 mg, 875 U) (Novozym 435: 3500 U/g) catalysts.<sup>14</sup>**

Entry	T - Pd (°C)	Conv (%) acetophenone	ee <sub>S</sub> (%)	ee <sub>P</sub> (%)	Conv (%) (R)-1-phenylethanol
1	150	68	41	>99	29
2	200	72	32	>99	24
3	150*	71	54	>99	35
4	150**	74	44	>99	30

**Reaction conditions:** pressure: 100 bar, CO<sub>2</sub> flow rate: 1 mL/min, substrate flow rate: 0.1 mL/min (acetophenone/vinyl acetate), H<sub>2</sub>:substrate ratio = 4:1, T (enzyme reactor) = 40 °C.

\* Reaction conditions: pressure: 100 bar, CO<sub>2</sub> flow rate: 0.5 mL/min, substrate flow rate: 0.05 mL/min (acetophenone/vinyl acetate), H<sub>2</sub>:substrate ratio = 4:1, T (enzyme reactor): 40 °C.

\*\* Reaction conditions: pressure: 100 bar, CO<sub>2</sub> flow rate: 1 mL/min, substrate flow rate: 0.1 mL/min (Acetophenone/vinyl acetate), H<sub>2</sub>:substrate ratio = 4:1, T (enzyme reactor): 50 °C.

#### 6.4. Conclusions

A two step chemoenzymatic catalytic cascade reaction for the production of (R)-1-phenylethyl acetate was investigated in a continuous flow scCO<sub>2</sub> system: hydrogenation of acetophenone catalysed by Pd Type 31 followed by the kinetic resolution of the product catalysed by Cal B CLEA. High conversion and enantioselectivity were observed for the cascade reaction. The reaction temperature had a more significant effect on both catalysts than the pressure. The kinetic resolution step gave excellent enantioselectivity ( $ee_R > 99\%$ ) at a higher temperature 60 °C. A decrease in the CO<sub>2</sub> flow rate increased the performance of both the hydrogenation and the kinetic resolution. Further flow rate slow down and/or use of a larger amount of catalyst may give a more significant improvement.

The continuous supercritical reactor designed to investigate catalytic cascade reactions possesses the following advantages.

- i) The catalysts can be physically separated.
- ii) The temperature of each step can be controlled separately.
- iii) The reactants can be introduced into the system at any point.

- iv) The number of reactors attached to the system and therefore number of steps of a catalytic cascade is unlimited.
- v) Ease of catalyst recovery and recycling.

Furthermore:

- vi)  $\text{ScCO}_2$  can provide advantages in dissolution of reactants (substrates and gases).
- vii) Possibility of solvent recycling.
- viii) Continuous production.

## References

1. Ratton, S., Heterogeneous catalysis in the fine chemicals industry: From dream to reality. *Chimica Oggi - Chemistry Today* **1998**, 16, 33-37.
2. Bruggink, A., Schoevaart, R., Kieboom, T., Concepts of nature in organic synthesis: Cascade catalysis and multistep conversions in concert. *Organic Process Research & Development* **2003**, 7, 622-640.
3. Larsson, A. L. E., Persson, B.A., Bäckvall, J.E., Enzymatic resolution of alcohols coupled with ruthenium-catalyzed racemization of the substrate alcohol *Angewandte Chemie International Edition* **1997**, 36, 1211-1212.
4. Sheldon, R. A., in Chirotechnology, The industrial synthesis of optically active compounds. *Marcel Dekker, New York* **1993**, 90-91.
5. Dinh, P. M., Howarth, J.A., Hudnott, A.R., Williams, J.M.J., Harris, W. , Catalytic racemisation of alcohols: Applications to enzymatic resolution reactions. *Tetrahedron Letters* **1996**, 37, 7623-7626.
6. Pamies, O., Bäckvall, J.E., Combination of enzymes and metal catalysts. A powerful approach in asymmetric catalysis. *Chemical Reviews* **2003**, 103, 3247-3261.
7. Riermeier, T. H., Gross, P., Monsees, A., Hoff, M., Trauthwein, H., Dynamic kinetic resolution of secondary alcohols with a readily available ruthenium-based racemization catalyst. *Tetrahedron Letters* **2005**, 46, 3403-3406.
8. Martin-Matute, B., Edin, M., Bogar, K., Bäckvall, J.E., Highly compatible metal and enzyme catalysts for efficient dynamic kinetic resolution of alcohols at ambient temperature. *Angewandte Chemie International Edition* **2004**, 43, 6535-6539.
9. Menashe, N., Shvo, Y., Catalytic disproportionation of aldehydes with ruthenium complexes. *Organometallics* **1991**, 10, 3885-3891.
10. Sheldon, R. A., Arends, I., Hanefeld, U., in Green Chemistry and Catalysis. *Wiley-VCH, Weinheim* **2007**.
11. Hitzler, M. G., Poliakoff, M., Continuous hydrogenation of organic compounds in supercritical fluids. *Chemical Communications* **1997**, 1667-1668.

12. Overmeyer, A., Schrader-Lippelt, S., Kasche, V., Brunner, G., Lipase-catalysed kinetic resolution of racemates at temperatures from 40 C to 160 C in supercritical CO<sub>2</sub>. *Biotechnology Letters* **1999**, *21*, 65–69.
13. Matsuda, T., Watanabe, K., Harada, T., Nakamura, R., Arita, Y., Misumi, Y., Ichikawa, S., Ikariya, T., High-efficiency and minimum-waste continuous kinetic resolution of racemic alcohols by using lipase in supercritical carbon dioxide. *Chemical Communications* **2004**, 2286-2287.
14. Stephenson, P., PhD Thesis. *University of Nottingham, Nottingham (UK) 2005*.
15. Seki, T., Grunwaldt, J.D., Baiker, A., Heterogeneous asymmetric hydrogenation in supercritical fluids: Potentials and limitations. *Industrial & Chemical Engineering Research* **2008**, *47*, 4561-4585.

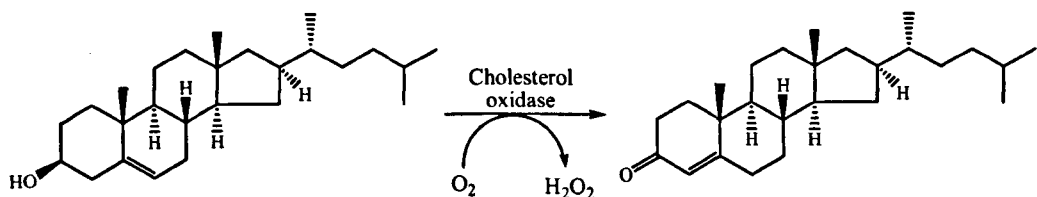
## Chapter 7

### Combi-CLEA of Cholesterol Oxidase and Catalase for the Continuous Oxidation of Cholesterol in scCO<sub>2</sub>

This Chapter describes the importance and characteristics of cholesterol oxidases, and gives an overview of enzyme catalysed coupled-/cascade reactions. The work in this Chapter investigates the oxidation of cholesterol catalysed by a combi-CLEA of cholesterol oxidase and catalase in scCO<sub>2</sub>.

#### 7.1. Cholesterol Oxidases

Bacterial cholesterol oxidases can be classified into two types: non-pathogenic (e.g. *Streptomyces*) and pathogenic (e.g. *Rhodococcus*). In non-pathogenic bacteria, cholesterol is used as carbon source, and the expression of cholesterol oxidase is induced by the presence of cholesterol.<sup>1, 2</sup> In pathogenic bacteria, cholesterol oxidase is used for infecting the host macrophages and again cholesterol regulates the expression of the enzyme in the bacteria.<sup>3, 4</sup> The pathway of infection in pathogenic bacteria is suggested to be the alteration of the physical structure of the lipid membrane (the lipid membrane contains cholesterol) by the conversion of cholesterol to 4-cholesten-3-one, but further evidence is needed to confirm this. The oxidation of cholesterol by cholesterol oxidase is shown in Scheme 7-1.



Scheme 7-1. The oxidation of cholesterol by cholesterol oxidase.

Cholesterol oxidase requires the cofactor Flavin Adenine Dinucleotide (FAD, flavin semiquinone) (Figure 7-1). The cofactor FAD is reduced to  $\text{FADH}^+$  during the reaction and is regenerated *via* the reduction of  $\text{O}_2$  to  $\text{H}_2\text{O}_2$ . Cholesterol oxidases are classed into two groups: I: with the cofactor (FAD) tightly but non-covalently bound to the protein (e.g. *Streptomyces* sp. and *Brevibacterium sterolicum*), and II: with the cofactor covalently bound to the enzyme *via* histidine residues (e.g. *Nocardia* (*Rhodococcus*) *erythropolis* and *Brevibacterium sterolicum*).<sup>5, 6</sup> Although cholesterol oxidases from the two groups share the same catalytic activity, they show no sequence homology and have significant differences in their redox and kinetic properties.<sup>7, 8</sup>

Cholesterol oxidase is a bifunctional monomeric flavoenzyme that catalyses the oxidation and subsequent isomerisation of steroids that contain a 3-OH group and a double bond in the C-5 position of the steroid ring system. The oxidation of cholesterol is performed in 2 steps: cholesterol is oxidised to cholest-5-en-3-one and then isomerised to cholest-4-en-3-one.<sup>5</sup> The reaction mechanisms of cholesterol oxidases illustrating the key residues for catalytic activity are shown in Scheme 7-2.

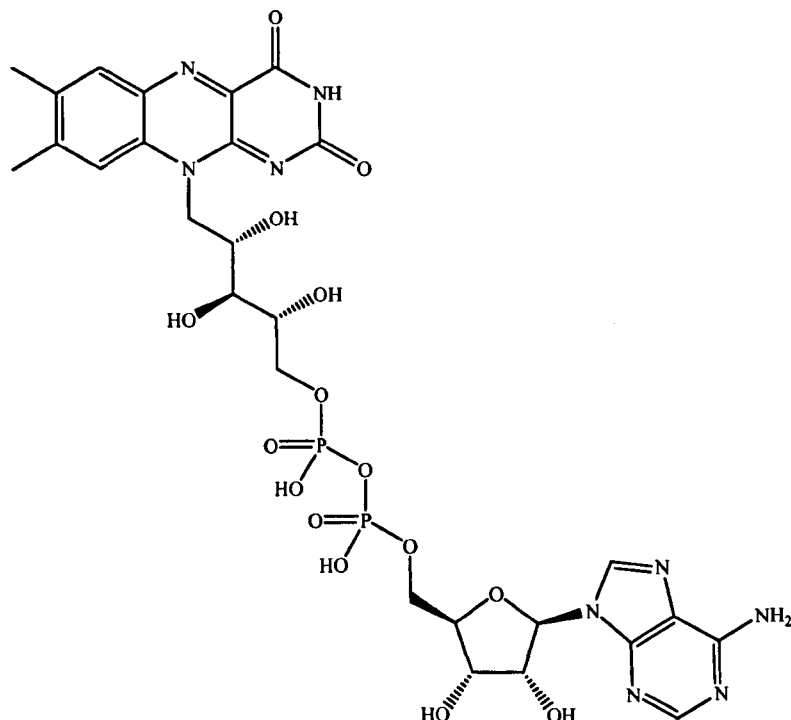
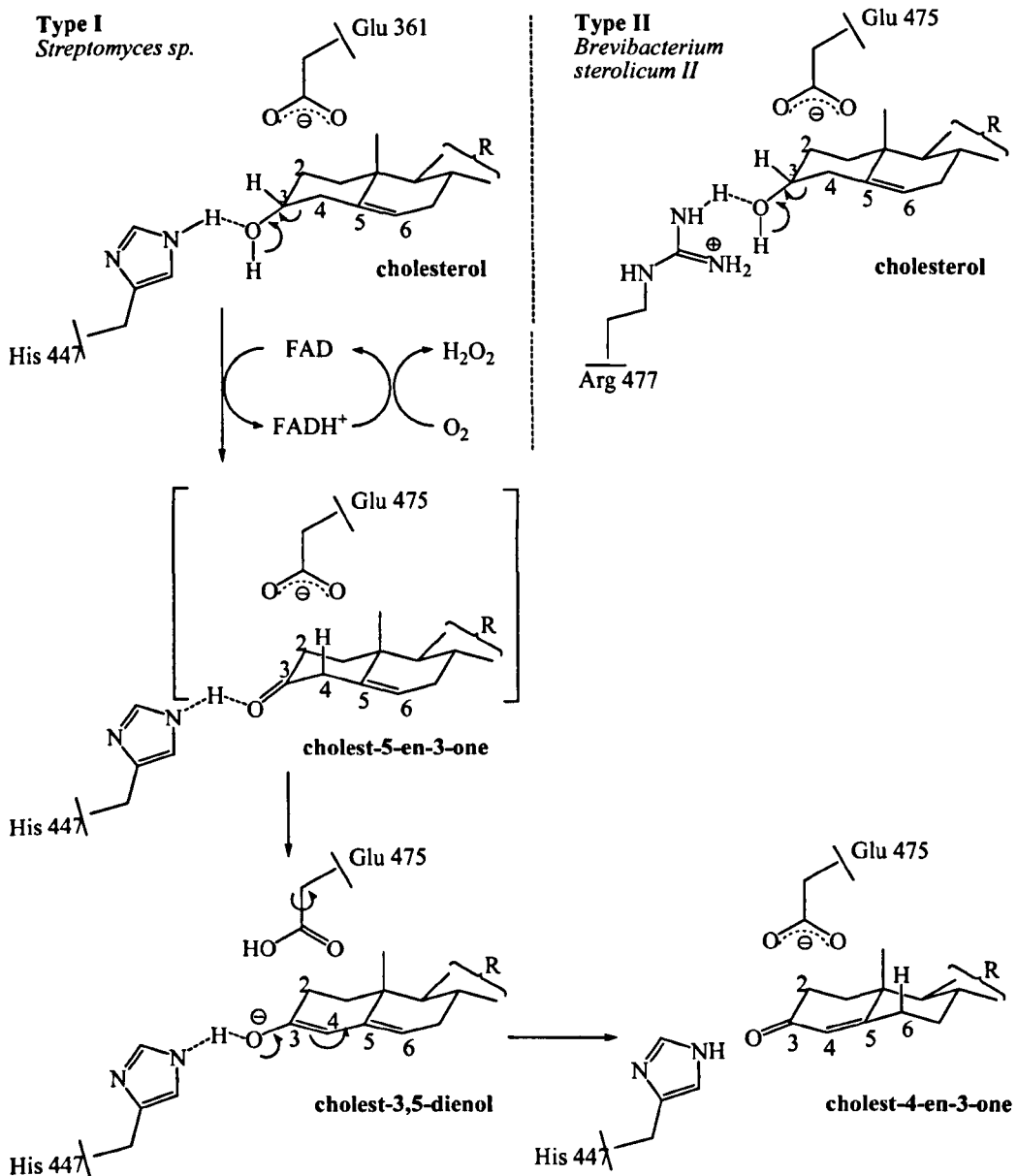


**Figure 7-1. The structure of Flavin Adenine Dinucleotide (FAD).**



**Scheme 7-2. Reaction catalysed by cholesterol oxidases Type I (*Streptomyces* sp.<sup>9</sup> and *Brevibacterium sterolicum* I<sup>10, 11</sup>) and Type II (*Brevibacterium sterolicum* II<sup>12</sup>). The proposed role of key active site residues is shown for the type I cholesterol oxidase. The analogous residues for the type II cholesterol oxidase are also illustrated.<sup>5, 6</sup>**

In this work, cholesterol oxidase from *Nocardia* sp. was used. Cholesterol oxidase from *Nocardia* sp. has been classed as a Type II cholesterol oxidase<sup>13</sup> and has already been used for determining total serum cholesterol<sup>13</sup> and for oxidising cholesterol<sup>14</sup> in organic solvents. The structure of cholesterol oxidase from

*Nocardia* sp. is not yet available in the literature. The structure of cholesterol oxidase from *Streptomyces* sp. (Type I) has been solved<sup>9</sup> and is presented in Figure 7-2.

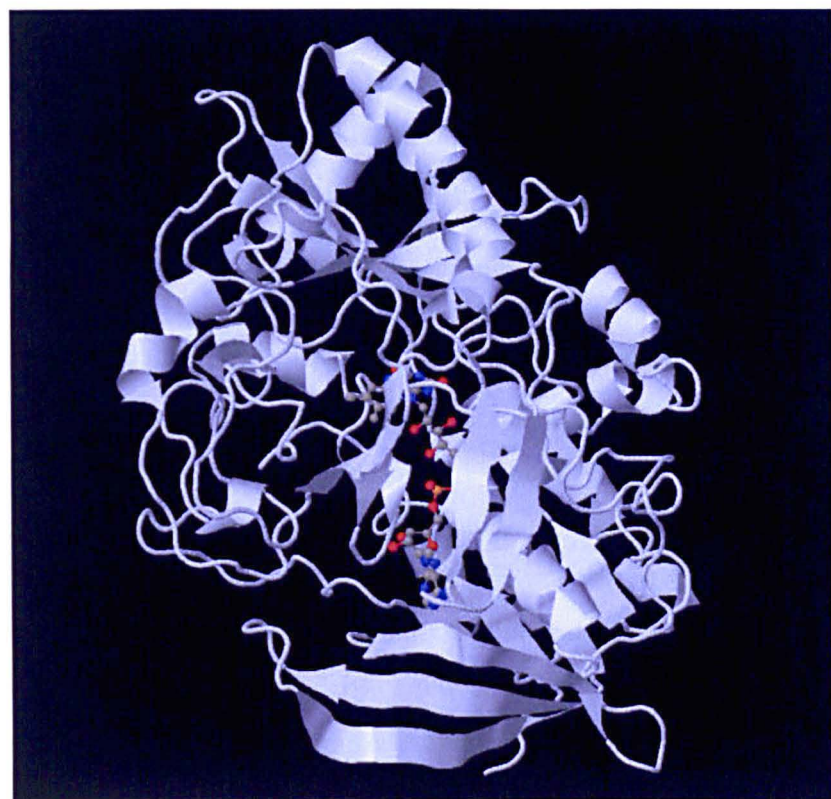


**Figure 7-2. The structure of cholesterol oxidase from *Streptomyces* sp. (1B4V).** The FAD cofactor is shown with ball-stick representation. The structure was obtained from Protein DataBank. The picture was created using Jmol.<sup>9</sup>

The major uses of cholesterol oxidases is in the quantification of serum cholesterol for the assessment of atherosclerosis, coronary heart disease and other lipid disorders, and also for the determination of risk of heart attack and thrombosis. The enzyme also is a potential larvicide<sup>15</sup> and a tool<sup>16-18</sup> in cell biology. The product of the oxidation of cholesterol, 4-cholest-3-one is a precursor of interest in the pharmaceutical industry.<sup>14</sup> The great advantage of cholesterol oxidases is that they have broad substrate specificity and therefore can be used in the transformation of steroids that can be used as intermediates for the synthesis of steroid hormones or other steroids.

The aim of this work was the production of 4-cholest-3-one (Scheme 7-1) with combi-CLEA of cholesterol oxidase and catalase in a continuous flow scCO<sub>2</sub> system. Cholesterol oxidase has been immobilised previously on glass beads and its activity has been studied for the oxidation of cholesterol<sup>19, 20</sup>, and for quantifying cholesterol<sup>21</sup> in edible oil samples and fat-containing food samples, in a continuous flow scCO<sub>2</sub> system. However, the immobilisation of cholesterol oxidase using a carrier-free immobilisation technique and the co-immobilisation of cholesterol oxidase with another enzyme in a carrier-free form have not yet been investigated.

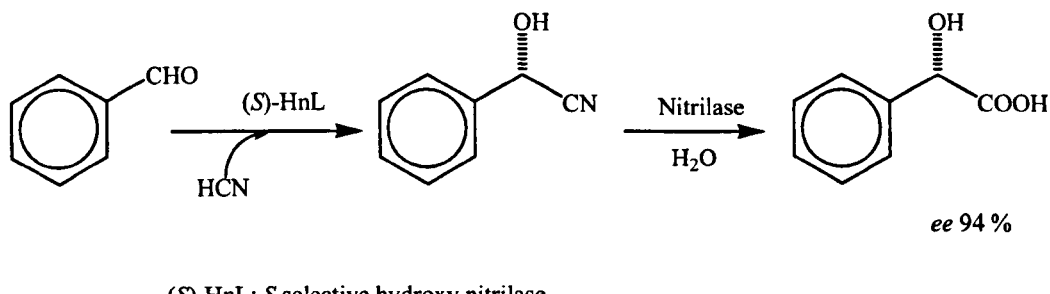
## 7.2. Enzyme Catalysed Coupled-/Cascade Reactions

The advantages of enzymes as biocatalysts are discussed in Chapter 5. A general discussion of multistep catalytic cascade reactions can be found in Chapter 6. Here, enzymatic cascade reactions are covered.

Enzymes have been shown to be suitable to catalyse chemical transformations and have also been used in cascade reactions.<sup>22-25</sup> In catalytic cascade reactions, the product of each step is instantly converted in the next step, and the reaction can therefore shift towards the favoured direction. This can be advantageous in enzymatic reactions where the inhibition by product is limiting, besides all other advantages of catalytic cascade reactions.

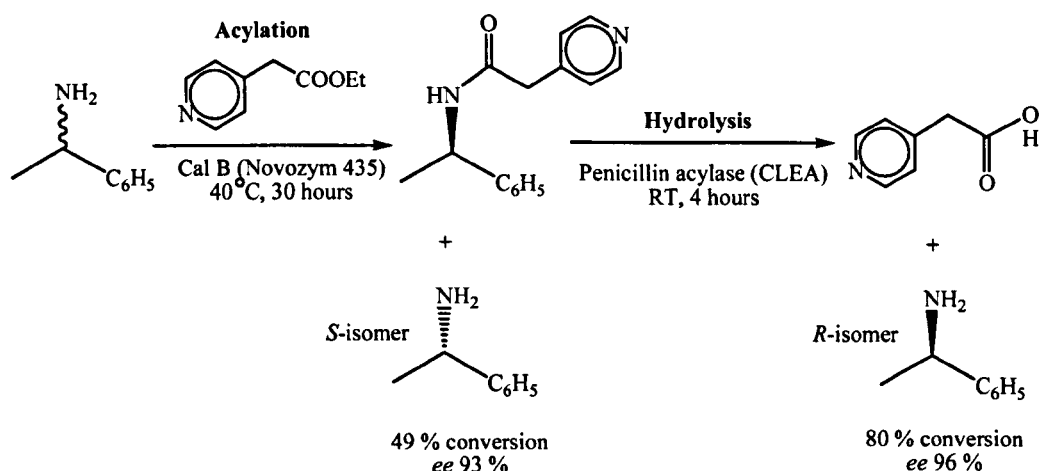
An example of enzymatic catalytic cascade reactions has been demonstrated by Sheldon.<sup>26</sup> The one pot conversion of benzaldehyde to (*S*)-mandelic acid was investigated with combi-CLEA (Scheme 7-3).<sup>26</sup> The limitations of this cascade reaction could be overcome by optimising the reaction conditions (pH and reaction medium). A major improvement could be achieved by using immobilised enzymes (*S*-selective oxynitrilase and a non-selective nitrilase) in the CLEA form. The enzymes were co-immobilised to make a combi-CLEA. The nitrile intermediate was immediately hydrolysed in the combi-CLEA particles, which suppressed diffusion into the water phase and possible racemisation. In addition, this process overcomes the limitations of the industrial process (the production of enantiopure 2-hydroxy acids *via* a dynamic kinetic resolution of the chemically synthesise

cyanohydrin in the presence of an enantioselective nitrilase) that is restricted to (*R*)-2-hydroxy acids, because no (*S*)-selective nitrilases for cyanohydrin substrates have yet been identified.

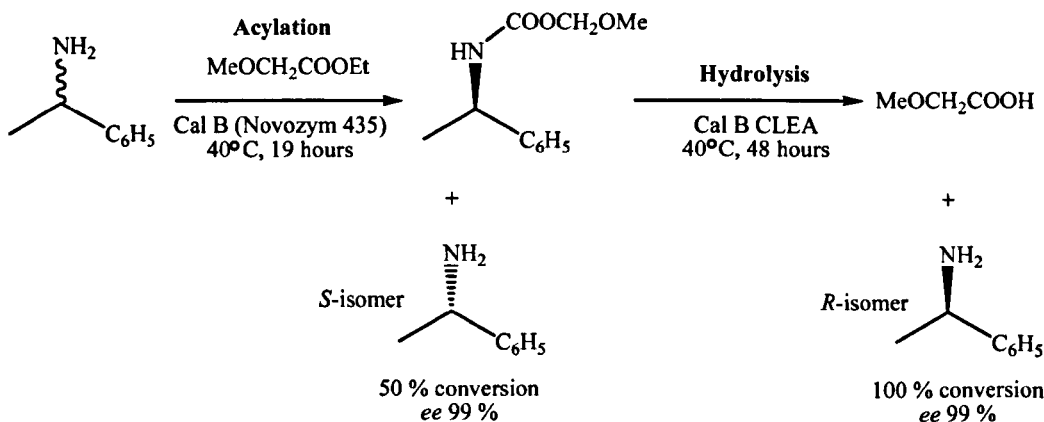


**Scheme 7-3.** Enzymatic route to the production of (*S*)-mandelic acid from benzaldehyde. A combi-CLEA of an *S*-selective oxynitrilase and a non-selective nitrilase in a two enzyme cascade.<sup>26</sup>

Another example of enzymatic cascade reactions has been reported by the same group. The combination of acylation catalysed by Cal B (Novozym 435) and hydrolysis (deacylation) catalysed by penicillin G acylase from *A. faecalis* (CLEA) was conducted with high enantioselectivity and high conversion (Scheme 7-4).<sup>25, 27</sup> The production of enantiomerically pure amines with chemical hydrolysis usually generates a large amount of waste (strongly alkaline conditions that also is incompatible with sensitive functional groups). The cascade reaction reported by Sheldon for the production of chiral amines reduces the waste generation and provides mild reaction conditions (aqueous medium, pH 7.0). The cascade reaction was further developed to the fully enzymatic resolution of amines with Cal B for both steps of the cascade reaction.<sup>28</sup> The schematic of the reaction is shown in Scheme 7-5.



**Scheme 7-4. Two enzyme resolution of amines by two consecutive enzymes.<sup>27</sup>**



**Scheme 7-5. Amine resolution with Cal B for acylation and deacylation.<sup>28</sup>**

The examples shown here demonstrate that catalytic cascade reactions have great potential and the limitations can be overcome by careful optimisation of the reaction conditions. Here the oxidation of cholesterol by cholesterol oxidase was investigated with a combi-CLEA of two enzymes because cholesterol oxidase can be inhibited by H<sub>2</sub>O<sub>2</sub>, the by-product of the oxidation. H<sub>2</sub>O<sub>2</sub> was removed from the system with catalase (catalase from bovine liver, Figure 7-3) that reduces H<sub>2</sub>O<sub>2</sub> to O<sub>2</sub> and H<sub>2</sub>O. The final aim of the study was the use of a combi-CLEA of cholesterol oxidase and catalase for the production of 4-cholestene-3-one in a continuous flow scCO<sub>2</sub> system.

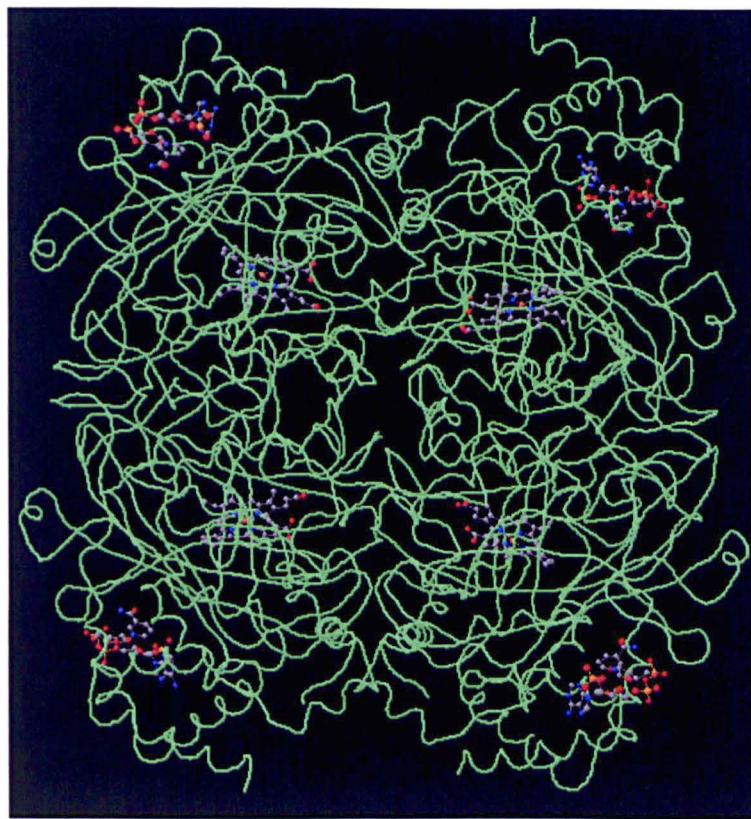


**Figure 7-3.** The structure of catalase from beef liver (8cat). Catalase is a tetramer where each subunit contains an active heme group (ball and stick representation) that performs the transformation of peroxide using a cofactor NADPH (ball and stick representation). The structure was obtained from Protein DataBank. The picture was created using Jmol.<sup>29</sup>

### 7.3. Results and Discussion

The preparation of cholesterol oxidase CLEA and combi-CLEA of cholesterol oxidase and catalase was investigated, and the immobilised enzymes were examined for the oxidation of cholesterol in a continuous flow scCO<sub>2</sub> system. Cholesterol oxidase from *Nocardia sp.* was used in this study. A preliminary screening of cholesterol oxidases from different sources (*Nocardia sp.*, *Streptomyces sp.*, *Pseudomonas sp.*, and *Pseudomonas fluorescens*) was performed and only cholesterol oxidase from *Nocardia sp.* converted cholesterol to 4-cholesten-3-one. The immobilisation of catalase from bovine liver has already been studied using the CLEA technique<sup>30</sup> which is a promising starting point for

making a combi-CLEA of cholesterol oxidase and catalase. Cholesterol oxidase from *Nocardia sp.* (E.C. 1.1.3.6., Merck 228230) (batch 1: 19.5 U/mg protein - protein content 77.4 %; batch 2: 20.1 U/mg protein - protein content 84.2 %) and catalase from bovine liver (E.C. 1.11.1.6, Sigma C-9322) (batch 1: 2140 U/mg protein - protein content 63 %; batch 2: 4540 U/mg protein - protein content 65 %) were used. The parameters used to the particular batches are presented along with the activity results.

### **7.3.1. Results of the Precipitation Screen of the Enzymes**

The first step of the CLEAtion (detailed description in Chapters 1 and 2) is enzyme aggregation. The recovered activity after precipitation must be high (above 90%) for preparing CLEA with potentially high activity. Here, iso-propanol, acetone, ethanol, dimethoxyethane (ethyleneglycol dimethyl ether), acetonitrile 90 % (v/v) and ammonium sulfate were examined as precipitants for both cholesterol oxidase and catalase. (A detailed description of the process can be found in Chapter 2.) The activity tests of cholesterol oxidase and catalase were based on the oxidation of cholesterol to cholest-4-en-3-one and on the reduction of H<sub>2</sub>O<sub>2</sub>, respectively. A detailed description of the activity assays can be found in Chapter 2. The results of the precipitation screen are shown in Figure 7-4 and Figure 7-5.

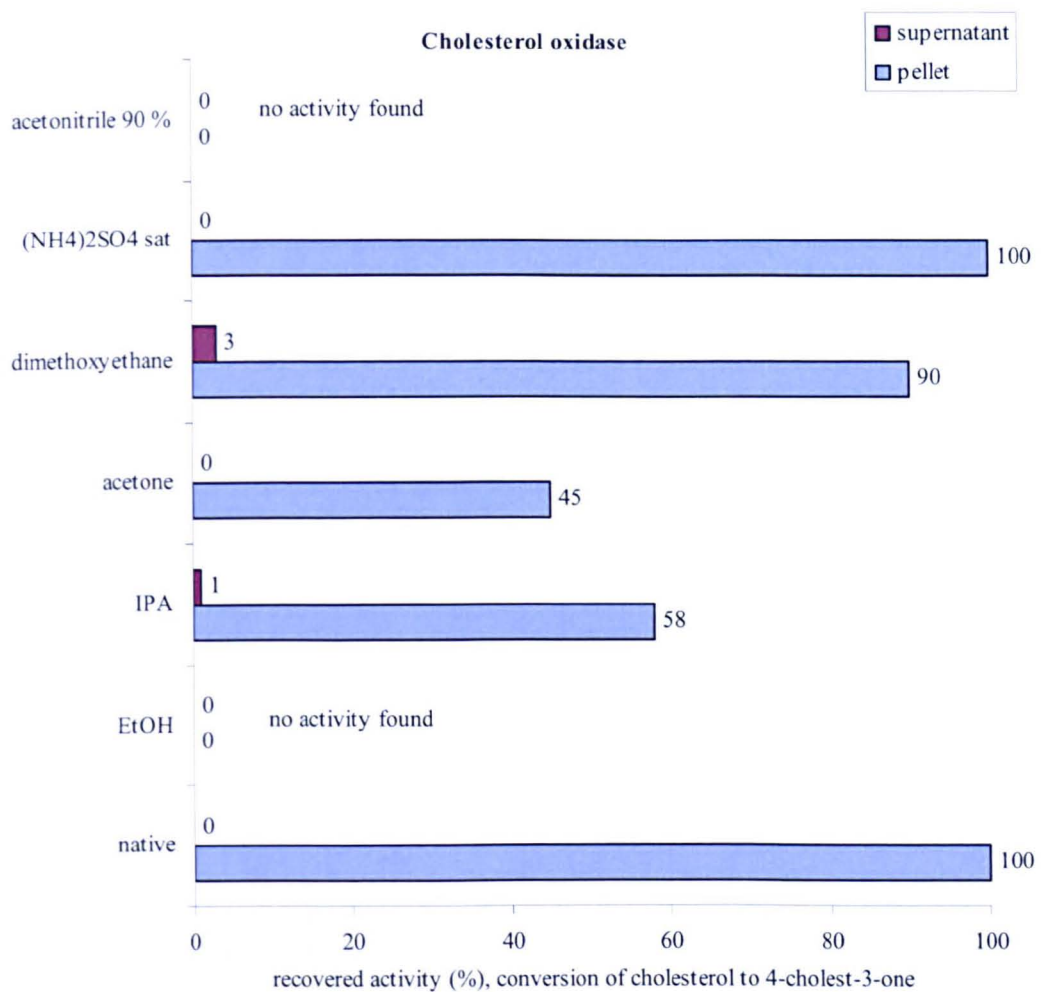


**Figure 7-4.** The activity of cholesterol oxidase from *Nocardia sp.* after precipitation. The precipitant was used in 1 : 5 volume ratio of enzyme aliquot to precipitant. The supernatant was removed and the pellet was redissolved in phosphate buffer. Cholesterol oxidase activity, conversion of cholesterol (%) is relative activity compared to native.

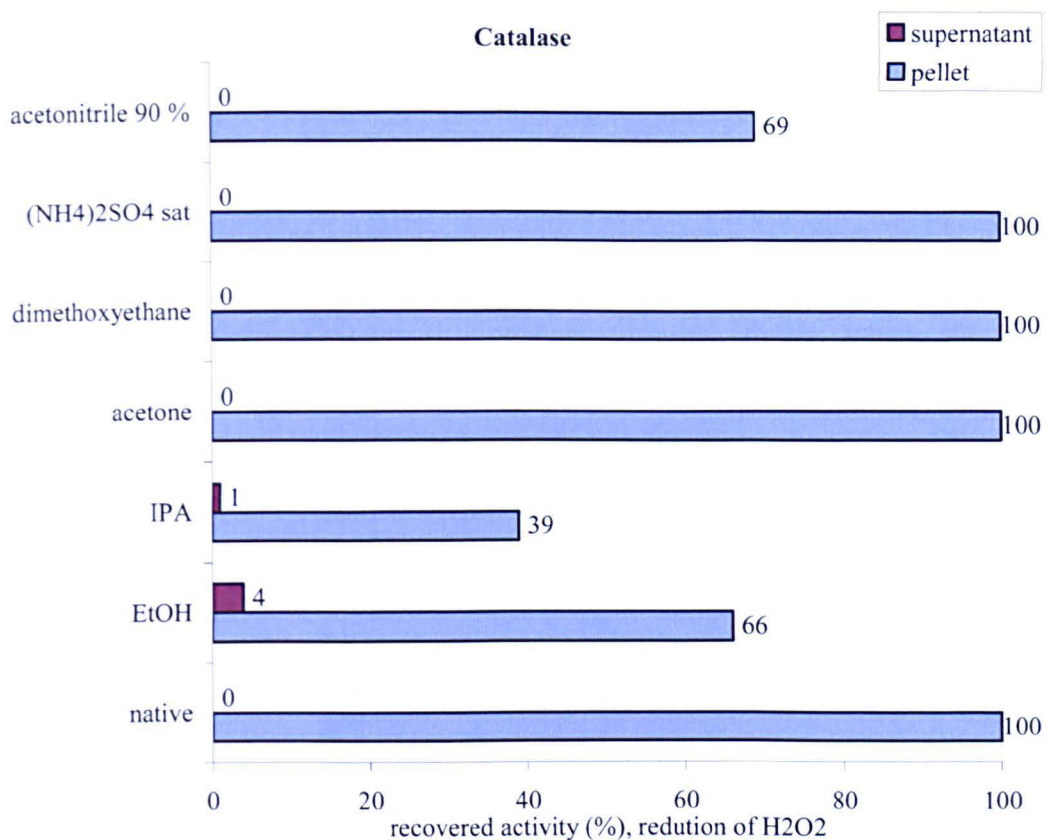


**Figure 7-5. The activity of catalase from bovine liver after precipitation.** The precipitant was used in 1 : 5 volume ratio of enzyme aliquot to precipitant. The supernatant was removed and the pellet was redissolved in phosphate buffer. Catalase activity, conversion of H<sub>2</sub>O<sub>2</sub> (%) is relative activity compared to native (catalase assay 1).

Cholesterol oxidase from *Nocardia sp.* was found to be sensitive to the presence of most precipitants (more than 30 % activity loss). Only ammonium sulfate was suitable to precipitate cholesterol oxidase without any loss of activity. Dimethoxyethane produced 10 % activity loss. Catalase from bovine liver could be precipitated without any activity loss with ammonium sulfate, dimethoxyethane and acetone. The enzyme was successfully precipitated using acetonitrile (90 % v/v), iso-propanol and ethanol but the activity loss was over 30 %.

Cholesterol oxidase CLEA was also prepared using dimethoxyethane as precipitant but the CLEA activity was very low in this case. Allowing 3 times longer reaction time, only 49 % conversion (relative to native) was obtained by the

CLEA (precipitant: dimethoxyethane, cross-linker: glutaraldehyde 10 mM). Dimethoxyethane might produce large aggregates or aggregates in unfavoured form that were thus cross-linked, in which the mass transport of the substrate to the active site of cholesterol oxidase could be highly limited. SEM was used to determine the morphology and the particle size of the CLEA. Figure 7-6 shows the SEM image of cholesterol oxidase CLEA prepared using dimethoxyethane as precipitant and glutaraldehyde (50 mM) as cross-linker. The image shows a paste-like structure that can indicate the presence of large aggregates.

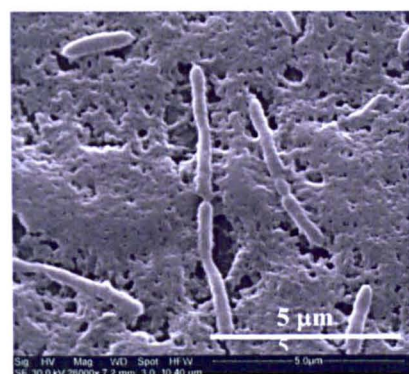


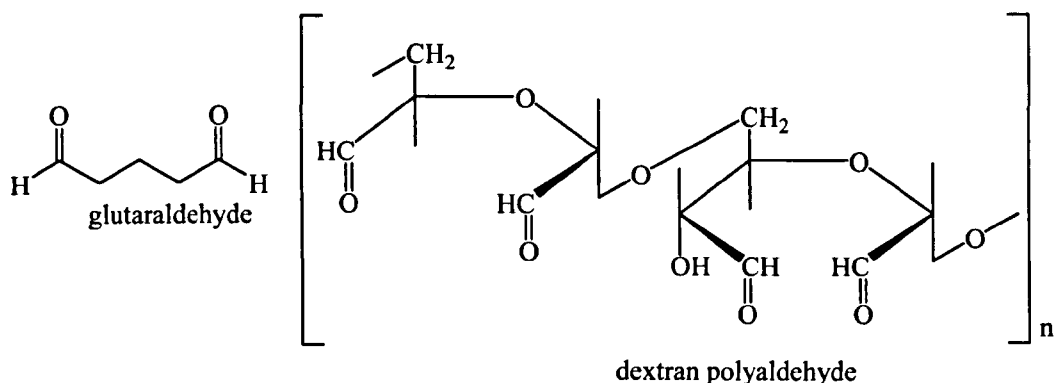
**Figure 7-6. SEM image of the individual cholesterol oxidase CLEA.** The CLEA was prepared using dimethoxyethane as precipitant and glutaraldehyde as cross-linker (50 mM) without a reduction step. The CLEA was prepared using cholesterol oxidase from *Nocardia sp.* (19.5 U/mg protein, 6.62 mg, 100 U).

### 7.3.2. CLEA Activity

In a CLEA, the solid enzyme particles are linked to each other using bifunctional linker molecules, usually dialdehydes. In this study, glutaraldehyde and dextran polyaldehyde were used as cross-linkers (Scheme 7-6). Glutaraldehyde was used at 10 mM and 50 mM concentrations; dextran polyaldehyde (aqueous solution of dextran polyaldehyde) was used in the following amounts 200  $\mu$ L DPA solution/mL enzyme solution and 400  $\mu$ L DPA solution/mL enzyme solution. The activity of the enzymes was examined by

- Cholesterol oxidase: oxidation of cholesterol in aqueous medium with  $O_2$  as oxidant
- Catalase: reduction of  $H_2O_2$  in aqueous medium.

(Detailed description of the enzyme assays can be found in Chapter 2.)



**Scheme 7-6. The cross-linkers: glutaraldehyde and dextran polyaldehyde.**

The third step of CLEA is reduction, however, it is not essential for making CLEA. The stability of CLEA can be enhanced by improving the stability of the linkages between the enzyme particles. It can be obtained by the reduction of ' $-\text{N}=\text{CH}-$ ' bonds to ' $-\text{NH}-\text{CH}_2-$ ' with  $\text{NaBH}_4$  or  $\text{Na}(\text{CN})\text{BH}_3$  (Scheme 1-2 in Chapter 1). The effect of the reduction was also studied in this work.

Cholesterol oxidase CLEA were prepared with ammonium sulfate as precipitant, and glutaraldehyde and dextran polyaldehyde as cross-linker, with and without reduction. The results of the CLEA activity test are shown in Table 7-1.

**Table 7-1.** The activity of the individual cholesterol oxidase CLEA. The precipitation was performed with saturated ammonium sulfate solution. Glutaraldehyde (GA) (10 mM and 50 mM) and dextran polyaldehyde (DPA) (200 µL DPA solution/mL enzyme solution and 400 µL DPA solution/mL enzyme solution) were used as cross-linkers. Cholesterol oxidase from *Nocardia* sp. (GA - 19.5 U/mg protein, 6.62 mg, 100 U and DPA - 20.1 U/mg protein, 5.92 mg, 100 U) was used. Cholesterol oxidase activity, conversion of cholesterol (%) is relative activity compared to native. GA = glutaraldehyde, DPA = dextran polyaldehyde, n/a = no measurement – the CLEA of the particular conditions was not prepared.

Cholesterol oxidase CLEA no reduction	Cholesterol oxidase activity (%)	Cholesterol oxidase activity (%), 20 days – fraction of ‘fresh’ (fresh: original activity)
GA 10	90	n/a
GA 50	91	n/a
DPA 200	91	100 (40 days)
DPA 400	95	90 (40 days)

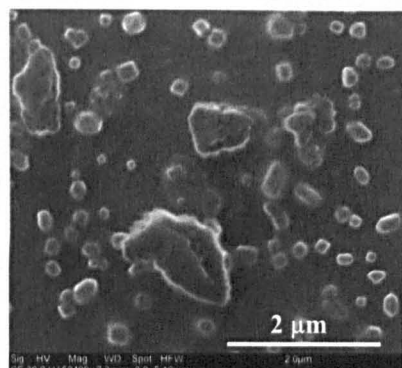
  

Cholesterol oxidase CLEA with reduction	Cholesterol oxidase activity (%)	Cholesterol oxidase activity (%), 20 days – fraction of ‘fresh’ (fresh: original activity)
DPA 200	98	75
DPA 400	74	100

The results of the cholesterol oxidase CLEA activity tests (Table 7-1) showed no significant effect of the cross-linker on the CLEA activity, however, CLEA made with glutaraldehyde as cross-linker had slightly lower activity. This may be due to the fact that glutaraldehyde is a small and reactive molecule that might produce a more compact structure in the CLEA than dextran polyaldehyde that is larger and less reactive. Glutaraldehyde could also interact with key amino acids in the active centre of the enzyme or with the flavin cofactor, and therefore block the enzyme activity. The long term stability of the cholesterol oxidase CLEA was high when stored as suspension. Further data is required to confirm how the reduction influences the activity of individual cholesterol oxidase CLEA.

SEM was used to determine the size and morphology of the CLEA particles. A number of enzyme molecules are expected to be packed together in an aggregate

which can have a significant influence on the activity as a whole. The SEM images of the cholesterol oxidase CLEA can be seen in Figures 7-7, 7-8 and 7-9.



**Figure 7-7.** SEM image of the individual cholesterol oxidase CLEA. The CLEA was prepared using ammonium sulfate as precipitant and glutaraldehyde as cross-linker (10 mM) without a reduction step. Cholesterol oxidase from *Nocardia* sp. (19.5 U/mg protein, 6.62 mg, 100 U) was used for making the CLEA. The particle is 0.2 μm in diameter with a small deviation but larger aggregates are also present.

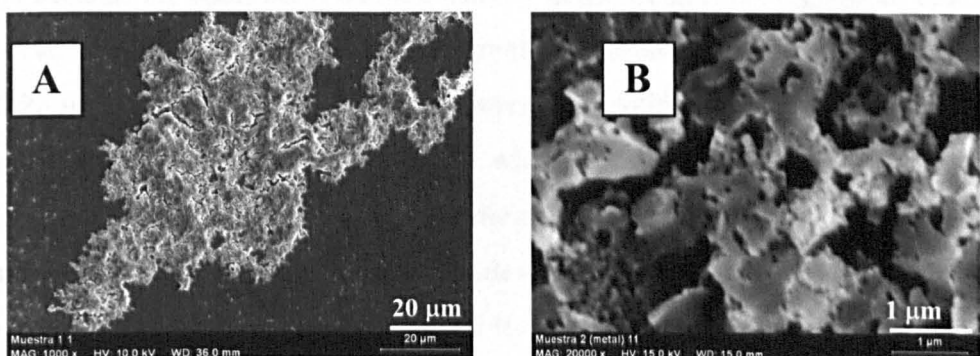


**Figure 7-8.** SEM image of the individual cholesterol oxidase CLEA. The CLEA was prepared using ammonium sulfate as precipitant and dextran polyaldehyde as cross-linker (A: 200 μL DPA solution/mL enzyme solution, B: 400 μL DPA solution/mL enzyme solution) without a reduction step. Cholesterol oxidase from *Nocardia* sp. (20.1 U/mg protein, 5.92 mg, 100 U) was used for making the CLEA.

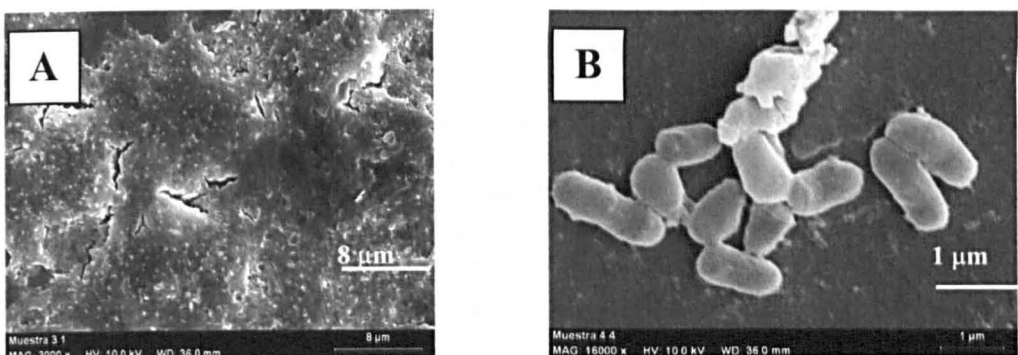


**Figure 7-9.** SEM image of the individual cholesterol oxidase CLEA. The CLEA was prepared using ammonium sulfate as precipitant and dextran polyaldehyde as cross-linker (A: 200  $\mu$ L DPA solution/mL enzyme solution, B: 400  $\mu$ L DPA solution/mL enzyme solution) including a reduction step. Cholesterol oxidase from *Nocardia* sp. (20.1 U/mg protein, 5.92 mg, 100 U) was used for making the CLEA. The size of the particles is A: cannot be determined, B: 1.5  $\mu$ m with a small deviation.

Well defined particles were obtained in some cases while others showed paste-like material. The morphology should not have a great effect on the activity of the CLEA because the cholesterol oxidase activity in the CLEA was high in all cases. However, the presence of larger particles might affect the CLEA activity. Particles of 0.2  $\mu$ m were obtained using ammonium sulfate as precipitant and glutaraldehyde as cross-linker (10 mM), which exhibited 90 % activity in the CLEA (relative to native). Larger particles, 1.5  $\mu$ m, were obtained using ammonium sulfate as precipitant and dextran polyaldehyde as cross-linker (400  $\mu$ l/ml solution), which exhibited 74 % activity (compared to native). The particle size might have an effect on the CLEA activity but further evidence is required to confirm this.

Catalase CLEA has been reported previously.<sup>30</sup> This work expands the examination of different factors, which could also be well utilised in the making of a combi-CLEA of cholesterol oxidase and catalase. Catalase CLEA was prepared using ammonium sulfate and dimethoxyethane as precipitant, and glutaraldehyde and dextran polyaldehyde as cross-linker. The results of the CLEA activity tests can be seen in Table 7-2.

**Table 7-2. Activity of the individual catalase CLEA.** The precipitation was performed with saturated ammonium sulfate solution (amms) or dimethoxyethane (DME). Glutaraldehyde (GA) (10 mM and 50 mM) and dextran polyaldehyde (DPA) (200 µL DPA solution/mL enzyme solution and 400 µL DPA solution/mL enzyme solution) were used as cross-linkers. Catalase from bovine liver (4540 U/mg protein, 250 mg, 737500 U) was used for making the CLEA. Catalase activity, conversion of H<sub>2</sub>O<sub>2</sub> (%), is relative activity compared to native (catalase assay 2). Amms = ammonium sulfate, DME = dimethoxyethane, GA = glutaraldehyde, DPA = dextran polyaldehyde.

Catalase CLEA no reduction	Catalase activity (%)	Catalase activity (%) 20 days – fraction of ‘fresh’ (fresh: original activity)
Amms - GA 10	0	7
Amms - GA 50	12	66
DME - GA 10	46	77
DME - GA 50	39	100
Amms - DPA 200	36	72
Amms - DPA 400	20	75
DME - DPA 200	39	90
DME - DPA 400	43	100

Catalase CLEA with reduction	Catalase activity (%)	Catalase activity (%) 20 days – fraction of ‘fresh’ (fresh: original activity)
Amms - GA 10	3	0
Amms - GA 50	39	44
DME - GA 10	40	0
DME - GA 50	29	0
Amms - DPA 200	38	54
Amms - DPA 400	54	57
DME - DPA 200	28	13
DME - DPA 400	29	0

Catalase CLEA was more active and more stable with dimethoxyethane as precipitant than with ammonium sulfate as precipitant. The reason for lower

activity of catalase in the CLEA prepared using ammonium sulfate as precipitant could be due to a less favoured form of enzyme aggregation, which could also affect the efficiency of the cross-linking (the lysine residues of the protein might become unavailable for the cross-linker). The efficiency of the cross-linking, the determination of the amount of non-cross-linked protein was examined using SDS-PAGE (results are discussed below).

Glutaraldehyde and dextran polyaldehyde were examined as cross-linkers for catalase CLEA. The CLEA prepared with glutaraldehyde as cross-linker exhibited lower activity than those prepared with dextran polyaldehyde as cross-linker in most cases. The effect of different cross-linkers due to their size and reactivity could affect the structure of the CLEA. The more significant parameter of the cross-linker may be its size when making catalase CLEA. Catalase is a large protein (250 kDa), that is a tetramer built of four subunits (62.5 kDa) with an active centre in each subunit (Figure 7-3). Dextran polyaldehyde may link the enzyme particles in a more favoured structure that may be closely bound by glutaraldehyde. The CLEA with dextran polyaldehyde can thus benefit of lower steric inhibition that may block less active sites, and also better mass transport. Differences in CLEA activity using different cross-linkers was also shown for cholesterol oxidase CLEA, however, only slight difference was observed there. Due to the more complex structure of catalase, the effect of the cross-linker can increase.

The drop in the activity of catalase in the CLEA might also be due to loss of protein (non-cross-linked or loosely bound to the cross-linked bulk). The efficiency of the cross-linking was determined by Sodium Dodecyl Sulfate Polyacrylamide Gel Electrophoresis (SDS-PAGE, to determine the quantity and size of proteins). The protein samples were boiled before running on the gel which breaks the catalase tetramer to subunits that can be determined by electrophoresis. The supernatants collected during the preparation of the CLEA (detailed description of the procedure can be found in Chapter 2) were analysed, which should contain the non-cross-linked protein. The strength of the bands appearing in the gel should correspond to the efficiency of the CLEA: the less intense

bands (less protein loss) the more efficient cross-linking. The bands in the gel shown in Figure 7-10 have a size of approximately 60 kDa that corresponds to the size of catalase subunits, 62.5 kDa. Band appeared in the sample of CLEA prepared using ammonium sulfate as precipitant (1, 2 and 5, 6 in Figure 7-10), while no bands were found in the samples of CLEA prepared using dimethoxyethane as precipitant (3, 4 and 7, 8 in Figure 7-10) with either cross-linker. The results of the SDS-PAGE suggest that the precipitant is important to produce CLEA with high retained activity. Dimethoxyethane may produce protein aggregates of catalase in a more favoured form to be cross-linked and/or it may be a more suitable the reaction medium for the cross-linking. Using ammonium sulfate as precipitant, dextran polyaldehyde was shown to be a more efficient cross-linker as the bands were less intense in these samples (1, 2 in Figure 7-10) than those with glutaraldehyde (5, 6 in Figure 7-10). (No band appeared in the samples of the CLEA made with dimethoxyethane as precipitant with either cross-linker (3, 4, 7, 8 in Figure 7-10.)) Dextran polyaldehyde may link the enzyme particles that cannot be bound by glutaraldehyde due to its larger size.

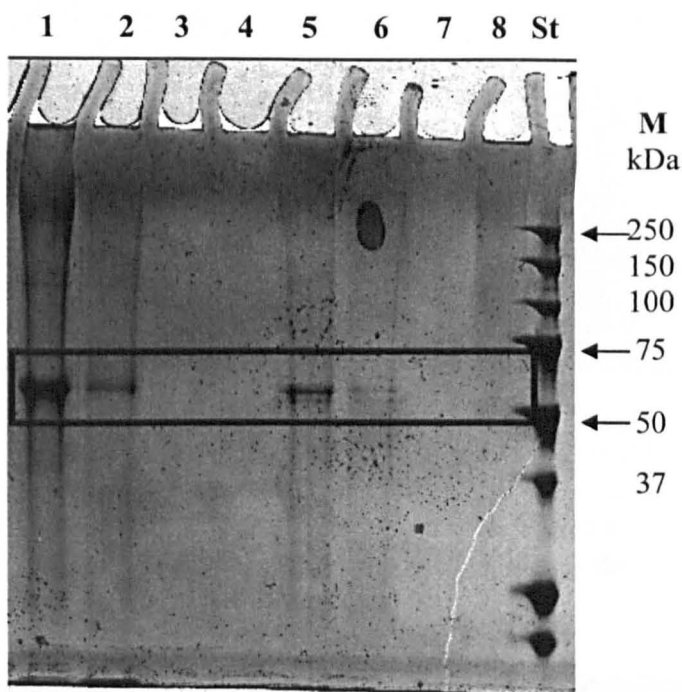


**Figure 7-10.** SDS-PAGE analysis of the protein fractions of catalase. Samples are as follows: 1: GA10 - amms, 2: GA 50 - amms, 3: GA 10 - DME, 4: GA 50 - DME, 5: DPA 200 - amms, 6: DPA 400 - amms, 7: DPA 200 - DME, 8: DPA 400 - DME, St: standard. Amms = ammonium sulfate, DME = dimethoxyethane, GA = glutaraldehyde, DPA = dextran polyaldehyde. The samples of the supernatant collected during the preparation of the CLEA were analysed.

Catalase is very unstable when stored in solution. Therefore the stability of the immobilised enzyme is important for industrial applications. The stability of catalase CLEA was high when stored as suspension in most cases, and therefore CLEA of catalase may have potential for industrial applications.

The effect of the reduction on the catalase CLEA was also examined (Table 7-2). The activity of 'reduced' catalase CLEA varied when compared to the activity of 'non-reduced' CLEA. Further chemical stability is expected by reduction but it was not observed clearly in this case.

The morphology and particle size of the CLEA was investigated by SEM. The SEM images of catalase CLEA are presented in Figures 7-11 and 7-12.

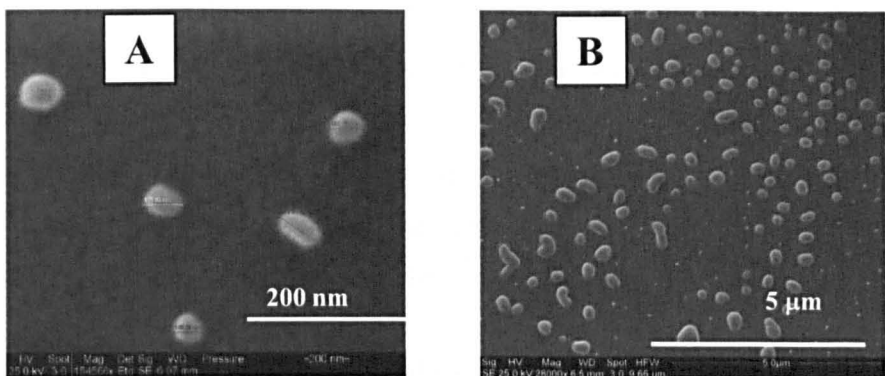


**Figure 7-11.** SEM image of the individual catalase CLEA. The CLEA was prepared using ammonium sulfate as precipitant and glutaraldehyde as cross-linker (A: 10 mM, B: 50 mM) without reduction. The CLEA were prepared using catalase from bovine liver (2140 U/mg protein, 250 mg, 335000 U). The size of the particles is A: 0.2  $\mu\text{m}$  with a small deviation and B: 0.2-0.6  $\mu\text{m}$ .

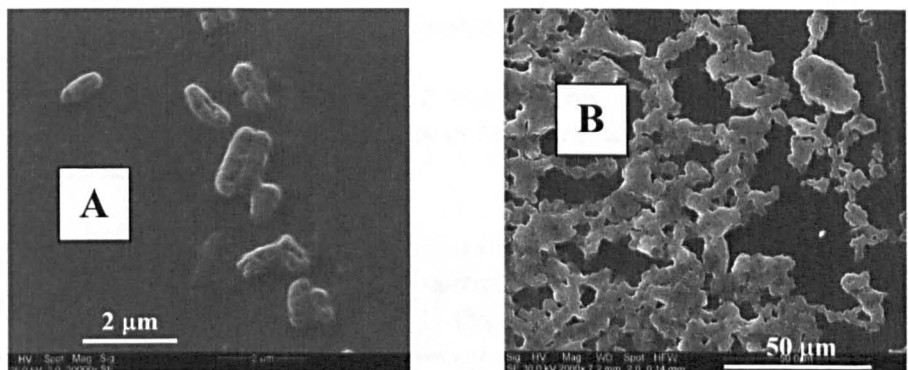


**Figure 7-12.** SEM image of the individual catalase CLEA. The CLEA was prepared using dimethoxyethane as precipitant and glutaraldehyde as cross-linker (A: 10 mM, B: 50 mM) without reduction. The CLEA were prepared using catalase from bovine liver (2140 U/mg protein, 250 mg, 335000 U). The size of the particles is A: 1-1.5  $\mu\text{m}$ , B: cannot be determined.

The SEM images of the individual catalase CLEA (Figures 7-11 and 7-12) showed well defined particles with particle size below 1.5  $\mu\text{m}$ . The only exception was catalase CLEA prepared using dimethoxyethane as precipitant and glutaraldehyde (50 mM) as cross-linker (Figure 7-12 B), which showed paste-like structure. The precipitating agent and the cross-linker both were shown influence the size of the CLEA. The particles were smaller using ammonium sulfate as precipitant than

those using dimethoxyethane as precipitant, with glutaraldehyde as cross-linker. The particles were larger using glutaraldehyde in a higher concentration.

Combi-CLEA of cholesterol oxidase and catalase were examined using ammonium sulfate as precipitant, and glutaraldehyde and dextran polyaldehyde as cross-linker. The results are shown in Table 7-3.

**Table 7-3. The activity of the combi-CLEA of cholesterol oxidase and catalase. The precipitation (co-precipitation) was performed with saturated ammonium sulfate solution and glutaraldehyde (GA) (10 mM and 50 mM) and dextran polyaldehyde (DPA) (200 µL DPA solution/mL enzyme solution and 400 µL DPA solution/mL enzyme solution) were used as cross-linkers. Cholesterol oxidase from *Nocardia sp.* (20.1 U/mg protein, 5.92 mg, 100 U) and catalase from bovine liver (4540 U/mg protein, 250 mg, 737500 U) were used. Cholesterol oxidase activity, conversion of cholesterol (%) is relative activity compared to native. Catalase activity, conversion of H<sub>2</sub>O<sub>2</sub> (%) is relative activity compared to native (catalase assay 2). GA = glutaraldehyde, DPA = dextran polyaldehyde.**

\* The activity assay was performed 2 weeks after the CLEA were prepared due to technical problems. The values in brackets are the activity data of the fresh combi-CLEA.

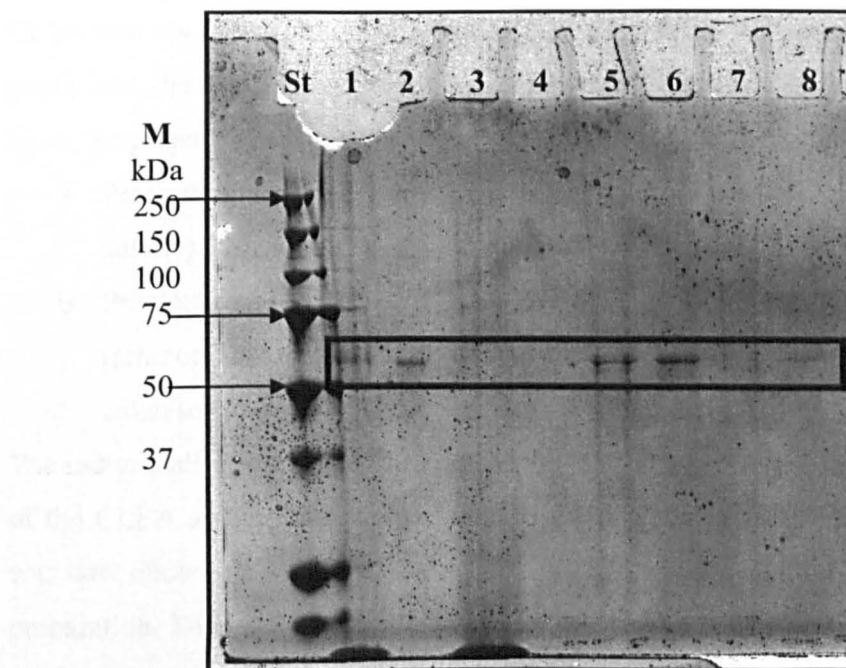
Combi-CLEA no reduction	Cholesterol oxidase activity (%)	Catalase activity (%)	Remaining H <sub>2</sub> O <sub>2</sub> (% - fraction of the amount of H <sub>2</sub> O <sub>2</sub> produced by the native oxidase)
GA 10	47* (66)	12	10
GA 50	17* (16)	17	0
DPA 200	69* (83)	53	6
DPA 400	60* (47)	40	10

Combi-CLEA with reduction	Cholesterol oxidase activity (%)	Catalase activity (%)	Remaining H <sub>2</sub> O <sub>2</sub> (% - fraction of the amount of H <sub>2</sub> O <sub>2</sub> produced by the native oxidase)
GA 10	53* (49)	6	33
GA 50	11* (8)	13	4
DPA 200	48* (54)	46	0
DPA 400	43* (50)	36	0

Cholesterol oxidase exhibited lower activity in combi-CLEA than in individual cholesterol oxidase CLEA. The reason for the lower activity could be due to mass transport limitations as a large amount of catalase surrounded cholesterol oxidase in combi-CLEA (cholesterol oxidase : catalase = 100 U (5.92 mg) : 737500 U (250 mg)). The activity of catalase in combi-CLEA was comparable with the activity in the individual catalase CLEA. The activity of both enzymes was lower using glutaraldehyde as cross-linker when compared with using dextran polyaldehyde as cross-linker at all conditions. This suggests that the cross-linker highly influences the enzyme activity in the combi-CLEA.

Free/released protein fractions of proteins can be determined by SDS-PAGE analysis. SDS-PAGE was performed previously for determining the efficiency of the CLEAtion in the individual catalase CLEA (Figure 7-10). In the combi-CLEA, the effect of cross-linking and the reduction step were examined. The results are shown in Figure 7-13.



**Figure 7-13. SDS-PAGE analysis of the protein fractions of catalase.** Samples are as follows 1: GA10 - amms, 2: GA10 R - amms, 3: GA50 - amms, 4: GA50 R - amms, 5: DPA 200 - amms, 6: DPA 200 R - amms, 7: DPA 400 - amms, 8: DPA 400 R - amms, St: standard. Amms = ammonium sulfate, GA = glutaraldehyde, DPA = dextran polyaldehyde, R = reduced.

The SDS-PAGE analysis showed that the efficiency of the cross-linking was higher using the cross-linker in a higher concentration. Weak bands (when present) were found in these samples (3, 4 and 7, 8 in Figure 7-13). The cross-linker used in a higher concentration might affect the structure of the immobilised biocatalyst by causing mass transport limitations and therefore lower activity (Table 7-3), which was observed in most cases. The bands were more intense when the reduction step was also included (2, 4, 6, 8 in Figure 7-13). Including an additional step in the procedure for preparation of the CLEA can increase the loss of protein.

Further studies were performed on the effect of the precipitation on the activity of combi-CLEA. It is possible to prepare individual CLEA and cross-link them to produce a combi-CLEA, however, an additional cross-linking step should be included in the procedure that is labour intensive and increases the possibility of enzyme loss. Also, this combi-CLEA may consist of large branches of individual CLEA and not of a homogeneous mixture of the enzymes. Another approach is to precipitate the enzymes separately and mix the aggregates before cross-linking. Here, the preparation of combi-CLEA was examined using the following methods.

- A. Precipitating the enzymes separately with the same precipitant (ammonium sulfate).
- B. Precipitating the enzymes separately with different precipitants (ammonium sulfate for cholesterol oxidase and dimethoxyethane for catalase).

The individually precipitated enzymes were mixed before cross-linking. The result of the CLEA activity can be seen in Table 7-4. (The major interest of this study was how cholesterol oxidase activity was affected by the conditions of the CLEA preparation. Therefore the catalase activity is not presented and discussed here.)

**Table 7-4. The activity of the combi-CLEA of cholesterol oxidase and catalase prepared with co- and separate precipitation of the enzymes. Glutaraldehyde (GA) (10 mM and 50 mM) was used as cross-linker. Cholesterol oxidase activity, conversion of cholesterol (%) is a relative activity compared to native. GA = glutaraldehyde.**

Combi-CLEA no reduction	Cholesterol oxidase activity (%)	Remaining H <sub>2</sub> O <sub>2</sub> (% - fraction of the amount of H <sub>2</sub> O <sub>2</sub> produced by the native oxidase )
A) GA 10 *	99	26
A) GA 50 *	90	45
A) GA 10 **	99	59
A) GA 50 **	75	34
B) GA 10 *	99	19
B) GA 50 *	59	1
B) GA 10 **	99	14
B) GA 50 **	66	56

A) Cholesterol oxidase from *Nocardia sp.* (19.5 U/mg protein, 6.62 mg, 100 U) and catalase from bovine liver (2140 U/mg protein, 62.5 mg, 83750 U) were used. The precipitation was performed with saturated aqueous ammonium sulfate solution.

B) Cholesterol oxidase from *Nocardia sp.* (19.5 U/mg protein, 6.62 mg, 100 U) and catalase from bovine liver (2140 U/mg protein, 250 mg, 335000 U) were used. The precipitation was performed using saturated aqueous ammonium sulfate solution for cholesterol oxidase and dimethoxyethane for catalase. Dimethoxyethane was removed from the catalase particles. The cholesterol oxidase particles were transferred to the pot containing the catalase aggregates. The cross-linking was performed in ammonium sulfate in appropriate concentration.

\* Co-precipitation

\*\* Separate precipitation. The aggregates were mixed before cross-linking.

The results in Table 7-4 show that the precipitation method did not have a significant effect on the cholesterol oxidase activity in the combi-CLEA. It suggests that the aggregates of different enzymes can be well mixed even when precipitated separately. It can give a great advantage in the making of a combi-CLEA where its enzyme are required to be precipitated in different solvent in order to retain high activity.

The particle size and morphology of the combi-CLEA was determined by SEM. Images of several combi-CLEA are shown in Figures 7-14 – 7-16. The conditions of the preparation are described in the caption below the images.

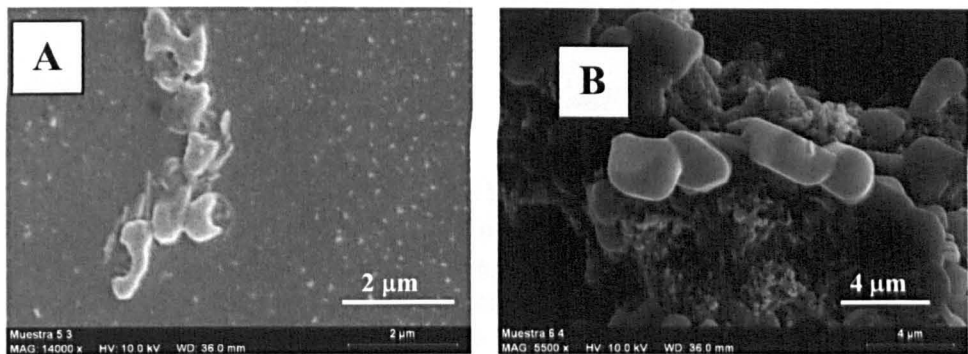


**Figure 7-14.** SEM image of the combi-CLEA. The CLEA was prepared using ammonium sulfate as precipitant and glutaraldehyde as cross-linker (A: 10 mM, B: 50 mM) without a reduction step. Cholesterol oxidase from *Nocardia* sp. (20.1 U/mg protein, 5.92 mg, 100 U) and catalase from bovine liver (4540 U/mg protein, 250 mg, 737500 U) were used.

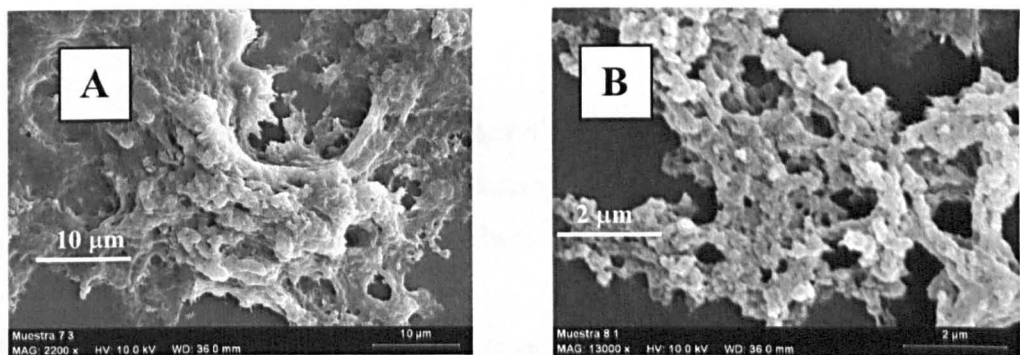


**Figure 7-15.** SEM image of the combi-CLEA. The CLEA was prepared using ammonium sulfate as precipitant and glutaraldehyde as cross-linker (A: 10 mM, B: 50 mM) including a reduction step. Cholesterol oxidase from *Nocardia* sp. (20.1 U/mg protein, 5.92 mg, 100 U) and catalase from bovine liver (4540 U/mg protein, 250 mg, 737500 U) were used.

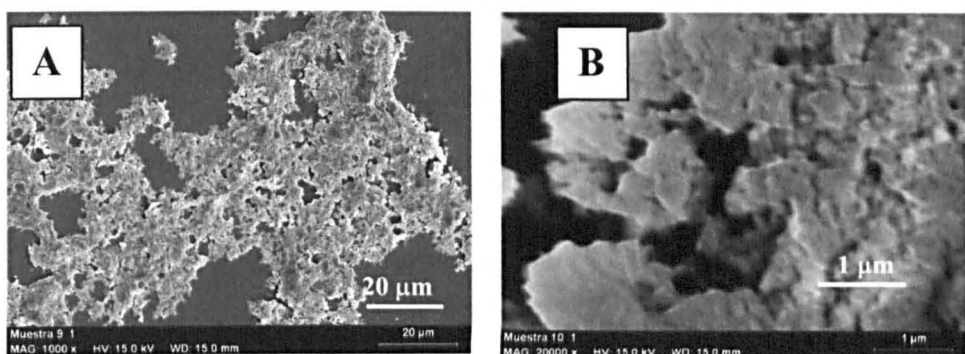


**Figure 7-16.** SEM image of the combi-CLEA. The CLEA was prepared using ammonium sulfate as precipitant and dextran polyaldehyde as cross-linker (A: 200  $\mu$ L DPA solution/mL enzyme solution, B: 400  $\mu$ L DPA solution/mL enzyme solution) without a reduction step. Cholesterol oxidase from *Nocardia* sp. (19.5 U/mg protein, 6.62 mg, 100 U) and catalase from bovine liver (4540 U/mg protein, 250 mg, 737500 U) were used.

The SEM images showed very similar structures for all combi-CLEA regardless the conditions of preparation. Paste-like structure was observed in all cases which suggest that the combi-CLEA contain large aggregates. As similar structures were shown for all combi-CLEA, unfortunately, no major conclusion can be drawn from the SEM images.

The CLEA was examined for the oxidation of cholesterol in a continuous flow scCO<sub>2</sub> system. A CLEA normally contains a small amount of H<sub>2</sub>O that was expected to be sufficient for the enzyme to function in a water-free environment.

### 7.3.3. Oxidation of Cholesterol in a Continuous Flow scCO<sub>2</sub> system

Enzymatic conversion of steroids may be advantageous in SCFs because steroids are nearly insoluble in H<sub>2</sub>O. For example, cholesterol solubility in H<sub>2</sub>O is 4.7  $\mu$ M<sup>31</sup>, while it is significantly more soluble in CO<sub>2</sub> 184  $\mu$ M (40 °C and 100 bar)<sup>32</sup>. Furthermore, scCO<sub>2</sub> is miscible with O<sub>2</sub> and the single phase can also be an advantage for oxidations in scCO<sub>2</sub>. The oxidation of cholesterol (Scheme 7-1) has been investigated here with A of cholesterol oxidase and combi-CLEA of cholesterol oxidase and catalase in a continuous flow scCO<sub>2</sub>

system. The oxidation of cholesterol with immobilised cholesterol oxidase (cholesterol oxidase immobilised on glass beads) has been reported previously to be successful in scCO<sub>2</sub>.<sup>19-21, 33, 34</sup> Here, the enzyme was immobilised using the CLEA technique which has not yet been investigated. In the continuous oxidation in flow scCO<sub>2</sub> system, cholesterol was extracted ‘in-flow’ which required optimisation prior to the investigation the oxidation.

#### **7.3.3.1. ‘In-flow’ Cholesterol Extraction in a Continuous Flow scCO<sub>2</sub> system**

In a continuous flow high pressure system, cholesterol can be introduced into the system in two ways.

- a) A solution of cholesterol can be pumped into the high pressure system using a liquid pump.
- b) Cholesterol can be extracted ‘in-flow’ by scCO<sub>2</sub> (solid cholesterol is loaded in a vessel that is attached to the flow system).

If cholesterol is pumped into the system as a solution, a cosolvent is required to bring the cholesterol into solution. A large amount of organic solvent may deactivate the enzyme<sup>35</sup> and therefore ‘in-flow’ extraction (b) was used in this work. There are several possibilities for sample collection:

- a) The effluent of the reactor can be bubbled through an organic solvent to dissolve the oxidation product and the unreacted cholesterol.
- b) A filter attached to the outlet of the BPR (elongated with a short tube) allows the collection of the oxidation product and the unreacted cholesterol as solid material.
- c) An organic solvent can be pumped into the system after the reactor to dissolve the oxidation product and the unreacted cholesterol.

The sample collection was performed using method ‘c’ in this work.

Several different reactors were studied in order to achieve reproducible and constant cholesterol concentration in the effluent. The schematic of the reactors is shown in Figures 7-17 – 7-20.

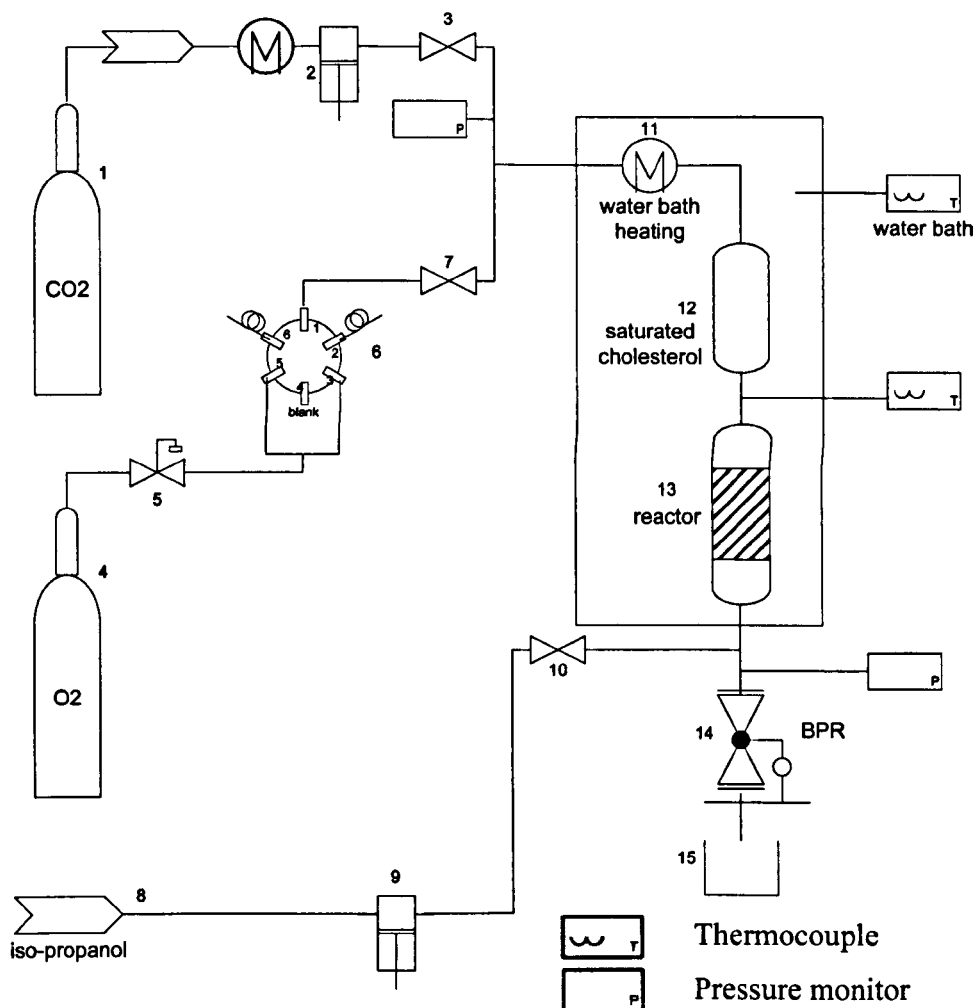


**Figure 7-17. The small scale continuous flow reactor. Setup 1 & Setup 2. Parts are labelled as follows. 1: CO<sub>2</sub> cylinder, 2: CO<sub>2</sub> cooling unit and HPLC pump, 3: Parker ball valve, 4: O<sub>2</sub> cylinder, 5: Manual pressure regulator, 6: Waters switching valve for O<sub>2</sub> dosage (two-position six-port switching valve), 7: Parker ball valve, 8: substrate/solvent reservoir, 9: HPLC pump, 10: Parker ball valve, 11: Water bath heater, 12: Cholesterol vessel, 13: Reactor, 14: GO valve - manual back pressure regulator (BPR), 15: Collection vial. All components were connected by 1/16" 316 stainless steel tubing. The feed streams were mixed in a heated T-piece mixer before being passed through the cholesterol vessel and the reactor. Products were collected by continuous depressurisation of the system using a manual backpressure regulator, and analysed by reverse phase HPLC.**

Setup 1 and Setup 2 are shown in Figure 7-17. The two reactor setups differentiate in the following parameters.

Setup 1.	Setup 2.
Part 12: Cholesterol vessel ( $0.7 \text{ cm}^3$ ) ( $\frac{1}{4}$ " tube, $d_{\text{inner}} = 3 \text{ mm}$ , length 10 cm)	Part 12: Cholesterol vessel ( $14.92 \text{ cm}^3$ ) ( $d_{\text{inner}} = 1 \text{ cm}$ , length 19 cm)
Part 13: Reactor ( $0.7 \text{ cm}^3$ ) ( $\frac{1}{4}$ " tube, $d_{\text{inner}} = 3 \text{ mm}$ , length 10 cm)	Part 13: Reactor ( $0.7 \text{ cm}^3$ ) ( $\frac{1}{4}$ " tube, $d_{\text{inner}} = 3 \text{ mm}$ , length 10 cm)

Cholesterol was loaded into the vessel used in the following ways.

Setup 1.

- A) Cholesterol (as received).
- B) The vessel was loosely filled with glass wool. Cholesterol was dissolved in dichloromethane and pipetted in the vessel and the solvent was evaporated by incubation the vessel at  $50^\circ\text{C}$ . In all other cases, solid cholesterol was loaded in the reactor.
- C) Ground cholesterol.

Setup 2.

- A) Alternate layers of cholesterol and glass wool were loaded in the 'cholesterol vessel'.
- B) Ground cholesterol was loaded in the vessel. The cholesterol extraction was performed in up flow.
- C) Alternate layers of ground cholesterol and glass beads were loaded in the vessel.
- D) Ground cholesterol was mixed with glass beads before loading. A thin layer of cholesterol was obtained on the surface of the glass beads.

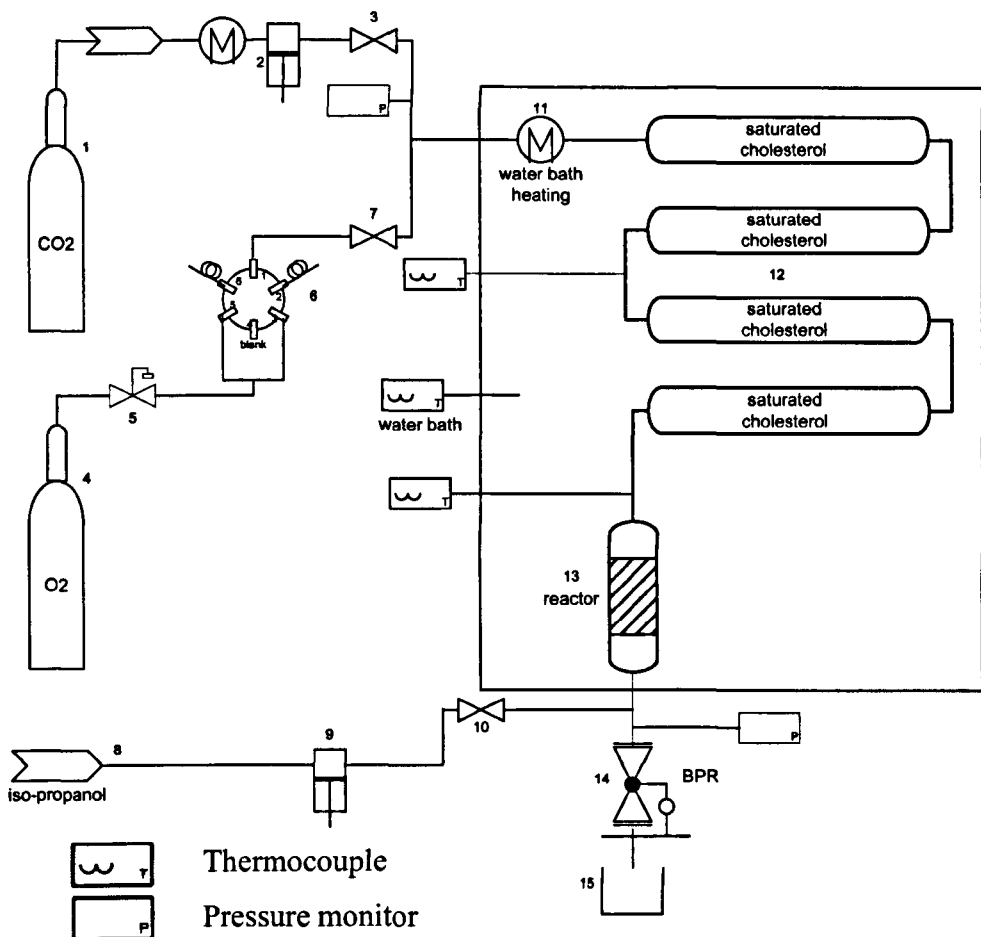


**Figure 7-18. The small scale continuous flow reactor. Setup 3.** Parts are labelled as follows. 1: CO<sub>2</sub> cylinder, 2: CO<sub>2</sub> cooling unit and HPLC pump, 3: Parker ball valve, 4: O<sub>2</sub> cylinder, 5: Manual pressure regulator, 6: Waters switching valve for O<sub>2</sub> dosage (two-position six-port switching valve), 7: Parker ball valve, 8: substrate/solvent reservoir, 9: HPLC pump, 10: Parker ball valve, 11: Water bath heater, 12: Cholesterol vessel ( $d_{inner}=3$  mm, length 100 cm), 13: Reactor ( $\frac{1}{4}$ "  $d_{inner}=3$  mm, length 10 cm), 14: GO valve - manual back pressure regulator (BPR), 15: Collection vial. All components were connected by 1/16" 316 stainless steel tubing. The feed streams were mixed in a heated T-piece mixer before being passed through the cholesterol vessel (7.07 cm<sup>3</sup> volume) and the reactor (0.7 cm<sup>3</sup> volume). Products were collected by continuous depressurisation of the system using a manual backpressure regulator, and analysed by reverse phase HPLC.

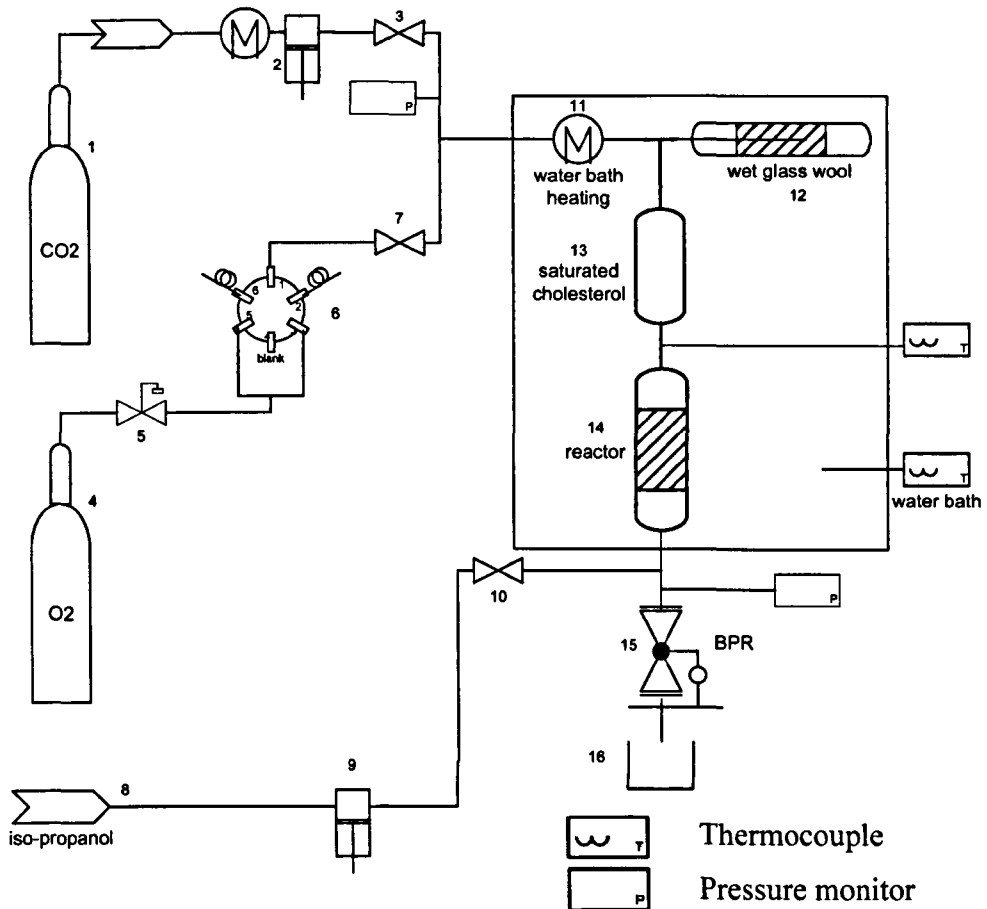


**Figure 7-19.** The small scale continuous flow reactor. Setup 4. Parts are labelled as follows. 1: CO<sub>2</sub> cylinder, 2: CO<sub>2</sub> cooling unit and HPLC pump, 3: Parker ball valve, 4: O<sub>2</sub> cylinder, 5: Manual pressure regulator, 6: Waters switching valve for O<sub>2</sub> dosage (two-position six-port switching valve), 7: Parker ball valve, 8: substrate/solvent reservoir, 9: HPLC pump, 10: Parker ball valve, 11: Water bath heater, 12: Vessel for CO<sub>2</sub> saturation with H<sub>2</sub>O 13: Cholesterol vessel ( $d_{inner}=1$  cm, length 19 cm), 14: Reactor ( $\frac{1}{4}$ "  $d_{inner}=3$  mm, length 10 cm), 15: GO valve - manual back pressure regulator (BPR), 16: Collection vial. Ground cholesterol was used. Alternate layers of cholesterol and glass beads were loaded. All components were connected by 1/16" 316 stainless steel tubing. The feed streams were mixed in a heated T-piece mixer before being passed through the cholesterol vessel (14.92 cm<sup>3</sup> volume) and the reactor (0.7 cm<sup>3</sup> volume). The cholesterol extraction was performed in an up flow configuration. Products were collected by continuous depressurisation of the system using a manual backpressure regulator, and analysed by reverse phase HPLC.

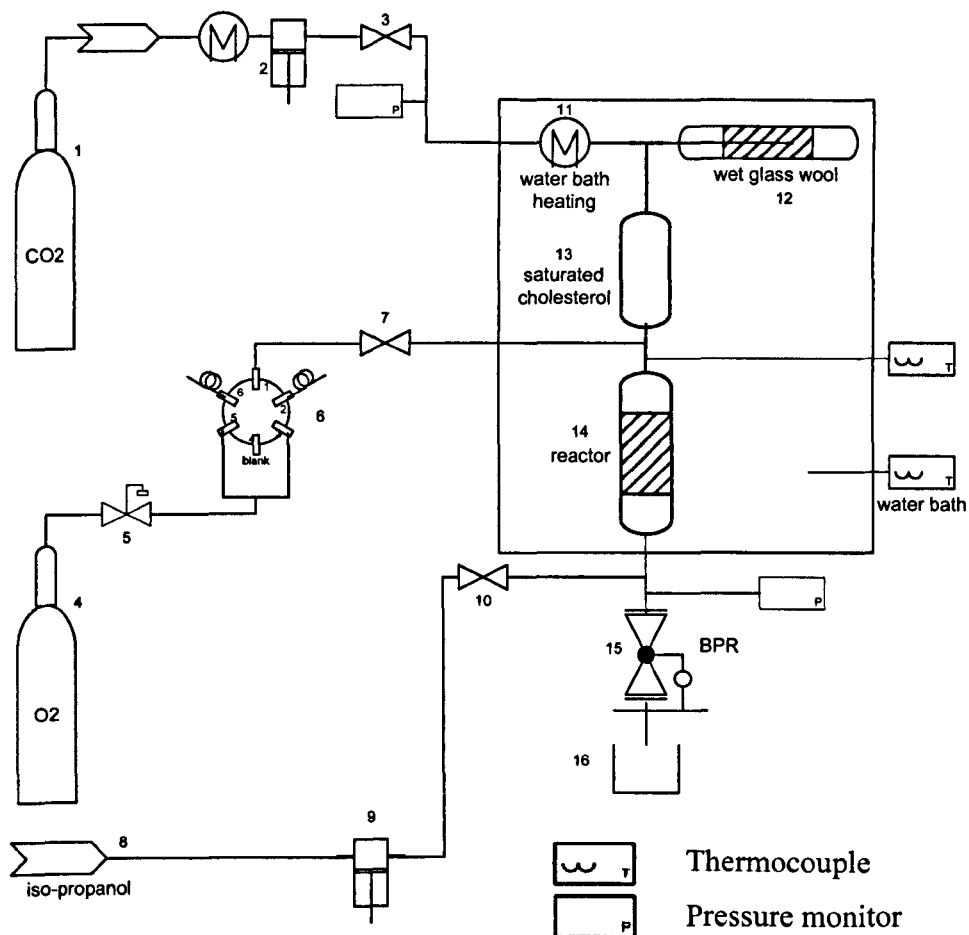


**Figure 7-20. The small scale continuous flow reactor. Setup 5 & Setup 6.** Parts are labelled as follows. 1: CO<sub>2</sub> cylinder, 2: CO<sub>2</sub> cooling unit and HPLC pump, 3: Parker ball valve, 4: O<sub>2</sub> cylinder, 5: Manual pressure regulator, 6: Waters switching valve for O<sub>2</sub> dosage (two-position six-port switching valve), 7: Parker ball valve, 8: substrate/solvent reservoir, 9: HPLC pump, 10: Parker ball valve, 11: Water bath heater, 12: Vessel for CO<sub>2</sub> saturation with H<sub>2</sub>O 13: Cholesterol vessel, 14: Reactor, 15: GO valve - manual back pressure regulator (BPR), 16: Collection vial. Ground cholesterol was used. Alternate layers of cholesterol and glass beads were loaded. All components were connected by 1/16" 316 stainless steel tubing. The feed streams were mixed in a heated T-piece mixer before being passed through the cholesterol vessel and the reactor. The cholesterol extraction was performed in an up flow configuration. Products were collected by continuous depressurisation of the system using a manual backpressure regulator, and analysed by reverse phase HPLC.

Setup 5 and Setup 6 are shown in Figure 7-20. The two reactor setups differentiate in the following parameters.

**Setup 5.**

Part 13: Cholesterol vessel ( $14.92 \text{ cm}^3$ )  
( $d_{\text{inner}} = 1 \text{ cm}$ , length 19 cm)  
Part 14: Reactor ( $0.7 \text{ cm}^3$ ) ( $\frac{1}{4}'' d_{\text{inner}} = 3 \text{ mm}$ , length 10 cm)

**Setup 6.**

Part 13: Cholesterol vessel ( $0.7 \text{ cm}^3$ )  
( $\frac{1}{4}'' \text{ tube}$ ,  $d_{\text{inner}} = 3 \text{ mm}$ , length 10 cm)  
Part 14: Reactor ( $0.7 \text{ cm}^3$ ) ( $\frac{1}{4}'' \text{ tube}$ ,  $d_{\text{inner}} = 3 \text{ mm}$ , length 10 cm)

The results of the 'in-flow' cholesterol extraction are shown in Table 7-5.

**Table 7-5. 'In-flow' extraction of cholesterol in continuous flow scCO<sub>2</sub> system. The reactor setups can be seen in Figures 7-17 – 7-20. The error in the table is the error in cholesterol area of the experiments repeated at particular conditions (HPLC analysis).**

Entry	Reactor setup	T (°C)	CO <sub>2</sub> flow (mL/min)	P (bar)	O <sub>2</sub>	Cholesterol concentration (mM)
1	setup 1A	40	2	100	yes	0.08-0.42
2	setup 1B	40	2	100	yes	0.24-0.28
3	setup 1B	50	2	100	yes	0.05
4	setup 1C	40	2	100	no	0.68-0.71
5	setup 1C	40	2	100	yes	0.37-0.5
6	setup 2A	40	2	100	yes	0.21-0.69
7	setup 2A	40	2	160	yes	2.31-3.43
8	setup 2B	40	2	100	yes	0.01-0.02
9	Setup 2C	40	2	100	yes	0.56-1.57
10	setup 2C *	40	2	100	yes	0.16-0.71
11	setup 2D	40	2	100	yes	0.75-1.46
12	setup 2D *	40	2	100	yes	0.29-0.79
13	setup 3	40	2	100	yes	0.19-0.57
14	setup 4 **	40	2	100	yes	0.16-0.32
15	setup 4 **	40	2	160	yes	2.1-2.37
16	setup 5**	40	2	130	no	2.3-3.48
17	setup 5 **	40	2	160	no	3.39-3.49
18	setup 6 **	40	1	100	yes	0.07-0.17
19	setup 6 **	40	1	160	yes	0.81-1.14
20	setup 6 **	40	1	100	no	0.51-1.82
21	setup 6 **	40	1	160	no	1.79-2.03

\* Reaction time 120 minutes.

\*\* Water-saturated CO<sub>2</sub> was used.

Setup 1 and Setup 2: Figure 2-17, Setup 3: Figure 2-18, Setup 4: Figure 2-19, Setup 5 and Setup 6: Figure 2-20.

As shown in Table 7-5, the concentration of cholesterol in the effluent fluctuated significantly using all reactors. The consistency of the cholesterol concentration was higher at a higher pressure (160 bar) (Entries 15, 16, 17, 19, 21 except Entry 7) than at a lower pressure (100 bar). The changes in mass transfer and also in the properties of CO<sub>2</sub> at the different conditions might influence the extraction. The effect of temperature has not yet been investigated extensively (Entries 2, 3). It can be seen from the results shown in the Table 7-5 (Entries 4-5, 18-20, 19-21) that the presence of O<sub>2</sub> had no significant effect on the cholesterol extraction (except Entries 4, 5). O<sub>2</sub> should not be the major influencing factor on the cholesterol extraction as the cholesterol concentration was still highly inconsistent even when O<sub>2</sub> was not present.

The particle size of the material to be extracted can influence the performance of the extraction. Cholesterol received as pellets was milled in order to obtain small particles (Entries 2-3, 4-5, 8-12, 14-15 and 18-21) or was dissolved in dichloromethane (and the solvent was evaporated) before loading which produced smaller particles (visual observation). Unfortunately, the use of ground cholesterol was unsuccessful as inconsistency in the cholesterol concentration was still observed. Cholesterol dissolved in dichloromethane (and the solvent evaporated) before loading (Entries 2 and 3) resulted in a highly consistent cholesterol concentration in the effluent of the system but the reproducibility between two runs using the same setup was poor.

Although the ‘in-flow’ cholesterol extraction could not be optimised in the continuous flow scCO<sub>2</sub> system, the oxidation of cholesterol was investigated.

#### **7.3.3.2. Oxidation of Cholesterol in a Continuous Flow scCO<sub>2</sub> system**

The oxidation was examined using a small scale high pressure equipment shown in Figure 7-20 above (Setup 5). A detailed description can be found in Chapter 2. The results of the continuous oxidation of cholesterol with CLEA in scCO<sub>2</sub> are shown in Table 7-6.

**Table 7-6. The results of cholesterol oxidation in a continuous flow scCO<sub>2</sub> system. Cholesterol oxidase from *Nocardia sp.* (20.1 U/mg protein, 5.92 mg, 300 U), cholesterol oxidase from *Nocardia sp.* CLEA (20.1 U/mg protein, 5.92 mg, 300 U) and combi-cholesterol oxidase-catalase-CLEA (cholesterol oxidase: 20.1 U/mg protein, 5.92 mg, 200 U and catalase from bovine liver 4540 U/mg protein, 500 mg, 1475000 U) were used as catalysts. The CLEA were prepared with ammonium sulfate as precipitant and dextran polyaldehyde (200 µL DPA solution/mL enzyme solution) cross-linker. The reactor setup is shown in Figure 7-22. n/a = not available.**

Cholesterol oxidase – yield of 4-cholest-en-3-one (%)				
CO <sub>2</sub> flow (ml/min)	40 °C 130 bar	40 °C 160 bar	50 °C 130 bar	50 °C 160 bar
2 ml/min	< 0.02	< 0.5	0	0
4 ml/min	0	< 0.2	0	0
6 ml/min	< 0.2	< 0.5	0	0
8 ml/min	0	< 0.2	0	0

Cholesterol oxidase CLEA - yield of 4-cholest-en-3-one (%)				
CO <sub>2</sub> flow (ml/min)	40 °C 130 bar	40 °C 160 bar	50 °C 130 bar	50 °C 160 bar
2 ml/min	< 0.2	< 1.2	0	< 0.1
4 ml/min	0	0	< 0.1	< 0.2
6 ml/min	< 0.1	< 0.1	< 0.1	< 0.1
8 ml/min	0	0	< 0.1	< 0.1

Combi-CLEA - yield of 4-cholest-en-3-one (%)				
CO <sub>2</sub> flow (ml/min)	40 °C 130 bar	40 °C 160 bar	50 °C 130 bar	50 °C 160 bar
2 ml/min	0	0	n/a	0.00
4 ml/min	0	0	n/a	0.00
6 ml/min	0	0	n/a	< 0.1
8 ml/min	< 0.6	0	n/a	< 0.1

Reaction conditions: pressure: 100 bar, O<sub>2</sub> : substrate ratio = 10 : 1 (calculated).

Unfortunately, the oxidation of cholesterol in a continuous flow scCO<sub>2</sub> system was unsuccessful using all enzymes. The yield of 4-cholest-en-3-one was very low and therefore the effect of pressure, temperature and flow rate on the reaction could

not be determined. It has been reported previously that an increase in flow rate can positively influence the enzyme activity<sup>20</sup> but this could not be demonstrated here. The activity of cholesterol oxidase may decrease significantly in a water-free environment or in an environment containing a small amount of water.<sup>14, 20</sup> Water-saturated CO<sub>2</sub> was used here which contained probably an insufficient amount of water for the enzyme to function. On the other hand, the reaction rate might be very slow and therefore no conversion could be obtained if a short residence time was provided. The residence time in the reactor has been calculated to be 0.354 min at 2 mL/min CO<sub>2</sub> flow rate if the whole volume of the reactor is filled with catalyst. Higher conversion may be obtained if a longer reaction time is provided, however, low yield of 4-cholesten-3-one was observed at slower CO<sub>2</sub> flow rates 0.5 mL/min and 1 mL/min (the results are not presented here).

The aggregation of cholesterol under supercritical conditions<sup>33</sup> might have suppressed the activity of cholesterol oxidase from *Nocardia sp.* Cholesterol oxidase from *G. chrysocreas* was examined under supercritical conditions and was shown to produce benefit from the presence of cholesterol aggregation at a higher level.<sup>19</sup> The aggregation of cholesterol may be a disadvantage for cholesterol oxidase from *Nocardia sp.* because it can have a different cholesterol uptake mechanism than that of cholesterol oxidase from *G. chrysocreas*.

Cholesterol oxidase from *G. chrysocreas* was examined under supercritical conditions and no conformational changes were observed in the protein structure.<sup>33</sup> These results suggest that conformational changes of the CLEA of cholesterol oxidase *Nocardia sp.* should not occur under supercritical conditions.

#### 7.3.3.3. Oxidation of Cholesterol in a Batch scCO<sub>2</sub> system

The oxidation of cholesterol was examined in a batch scCO<sub>2</sub> system to determine the cause of low activity in the continuous flow scCO<sub>2</sub> system. The experimental setup and the reactor are described in Chapter 2. The results of the batch oxidation are shown in Table 7-7.

**Table 7-7. The result of cholesterol oxidation in batch scCO<sub>2</sub>. The CLEA was prepared with ammonium sulfate as precipitant and glutaraldehyde (10 mM) as cross-linker. Combi-cholesterol oxidase-catalase-CLEA was used as catalysts (cholesterol oxidase from *Nocardia sp.*: 17.3 U/mg protein, 6.85 mg, 100 U and catalase from bovine liver 4540 U/mg protein, 250 mg, 737500 U). A small scale clamp autoclave was used to perform the reactions. A detailed description of the autoclave can be found in Chapter 2. The experimental setup of the batch oxidation reaction is discussed in detail in Chapter 2. Reactor volume was 8 mL.**

Entry	Reaction time (hour)	Wet or dry?	T (°C)	Pressure (bar)	Yield of cholest-4-en-3-one (%)
1	5	wet	40	4 *	100
2	5	wet	40	100	8
3	5	dry	40	100	0
4	5	dry	40	100	0
5	20	dry	40	100	0

**Reaction conditions:**

**Entry 1:** O<sub>2</sub> : 4 bar, phosphate buffer (20 mM, pH 7.0): 3.8 mL, alcoholic solution of cholesterol (IPA, 12 mM): 1 mL, enzyme suspension (combi-CLEA): 0.2 mL, 0.67 U.

\* Pressure of O<sub>2</sub>.

**Entry 2:** O<sub>2</sub> : 4 bar, CO<sub>2</sub>: 100 bar, phosphate buffer (20 mM, pH 7.0): 3.8 mL, alcoholic solution of cholesterol (IPA, 12 mM): 1 mL, enzyme suspension (combi-CLEA): 0.2 mL, 0.67 U.

**Entry 3:** O<sub>2</sub> : 4 bar, CO<sub>2</sub>: 100 bar, alcoholic solution of cholesterol (IPA, 12 mM): 1 mL, enzyme (combi-CLEA) - dry powder: 0.67 U.

**Entry 4 & 5:** O<sub>2</sub> : 4 bar, CO<sub>2</sub>: 100 bar, cholesterol: 4.6 mg, enzyme (combi-CLEA) - dry powder: 0.67 U.

As mentioned previously, the continuous flow oxidation was possibly unsuccessful due to i) the lack of H<sub>2</sub>O, or ii) aggregation of cholesterol under supercritical conditions. The oxidation of cholesterol was investigated in batch with a large amount of H<sub>2</sub>O present without CO<sub>2</sub> (Entry 1) and with CO<sub>2</sub> (Entry 2). The enzyme produced 8 % yield of 4-cholest-4-en-3-one in a 5-hour reaction (Entry 2), which was significantly lower than that observed in the oxidation performed without CO<sub>2</sub> (Entry 1). Cholesterol oxidase from *G. chrysocreas* (Type I cholesterol oxidase) was reported to benefit from cholesterol aggregation.<sup>19, 20, 33</sup> In this work, cholesterol oxidase from *Nocardia sp.* (Type II cholesterol oxidase) was used which may work

differently: cholesterol aggregation at a higher level under supercritical conditions may suppress the catalytic activity of cholesterol oxidase from *Nocardia sp.*

No activity was observed in the oxidation of cholesterol without H<sub>2</sub>O in the batch scCO<sub>2</sub> system (Table 7-7, Entries 3-5). A CLEA normally contains a small amount of H<sub>2</sub>O which should be sufficient for the enzyme to function, but unfortunately no activity was observed here without H<sub>2</sub>O (Table 7-7, Entries 3-5). The activity of cholesterol oxidase was compared using wet cells and freeze-dried cells by Buckland: the activity of cholesterol oxidase dropped significantly using freeze-dried enzyme.<sup>14</sup> The addition of H<sub>2</sub>O to the reaction medium improved the catalyst performance of the freeze-dried enzymes but only 20 % of the activity displayed by wet cells could be achieved.<sup>14</sup> The CLEA used here were dried by freeze-drying. The freeze-drying procedure might remove all H<sub>2</sub>O from the CLEA and could also change the structure of the enzyme and the activity of the enzyme could therefore significantly decrease. The activity of cholesterol oxidase in the dry CLEA was examined in aqueous medium (CLEA dispersed in phosphate buffer) and the enzyme showed activity for the oxidation of cholesterol, but unfortunately no recovery data is available.

The oxidation was also examined in an IPA/scCO<sub>2</sub> system with dry CLEA (without H<sub>2</sub>O) (Entry 3). The lack of water was shown to significantly decrease the activity of the enzyme. Furthermore, the presence of IPA in a large quantity may deactivate the enzyme<sup>14,35</sup> and therefore the enzyme activity decreases.

#### 7.4. Conclusions

CLEA of cholesterol oxidase and combi-CLEA of cholesterol oxidase and catalase were successfully prepared with high retained activity. The effect of different precipitants, different cross-linkers, and the cross-linker concentration were examined. The precipitating agent was demonstrated to be important in order to obtain CLEA with high activity and stability. Cholesterol oxidase from *Nocardia sp.* was found to be sensitive to the presence of most precipitants, only ammonium sulfate was suitable to precipitate the enzyme without any loss of activity and dimethoxyethane produced 10 % activity loss. Catalase from bovine liver could be

precipitated without any activity loss with ammonium sulfate, dimethoxyethane and acetone.

Glutaraldehyde and dextran polyaldehyde were examined as cross-linkers. The cross-linker had no significant effect on the cholesterol oxidase CLEA. Catalase CLEA was generated with higher activities using dextran polyaldehyde as cross-linking agent. The concentration of the cross-linker had similar effect in most cases: the cross-linker used in a higher concentration resulted in a CLEA with lower activity that may be caused by mass transport limitations of the substrate to the active site of the enzyme due to a more rigid structure of the CLEA.

The activity of cholesterol oxidase was lower in combi-CLEA than that in individual cholesterol oxidase CLEA. In combi-CLEA, the transport of the substrate to the active site of the enzyme might be slower than that in the individual cholesterol oxidase CLEA because of a large amount of catalase present around cholesterol oxidase. The active site of several cholesterol oxidase molecules might also have become blocked in the combi-CLEA.

SEM images were taken to determine the morphology and size of the CLEA. Cholesterol oxidase CLEA prepared using glutaraldehyde and dextran polyaldehyde as cross-linker in a higher concentration gave CLEA with well defined particles of 0.2-1.5 µm size in diameter. The structure of all other CLEA could not be clearly determined: paste-like structure was observed that can refer to the presence of large aggregates.

Unfortunately, the 'in-flow' extraction of cholesterol in scCO<sub>2</sub> could not be optimised. A number of different reactors were designed and examined where the following parameters were varied.

- Length of the extraction vessel.
- Particle size of cholesterol.
- Flow rate of CO<sub>2</sub>.
- Temperature, pressure.

Unfortunately, the extraction could not be optimised because the concentration of cholesterol in the effluent of the reactor was highly inconsistent in all cases.

Although, the 'in-flow' cholesterol extraction could not be optimised, the oxidation of cholesterol was examined in a continuous flow scCO<sub>2</sub> system with cholesterol oxidase (as received), cholesterol oxidase CLEA, and combi-CLEA of and cholesterol oxidase and catalase. Unfortunately, very low yield was obtained in all cases and therefore the effect of pressure, temperature and flow rate on the reaction could not be determined. The low activity in the continuous flow system could be due to the lack of water that is required by the enzyme to function or the presence of CO<sub>2</sub> that can inhibit the enzyme activity.

The yield of the oxidation of cholesterol in a batch scCO<sub>2</sub> system dropped significantly when CO<sub>2</sub> was present even with a large amount of H<sub>2</sub>O. The oxidation produced 0 % yield without H<sub>2</sub>O in scCO<sub>2</sub>. A CLEA normally contains a small amount of H<sub>2</sub>O but it was shown to be insufficient in this case. The drying procedure (freeze-drying) of the CLEA could also influence the activity of cholesterol oxidase that may be sensitive to freeze-drying. The results suggest that cholesterol oxidase form *Nocardia* sp. may require a small amount of water to function and that the drying of enzyme can also be highly influencing.

## References

1. Av-Gay, Y. S., R., Cholesterol is accumulated by mycobacteria but its degradation is limited to non-pathogenic fast-growing mycobacteria. *Canadian Journal of Microbiology* 2000, 46, 826-831.
2. Uwajima, T. Y., H.; Nakamura, S.; Terada, O., Isolation and crystallization of extracellular 3 $\alpha$ -hydroxysteroid oxidase of *Brevibacterium sterolicum nov. sp.* *Agricultural and Biological Chemistry* 1973, 37, 2345-2350.
3. Fernandez-Garayzabal, J. F. D., C.; Dominguez, L., Cholesterol oxidase from *Rhodococcus equi* is likely the major factor involved in the cooperative lytic process (CAMP reaction) with *Listeria monocytogenes*. *Letters in Applied Microbiology* 1996, 22, 249-252.
4. Navas, J. G.-Z., B.; Ladron, N.; Garrido, P.; Vazquez-Boland, J. A., Identification and mutagenesis by allelic exchange of choE, encoding a cholesterol oxidase from the intracellular pathogen *Rhodococcus equi*. *Journal of Bacteriology* 2001, 183, 4796-4805.
5. Sampson, N. S., Vrielink, A., Cholesterol oxidases: A study of nature's approach to protein design. *Accounts of Chemical Research* 2003, 36, 713-722.
6. Aparicio, J. F., Martin, J.F., Microbial cholesterol oxidases: bioconversion enzymes or signal proteins? *Molecular biosystems* 2008, 4, (8), 804-809.

7. Gadda, G., Wels, G., Pollegioni, L., Zucchelli, S., Ambrosius, D., Pilone, M.S., Ghisla, S., Characterization of cholesterol oxidase from *Streptomyces hygroscopicus* and *Brevibacterium sterolicum*. *European Journal of Biochemistry* **1997**, 250, 369-376.
8. Pollegioni, L., Wells, G., Pilone, M.S., Ghisla, S., Kinetic mechanisms of cholesterol oxidase from *Streptomyces hygroscopicus* and *Brevibacterium sterolicum* *European Journal of Biochemistry* **1999**, 264, 140-151.
9. Yue, Q. K., Kass, I.J., Sampson, N.S., Vrielink, A., Crystal Structure Determination of Cholesterol Oxidase from *Streptomyces* and Structural Characterization of Key Active Site Mutants. *Biochemistry* **1999**, 38, 4277-4286.
10. Li, J., Vrielink, A., Brick, P., Blow, D.M., Crystal Structure of Cholesterol Oxidase Complexed with a Steroid Substrate: Implications for Flavin Adenine Dinucleotide Dependent Alcohol Oxidases. *Biochemistry* **1993**, 32, 11507-11515.
11. Vrielink, A., Lloyd, L.F., Blow, D.M., Crystal structure of cholesterol oxidase from *Brevibacterium sterolicum* refined at 1.8 Å resolution. *Journal of Molecular Biology* **1991**, 219, 533-554.
12. Coulombe, R., Yue, K.Q., Ghisla, S., Vrielink, A., Oxygen access to the active site of cholesterol oxidase through a narrow channel is gated by an Arg-Glu pair. *Journal of Biological Chemistry* **2001**, 276, 30435-30441.
13. Richmond, V., Preparation and Properties of Cholesterol Oxidase from *Nocardia* sp. and Its Application to the Enzyme Assay of Total Serum Cholesterol. *Clinical Chemistry* **1973**, 19, (12), 1350-1356.
14. Buckland, B. C., Dunnill, P., Lilly, M.D., The enzymatic transformation of water-insoluble reactants in nonaqueous solvents, Conversion of cholesterol to cholest-4-en-3-one by a *Nocardia* sp. *Biotechnology and Bioengineering* **1975**, 17, 815-826.
15. Corbin, D. R. G., J. T.; Purcell, J. P., The identification and development of proteins for control of insects in genetically modified crops. *Hortscience* **1998**, 33, 614-617.
16. Lange, Y. J., Tracking cell cholesterol with cholesterol oxidase. *Lipid Research* **1992**, 33, 315-321.
17. London, E., Insights into lipid raft structure and formation from experiments in model membranes. *Current Opinion in Structural Biology* **2002**, 12, 480-486.
18. Ahn, K. W., Sampson, N.S., Cholesterol oxidase senses subtle changes in lipid bilayer structure. *Biochemistry* **2004**, 43, 827-836.
19. Randolph, T. W., Enzymatic oxidation of cholesterol aggregates in supercritical carbon dioxide. *Science* **1988**, 238, 387-390.
20. Randolph, T. W., Enzyme-catalyzed oxidation of cholesterol in supercritical carbon dioxide. *AICHE Journal* **1988**, 34, 1354-1360.
21. Bauza, R., Ríos, A., Valcárcel, M., Coupling immobilized enzymes flow reactors with supercritical fluid extraction for analytical purposes. *Analyst* **2002**, 127, 241-247.

22. Sheldon, R. A., van Rantwijk, F., Biocatalysis for sustainable organic synthesis. *Australian Journal of Chemistry* **2004**, 57, 281-289.
23. Anthonsen, F., Ed Straathof, A.J.J., in Applied Biocatalysis. *Harwood Academic Publishers* **2000**.
24. Demirjam, D. C., Shah, P.C., Moris-Varas, F., Ed Fessner, W.D., in Biocatalysis - From Discovery to Application. *Springer, Berlin* **1999**.
25. Sheldon, R. A., Arends, I., Hanefeld, U., in Green Chemistry and Catalysis. *Wiley-VCH, Weinheim* **2007**.
26. Mateo, C., Chmura, A., Rustler, S., van Rantwijk, F., Stoltz, A., Sheldon, R.A., Synthesis of enantiomerically pure (S)-mandelic acid using an oxynitrilase–nitrilase bienzymatic cascade: a nitrilase surprisingly shows nitrile hydratase activity. *Tetrahedron: Asymmetry* **2006**, 17, 320-323.
27. Ismail, H., Lau, R.M., van Langen, L.M., van Rantwijk, F., Svedasb, V.K., Sheldon, R.A., A green, fully enzymatic procedure for amine resolution, using a lipase and a penicillin G acylase. *Green Chemistry* **2008**, 10, 415-418.
28. Ismail, H., Lau, R.M., van Rantwijk, F., Sheldon, R.A., Fully enzymatic resolution of chiral amines: Acylation and deacylation in the presence of *Candida antarctica* lipase B *Advanced Synthesis & Catalysis* **2008**, 350, 1511-1516.
29. Fita, I., Rossmann, M.G., The NADPH binding site on beef liver catalase. *Proceedings of the National Academy of Sciences USA* **1985**, 82, 1604-1608.
30. Wilson, L., Betancor, L., Fernandez-Lorente, G., Fuentes, M., Hidalgo, A., Guisan, J.M., Pessela, B.C.C., Fernandez-Lafuente, R., Cross-linked aggregates of multimeric enzymes: A simple and efficient methodology to stabilize their quaternary structure. *Biomacromolecules* **2004**, 5, 814-817.
31. Haberland, M. E., Reynolds, J.A., Self-association of cholesterol in aqueous solution. *Proceedings of the National Academy of Sciences USA* **1973**, 70, 2313-2316.
32. Yun, S. L. J., Lioung, K.K., Gurdial, G.S., Foester, N.R., Solubility of Cholesterol in Supercritical Carbon Dioxide. *Industrial & Chemical Engineering Research* **1991**, 30, 2476-2482.
33. Randolph, T. W., Clark, D.S., Blanch, H.W., Prausnitz, J.M., Cholesterol aggregation and interaction with cholesterol oxidase in supercritical carbon dioxide. *Proceedings of the National Academy of Sciences USA* **1988**, 85, 2979-2983.
34. Kane, M. A., Baker, G.A., Pandey, S., Bright, F.V., Performance of cholesterol oxidase sequestered within reverse micelles formed in supercritical carbon dioxide. *Langmuir* **2000**, 16, 4901-4905.
35. Cheetham, P. S. J., Dunnill, P., Lilly, M.D., The characterisation and interconversion of three forms of cholesterol oxidase extracted from *Nocardia rhodochorus*. *Biochemistry Journal* **1982**, 201, 515-521.

# Chapter 8

## Thesis Conclusions and Future Directions

This Chapter describes the findings of this Thesis. The results of Chapter 3, 4, 5, 6, and 7 are summarised here and future directions are also suggested.

### 8.1. Continuous Asymmetric Hydrogenation with Supported Homogeneous Chiral Rh Catalysts on Alumina in scCO<sub>2</sub>

Continuous catalytic asymmetric hydrogenation in supercritical fluids has been investigated previously where the chiral modifier was continuously fed.<sup>1,2</sup> The work in this Thesis demonstrates one of the first examples of continuous enantioselective hydrogenation in scCO<sub>2</sub> with a supported homogeneous chiral catalyst without the need for the addition of the chiral modifier.

The chiral catalyst [Rh(COD)(ligand)]<sup>+</sup>[BF<sub>4</sub>]<sup>-</sup>/PTA/Alumina modified with different bisphosphine ligands (Josiphos type ligands, Solvias AG, Basel, Switzerland) was examined for the continuous enantioselective hydrogenation of dimethyl itaconate in scCO<sub>2</sub>. The asymmetric hydrogenation gave the highest enantioselectivity with [Rh(COD)(Josiphos 001)]<sup>+</sup>[BF<sub>4</sub>]<sup>-</sup>/PTA/Alumina *ees* = 83 % at 55 °C and 100 bar. The bisphosphine ligand attached to the Rh complex highly influenced the enantioselectivity of the hydrogenation possibly due to differences in electron withdrawing/donating properties, size, and steric effect of the ligand.

In addition, the continuous asymmetric hydrogenation of dimethyl itaconate was examined in a biphasic system ionic liquid/scCO<sub>2</sub>. The ionic liquids (ILs) [BMIM][BF<sub>4</sub>], [BMIM][NTf<sub>2</sub>], and [BMIM][N(CN)<sub>2</sub>] were investigated to immobilise [Rh(COD)(Josiphos 001)]<sup>+</sup>[BF<sub>4</sub>]<sup>-</sup>. The highest enantioselectivity *eef* = 76 % was observed in [BMIM][NTf<sub>2</sub>]/scCO<sub>2</sub> at 70 °C and 100 bar. The variation in enantioselectivity using different ILs was possibly due to i) differences in solubility of H<sub>2</sub> in various ILs ii) differences in solubility of CO<sub>2</sub> in various ILs and therefore differences in mass transfer, and iii) differences in nucleophilicity/coordination strength of the IL anion.

This work on asymmetric hydrogenation showed that the nature of the bisphosphine ligand attached to the Rh was crucial to achieve high enantioselectivity. Modifications on the substituent attached to the ligand backbone by altering the electron withdrawing/donating properties to increase the chiral performance of the catalyst would be an interesting area to investigate in the future. This concept has already been demonstrated to be successful: an increase in enantioselectivity was obtained.<sup>3</sup> The ligand tuning of Walphos type ligands gave enantioselectivity up to 95 % and 97 % in Ru and Rh catalysed hydrogenations of alkenes and ketones, respectively. The success of this approach demonstrated on Walphos type ligands is promising to develop the chiral motif of other bisphosphine ligands of the Josiphos family.

## 8.2. Continuous Kinetic Resolution of $\alpha$ -tetralol Catalysed by Cal B CLEA in scCO<sub>2</sub>

Enzymes can also be used as catalysts of selective reactions. The kinetic resolution of 1-phenylethanol has already been studied in various reaction media including scCO<sub>2</sub> with Novozym<sup>4</sup> 435 and Cal B CLEA.<sup>5</sup> Here, the continuous kinetic resolution of another secondary alcohol,  $\alpha$ -tetralol, catalysed by Cal B CLEA was investigated using different acyl donors (vinyl acetate, phenyl acetate, p-nitrophenyl acetate) in scCO<sub>2</sub>. By investigating the kinetic resolution  $\alpha$ -tetralol, the substrate specificity of the enzyme could be determined.

The selective esterification of  $\alpha$ -tetralol gave high enantioselectivity  $ee_R$  up to 99 % in a continuous flow scCO<sub>2</sub> system. The acyl donor significantly influenced the enantioselectivity of the reaction: the reaction may be driven towards the product more depending on the stability of the by-product remaining from the acyl donor. Cal B CLEA displayed lower enantioselectivity and conversion in the kinetic resolution of  $\alpha$ -tetralol than in the kinetic resolution of 1-phenylethanol. This suggests that the enzyme may be more specific for 1-phenylethanol than for  $\alpha$ -tetralol, which can be due differences in size of the two substrates:  $\alpha$ -tetralol is larger than 1-phenylethanol, and therefore the active site of Cal B may accommodate  $\alpha$ -tetralol poorly, while it accommodates 1-phenylethanol well.<sup>6</sup>

The rate limiting step of the kinetic resolution of  $\alpha$ -tetralol by Cal B CLEA could not be determined due to the limited amount of materials available in the lab. It would be interesting to investigate this in the future. It would also be interesting to perform molecular modelling for  $\alpha$ -tetralol and 1-phenylethanol to determine whether Cal B distinguishes these molecules due to their size.

### 8.3. Catalytic Cascade Reaction in a Continuous Flow scCO<sub>2</sub> system: Hydrogenation followed by the Kinetic Resolution of the Product

A two step chemoenzymatic catalytic cascade reaction for the production of (*R*)-1-phenylethyl acetate was investigated in a continuous flow scCO<sub>2</sub> system: hydrogenation of acetophenone catalysed by Pd Type 31 followed by the kinetic resolution of the product catalysed by Cal B CLEA. Two separate reactors were used in the continuous flow system which helped to overcome the problem of catalyst incompatibility and also allowed separate control of the temperature of each step. The cascade reaction gave high enantioselectivity and conversion:

- Step 1 (hydrogenation of acetophenone): conversion up to 91 %
- Step 2 (kinetic resolution): conversion up to 22 %, enantioselectivity  $ee_R > 99 \%$ .

A decrease in CO<sub>2</sub> flow rate increased the performance of both hydrogenation and kinetic resolution. The optimisation of the cascade reaction would be interesting to perform in the future.

The continuous supercritical reactor used in this work may be suitable for conducting other series/cascade reactions. It provides a great advantage for multistep reactions where the catalysts are incompatible as the physical separation of the catalysts is easily attainable.

### 8.4. Combi-CLEA of Cholesterol Oxidase and Catalase for the Continuous Oxidation of Cholesterol in scCO<sub>2</sub>

The aim of the work was to optimise the process for the preparation of CLEA of cholesterol oxidase, and combi-CLEA of cholesterol oxidase and catalase,

and to investigate their activity for the continuous oxidation of cholesterol in scCO<sub>2</sub> with 'in-flow' cholesterol extraction.

The optimisation of the process for the preparation of CLEA was performed by examining effect of different precipitating agents, different cross-linkers, and the cross-linker concentration, which resulted in CLEA with high retained activity:

- Individual cholesterol oxidase CLEA: activity of cholesterol oxidase up to 99 % (relative to native)
- Combi-CLEA: activity of cholesterol oxidase up to 99 % (relative to native), activity of catalase up to 53 % (relative to native).

The precipitating agent was shown to be important in order to produce CLEA with high retained activity and high stability. Cholesterol oxidase was shown to be highly sensitive to the presence of a precipitant, while catalase was found to be less sensitive. The cross-linker, glutaraldehyde and dextran polyaldehyde, and its concentration had a significant effect on the enzyme activity in the CLEA. The cross-linker itself had a small effect on cholesterol oxidase CLEA, while it had a more significant effect on catalase CLEA that was generated with a much higher activity using dextran polyaldehyde as cross-linker. The concentration of the cross-linker had a similar effect in most cases: the cross-linker used in a higher concentration resulted in CLEA with lower activity possibly due to mass transport limitations of the substrate to the active site of the enzyme in a more rigid structure of the CLEA. In the combi-CLEA, the activity of cholesterol oxidase was highly dependent on the amount of catalase present: higher cholesterol oxidase activity was observed with less catalase. The lower cholesterol oxidase activity might be due to mass transport limitations of the substrate to the active site of the cholesterol oxidase which was probably due to the large mass of catalase present in the combi-CLEA.

The CLEA was examined for the continuous oxidation of cholesterol in scCO<sub>2</sub> with 'in-flow' extraction of cholesterol. Although, the 'in-flow' extraction of cholesterol could not yet be optimised (high inconsistency in the concentration of cholesterol in the effluent of the reactor using either reactor setup), the continuous oxidation of cholesterol was examined with cholesterol oxidase CLEA and combi-CLEA of cholesterol oxidase and catalase in scCO<sub>2</sub>. Unfortunately, very low yield was obtained with all catalysts at all conditions

in the continuous flow system which could be due to the lack of water. The oxidation of cholesterol in a batch scCO<sub>2</sub> system also showed that the lack of water may be the main limiting factor. A CLEA normally contains a small amount of H<sub>2</sub>O but it was shown to be insufficient in this case. The drying procedure (freeze-drying) of the CLEA could also influence the activity of cholesterol oxidase that may be sensitive to freeze-drying. The results suggest that cholesterol oxidase form *Nocardia sp.* may require a small amount of water to function and that the drying can highly influence the enzyme activity.

The continuous oxidation of cholesterol in scCO<sub>2</sub> can have potential in the manufacture of the oxidation products of cholesterol and derivatives. The findings of this work can aid the development of the process. The catalyst performance may increase if H<sub>2</sub>O is present which would be interesting to examine in a continuous flow scCO<sub>2</sub> system in the future. Cholesterol oxidase from *Nocardia sp.* may be sensitive to freeze-drying, the method used here to dry the CLEA, which would be important to investigate in the future. The stability of the CLEA and the combi-CLEA against organic solvents and temperature would also be important to investigate in the future. Cholesterol oxidases from different groups share the same catalytic activity, but they show no sequence homology and the FAD cofactor binding is also different.<sup>7, 8</sup> CLEAtion of cholesterol oxidase from different sources would be interesting to investigate to demonstrate whether these differences between cholesterol oxidases from different groups influence the immobilisation of the enzyme. A number of factors have been investigated to optimise the ‘in-flow’ cholesterol extraction in a continuous flow scCO<sub>2</sub> system but unfortunately it was unsuccessful. Foster and co-workers reported a solubility study on cholesterol in a flow scCO<sub>2</sub> system.<sup>9</sup> The reactor designed by Foster and by us differentiated only in the sample collection method that may be key to achieve steady state, however, we are convinced that the sample collection method of our system was also highly suitable. The optimisation of the ‘in-flow’ extraction in our continuous flow system would be interesting to perform in the future.

## 8.5. Thesis Summary

This Thesis has investigated the use of several immobilised catalysts for continuous enantioselective reactions in scCO<sub>2</sub>. The aim of the research was to achieve high enantioselectivity using metal complexes and enzymes as catalysts. The compatibility of supported homogeneous chiral Rh catalysts and Cross-Linked Enzyme Aggregates of different enzymes in continuous flow supercritical reactions was demonstrated successfully, which have great potential to perform exciting and productive research in the future.

This work also demonstrated examples for individual CLEA and combi-CLEA. Although CLEA of several different enzymes have already been prepared successfully, CLEAtion still is an intriguing research field and yet to be explored in a greater extent.

## References

1. Wandeler, W., Künzle, N., Schneider, M., Mallat, T., Baiker, A., Continuous platinum-catalyzed enantioselective hydrogenation in 'supercritical' solvents. *Chemical Communications* **2001**, 673-674.
2. Szöllősi, G., Hermán, B., Fülöp, F., Bartók, M., Continuous enantioselective hydrogenation of activated ketones on a Pt-CD chiral catalyst: use of H-Cube reactor system. *Reaction Kinetics and Catalysis Letters* **2006**, 88, (2), 391-398.
3. Wang, Y., Strum, T., Steuerer, M., Arion, V.B., Mereiter, K., Spindler, F., Weissensteiner, W., Synthesis, coordination behaviour, and use in asymmetric hydrogenation of Walphos-type ligands. *Organometallics* **2008**, 27, 1119-1127.
4. Matsuda, T., Watanabe, K., Harada, T., Nakamura, R., Arita, Y., Misumi, Y., Ichikawa, S., Ikariya, T., High-efficiency and minimum-waste continuous kinetic resolution of racemic alcohols by using lipase in supercritical carbon dioxide. *Chemical Communications* **2004**, 2286-2287.
5. Stephenson, P., PhD Thesis. *University of Nottingham, Nottingham (UK) 2005*.
6. Ottosson, J., Fransson, L., King, J.W., Hult, K., Size as a parameter for solvent effects on *Candida antarctica* lipase B enantio selectivity. *Biochimica et Biophysica Acta - Protein Structure and Molecular Enzymology* **2002**, 1594, 325-334.
7. Gadda, G., Wels, G., Pollegioni, L., Zucchelli, S., Ambrosius, D., Pilone, M.S., Ghisla, S., Characterization of cholesterol oxidase from *Streptomyces hygroscopicus* and *Brevibacterium sterolicum*. *European Journal of Biochemistry* **1997**, 250, 369-376.
8. Pollegioni, L., Wells, G., Pilone, M.S., Ghisla, S., Kinetic mechanisms of cholesterol oxidase from *Streptomyces hygroscopicus* and *Brevibacterium sterolicum* *European Journal of Biochemistry* **1999**, 264, 140-151.

9. Yun, S. L. J., Liong, K.K., Gurdial, G.S., Foester, N.R., Solubility of Cholesterol in Supercritical Carbon Dioxide. *Industrial & Chemical Engineering Research* 1991, 30, 2476-2482.

## Appendix

### Publications

1. Stephenson, P., Kondor, B., Licence, P., Scovell, K., Ross, S.K., Poliakoff, M. Continuous Asymmetric Hydrogenation in Supercritical Carbon Dioxide using an Immobilised Homogeneous Catalyst, *Advanced Synthesis and Catalysis* **2006**, 348, 1605-1610.
2. Hobbs, H.R., Kondor, B., Stephenson, P., Sheldon, R.A., Thomas, N.R., Poliakoff, M. Continuous Asymmetric Hydrogenation in Supercritical Carbon Dioxide using an Immobilised Homogeneous Catalyst. *Green Chemistry* **2006**, 8, 816-821.